Emergence d'une dynamique neuronale préfrontale par l'entraînement cognitif

Marion Ducret

Université Claude Bernard Lyon 1

THESE de DOCTORAT DE
L'UNIVERSITE CLAUDE BERNARD LYON 1

Ecole Doctorale 476
Neurosciences et Cognition

Discipline : Neurosciences

Soutenue publiquement à Lyon le 03/12/2024, par :
Marion DUCRET

Emergence of prefrontal neural dynamics through cognitive training

---

Devant le jury composé de :

Dr. BURLE Boris	CNRS, LNC Marseille	Rapporteur
Dr. KILAVIK Bjørg	CNRS, INT Marseille	Rapporteure
Dr. BOURET Sébastien	CNRS, ICM Paris	Examinateur
Dr. COUTUREAU Etienne	CNRS, Bordeaux	Président
Dr. CRISTOFORI Irene	Université Lyon 1	Examinatrice
Dr. SLIWA Julia	CNRS, ICM Paris	Examinatrice
Dr. PROCYK Emmanuel	CNRS, SBRI Lyon	Directeur de thèse
Dr. WILSON Charles R. E.	INSERM, SBRI Lyon	Directeur de thèse

ABSTRACTS

English version

Learning to learn refers to the ability to extract general rules from specific experiences to accelerate future learning, a process facilitated through cognitive training. Although the lateral prefrontal cortex-midcingulate cortex network is known to be involved in this process (Browning et al., 2007; Procyk et al., 2016), the neural changes occurring from a naïve state to the learning to learn level remain poorly studied. To address this, we first refined the rostro-caudal functional organisation of this network using resting-state fMRI in 15 monkeys. Then we conducted longitudinal electrophysiological recordings, including single-unit activity, event-related potentials from local field potentials, and functional connectivity using two monkeys who were task naïve at the start of recordings. The monkeys performed a series of tasks, ranging from a baseline non-cognitive task to discrimination learning and reversal learning tasks, allowing us to track neural adaptations over time. Feedback processing was central to our approach, as it drove the learning process, enabling the subjects to adjust their strategies and improve their performance. We also conducted a comprehensive behavioural analysis, demonstrating how our subjects learned and adapted across tasks, progressively acquiring more efficient learning strategies. Interestingly, our monkeys did not learn in the same way as reported in previous studies (Faraut et al., 2016; Harlow, 1949; Wilson & Gaffan, 2008). Both monkeys successfully reached the learning to learn level, but each displayed distinct patterns of neural changes across all measured levels, including single-unit activity, LFPs, and functional connectivity. Moreover, the two monkeys exhibited different motivational profiles, which allowed us to identify specific effects of motivation on feedback processing and overall task performance. These differences in motivational states provided unique insights into how internal states can modulate neural activity and influence learning efficiency.

Our findings demonstrated distinct neural changes that accompany the transition from task-specific learning to the more generalized learning to learn level. Furthermore, motivational analysis highlighted its crucial role in modulating feedback processing and neural dynamics. These results contribute to a larger project aimed at understanding the neural basis of cognitive training. Additional analyses, such as oscillatory activity or those focused on

aspects beyond feedback processing, like action planning, may further clarify the neuronal dynamics underlying cognitive training and contribute to a more comprehensive understanding of the mechanisms of learning to learn.

French version

Apprendre à apprendre fait référence à la capacité d'extraire des règles générales à partir d'expériences spécifiques pour accélérer les apprentissages futurs, un processus facilité par l'entraînement cognitif. Bien que le réseau formé par le cortex préfrontal latéral et le cortex cingulaire moyen soit reconnu pour jouer un rôle clé dans ce processus (Browning et al., 2007; Procyk et al., 2016), les changements neuronaux qui se produisent depuis un état naïf jusqu'au niveau d'apprendre à apprendre restent peu étudiés. Pour pallier ce manque, nous avons d'abord affiné l'organisation fonctionnelle rostro-caudale de ce réseau à l'aide d'une étude utilisant l'IRM fonctionnelle au repos chez 15 singes. Ensuite, nous avons réalisé des enregistrements électrophysiologiques longitudinaux, incluant des analyses d'activité unitaire, des potentiels évoqués à partir des potentiels de champs locaux et de la connectivité fonctionnelle chez deux singes naïfs. Ces singes ont été soumis à une série de tâches allant d'une tâche de référence sans apprentissage cognitif à des tâches d'apprentissage discriminatif et d'inversion (« discrimination learning » et « reversal learning »), nous permettant ainsi de suivre les adaptations neuronales au fil du temps. Le traitement des retours, appelé « feedback », était au cœur de notre approche, car il guidait le processus d'apprentissage, permettant aux sujets d'ajuster leurs stratégies et d'améliorer leurs performances. Nous avons également mené une analyse comportementale complète, montrant comment nos sujets ont appris et se sont adaptés aux différentes tâches, en acquérant progressivement des stratégies d'apprentissage plus efficaces. Il est intéressant de noter que nos singes n'ont pas appris de la même manière que dans les études précédentes (Faraut et al., 2016; Harlow, 1949; Wilson & Gaffan, 2008). Bien que les deux singes aient appris à apprendre, chacun a montré des schémas distincts de changements neuronaux à tous les niveaux mesurés, incluant l'activité unitaire, les potentiels de champs locaux et la connectivité fonctionnelle. De plus, les deux singes ont présenté des profils motivationnels différents, ce qui nous a permis d'identifier des effets spécifiques de la motivation sur le

traitement des « feedbacks » et les performances globales. Ces différences d'états motivationnels ont offert des perspectives uniques sur la manière dont les états internes peuvent moduler l'activité neuronale et influencer l'efficacité de l'apprentissage.

Nos résultats ont démontré des changements neuronaux distincts qui accompagnent la transition de l'apprentissage spécifique à une tâche vers un niveau plus généralisé d'apprentissage à apprendre. Par ailleurs, l'analyse motivationnelle a mis en évidence son rôle crucial dans la modulation du traitement des « feedbacks » et des dynamiques neuronales. Ces résultats s'inscrivent dans le cadre d'un projet plus vaste visant à comprendre les bases neuronales de l'entraînement cognitif. Des analyses supplémentaires, telles que les oscillations ou celles centrées sur des aspects autres que le traitement des « feedbacks », comme la planification des actions, pourraient aider à mieux définir les dynamiques neuronales sous-tendant l'entraînement cognitif et à offrir une compréhension plus complète des mécanismes d'apprentissage à apprendre.

REMERCIEMENTS

Tout d'abord je voudrais remercier Charlie sans qui rien de tout ça n'aurait été possible. Merci d'avoir cru en moi il y a maintenant 5 ans et de m'avoir confié ton projet un peu fou. J'ai énormément appris en bossant avec toi, même à bricoler. Merci pour la liberté que tu m'as laissée et pour ton ouverture d'esprit qui a souvent mené à des débats très intéressants même en dehors de la science. Merci aussi pour les nombreuses pintes de bières et pour m'avoir fait découvrir mon cocktail préféré, le pornstar martini.

Manu, merci pour tes nombreux conseils et pour ta disponibilité. Merci également de m'avoir accueilli au sein de ton équipe et d'être un si bon modèle de rigueur scientifique. Merci aussi de m'avoir permis avec Céline de travailler à vos côtés et de m'avoir fait découvrir le monde de l'IRM pour mon premier papier.

Céline, merci pour ta bienveillance, pour tes précieux conseils et surtout pour le soutien que tu as su m'apporter toujours aux bons moments. Comme l'a déjà dit Camille l'année dernière, tu es un modèle pour bon nombre d'entre nous.

« Où est Jérôme ? » la question que j'ai le plus entendu en 4 ans. Merci de m'avoir montré comment fonctionnait une dremel. Grâce à toi j'ai pu prouver à Charlie que la duchesse n'était pas si nulle en bricolage. Je voulais aussi le remercier pour les fous rires de fin de journée et pour les nombreux post-its d'encouragement.

Je voudrais également remercier la team NEF dans son ensemble, on se le dit souvent mais c'est une chance incroyable de bosser dans une équipe aussi soudée et bienveillante. Ça a été 5 années de travail intenses mais aussi de sacrés moments de fun. Les mythiques NEF drinks même si on s'est calmé au fur et à mesure des années, les conférences au palais Hirsch, les esclaves de NeuroFrance (désolée Manu) mais surtout le célèbre aquarium. Ce bureau où le chauffage marche en été mais pas en hiver, qui voit plus de passage à la journée que la gare Part Dieu, mais où j'ai rencontré des personnes incroyables.

Clémence, mon binôme d'animalerie, je te rappelle qu'on devait faire une thèse à deux. Les longues heures avec les singes n'auraient vraiment pas été les mêmes sans toi, surtout quand il fallait nettoyer les volières en faisant un karaoké ou se battre contre des singes qui ne voulaient pas coopérer. Merci pour tout, ton écoute, ton soutien, tes câlins, tes mots justes et tes massages aussi. J'ai découvert une véritable amie et je te suis extrêmement reconnaissante du pilier que tu as été pour moi au cours de ces années.

Valentine, même s'il a fallu 2 ans pour que tu arrêtes de chanter en bossant, merci pour ta bonne humeur, ton humour et ton soutien mais surtout merci pour tes positions improbables sur ta chaise qui ont égayé mes journées. Merci aussi d'avoir été le meilleur des scribes pendant la préparation de ma soutenance. Tu as été un binôme incroyable pour les soirées tardives dans le bureau et une oreille attentive pour tous mes états d'âme.

Camille, on est arrivée ensemble mais finalement tu es partie avant moi. Ma grande sœur de la recherche, tu as été un vrai modèle pour moi et d'un tel soutien, toujours prête à m'écouter et me rassurer, autour d'une bière quand même si possible ou bien dans le taxi Ducret. Mes années de thèse auraient été bien différente sans toi et je ne sais pas comment je vais survivre dans ma vie pro sans pouvoir tout débriefer avec toi. J'ai trouvé en toi une véritable amie.

Julien, merci pour la Toki-thérapie, merci de m'avoir nourri de St Albray et de pâtisserie et merci pour tes conseils avisés. Clément, merci pour tout ce que tu m'as appris avec les singes et avec les spikes. Merci aussi pour ta disponibilité, même à distance. Merci également à Charles, pour tes bonjours les stars qui nous manquent beaucoup et tes questions improbables, à Amel, l'enfant adopté de l'équipe, pour ta bonne humeur et ton accent chantant. Et merci à tous les autres membres de l'équipe qui contribuent à la bonne ambiance générale !

Je voudrais également remercier tous mes copains, pour votre soutien incroyable mais surtout pour votre présence à ma soutenance qui m'a énormément touché. J'ai une chance folle d'être si bien entourée. Je crois que vous l'attendiez presque autant que moi cette fin de thèse ! Un

merci spécial à Zoé et Gaspard qui ont fait le trajet depuis St Etienne et à Rémi et Julie depuis Clermont.

Pauline, un petit mot spécial pour te remercier infiniment pour ta présence durant ces mois de rédaction, tu as été d'un soutien incroyable pour moi. Et je n'ai pas forcément eu l'occasion de te le dire avant mais j'ai toujours adoré te voir expliquer mon sujet de thèse avec tant d'entrain à de nombreuses personnes.

Merci à mon père et ma mère de m'avoir permis de faire des études aussi longues en toute tranquillité, promis cette fois c'est vraiment fini. Merci pour votre soutien sans faille et pour vos encouragements. Merci à mon frère, Guillaume, de ne jamais avoir vraiment compris ce que je faisais mais d'avoir répété souvent à qui voulait l'entendre que je passais ma journée à jouer avec des singes. Merci à toute ma famille, pour l'environnement incroyable dans lequel j'ai grandi. J'ai une pensée pour Opa et Oma qui ont suivi tout mon parcours et qui me soutiennent dans tous mes projets. Mais aussi pour Jean Louis et ma mamie qui aurait été très fier de me voir arriver au bout de ce doctorat.

Et enfin merci à toi, Lucas, mon mari, mon meilleur ami, mon plus gros soutien, cette thèse c'est un peu la tienne aussi finalement. Pendant 4 ans notre vie a tourné autour de ma thèse et tu ne t'es jamais plains. Tu as été un soutien sans faille à toutes les étapes et je ne suis pas certaine que j'aurais réussi sans toi. Merci pour tout.
Le petit mot de la fin pour dire que c'était finalement ma deuxième thèse, la première c'était il y a 28 ans dans le ventre de ma maman…

TABLE OF CONTENTS

INTRODUCTION

The ability to learn is one of the most fundamental aspects of human life, underpinning not only individual development but also the progress of entire societies. Learning enables humans to acquire new skills, adapt to changing environments and solve complex problems. It is through learning that knowledge is transmitted across generations, cultures are formed and innovation arises. In this context, understanding the mechanisms that govern learning is of huge importance, both for advancing scientific knowledge and for addressing societal challenges. Neuroscience seeks to unravel how the brain, an organ of immense complexity, supports the myriad cognitive functions that enable learning. How changes in brain activity correlate with changes in behaviour during the learning process have been one of the big questions in the last decades. This question is critical not only for understanding how the brain functions but also for developing ways to enhance learning and cognitive performance across different contexts, from education to rehabilitation. The societal implications of this research are profound. As the world becomes more complex and the demand for new skills increases, there is a growing need to understand how learning can be optimised. This includes not only the traditional educational settings but also the workplace, where continuous learning is essential for adapting to technological advances. Moreover, as populations age, understanding how to maintain cognitive function through targeted training becomes increasingly important. Insights into how cognitive training affects brain function could lead to more effective strategies for preserving cognitive health and enhancing quality of life in older adults. Furthermore, the implications of linking brain dynamics with learning extend to addressing cognitive impairments and mental health challenges. By understanding how learning processes can be influenced and improved, it may be possible to develop interventions that help individuals with learning disabilities, cognitive decline, or psychiatric conditions. The potential to improve cognitive outcomes through targeted interventions could have a transformative impact on public health and well-being.

Chapter 1. The cognitive basis of feedback processing in learning and learning to learn contexts

I. Learning and learning to learn

Learning, in its broadest sense, is defined as the process by which living beings acquire or modify knowledge, behaviour, skills, values or preferences through experience, education or training. It is one of the most important topics in contemporary psychology but it still remains an extremely difficult concept to define. One common assumption is that we can attribute a behavioural change to learning only if the change is relatively permanent and results from experiences (Watson, 1913).

There is a broad range of learning theories from behavioural theories, like the pavlovian classical conditioning (Pavlov, 1927) or the operant conditioning (Skinner, 1953), to cognitive theories in which the subject is solving complex problems by learning rules and concepts (Bandura, 1986; Köhler, 1929; Tolman, 1949).

In the field of neuroscience, learning is a core concept conceptualised as a set of neurobiological processes through which the brain encodes, stores and retrieves information. These processes enable individuals to adapt their behaviours in response to the ever-changing demands of the environment. Learning in neurosciences is a dynamic interplay of processes including neural encoding (Quian Quiroga & Panzeri, 2009), synaptic plasticity (Bliss & Collingridge, 1993), memory consolidation (McGaugh, 2000), neurogenesis (Zhao et al., 2008) and retrieval (Tulving, 2002). These processes work together to enable the brain to adapt behaviour based on experience, ensuring that an individual can respond effectively to changing environmental demands. Learning could be one of the most important human capacities as it represents not only the ability to acquire knowledge from experiences but also the capacity of shaping adaptive behaviour essential for survival.

Learning to learn, also known as meta-learning in the computational field, is a separate function from classical learning that refers to the process by which individuals develop strategies and skills to improve their ability to learn new information. Unlike classical learning, which focuses on acquiring specific knowledge, learning to learn is concerned with optimising

the learning process itself. The mechanism of learning to learn is the product of what is called the cognitive training. This process was demonstrated by Harlow and is now well established in primate species (Harlow & Warren, 1952). Harlow characterised this process as the acquisition of a 'learning set' (Harlow, 1949), a process considered one of task-specific strategy acquisition that does not rely on the same cognitive processes as the gradual learning of individual problems. It is a higher-order cognitive function that involves recognizing patterns in learning experiences, adapting to new situations/environments and applying generalised principles across different contexts. It would be possible to accelerate the learning by discovering and exploiting common elements, like rules, across problems (Kemp et al., 2010). This meta-cognitive approach enables learners to become more effective and flexible, making it easier to acquire new knowledge and skills in diverse areas. It is important to make a clear distinction between the two as they are two different cognitive processes. In fact, while classical learning is often domain-specific, the skills developed through learning to learn have broad applications. These skills contribute to lifelong learning, allowing individuals to continue adapting throughout their lives and they are increasingly recognized as a crucial skill in today's fast-paced, ever-changing world. The importance of learning how to learn efficiently has become a major subject in the educational field and studies have shown that learning to learn training can improve academic performance and foster deeper learning (Dignath & Büttner, 2008; Schraw, 1998). Beyond education, learning to learn skills have been associated with an increase of well-being and cognitive resilience in older adults (Cornford, 2002; Kyndt & Baert, 2013).

A key of this concept is the notion of timescales. Learning to learn refers to a scenario in which the subject learns at two levels. At the first level, learning happens quickly within the context of a specific example within a task. This involves acquiring knowledge or skills pertinent to the immediate challenge, such as learning about object properties accurately within a particular dataset. This type of learning is typically content-specific and occurs over a shorter time scale, driven by direct experience with the task at hand. The second level involves a slower, more gradual accumulation of knowledge across multiple tasks or repeated trials of the same task. Over this longer time scale, the subject extracts general rules or structures that may not be evident in individual tasks or trials. This type of learning enables the transfer of knowledge across different but related domains, enhancing the ability to adapt to new tasks

more efficiently (Constantinidis & Klingberg, 2016; Santoro et al., 2016; Thrun, 1996). As an example, an animal might learn about the qualities of fruit in the surrounding trees - ripeness, accessibility, etc. These experiences will allow them to extract general information that will be useful if they move to a new forest and encounter new fruit - for example fruit colour is linked to ripeness. These principles of learning to learn extend also to higher strategic learning in humans as well. For example, a chess player who has mastered the game's strategies may apply these learned principles when playing other strategic games like Go or shogi (japanese chess). Despite the differences in rules and game pieces, the underlying strategic thinking developed in chess, like anticipating opponent moves or controlling the centre of the board, can be transferred and adapted to new contexts.

In addition to this dual time scale concept, Lansdell and Kording proposed two distinct sub-categories within learning to learn, which further illustrate how these processes operate across different contexts (Lansdell & Kording, 2019). First, "learning to optimize" involves developing efficient learning rules that enable rapid convergence to good solutions, particularly when faced with many unrelated tasks. The focus here is on optimizing the learning process itself, making it quicker and more effective, regardless of the task's specific content. This approach is especially useful in environments where the subject encounters a wide variety of tasks that do not share a common structure (Finn et al., 2017). Secondly, the "structure learning" that occurs when the subject identifies and internalizes a common structure across related tasks, which then facilitates rapid learning on new tasks within the same family. This process requires that the tasks share meaningful similarities, allowing the subject to transfer learned strategies or rules effectively to new but related challenges (Tenenbaum et al., 2011). These sub-categories of learning to optimize and structure learning refine the learning to learn concept, providing insight into how different types of tasks influence the strategies used to enhance learning.

II. Feedback in learning and learning to learn processes

Feedback is a critical concept in both learning and cognitive science, referring to the process through which information about the outcomes of actions or behaviours is returned to

the individual, enabling adjustments and improvements in future performance. The term "feedback" originated in engineering and cybernetics (Ashby, 1956; Wiener, 1948), where it describes systems that use outputs to regulate and control processes, but its application has since expanded significantly to include various domains such as psychology, education, and neuroscience. At its most basic level, feedback is the information provided to a system or individual about their performance relative to a goal or desired outcome (Kluger & DeNisi, 1996). This information can take various forms, from the explicit (verbal instructions or numerical scores) to the implicit (sensory feedback) (Nicol & Macfarlane-Dick, 2006). The purpose of feedback is to inform the subject about the correctness, adequacy, or effectiveness of their actions, allowing them to modify future behaviours to achieve better results (Hattie & Timperley, 2007; Ramaprasad, 1983).

In cognitive tasks, feedback can be categorized into two types reflecting its roles in cognitive processes and learning: positive and negative feedback. Positive feedback reinforces or amplifies an initial behaviour, leading to an increase in that behaviour. Negative feedback works to correct or diminish a behaviour that deviates from a desired path (Ashby, 1956).

From a cognitive perspective, feedback is essential for learning because it helps individuals understand the gap between their current performance and the desired outcome. It also facilitates the development of self-regulation, as learners use feedback to monitor, evaluate, and adjust their learning strategies (Wessel, 2018; Zimmerman, 2002). According to the “Cognitive Load Theory”, feedback can reduce cognitive load by providing clear information that helps learners focus on relevant aspects of the task, thereby enhancing the efficiency of learning (Sweller, 1988). Feedback is deeply embedded in various learning theories, particularly in behaviourism and constructivism. Within the behaviourist framework, feedback is viewed primarily in terms of reinforcement. The “Law of Effect”, as proposed by Thorndike (1911), says that behaviours followed by positive outcomes are reinforced and thus more likely to be repeated, whereas those followed by negative outcomes are less likely to occur (Postman, 1947). In constructivist theories, feedback is seen as a critical element in the learner’s active construction of knowledge (Vygotsky, 1978). Overall, the feedback operates across various levels and forms, from the reinforcement of behaviours in behaviourist models to the facilitation of self-regulated learning in cognitive theories.

Using feedback during learning does not mean only correcting mistakes, it also develops skills that help to learn better in the future. Thanks to feedback, learners know when they are wrong and they can adjust their problem solving techniques. Over time, this will make them more efficient as they repeatedly use feedback to improve not just their knowledge but their learning processes. This means that they gradually develop the ability to learn how to learn by understanding how to acquire and apply knowledge more effectively across various contexts.

a) Positive feedback

In the context of cognitive tasks used in neuroscience, positive feedback is often delivered in the form of rewards. According to the Cambridge dictionary, a reward is "something good you are given or allowed because of something you do". In a more scientific way, Schultz defined it as "any positive or pleasurable outcome that we are motivated to obtain and that we will work for" (Schultz, 2015). One common notion in these two definitions is the necessity of an action to obtain a reward. A reward can have a lot of different forms, it is not defined by its physical properties but by the behavioural reactions they induce. There are three interlaced functions of reward: the learning process, the anticipatory behaviour and the decision-making linked to it and the positive emotion of pleasure. The anticipatory behaviour, or preparatory behaviour, leads to decision making which is driven by the attractive character of the reward that makes us exert an effort. This can also be referred to as the motivation, as Schultz said: 'reward makes you come back for more'. The latter one, the pleasure, is the more obvious one because it is the foremost emotion evoked by the reward. This pleasure signal associated with the reward motivates and helps individuals to learn in a better way (Schultz, 2015, 2016).

One of the primary roles attributed to the reward is their capacity to act as a positive reinforcer, increasing the likelihood that the behaviour leading to the reward will be repeated in the future. This process is rooted in the brain reward system, particularly involving the neurotransmitter dopamine, which plays a critical role in the reinforcement of behaviour (Schultz, 1998). When a learner receives a reward following a correct response, the brain

reward circuitry is activated and the dopaminergic neurons of the ventral tegmental area release dopamine. The dopamine targets the nucleus accumbens in the basal ganglia which reinforces the current behaviour by creating a sense of satisfaction (Di Chiara & Bassareo, 2007). Dopamine is also sent to the prefrontal cortex and helps reinforce the correct behaviour and link reward information to long-term behavioural strategies (Volkow et al., 2011). Dopamine release operates in two modes: phasic and tonic. Phasic one occurs in brief bursts in response to unexpected rewards, signalling a reward prediction error (Schultz, 2007). Tonic dopamine release is more stable and helps regulate overall motivation and brain's alertness to act over a longer period (Niv et al., 2007). This reinforcement process is essential for both learning specific tasks and developing the meta-cognitive skills associated with learning to learn (Berridge & Robinson, 1998). Furthermore, research has shown that the size, frequency, and predictability of rewards can significantly influence how effectively they function as feedback. For example, larger and more frequent rewards can lead to faster learning, but they can also diminish over time if they become too predictable, leading to a decrease in motivation (Kable & Glimcher, 2009). On the other hand, unpredictable or variable rewards can maintain engagement and motivation over longer periods, as the learner remains motivated by the uncertainty of the outcome. Thus, in addition to reinforcing behaviour, rewards play a critical role in motivation and goal-directed actions. The anticipation of a reward can drives individuals to engage in specific behaviours, thereby influencing learning and decision-making processes (Berridge & Robinson, 2003). This motivational aspect is fundamental.

Overall, rewards are frequently used to provide positive feedback in cognitive tasks, playing a critical role in reinforcing learning behaviours and enhancing the learning to learn process.

While rewards and feedback are closely related, they are not identical concepts and should not be used interchangeably. Feedback refers to any information provided to a learner about their performance, which can be used to guide future actions. This feedback can be positive or negative, explicit or implicit, and serves to inform the learner about the correctness, efficiency, or quality of their behaviour or decisions (Hattie & Timperley, 2007). Rewards, on the other hand, are specific outcomes or stimuli that are perceived as desirable and are given in response to a particular action or behaviour. The key difference lies in their primary function: feedback is informational, providing data about performance, while rewards are motivational,

designed to reinforce behaviour and encourage its repetition. However, rewards can also serve as a form of feedback by providing a clear, positive signal that a particular behaviour was correct or desirable. This is particularly true in the context of cognitive tasks, where the receipt of a reward delivers not just a pleasurable experience but also valuable information to the learner about the success of their actions. In this way, the reward becomes a feedback signal, informing the learner that their strategy or response was effective, which in turn reinforces the behaviour and strengthens the associated neural pathways (Berridge & Robinson, 2003; Schultz, 2015). The transition from reward to feedback occurs because the reward carries informational content by indicating that the action taken was appropriate and successful in achieving the desired outcome. This dual role of rewards is critical in learning processes, as it simultaneously motivates the learner and provides the feedback necessary to refine future behaviour (Schultz, 2016).

b) Negative feedback

In cognitive processes, negative feedback plays a crucial role in signalling errors or deviations from desired outcomes. Unlike positive feedback, which reinforces correct behaviours, negative feedback provides information that something has gone wrong, encouraging individuals to recognize and correct mistakes. This type of feedback is essential for refining strategies and improving future performance. In the context of cognitive tasks, negative feedback can take various forms and these signals are designed to indicate that an error has occurred.

An error in cognitive tasks typically refers to a mismatch between the expected outcome and the actual result, indicating that the current strategy or response was incorrect. Errors do not always mean failures, they are valuable opportunities for learning. Negative feedback, by highlighting these errors, helps the brain identify where and why the mistake occurred, facilitating the adjustment of cognitive strategies. This error-driven learning process is essential for adaptive behaviour, allowing individuals to refine their responses and improve performance over time (Holroyd & Coles, 2002). Another phenomenon in error processing is post-error slowing - the tendency for individuals to slow down their responses following an

error. This slowing is often thought to reflect a strategic attempt to avoid repeating the error by giving oneself more time to process the task. However, recent research has added nuance to this interpretation. Danielmeier and Ullsperger demonstrated that post-error slowing is not merely a strategic attempt to improve accuracy (Danielmeier & Ullsperger, 2011). It also reflects an impairment in the cognitive system's ability to prepare and execute correct responses, leading to an increased likelihood of repeating errors. This suggests that errors can temporarily disrupt cognitive processing, making immediate correction more difficult. Complementarily, Wessel proposed the "adaptive orienting theory," which suggests that errors trigger an initial global inhibition of both motor and cognitive processes (Wessel, 2018). This inhibition, although impairing immediate performance, is crucial for redirecting cognitive resources to address the error, thus facilitating longer-term adaptive adjustments. These findings underscore the complexity of error processing, revealing it as a balance between the immediate impairments caused by errors and the subsequent adaptive strategies that enhance learning and performance.

In cognitive tasks, the absence of a reward or the introduction of a latency period before the next trial can serve as a form of negative feedback. The absence of a reward is particularly effective because it disrupts the expected positive outcome, creating a clear indication that an error has occurred (Schultz, 2016). Similarly, a latency period can give the learner time to reflect on the error and consider alternative strategies (Holroyd & Coles, 2002). Both forms of negative feedback are critical for reinforcing the learning process, as they provide clear, immediate signals that help guide behaviour towards more successful outcomes.

Negative feedback is a powerful tool in cognitive processes, enabling individuals to detect errors, adjust strategies, and improve performance. By learning to understand negative feedback effectively, subjects can refine their cognitive strategies and achieve greater success in complex tasks.

Overall, both types of feedback are useful in the learning and learning to learn processes and have different impacts depending on the context. It is important to acknowledge the fact that feedback processing and learning to learn are not immutable processes. In fact, multiple factors could impact them and need to be taken into account.

III. Impact factors influencing feedback processing and learning to learn

The effectiveness of feedback processing and the development of learning to learn skills are also shaped by various non-pathological factors. These factors can significantly influence how individuals engage with learning tasks, interpret feedback, and refine their learning strategies over time. Among these factors, motivation, the level of task difficulty, and time on task are particularly crucial. Each of these elements plays a distinct role in shaping the cognitive and emotional environment in which learning occurs, ultimately impacting the learner's ability to process feedback and adapt their learning processes.

Motivation and learning are intrinsically linked, each influencing the other in a dynamic interplay. Motivation is not just a catalyst for engaging in learning tasks but also a critical component that shapes the way feedback is processed and utilised in the learning to learn process. Individuals with high motivation are more likely to engage deeply with learning tasks, set challenging goals, and employ effective strategies to achieve those goals (Deci & Ryan, 2000). This engagement favours a positive feedback loop: early successes, driven by motivation, boost self-efficacy, which in turn enhances motivation and encourages further learning efforts. Motivated learners are also more adept at interpreting feedback, using it not merely as a signal of success or failure but as valuable information for refining strategies and improving performance (Fishbach et al., 2010). Research indicates that such learners exhibit greater adaptability and resilience, crucial traits in the learning to learn process, which involves continually refining one's approach to learning in response to new challenges (Pintrich & Groot, 1990).

Another critical factor in learning, directly affecting the quality and quantity of cognitive engagement and linked to the motivation is the "time-on-task". It refers to the amount of time a learner actively spends engaged in a cognitive task (Carroll, 1963). It is often used as a metric in educational settings to evaluate student engagement and in cognitive research to measure factors like attention, fatigue or the effect of distributed practice. Extended time on task provides more opportunities for practice, reinforcement, and the application of feedback, leading to deeper learning and better retention (Ericsson et al., 1993). However, the relationship between time on task and learning outcomes is not linear. While more time spent on a task can enhance learning, there are reverse effects if that time is not managed

effectively. Prolonged engagement without sufficient pauses can lead to cognitive fatigue, which impairs the ability to process feedback and reduces overall performance (Reeve & Lee, 2014). Fatigue can also decrease motivation, leading to a drop in the quality of learning as the task becomes more of a burden than a challenge. Additionally, the concept of "spacing" learning sessions over time has been shown to improve long-term retention and the ability to apply learned knowledge in new contexts (Cepeda et al., 2006).

The difficulty level of cognitive tasks plays a pivotal role in determining the effectiveness of learning and the processing of feedback. Tasks that are too simple can lead to disengagement and boredom, reducing the learner's motivation to engage with feedback or apply it meaningfully (Cziksentmihalyi, 1990). In contrast, tasks that are too difficult can overwhelm the learner, leading to frustration which can diminish the effectiveness of feedback and reduce motivation to continue (Van Merriënboer & Sweller, 2005). Optimal learning occurs within what is often referred to as the "zone of proximal development" (ZPD), a concept introduced by Vygotsky (1978). The ZPD represents the range of tasks that are just beyond the learners' current abilities but can be mastered with appropriate guidance and feedback. Within this zone, feedback is most effective because it helps the learner to bridge the gap between what they can do independently and what they can achieve with support. Feedback that is tailored to the learners current level of difficulty can guide them through the ZPD, fostering progressive learning gains that build confidence and competence (Hattie & Timperley, 2007).

These factors have different impacts on the learning process which should not be ignored and an in-depth behavioural analysis to identify them should be essential in any project with a cognitive task.

IV. Pathologies associated with learning disabilities

We described in the previous parts the behavioural basis of the feedback processing in a learning to learn context in healthy subjects. However, non-healthy cases in which this processing is impaired exist and increase the necessity to have a clear description of these mechanisms. In fact, fundamental research projects like this thesis intend to serve as a

knowledge base in healthy subjects in order to develop interventions aimed at improving pathological conditions.

Various neurological and psychological conditions can significantly impact the brain's ability to process and integrate feedback, resulting in learning impairments. This includes specific learning disabilities such as dyslexia and dyscalculia, as well as broader conditions such as autism spectrum disorder (ASD) and attention deficit hyperactivity disorder (ADHD), all of which interfere with the feedback mechanisms critical for learning.

Dyslexia is a specific learning disability that primarily affects reading and writing abilities often resulting from altered phonological processing in the brain. Dyslexic individuals have atypical neural activation in areas like the left temporo-parietal cortex (Gabrieli, 2009; Shaywitz & Shaywitz, 2003). This impairment in processing phonological feedback impairs the development of fluent reading skills, as learners struggle to correct and adjust their reading strategies based on the feedback they receive from the text.

Similarly, dyscalculia impacts the ability to understand and manipulate numbers, and is associated with differences in the development of brain regions related to numerical processing, particularly the angular gyrus and the intra-parietal sulcus (Butterworth, 2010; Price et al., 2007). This deficit makes it difficult to learn from mistakes and develop effective strategies for numerical tasks.

Autism spectrum disorders (ASD) is also linked to learning challenges. Individuals with ASD may experience significant difficulties in social interaction, communication and repetitive behaviour, which affects their learning. One of the core deficits in ASD is the impaired ability to process social feedback, which is essential for learning social norms and communication skills (Baron–Cohen, 2000) (Baron-Cohen et al., 2000).

Attention deficit hyperactivity disorder (ADHD) is characterized by difficulties with attention, hyperactivity and impulsivity. These symptoms often disrupt the ability to maintain focus and control impulses, leading to challenges in academic settings (Barkley et al., 2006). One of the critical cognitive deficits in ADHD is the impaired processing of feedback, particularly in adjusting behaviour based on negative feedback (Luman et al., 2010). Individuals with ADHD may struggle to use feedback effectively to modify their behaviour, leading to repeated errors and difficulties in sustaining attention on learning tasks.

Overall, each of these conditions demonstrates how impairments in feedback processing can restrict the learning process, not only in specific areas such as reading or maths but also in general cognitive adaptation and flexibility. Feedback is essential for "learning to learn," as it allows individuals to refine their strategies, adapt to new challenges, and improve over time. When the feedback mechanisms are disrupted, individuals face greater challenges in learning to learn. By understanding how feedback processing is disrupted in these conditions, we can better appreciate the mechanisms that enable learning to learn and identify therapeutic interventions that could enhance feedback integration in both healthy and clinical populations.

V. The Brain Training business

The Brain Training encompasses a variety of structured exercises designed to enhance cognitive functions such as memory, attention, executive function, and problem-solving skills. This approach has gained popularity over the past few decades, driven by the promise of improving mental acuity/sharpness and potentially combatting age-related cognitive decline. The concept hinges on the idea that, like muscles, the brain can be strengthened through regular, targeted exercises that promote neuroplasticity. These exercises can be delivered through traditional methods, such as puzzles and memory games, or via digital platforms, including specialised software and mobile applications. Brain Training could have several applications.

Cognitive decline is a natural part of aging but it can also signal conditions like dementia and mild cognitive impairment (MCI). Brain Training has been explored as a non-pharmacological intervention to slow or counteract these declines. For example, Corbett and colleagues, developed a 6-month online Brain Training program for adults over 60, and showed improvements in daily living activities comparable to pharmacological treatments for dementia (Corbett et al., 2015). However, the study's limitations, such as focusing on participants with higher education levels, suggest that more inclusive and reproducible research is needed. Similarly, Ball and colleagues, demonstrated improvements in memory and reasoning skills in older adults (Ball et al., 2002) while Jaeggi and colleagues found that complex working memory tasks could enhance fluid intelligence in young adults (Jaeggi et al.,

2008). However, other studies failed to replicate the effect highlighted in Jaeggi's study, questioning the reproducibility of these results (Melby-Lervåg & Hulme, 2013a, 2013b; Redick et al., 2013).

Individuals with attention deficit hyperactivity disorder (ADHD) often struggle with executive functions, particularly working memory. Traditionally treated with psychostimulant medications, recent research has explored non-pharmacological interventions involving working memory training. Holmes and colleagues, found that such training significantly improves working memory in children with ADHD, sometimes surpassing the effects of medication (Holmes et al., 2010).

While brain training holds promise, there are significant limitations and potential misapplications. One of the main challenges is the "transfer effect"—the extent to which improvements in trained tasks generalise to untrained tasks and real-life situations. For example, a meta-analysis by Karbach and Verhaeghen indicated cognitive benefits in older adults following executive control and working memory training (Karbach & Verhaeghen, 2014). However, other studies, such as Owen and colleagues who conducted a large-scale study with over 11.000 participants, show that these improvements are often task-specific and may not translate to broader daily-life cognitive functions (Owen et al., 2010). The durability of these benefits is also debated; some research, like that by Melby-Lervåg and Hulme, suggests that cognitive gains may diminish over time without continuous training, raising questions about the long-term efficacy of these interventions (Melby-Lervåg & Hulme, 2013b). Additionally, individual differences such as age, baseline cognitive abilities, and the type of cognitive training program can significantly influence the outcomes, making it challenging to establish universal guidelines for cognitive training interventions. Finally, the rise of the commercial brain training industry has faced criticism for overstating the benefits of cognitive training programs. For example, the Federal Trade Commission has taken action against companies for misleading consumers, emphasising the need for rigorous scientific validation and ethical marketing practices in this field (Federal Trade Commission, 2016).

Overall, Brain Training has potential applications in mitigating age-related cognitive decline and enhancing cognitive functions in conditions like ADHD. However, its effectiveness varies, and the field is marred by limitations regarding the generalization and longevity of cognitive

improvements. The commercialization of Brain Training also raises ethical concerns, underscoring the importance of basing claims on robust scientific evidence.

To conclude, even if the concept of Brain Training was promising for several conditions, a larger work on defining the neural mechanisms that underlie the learning to learn process is necessary before reaching the commercialisation of an efficient method.

Chapter 2. Neural basis of feedback in learning and learning to learn context

I. General neural basis of feedback and learning

Feedback is a critical component in the learning process, enabling individuals to assess their actions, adapt to new information, and refine their behaviour to optimise outcomes. The neural basis of feedback processing involves multiple brain regions, each playing a distinct role in detecting, evaluating, and responding to feedback, whether positive or negative. These regions include the midcingulate cortex (MCC), prefrontal cortex (PFC), basal ganglia, cerebellum, insula, orbitofrontal cortex (OFC), and parietal cortex, forming an integrated network that supports cognitive control, decision-making, and motor coordination. Each of these regions are involved in the processing of specific types of feedback, from motor to sensory and cognitive ones.

Sensorimotor feedback relies particularly on the cerebellum, an area traditionally associated with motor coordination. The cerebellum is involved in the fine-tuning of motor actions, using feedback to correct errors in real-time and improve the precision of movements (Koziol et al., 2014). The parietal cortex also plays a significant role in sensorimotor feedback processing, through the integration of sensory information. It is involved in processing feedback related to spatial and motor tasks, helping to guide movements based on sensory feedback (Andersen & Cui, 2009). The parietal cortex interacts with the PFC and motor regions to adjust actions in response to feedback, especially in tasks that require precise motor control.

Other areas, like the insula or the OFC, are involved with sensory feedback. The insula, deeply embedded within the cerebral cortex, is involved in emotional awareness and sensorial information integration. It plays a significant role in processing internal body signals and is particularly active during the evaluation of errors and feedback, especially when feedback is perceived as negative or emotionally significant (Ullsperger et al., 2010). The insula modulates the emotional impact of feedback, influencing how individuals respond to errors and adjust

their behaviour accordingly. The OFC is essential for processing rewards and making decisions based on the expected value of outcomes. It is involved in updating the value of different options based on feedback and is particularly important for adjusting behaviour when the expected reward changes (Bechara et al., 2000). Overall, the OFC integrates sensory information with reward signals to guide decision-making.

Finally, in this project we are particularly interested in the impact of cognitive training on the feedback processing, thus our main interest is in areas that are linked to the cognitive aspect of the feedback. For example, MCC activity seems to be sensitive to the volatility of the environment and to encode values and prospective information useful for adaptive behaviours (Kolling et al., 2016). It could be implicated in evaluating the broader implications of errors for goal-directed behaviour, including the need for strategic adjustments to optimise future performance (Shenhav et al., 2013). Overall, the MCC is essential for integrating different information types over time to learn and adapt to changing environments (Procyk et al., 2021). Then, the PFC, especially the dorsolateral prefrontal cortex (dLPFC), is responsible for maintaining and manipulating information in working memory, which should be crucial for applying feedback to improve task performance over time (Miller & Cohen, 2001). The PFC is activated during tasks requiring high levels of cognitive control, especially when feedback is critical for adjusting behaviour and optimising performance (Ridderinkhof et al., 2004). Finally, the basal ganglia, particularly the striatum, play a pivotal role in reinforcement learning, helping to encode the value of different actions based on the feedback received (Schultz, 2016). This process is central to the concept of reward prediction error (RPE), which is the difference between expected and actual outcomes. Dopaminergic neurons in the basal ganglia signal RPE, guiding learning by reinforcing behaviours that lead to positive outcomes and discouraging those that do not (Schultz, 1998).

II. Focus on the LPFC-MCC network

The PFC is one of the most evolved and complex regions of the primate brain (Semendeferi et al., 2001; Smaers et al., 2017; Wise, 2008), playing a central role in high-order cognitive processes such as decision-making, executive function, and behavioural

adaptation. In primates, there are two groups of PFC areas: the agranular areas, which have homologues in other mammals, and the granular areas which have no homologue (Passingham, 2021). The PFC contains distinct subregions such as the MCC and the dLPFC (Preuss & Wise, 2022; Vogt, 2016; Vogt et al., 2003); see **Fig. 1**. These subregions are crucial for various aspects of cognitive control and are highly interconnected with other brain regions, enabling the integration of sensory, motor, and emotional information.

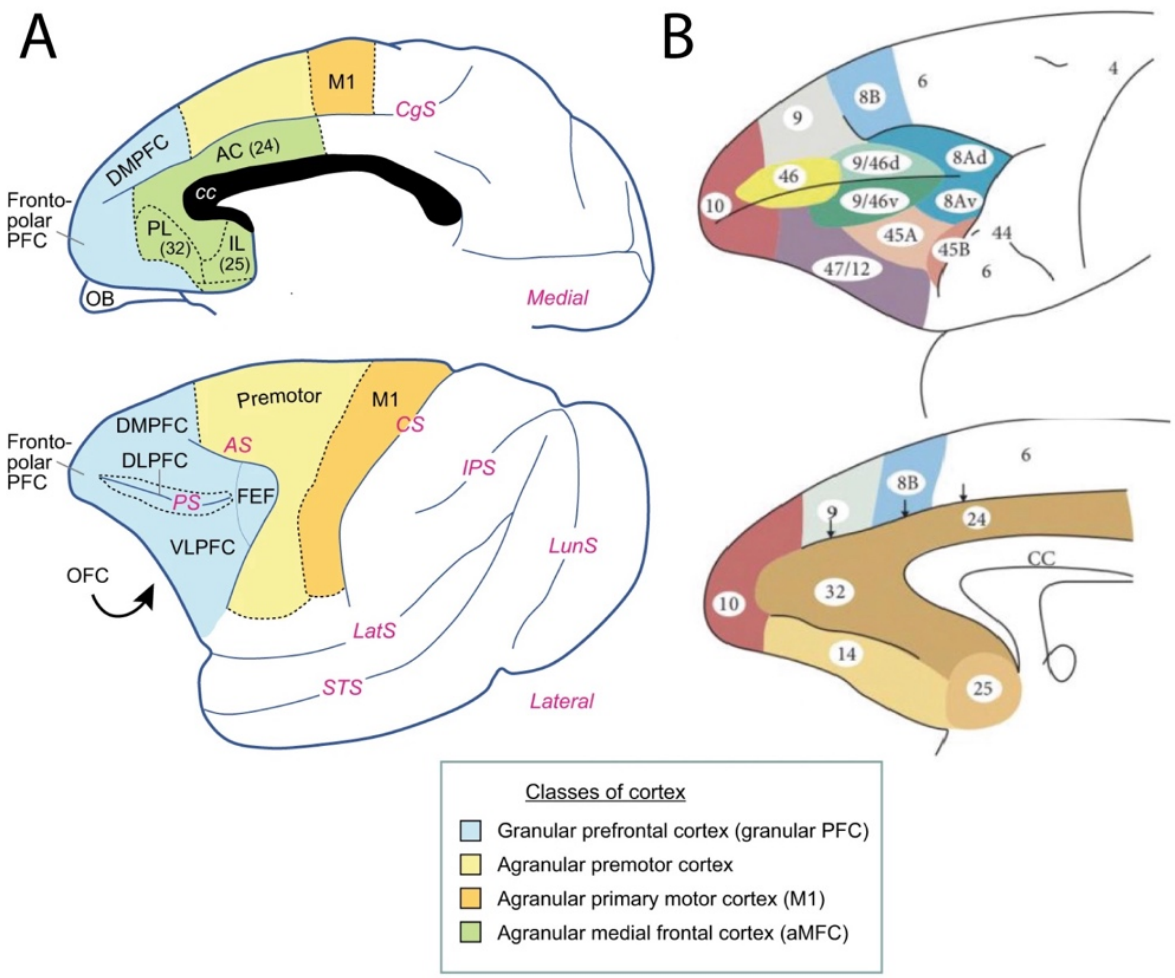

Figure 1. Prefrontal cortex organization in macaques. A) Granular and agranular parts of the PFC extracted from Preuss & Wise, 2022. B) Cytoarchitecture maps of the medial and lateral PFC extracted from Passingham 2021. Figure reproduced from Petrides and Pandya 1999.

a) The Midcingulate Cortex

The MCC is a distinct and heterogeneous region within the agranular mPFC, located posterior to the anterior cingulate cortex. It can be subdivided into the anterior MCC and posterior MCC, each with unique cytoarchitectural properties (Vogt, 2009; Vogt et al., 1995). The MCC encompasses the cingulate motor areas (CMAs), which are critical for motor planning and execution (**Fig. 2**). These CMAs include the rostral CMA, dorsal CMA, and ventral CMA, which are organised along a rostro-caudal gradient and represent different body parts for motor control (Amiez & Petrides, 2014; Dum & Strick, 2002).

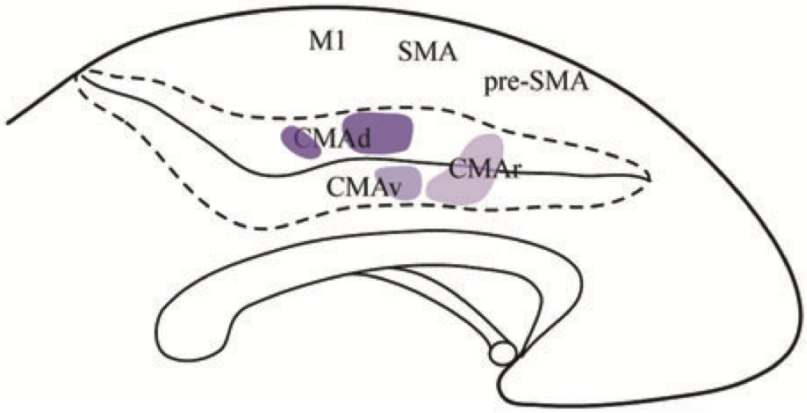

Figure 2. Motor cingulate regions in macaques. Figure extracted from Amiez & Petrides 2014.

The MCC has robust connections with various brain regions, including the PFC, premotor cortex, primary motor cortex, supplementary motor area, and insula (Carmichael & Price, 1995; Morecraft et al., 2012). These connections facilitate the integration of sensory and motor information, supporting complex cognitive and motor functions. Notably, the MCC is also connected to the superior temporal gyrus, superior temporal sulcus, parietal cortex, and the amygdala, suggesting its role in integrating cognitive and emotional information for adaptive behaviour.

Functionally, the MCC is pivotal in executive functions, particularly in performance monitoring, error detection, and decision-making. It plays a significant role in detecting and evaluating errors, with error-related signals such as the error-related negativity (ERN) being prominent in this region (Holroyd & Coles, 2002). The MCC is also involved during so-called conflict tasks, with a potential role in facilitating adjustments in behaviour to optimise

performance, although data on these aspects are contradictory (Burle et al., 2008; Hochman et al., 2014). This is especially relevant in tasks requiring motor preparation and execution, where the MCC coordinates motor planning through its connections to the CMAs (Amiez et al., 2019). Moreover, research in macaques has shown prominent MCC activity for goal-directed behaviour and performance monitoring, including error prediction and behavioural adaptation in response to feedback (Procyk et al., 2016; Quilodran et al., 2008).

b) The Lateral Prefrontal Cortex

The LPFC covers the lateral surface of the frontal cortex and is divided into dorsal and ventral regions, known as the dorsolateral prefrontal cortex (dLPFC) and ventrolateral prefrontal cortex (vLPFC), respectively. The dLPFC, which includes cytoarchitectonic areas 8, 9/46, and 46, is particularly well-developed in primates (Garey, 1999; Preuss & Wise, 2022) and plays a key role in higher-order cognitive functions (Petrides & Pandya, 1994, 2002). The LPFC in non-human primates like macaques shows a similar cytoarchitectural organisation to that of humans, with only a few differences in sulcal patterns and the relative expansion of certain areas, such as areas 10, 46, and 9, which are more prominent in humans and great apes (Amiez et al., 2023).

The network in which the dLPFC is embedded suggests important roles in the integration of multimodal sensory inputs and coordination of complex cognitive processes. It has strong structural connections with the superior temporal sulcus, frontal eye fields, lateral intraparietal cortex, motor cortex, premotor cortex, supplementary motor area, and MCC (Borra et al., 2008; Morecraft et al., 2012; Petrides & Pandya, 1999). This connectivity profile enables the dLPFC to access processed sensory information, memory systems via connections with the retrosplenial cortex and hippocampus, and motor outputs, supporting its role in cognitive control, working memory, and behavioural planning.

The dLPFC is central to executive functions such as working memory, cognitive flexibility, and decision-making. It is involved in monitoring, manipulating, and integrating information necessary for behaviour planning and execution (Miller & Cohen, 2001; Tanji & Hoshi, 2008). In macaques, the dLPFC plays a crucial role in cognitive control, particularly in

tasks requiring the maintenance and manipulation of information over time, which are essential for adaptive decision-making (Petrides, 2005).

While the general organisation and functions of the MCC and LPFC are conserved across primates, including humans and macaques, there are notable differences. In humans, the expansion of the frontal lobe, particularly the LPFC, has led to more pronounced capabilities in abstract thinking, social cognition, and language (Semendeferi et al., 2011; Teffer & Semendeferi, 2012). Additionally, the presence of secondary sulci, such as the paracingulate sulcus, which is more frequently found in humans and great apes, is associated with the expansion and increased complexity of the PFC (Amiez et al., 2019). These anatomical differences likely contribute to the enhanced cognitive abilities observed in humans compared to other primates.

The MCC and LPFC are integral components of the frontal cortex, each contributing uniquely to the regulation of cognitive functions in primates. The MCC, with its role in performance monitoring, error detection, and motor planning, and the LPFC, with its involvement in cognitive control and decision-making, form a network that is essential for learning and learning to learn processes. In fact, this network seems to have a specific organization. Badre & D'Esposito showed a rostro-caudal organization in the frontal lobe with the more rostral areas supporting more abstract representations and more complex rules (Badre & D'Esposito, 2009). This rostro-caudal organization was also highlighted precisely between the LPFC and the MCC for motivating and selecting behaviours (Kouneiher et al., 2009). These studies support the theory of a rostro-caudal anatomo-functional organization of the frontal networks contributing to a hierarchy of cognitive-motor controls (Duncan et al., 2020).

c) Neural basis specifications in learning to learn

Learning to learn involves the brain ability to refine its learning strategies over time, leading to more efficient and adaptable behaviour. This process relies heavily on the LPFC (Browning et al., 2007) and also implies the performance monitoring in the MCC (Procyk et

al., 2016). These regions are crucial for integrating feedback across multiple time scales, allowing for the generalisation of learned strategies to new contexts.

The LPFC has been shown in macaques to be critical for learning to learn. Its role has been linked to the capacities of the prefrontal regions to integrate information across extended time periods, which is essential for the development of the performance strategies that lead to accelerated learning. Browning and colleagues trained macaque monkeys on a simple discrimination learning task, and they acquired a learning set over a series of problems, showing significantly improved performance. Monkeys then received frontal-temporal disconnection through crossed unilateral ablation - a preparation which leaves intact regions of prefrontal and temporal cortex but abolishes any possibility of interaction between them. The effect in this context was to remove any effect of the frontal cortex on object learning processes in the temporal lobe. After frontal-temporal disconnection monkeys retained the ability to learn object discriminations, but they did so at the rate of task naïve monkeys with no learning set (**Fig. 3**). This finding suggests that while fundamental visual learning mechanisms remain intact within the temporal lobe, the process of learning to learn relies on the ability of the LPFC to interact with this information, presumably to use its ability to integrate information across time.

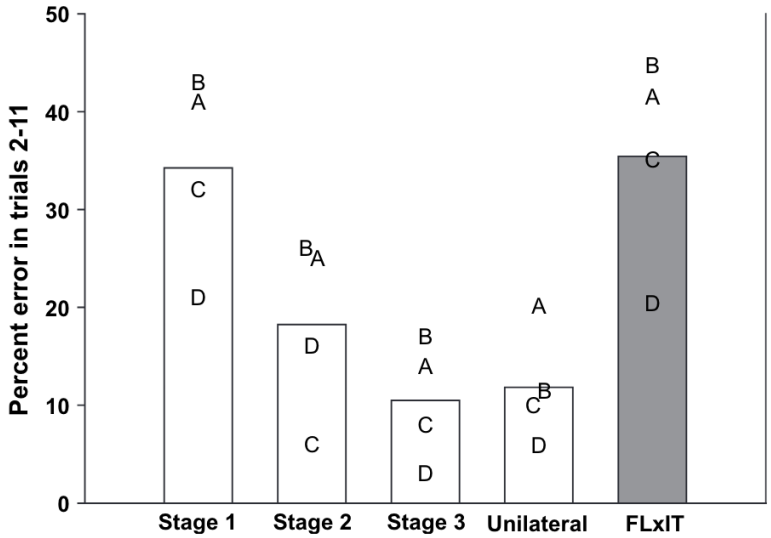

Figure 3. Fronto-temporal disconnection effect on learning and learning to learn processes. Stages 1 to 3 represent the training course. Unilateral is the control and FLxIT indicates the final step after the disconnection lesion. Figure extracted from Browning & al., 2007.

The MCC might contribute to learning to learn in the context of its roles in monitoring ongoing performance, detecting discrepancies between expected and actual outcomes, and signalling when adjustments are necessary (Procyk et al., 2016). The MCC is particularly engaged during tasks that require strategic adaptations in response to feedback, making it essential for the ongoing process of refining cognitive strategies and optimising learning efficiency. In particular in the example of the simple acquisition of learning set from discrimination learning as cited in Browning et al. above and the foundational work of Harlow, it is proposed that learning set is expressed as the formation of a prospective Win-Stay Lose-Shift strategy. In this case, outcome processing becomes no longer simply reactive ("I received a reward" or "I lost") but also brings immediate prospective information ("I should change response" or "that is the response I should follow"). This of course implies a modification of the outcome responding throughout the process of learning to learn. We would hypothesise that elements of this change would be expressed in the well-studied outcome processing in MCC - perhaps in a manner analogous to the shifts in response timing that have been shown to occur as animals move from exploratory to exploitative phases of a problem-solving task as demonstrated by Quilodran et al 2008.

In addition to a specific outcome processing role, the MCC is also well established in the motivational aspects of learning, evaluating the effort required for tasks and influencing the willingness to engage in challenging activities (Shenhav et al., 2013). As described above, learning to learn is the fruit of a long, engaged learning process over multiple exemplars that allow extraction of the regularities of the task. Levels of such motivation or engagement are therefore likely to impact learning to learn success.

Moreover, advances in artificial intelligence have provided additional insights into the neural mechanisms underlying learning to learn. Doya proposed that meta-parameters in reinforcement learning could be analogous to neuromodulators in the basal ganglia, with dopamine signalling reward prediction errors, serotonin controlling action selection randomness, and acetylcholine regulating memory update speed (Doya, 2002). In this framework, the PFC, in conjunction with the MCC, could act as a meta-reinforcement learning (meta-RL) system, guiding adaptive behaviour through feedback processing (Lansdell & Kording, 2019; J. X. Wang et al., 2018). In the Wang model, the PFC does not just respond to immediate stimuli but learns how to learn by continually adjusting how it processes information

from feedback. This meta-RL process involves two levels: one at which the PFC interacts with subcortical regions, like the basal ganglia, to receive signals such as dopamine to adjust behaviour and learning, and another where the PFC monitors how the brain's responses change over time. In this way, the PFC learns to modify learning strategies across tasks, which helps in rapidly adapting to new tasks and environments. This model demonstrates how the brain efficiently implements reinforcement learning strategies to generalize across various tasks. Lansdell & Kording draw connections between machine learning approaches and biological systems, explaining that neural networks in artificial intelligence and the brain learn faster when exposed to related tasks. In this context, the PFC could serve as a meta-learner, optimizing cognitive strategies based on feedback. The PFC implements learning rules that are dynamically updated, improving both task performance and generalization to new tasks.
Khamassi and colleagues supported this idea by demonstrating that the MCC might play a crucial role in adjusting reinforcement learning parameters like exploration-exploitation balance in response to task demands (Khamassi et al., 2013). They highlighted how the MCC, in conjunction with the LPFC, monitors performance and detects errors, which is vital for guiding adaptive behaviour (Khamassi et al., 2011). Furthermore, the 2015 work by Khamassi et al. expanded on this by illustrating how the MCC role in feedback processing could optimise decision-making and behavioural flexibility in complex and changing environments (Khamassi et al., 2015).

The adjusting role of the MCC highlighted by computational work was also supported by biological lesion studies (Kennerley et al., 2006; Walton et al., 2003). Moreover, Amiez and colleagues deactivated the MCC with a pharmacological approach (muscimol) and argued that MCC contributes to the long-term regulation of reward-driven voluntary behaviours by encoding the general task values and the reward received (Amiez et al., 2006).

d) Neural changes induced by training

As discussed above, learning and learning to learn are two distinct processes, and the data suggest that they involve at least partially distinct brain areas. However, even if this distinction is really important to understand the implications of each process, their limits are

not clear-cut. Passing from initial slow and incremental learning to highly efficient learning that has benefited from a process of learning to learn is achieved by cognitive training, and the effect of this training on the PFC neural correlates has been poorly studied. Studies focused on comparing neural activity of the PFC before learning to activity after learning steps. In their earlier work, Meyer et al. provided critical insights into the neural plasticity of the PFC during cognitive tasks (Meyer et al., 2011). Their study showed that, after training on a visual working memory task, there was an increased number of PFC neurons that responded to specific aspects of the task. These findings laid the foundation for understanding how PFC neurons become tuned to task-relevant information following training, suggesting a stronger representation of learned material. Building on this work, Qi and colleagues extended these findings by investigating the decision-making processes and neural correlates in the PFC before and after learning (Qi et al., 2012). In their study, they observed a reduction in noise correlation - essentially the reduction of shared variability between neurons that do not directly contribute to task performance. This reduction was seen as a sign of increased neural efficiency after training. Additionally, they reported an enhancement in the precision of neural responses linked to task demands, implying that cognitive training enhances not just the quantity but the quality of neural responses. Subsequent work by Qi and Constantinidis expanded the scope of this research by examining cognitive tasks across multiple stages of training (Qi & Constantinidis, 2013). They found similar patterns, with an increase in task-responsive units, further reduction of noise correlation, and refinement in PFC neural activity. These studies collectively emphasize the idea that PFC neurons adapt through training by refining their responses to task-relevant stimuli, improving overall performance in cognitive tasks. More recently, Tang and colleagues provided an even more detailed look at these neural adaptations by assessing the working memory training across multiple stages (Tang et al., 2022). Their findings confirmed earlier reports of increased task-responsive units and reduced noise correlation but also introduced novel insights into the role of local field potentials (LFP) in cognitive training. They observed an increase in high-beta and low-gamma power in LFP after training, indicating that these frequency bands may play a role in reinforcing neural synchrony during task performance. This study advanced the understanding of the neural oscillations that accompany cognitive training and provided a clearer picture of the temporal dynamics of training-induced plasticity. Collectively, these studies reveal a pattern of neural

adaptation in the PFC characterized by increased task-specific neuronal responsiveness, reduced noise correlation, and changes in neural oscillations. However, while these studies provide invaluable insights into pre- and post-training differences, they often overlook the neural changes occurring during the training itself. It is necessary to address this gap by exploring how neural activity evolves across the entire learning process, rather than just comparing the beginning and end stages. This would offer a more comprehensive view of how cognitive training shapes neural circuits in real-time.

e) Feedback-related changes in LPFC-MCC network

Several studies have demonstrated how the MCC and LPFC adjust their neuronal networks and firing patterns in response to feedback during cognitive tasks. Quilodran and colleagues demonstrated that the MCC exhibits distinct neuronal activity in response to both positive and negative feedback, particularly during the transition from exploration to exploitation in monkeys (Quilodran et al., 2008). The MCC shows increased gamma-band oscillations after the first reward, signalling the end of exploration, highlighting its role in feedback-based learning and decision-making. Rothe and colleagues expanded on this by exploring the dynamic interplay between the MCC and LPFC, showing that after negative feedback, the MCC increases gamma-band synchronization, particularly during exploratory behaviour, while the LPFC shows transient gamma activity following positive feedback (Rothe et al., 2011). These findings suggest that the MCC processes feedback over extended periods, guiding long-term behavioural adjustments, whereas the LPFC rapidly integrates feedback to refine immediate strategies based on positive outcomes. Seo and Lee investigated the role of the MCC and LPFC in processing reward-based feedback during a decision-making task (Seo & Lee, 2007). They found that MCC neurons exhibit strong gamma synchronization in response to negative, unexpected feedback (particularly when outcomes were worse than expected), reflecting a reorganization of neuronal networks that facilitates error processing and behavioural adjustment. In contrast, the LPFC displayed transient desynchronized activity following feedback, particularly positive feedback, indicating a rapid recalibration of the cognitive strategy. Together, these studies highlight the differential yet coordinated roles of

the MCC and LPFC in feedback processing. The MCC engages in sustained synchronization and network reorganization to process both errors and rewards over time, facilitating long-term adjustments. In contrast, the LPFC quickly integrates feedback through transient bursts of activity, enabling immediate strategy shifts. This dynamic interaction, particularly reflected in changes in gamma-band oscillations, underscores the importance of these regions in adaptive behaviour based on feedback.

III. Event-related potentials components in feedback processing and learning

In the context of learning to learn, ERP components provide crucial insight into how the brain processes feedback, errors, and rewards. Several key components, including the error-related negativity (ERN), feedback-related negativity (fERN), error positivity (Pe), N200, and P300, are associated with distinct cognitive processes that reflect different stages of feedback evaluation and adaptation.

The ERN is a negative deflection typically observed shortly after an error is made, peaking within 100 ms. This early automatic response is associated with the detection of errors, and it primarily reflects the brain's conflict-monitoring system, located in the anterior cingulate cortex. It signals the need for cognitive adjustments to correct ongoing actions (Holroyd & Coles, 2002). Studies suggest that as individuals become more proficient at tasks, the amplitude of the ERN may increase, reflecting heightened sensitivity to errors and more effective error processing (Fu et al., 2023). Following the ERN, the Pe, a positive deflection, occurs around 200-500 ms post-error and is linked to the conscious awareness of an error. The Pe is thought to reflect the motivational significance of errors, encouraging individuals to correct their behaviour (Overbeek et al., 2005). As learners progress and become more experienced, changes in Pe amplitude can indicate shifts in how errors are consciously recognized and acted upon (Fu et al., 2023).

The fERN, an ERP component related to feedback processing, emerges 200-300 ms after feedback presentation. The fERN is larger in response to negative feedback than positive feedback, indicating its role in reinforcement learning and the evaluation of feedback for future behavioural adjustments (Fu et al., 2023; Holroyd & Coles, 2002). This negative component

plays a critical role in learning contexts where feedback is used to guide decision-making and adapt behaviour. The P300, a positive deflection which occurs around 300-500 ms post-feedback, is associated with attentional allocation and memory updating. The amplitude of the P300 often reflects how much cognitive effort is needed to process the feedback. In learning contexts, the P300 amplitude tends to decrease as learners become more familiar with tasks, indicating a shift from active attention to more automatic processing (Fu et al., 2023; Polich, 2007). The N200, typically negatively peaking 200-350 ms after a stimulus, is linked to cognitive control and conflict monitoring. It is more prominent in tasks that require response inhibition or adaptation to new rules, such as during the early phases of learning. Over time, reductions in N200 amplitude can suggest that learners are becoming more efficient at detecting and resolving conflicts as they acquire greater task proficiency (Folstein & Van Petten, 2008; Fu et al., 2023).

The interaction of these components reveals the brain's dynamic response to feedback throughout the learning process. As tasks become more familiar, learners exhibit a transition from effortful processing, reflected in larger P300 and N200 amplitudes, to more automatic and efficient responses. Over the course of training, shifts in ERP components like the ERN and Pe demonstrate changes in error sensitivity and conscious error awareness, further refining learning strategies (Fu et al., 2022).

However, the ERN has been shown to reflect more than just error detection. Vidal et al. (2000) explored the possibility that the ERN might not be exclusive to errors by examining EEG data from simple reaction time tasks (Vidal et al., 2000). They found that small ERN-like components could be observed even on correct trials, albeit with lower amplitude compared to error trials. These findings suggest that the ERN may represent a broader response-monitoring process that is triggered not only by errors but also by conflict or uncertainty during correct responses. Vidal and colleagues further investigated this phenomenon by analyzing ERN activity on correct trials in more detail, using a task where participants had to respond to stimuli under high time pressure (Vidal et al., 2003). They confirmed the presence of small ERN during correct trials, thus supporting the idea that the ERN reflects a general response evaluation process rather than being specific to error detection alone. This suggests that the ERN is involved in continuously monitoring performance to optimize future actions, not just in signalling when an error occurs. Extending this idea, Bonini and colleagues proposed that

error processing follows a hierarchical organization, with the supplementary motor area (SMA) playing a leading role in monitoring both correct and incorrect actions (Bonini et al., 2014). Using intracerebral recordings in humans, they demonstrated that the SMA produces early signals in response to both correct and incorrect actions, which are subsequently followed by activation in the MCC for errors. This hierarchy suggests that the ERN may be part of a broader system of action monitoring, where both the SMA and the MCC are involved in evaluating ongoing actions and determining the need for cognitive adjustments. The SMA's early involvement highlights its role in initiating the evaluation process before error-specific signals emerge from the MCC. These findings suggest that the ERN is not just a signal for error detection, but rather a component of a hierarchical, distributed system for monitoring all actions.

Research in non-human primates has provided critical insights into the neural basis of feedback and error processing through ERP. Vezoli and Procyk demonstrated the presence of feedback-related potentials (FRP) in macaque monkeys during trial-and-error learning tasks (Vezoli & Procyk, 2009). They recorded neural activity in the frontal cortex and found that, as in humans, the FRP in monkeys was stronger following negative feedback compared to positive feedback. This observation is consistent with human findings where the fERN reflects the brain's sensitivity to negative feedback, a key mechanism in reinforcement learning (Holroyd et al., 2002). Vezoli and Procyk's work provided direct evidence that monkeys exhibit similar neural responses to feedback, thus supporting the idea of conserved feedback-processing mechanisms across species. Building on this, Wilson and colleagues focused on the role of dopamine in modulating these FRP (Wilson et al., 2016). By inducing progressive dopamine lesions in macaque monkeys and recording their neural responses during feedback, they observed that the ability to differentiate between positive and negative feedback through FRP gradually diminished as dopamine levels decreased, yet critically the monkeys maintained their ability to use feedback to do perform the task near optimally. The modulation with dopamine levels is consistent with human studies showing that dopamine plays a crucial role in modulating the ERN and fERN, as these potentials are sensitive to dopaminergic modulation, particularly in tasks involving reward prediction errors (Holroyd et al., 2002; Jocham & Ullsperger, 2009). Yet the absences at the end of the study of an ERP that differentiates positive and negative feedback, despite the monkeys' continued ability to

successfully use feedback to perform the task, questions the direct link between the FRPs and feedback processing. Further work by Godlove and colleagues provided direct evidence of an error-related ERP component in monkeys (Godlove et al., 2011). Using a stop-signal task, they recorded ERP following errors and found that these signals closely resembled the human ERN in terms of timing and scalp distribution (Gehring et al., 1993). The study demonstrated that monkeys, like humans, generate neural signals that reflect error processing, and these can be captured using ERP techniques. Finally, Sajad and colleagues provided more detailed insights into the neural circuits generating these error-related ERP components by focusing on the supplementary eye field (SEF). They found that error-related signals in the SEF were strongest in layers 2/3, and this activity was closely linked to behavioural adjustments, such as changes in reaction time after errors (Sajad et al., 2022). This aligns with human findings that show error-related brain activity is often linked to subsequent behavioural adjustments in tasks requiring cognitive control (Holroyd et al., 2002). By mapping these neural circuits, the study connected the cellular origins of error-related signals with the broader ERP framework, showing how specific cortical layers drive error-monitoring processes visible in both localized neural activity and scalp-recorded ERP. Together, these studies provide strong evidence that monkeys exhibit ERP components like FRP (or fERN) and ERN that closely resemble those found in humans. They explicitly showed that feedback and error-related potentials are conserved across species, with dopamine playing a critical modulatory role.

Chapter 3. Systems and mechanisms of learning and habit formation

Understanding the neural systems and mechanisms that underpin learning and habit formation is essential for understanding how individuals adapt their behaviour in response to changing environments. These processes are not only fundamental to acquiring new skills but also to the concept of learning to learn. The neural mechanisms involved in both goal-directed actions and automatic habits, as well as the interplay between reinforcement learning, cognitive control, and habit formation are central elements of learning and learning to learn processes.

Learning processes are governed by neural networks that balance the need for flexibility and efficiency. One of the primary distinctions within these systems is between goal-directed behaviours, which are flexible and outcome-oriented, and habits, which are more rigid and stimulus-driven. Goal-directed behaviour relies on an evaluative process where the potential outcomes of different actions are considered before a decision is made. This process is supported by the medial PFC and the dorsomedial striatum which are crucial for maintaining and updating information related to goals and expected outcomes (Killcross & Coutureau, 2003). In contrast, habitual behaviour, which emerges through repeated reinforcement, is controlled primarily by the dorsolateral striatum. Habits are triggered by specific environmental cues and operate with minimal conscious thought, enabling responses that are more efficient but less adaptable. Once a behaviour is habitual, it becomes less sensitive to changes in outcome value, a phenomenon often referred to as "habitual insensitivity" (Coutureau & Killcross, 2003).

Reinforcement learning (RL) provides a computational framework for understanding how goal-directed and habitual behaviours are learned and expressed. In RL, behaviour is shaped by the outcomes of past actions, with two main strategies emerging: model-based and model-free learning (Daw & O'Doherty, 2014; Sutton & Barto, 2014). Model-based learning, which aligns with goal-directed behaviour, involves constructing and using a model of the environment to predict the outcomes of actions. This type of learning is computationally

intensive but allows for greater adaptability, as the agent can simulate various scenarios before acting. The dLPFC plays a key role in supporting model-based learning by integrating information about potential future rewards and guiding decision-making accordingly. In contrast, model-free learning corresponds more closely to habitual behaviour. In this strategy, actions are selected based on the accumulated value of past rewards, without the need for a detailed model of the environment. This approach is less flexible but more efficient, allowing for the rapid execution of well-learned behaviours. The dorsolateral striatum and basal ganglia are central to this process, as they encode the value of actions based on past reinforcement and drive the formation of habits through repeated practice and reward (Daw et al., 2005).

The transition from goal-directed to habitual behaviour can be seen as a shift from controlled to automatic processes. This transition is essential for optimising cognitive resources, allowing the brain to delegate routine tasks to automatic systems while reserving cognitive control for more complex, non-routine actions. The supervisory attentional system (SAS) proposed by Norman and Shallice provides a theoretical framework for understanding how the brain manages this balance (Norman & Shallice, 1986). The SAS, situated in the prefrontal cortex, is responsible for overseeing tasks that require conscious control and decision-making. In contrast, routine actions that have become habitual are managed by contention scheduling mechanisms, which operate in a more automatic fashion and involve subcortical structures like the basal ganglia. However, it should be noted that robotics works pointed out an alternation between the goal-directed step and the habitual behaviour one rather than a clear distinction (Chatila et al., 2018; Khamassi & Humphries, 2012). Moreover, electrophysiological components such as specific event-related potentials were proposed as markers of goal-directed versus habitual control (Yousuf et al., 2019).

The cognitive control is further explained by the Expected Value of Control (EVC) theory, which suggests that the brain allocates cognitive resources based on a cost-benefit analysis of exerting control. According to Shenhav and colleagues, the PFC evaluates the expected value of different actions, considering both the potential rewards and the cognitive effort required (Shenhav et al., 2013). This theory helps to explain how the brain decides when to engage in goal-directed behaviour versus relying on habitual responses, optimising performance by prioritising actions that are likely to yield the highest payoff with the least effort.

Another significant model that connects these processes is the Collins and Koechlin model, which describes how the PFC manages multiple behavioural strategies simultaneously (Collins & Koechlin, 2012). According to their model, the PFC is organised hierarchically, with different levels responsible for managing various types of control processes. The higher levels of this hierarchy are involved in goal-directed actions, managing abstract strategies and adapting to new information, while the lower levels are responsible for the execution of more concrete, habitual behaviours. This hierarchical organisation allows for the flexible switching between strategies depending on the context and the demands of the task, which is crucial for both learning new behaviours and refining existing ones.

Overall, the systems and mechanisms underlying learning and habit formation are deeply interconnected, involving a dynamic interplay between goal-directed and habitual processes. The brain's ability to learn and adapt is based on its capacity to balance flexibility with efficiency, employing cognitive control when necessary and relying on automatic processes for routine tasks.

Chapter 4. Project overview

I. Objectives

Historically many studies of electrophysiological recordings in awake behaving non-human primates used an acute preparation because of the lack of technical capacities to leave electrodes in the brain for a long period of time and obtain chronic recordings. In recent years the technology for consistent chronic recordings with good yield has developed, and this now permits, to some extent, longitudinal neurophysiological recordings in awake animals. In these studies, however, the implantation surgery is generally performed after extensive training of the subject on the task in hand. This approach is logical and justifiable - it means that recordings can be made during a period of stable behaviour during a learning plateau - essential particularly when the recordings are acute and therefore not comparable from day to day. But this does mean that the very first stage of learning in any process is almost never studied. Therefore, even for a well-described field such as learning, we lack some essential information about how well-studied systems and well-established neural correlates emerge at the very beginning. There is also a huge amount of literature about how to use the feedback to learn efficiently as it is one of the key processes of learning. In contrast, there are relatively few recordings, above all in the primate literature, that follow the process of learning to use cognitive feedback for the very first time, and no longitudinal studies on the neural basis of the emergence of learning to learn from an initial naïve state. The principal aim of this thesis project was to focus on this ignored early stage of learning and describe the implementation of the use of feedback for learning and the evolution through the different steps leading to the learning to learn level. We chose to focus on two areas known to be connected together, the MCC and the LPFC. Beyond their well-established roles in outcome processing and adaptive behaviour, these two regions are directly (in the case of LPFC, Browning et al 2007) and very probably (in the case of MCC, see discussion above) heavily involved in the network changes needed to implement learning to learn over an extended period of cognitive training. We therefore chose a well-known and simple cognitive task of object discrimination learning, which was fundamental to the early description of learning to learn processes in the form of learning

set (Harlow, 1949), in order to have an easy and clear distinction between the learning and learning to learn processes. To our knowledge we are the first to record frontal neural activity throughout the learning set formation described in this task.

The experimental part of this thesis employed a multi-methodological approach to explore the neural mechanisms of learning to learn. First, a resting-state MRI (rsMRI) study was conducted to investigate the functional connectivity between the MCC and LPFC, providing a detailed, fine-grained analysis of their rostro-caudal organization. Next, a detailed behavioural analysis was carried out to elucidate the learning strategies employed by the monkeys. By comparing their behaviour with previous similar studies, we were able to identify key behavioural markers and factors that could influence the learning process. This analysis served as a reference for tracking the progression of learning strategies over time. The electrophysiological component of the study was divided into three parts. The first involved analyzing event-related potentials (ERP) focused on two types of feedback: positive and negative. This allowed us to assess changes in local field potentials (LFP) as learning progressed. A peak analysis was conducted for each type of feedback, along with an examination of the signal differences between them. Additionally, we analyzed sorted single-unit activity to explore whether neural changes at different scales were coherent or correlated. The second focus was on functional connectivity between brain areas and within the antero-posterior axes of each area. This was achieved using various measures, including coherence, amplitude envelope correlation, phase-locking value, and Granger causality, providing a detailed understanding of how different regions of the brain interact during learning. Finally, the impact of motivation on LFP learning markers was assessed, aiming to separate the effects of motivation from the learning process itself. This analysis helped clarify whether changes in neural activity were driven by learning or by motivational factors.

Overall, we divided the experimental part of this project on different sub-objectives:

1) Defining precisely the pattern of functional connectivity between our two areas of interest
2) Describing the learning pattern of our monkeys, comparing it with previous studies and highlighting the impact factors present in our specific cognitive design

3) Studying the evoked responses to feedback at different scales (local-field potentials and sorted single-units scales)
4) Tracking changes of functional connectivity across learning
5) Assessing the impact of the motivation on evoked responses to feedback

II. Multi-scale approach

In this thesis, a multi-scale approach was central to investigating the neural dynamics underpinning learning, particularly within the LPFC-MCC network, which plays a crucial role in cognitive control and decision-making. By combining resting-state magnetic resonance imaging (rsMRI) and electrophysiological recordings, we aimed to bridge the gap between large-scale brain network interactions and the fine-scale neural dynamics that evolve throughout the learning process.

Resting-state MRI offered a macroscopic view of brain connectivity, enabling us to assess functional networks through spontaneous fluctuations in the BOLD signal. This approach allowed us to identify the functional specificity of the LPFC-MCC network in the resting state, providing a foundational map of connectivity that we used to guide our subsequent electrophysiological analyses.

The electrophysiological recordings, which included local field potentials (LFP) and single-unit activity, were crucial for examining neural activity at a finer resolution. LFPs reflect the collective activity of neuron populations, shedding light on oscillatory patterns and synchrony within brain regions. Meanwhile, single-unit recordings provided the most detailed insight into individual neuron firing patterns, allowing us to explore how neurons within the LPFC and MCC respond to learning tasks.

By employing this multi-scale approach, we could capture neural changes across both individual neurons and larger neural populations, enabling us to form a more comprehensive view of how learning unfolds in the brain. This integration of rsMRI and electrophysiology was particularly suited for studying complex brain regions like the LPFC and MCC, as it allowed us to explore both the large-scale functional connectivity and the micro-level neural dynamics involved in learning. This method also helped mitigate the risk of being overly specific or biased

toward particular neural mechanisms, thus providing a holistic understanding of learning and learning to learn processes.

III. Neural correlates and cognitive task

In our project, the focus on neural correlates of learning is key to understanding the specific processes that underlie adaptive behaviour in the LPFC-MCC network. Unlike general approaches that examine large brain areas or global network changes, this study targets precise neural signatures linked to distinct stages of learning. The goal is to uncover how dynamic changes at the neuronal level translate into specific behavioural adaptations. By studying the neural correlates, we aim to isolate the specific activity patterns associated with particular learning mechanisms like feedback processing. The LPFC and MCC are regions known to be involved in multiple cognitive processes, such as task-switching, error monitoring, and goal-directed actions. Therefore, dissecting their role in learning requires a fine-grained analysis to distinguish between different cognitive operations. Our approach combines electrophysiological data, which captures neural activity at the level of individual neurons and local populations, with functional connectivity measures that reveal how these regions communicate and coordinate together during learning. This dual approach enables us to focus specifically on the neural dynamics that underpin learning, while minimizing the risk of broad, non-specific analyses that might miss key task-related neural activity. By integrating both local neuronal activity and larger-scale network interactions, we can gain a more detailed understanding of how neural circuits adapt during the learning process, ensuring that the findings remain closely tied to the cognitive mechanisms being studied.

By investigating these neural correlates, the project aims to highlight the specificity of neural processes in learning. This will not only provide insights into the fundamental neurobiological mechanisms of learning but also offer potential applications for understanding and improving learning in pathological conditions, where these processes are disrupted.

GENERAL MATERIALS AND METHODS

I. Subjects

Two female rhesus monkeys (*macaca mulatta*) were assessed in this study: monkey B 13 years old weighing 7kg at the start of the study, and monkey I 8 years old weighing 8kg. All procedures followed the European Community Council Directive (directive 2010/63/UE) (Ministère de l'Agriculture et de la Forêt, Commission nationale de l'expérimentation animale) and were approved by the local ethical committee (Comité d'Ethique Lyonnais pour les Neurosciences Expérimentales, CELYNE, C2EA #42) under references APAFIS#14704 and APAFIS#44461.

II. Tasks

Prior to implantation and recordings, monkeys were habituated to the testing procedure, brought to the recording box, and habituated to the touchscreen and the delivery of rewards. In contrast to most electrophysiological recording studies, however, monkeys were not extensively trained on a cognitive task prior to recordings. Instead, we recorded throughout the process of task acquisition.

a) Baseline task

Prior to teaching the monkeys any cognitive operations, we sought to record from a baseline task in which the motor and reward-based operations were common to the subsequent cognitive tasks, but there was little classical cognitive requirement (**Fig. 4**). The aim is to characterise frontal neurophysiological responses prior to the formal cognitive training, providing a neural dynamic baseline. As such the task requires a simple motor action for the obtention of reward, to train the monkey to interact with the touch screen and take the liquid reward. Monkeys had to learn to first touch and maintain hand fixation on a "lever" stimulus on the touchscreen (500 to 1000 ms). This lever stimulus, procedure and duration was common to all subsequent tasks - it provides a signal that the animal has decided to

engage in another trial, and provides a stable pre-trial analysis period where there is an element of behavioural control because hand fixation must be maintained. After validating the lever, monkeys then had to touch an abstract image and maintain hand fixation (300 to 700ms) to obtain a reward. The notions of choice and error are not present in this task.

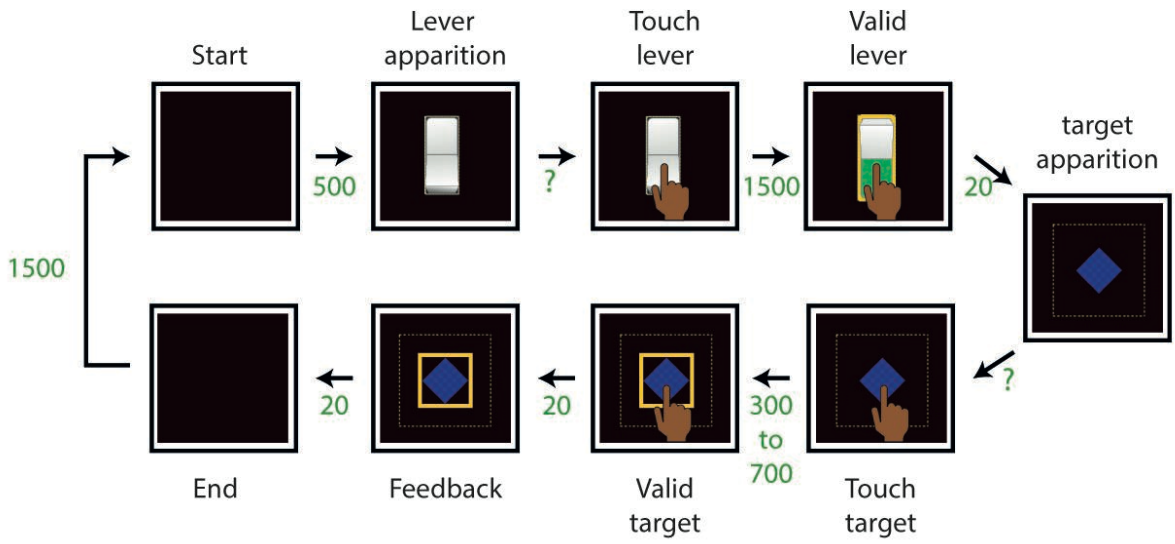

Figure 4. Baseline task timeline. The "feedback" step represents the reward delivery in correct trials and the absence of reward in incorrect trials. Numbers in green represent the timing between steps in ms. The question marks indicate that times are variable.

b) Discrimination learning task

The discrimination learning task is a central experimental paradigm in cognitive neurosciences, essential for understanding the cognitive and neural mechanisms underlying sensory perception, learning, and decision-making. It involves training subjects to distinguish between different stimuli based on specific attributes, such as visual or spatial features. This task is a classical serial 2-object discrimination, for example used across a series of important studies by Harlow (1949). In particular relevance for our study, Harlow describes that monkeys can over time acquire what he defined as a learning set. The stimuli vary along predetermined dimensions (colour, shape and spatial location). For a given problem, monkeys are presented concurrently with a pair of image stimuli on the touchscreen, pseudo randomly above and to the left or right of the lever. Based on the visual object identity only one stimulus corresponds

to the correct response. Successfully touching the correct stimulus leads to positive reinforcement with liquid reward (50% diluted apple juice, 0.8 mL per reward). Incorrect responses are followed by an extended latency time before the next trial (5s for monkey B and 7s for monkey I). Monkeys perform a series of these problems on the same pair of stimuli until they reach a performance criterion for that pair of stimuli (**Fig. 5**). After this they pass to the next problem, with a new unique pair of stimuli. The progression of learning is monitored by measuring performance metrics, specifically the progression towards the learning criterion. In parallel a series of performance measures is recorded (reaction & movement time, accuracy, error & trial engagement rates). All responses are recorded through hand movements to the touchscreen. As in the baseline task monkeys need to manually maintain a lever (1000ms) in order to initiate each trial. Touch choices to the task stimuli must be maintained on the stimulus (300ms) to validate choices. The trial was finished after the validation of a stimulus or if the monkeys did not validate one within 10 seconds. This means that the monkey could change his stimuli choice if he did not hold the entire validation time.

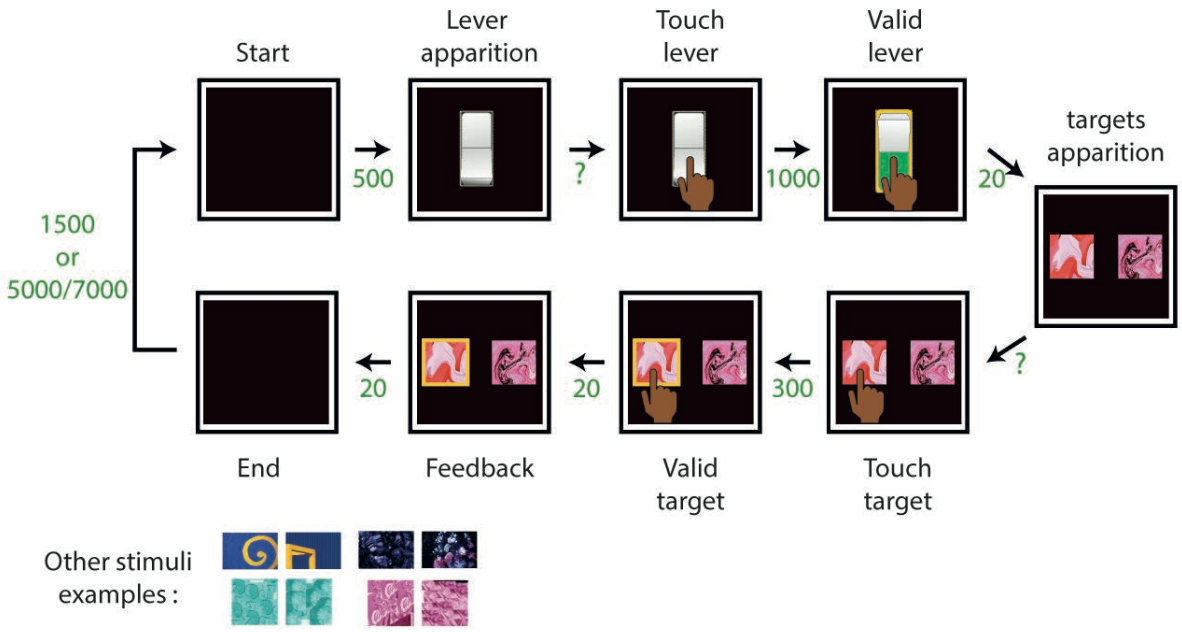

Figure 5. DL task timeline. The "feedback" step represents the reward delivery in correct trials and the absence of reward in incorrect trials. Numbers in green represent the timing between steps in ms. The question marks indicate that times are variable.

c) Reversal learning task

Reversal learning task is a pivotal experimental paradigm in cognitive neurosciences, designed to investigate cognitive flexibility, the ability to adapt behaviour in the ever-changing environment, so in response to changing reinforcement contingencies. This task allows the study of how subjects adjust their responses when previously learned associations (between stimuli and feedback) are reversed. The cognitive flexibility is assessed by evaluating adaptive responses in changing contingencies (Izquierdo, 2017). Living in a complex and uncertain environment, the ability to perform reversal learning is essential to good adaptive behaviour. In this sense, the reversal learning task imposes rather different cognitive demands on subjects than discrimination learning. Discrimination focuses on associative strength of a novel pair of stimuli, in reversal learning the classical focus has been on the suppression of prior knowledge to perform the reversal. Yet Harlow and colleagues demonstrated that a learning set can be formed to serial 2-choice reversals just as it can to the discriminations described above, and indeed it has been shown that the learning set can, in certain circumstances, transfer between reversals and discriminations (Faraut et al., 2016; Harlow & Warren, 1952; Schrier, 1966). This suggests that the cognitive operations are not so different, at least once animals have acquired a learning set. A key aim of the current study is to seek to address this through the neurophysiological basis of this transfer.

As such, and following the work of Schrier, Harlow, and Faraut, the reversal task here is designed with overarching parameters the same as the discrimination task. Monkeys are making serial 2-choice decisions between two visual stimuli. Timings, stimulus placements, criteria, and reward parameters are identical to the discrimination task. Once criterion is reached on the first problem, however, the contingencies are reversed without warning and monkeys must relearn the exact same stimuli with reversed contingencies - adapting their behaviour to new rules. The task continues as a sequence of reversals of the same 2 stimuli - so monkeys must serially relearn original stimulus-outcome rules multiple times.

III. Water control

To maintain motivation, provide similar conditions across days, and obtain sufficient numbers of trials per day for electrophysiological analysis, the monkeys were placed under a water control protocol. Prior to the start of the experiment we calculated their daily water intake over two weeks and used this average intake as a reference value to provide the minimum daily quantity of liquid consumed during the protocol. Over the initial weeks of training (and prior to recordings), animals were gradually habituated to obtain the majority of this liquid through work on the initial task, and through the fruit rewards provided after work sessions. They did not have access to water in the early morning prior to work sessions, and received post-session top-up water when necessary to bring them above their reference intake. By the time of the start of the DL task and recordings, monkeys were well habituated to this procedure and obtained more than their reference volume of liquid on the vast majority of sessions in the experiment.

IV. Surgery

We performed the implantation surgery in aseptic conditions. Monkeys received full anaesthetic along with appropriate antibiotic and analgesic treatments during and after the surgery, along with extensive monitoring. Before anaesthesia, monkeys were administered glycopyrrolate (Robinul: 0.06 mg/kg), an anticholinergic agent. After a 20-minute interval, anaesthesia was induced with an intramuscular injection of tiletamine and zolazepam (Zoletil: 7 mg/kg). Once sedated, the monkey was given antibiotic (amoxicillin, 8.75 mg/kg) for prophylaxis of infection, a steroidal anti-inflammatory (dexamethasone, 0.1 mg/kg), and an opioid agent for analgesia (buprenorphine, 0.01mg/kg). The head was shaved and an intravenous cannula put in place for intraoperative delivery of fluids (sterile saline drip, 5 mL/h/kg). The monkey was intubated, placed on isoflurane anaesthesia (1–2%, to effect, in an O2 and NO2 mix), and then mechanically ventilated. A stereotaxic frame (Rogue Research) secured the monkeys' heads in a sphinx position. Breathing volume and frequency were adjusted based on the animals' weights. Physiological parameters, including heart rate

and ventilation parameters (spO2 and CO2), were continuously monitored during the surgery. Body temperature was maintained using warm air circulating blankets.

The Floating Micro-Array (FMA) implantation part was guided by the Brainsight robot (Rogue Research). We defined the precise location of each FMA prior to the surgery (**Fig. 6A**). We used an in-house needle suction system attached to the arm of the robot to maintain the FMA. This permitted us to register the needle with the Brainsight software, thereby allowing us to use Brainsight to calculate the necessary trajectory for insertion. Trajectories were calculated to leave the FMA perpendicular to the surface of cortex, for the most secure implantation possible. The FMA electrode lengths had been specifically calculated to leave the electrodes at the desired depth within the cortex if the FMA was correctly placed on that trajectory and left perpendicular to the surface of cortex. Once the trajectory was calculated, the needle in position and the FMA attached, we removed the sucrose protective coating by dissolving it with heated saline water (**Fig. 6B**). We then used the robot as a micro descender for the insertion. The electrodes were lowered into the brain using the robotic arm and the position was adjusted visually if necessary, to account for the presence of blood vessels for example (**Fig. 6C**).

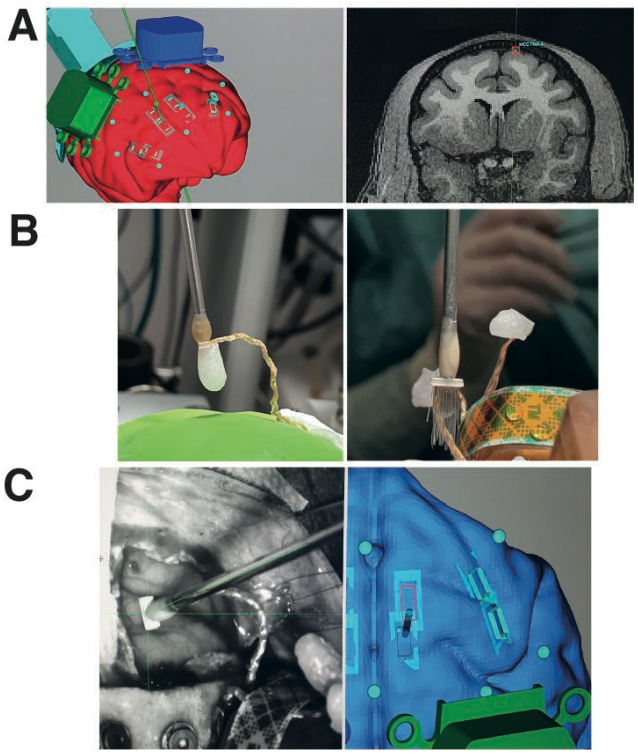

Figure 6. Surgery steps. All the screenshots are from Brainsight software and photos were taken during surgery. A) Placement of the FMA on Brainsight with a brain reconstruction on the left and an anatomical MRI on the right. B) In-house needle suction system to maintain FMA during surgery. C) FMA being guided down to the brain by the Brainsight robot - actual image on the left and Brainsight guidance on the right.

V. Electrophysiological and behavioural data acquisition

The monkeys were trained to perform tasks sitting in a primate chair (Crist Instrument Co., USA) in front of a tangent touch screen (Microtouch System, Methuen, USA). An open window in front of the chair allowed them to use their favourite hand to interact with the screen (monkey I is left-handed, monkey B is right-handed). The presentation of visual stimuli and the recording of the positions and accuracy of touch were performed by EventIDE software (Okazolab Ltd, www.okazolaBcom). During the tasks, eye movements were monitored using an Iscan infrared system (Iscan, Inc.). Electrophysiological data were recorded using an Intan multi-channel system (Intan Technologies). Water control protocols were used in order to train monkeys to perform tasks with high trial counts per session necessary for electrophysiological recordings, and to regulate their motivation level.

VI. Electrophysiological data pre-processing

a) Local-field potential analysis

The raw data were downsampled to 1kHz and filtered between 1Hz and 100Hz. A notch filter at 50Hz was applied with a 'spectrum fit' method (MNE toolbox, Python). We defined outliers at the session level by calculating the threshold on the average LFP signals for all sessions for each FMA: mean + 3.5*standard deviation. We removed all the FMA of a session if parts of the signal were superior to the threshold.

b) Multi and single units activity

The spike sorting was done using Kilosort2 (Pachitariu et al., 2016) then a visual verification was manually done. We used different information on the pre-sorted clusters to validate or refute them: the inter-spike interval, the amplitude, the shape and the correlogram. These informations allowed us to group together clusters that have been wrongly sorted

separately, to separate clusters of multi-units to different single-units and to identify and remove artefacts. We removed units that had less than 1000 spikes in one session. We did this for all electrodes of controlateral hemisphere of monkeys, for all DL task sessions. Then we combined single unit information with behavioural information for each session.

VII. Location of electrodes

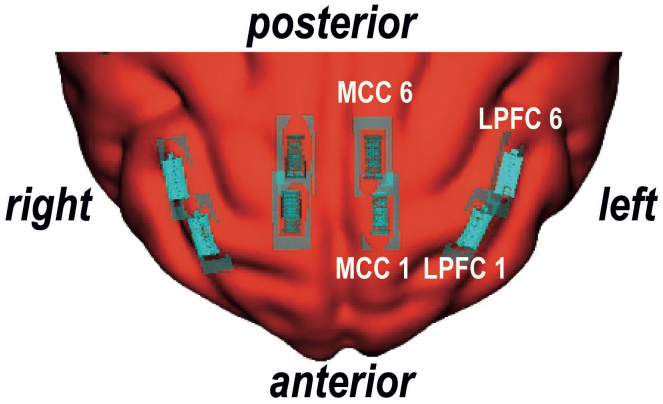

Figure 7. FMA placement in brain reconstruction. Brain reconstruction made with Brainsight software. MCC1/LPFC1 and MCC6/LPFC6 represent the extremity of the antero-posterior groups described below.

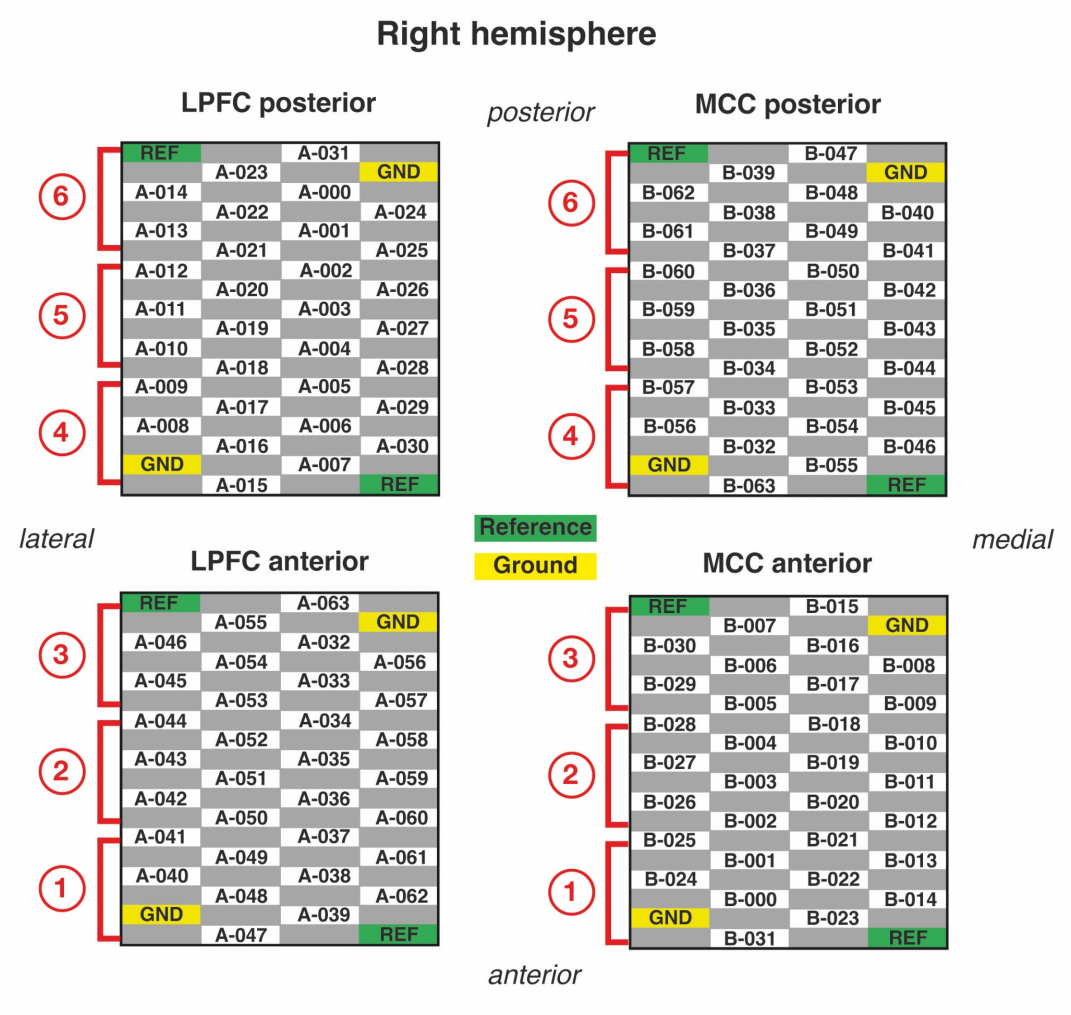

Figure 8. FMA placement in brain and electrodes names for the right hemisphere. Grids of the specific placement of each electrode for both hemispheres and areas (LPFC and MCC). Red brackets and numbers represent the 6 antero-posterior groups that we made. The reference is an electrode which is not in neural tissue and serves as a comparison to eliminate common noise. The ground is an electrical reference to avoid noise and artefacts due external electrical sources.

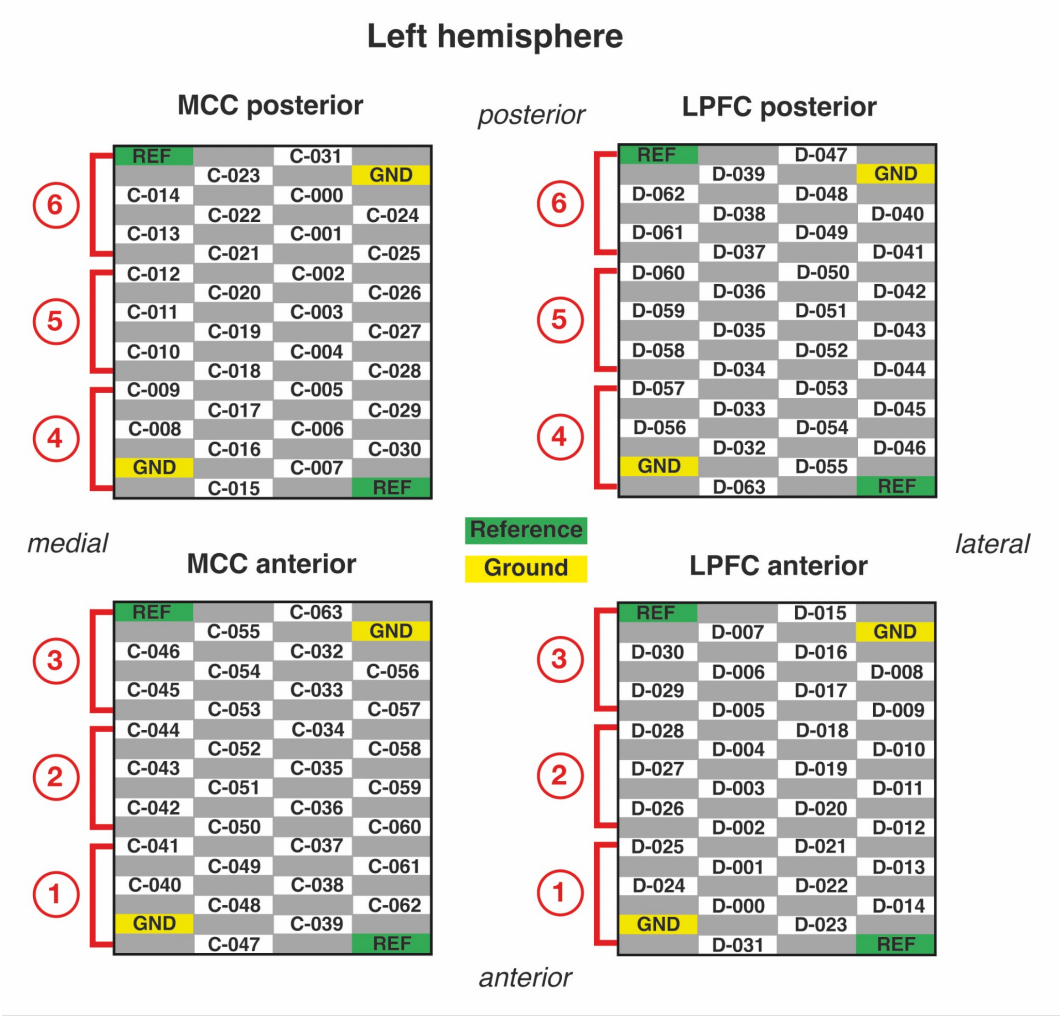

Figure 9. FMA placement in brain and electrodes names for the left hemisphere. Grids of the specific placement of each electrode for both hemispheres and areas (LPFC and MCC). Red brackets and numbers represent the 6 antero-posterior groups that we made. The reference is an electrode which is not in neural tissue and serves as a comparison to eliminate common noise. The ground is an electrical reference to avoid noise and artefacts due external electrical sources.

In each hemisphere of each monkey brain, we positioned four arrays (Floating micro-electrode array, Microprobes): two in the dorsolateral prefrontal cortex and two in the midcingulate cortex (**Fig. 7**). All FMAs were placed following an antero-posterior axis with 5-6mm between the centre points. The long axis of the FMAs is 4mm long, so this left 1-2 mm between them, with a little variation depending on placement avoiding blood vessels. We defined 6 antero-posterior groups for each area of each hemisphere that we used to group our data in the experimental part (**Fig. 8 & 9**). The exact positions were defined with the Brainsight software using precise landmark locations and adjustments were performed during the surgery according to the brain morphology (vessels, etc.) of each monkey. Each array contains 32

contacts with two different lengths in the LPFC and many in the MCC (*contralateral hemisphere:* **Fig. 10**). We designed different depths to record information in different layers of each area. There were two different depths in the LPFC as it was in the cortical surface, for the MCC we defined different lengths according to the morphology of the cortex.

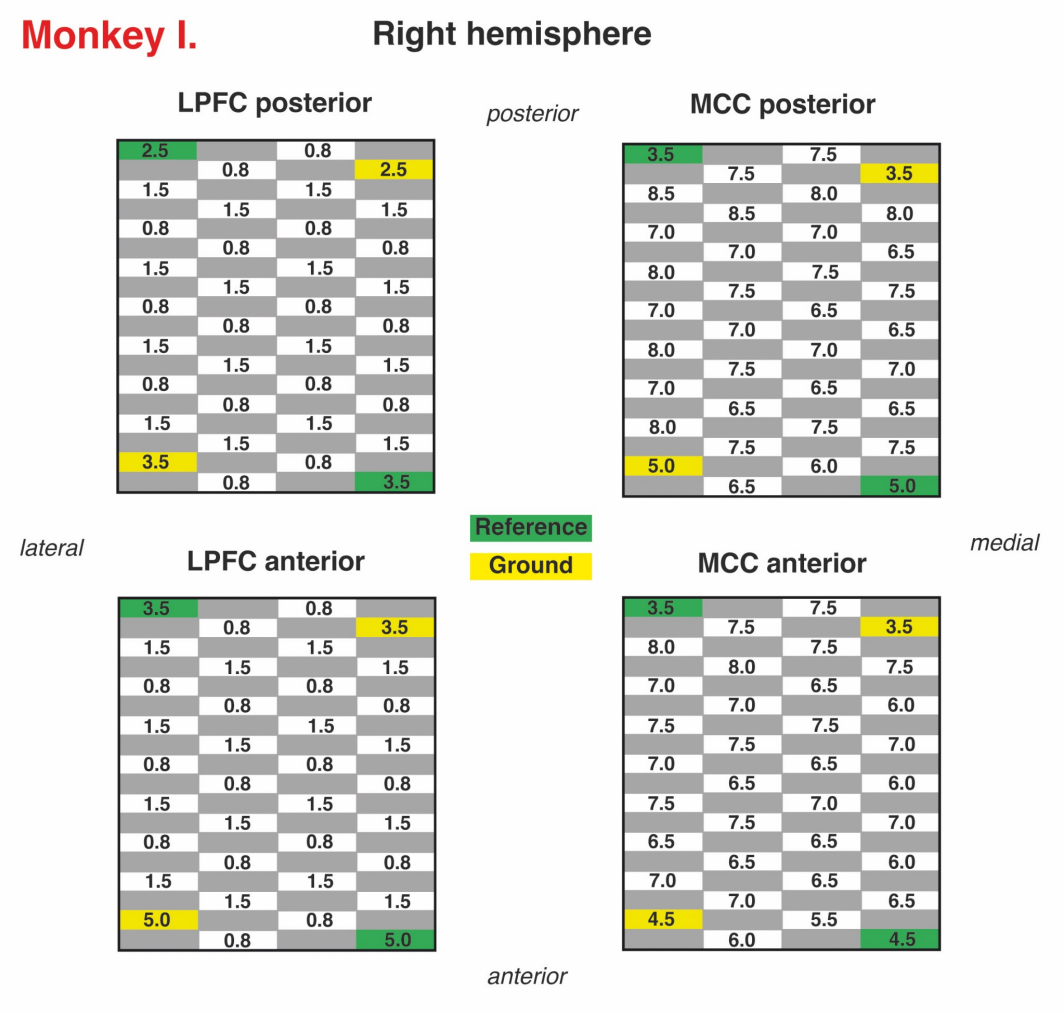

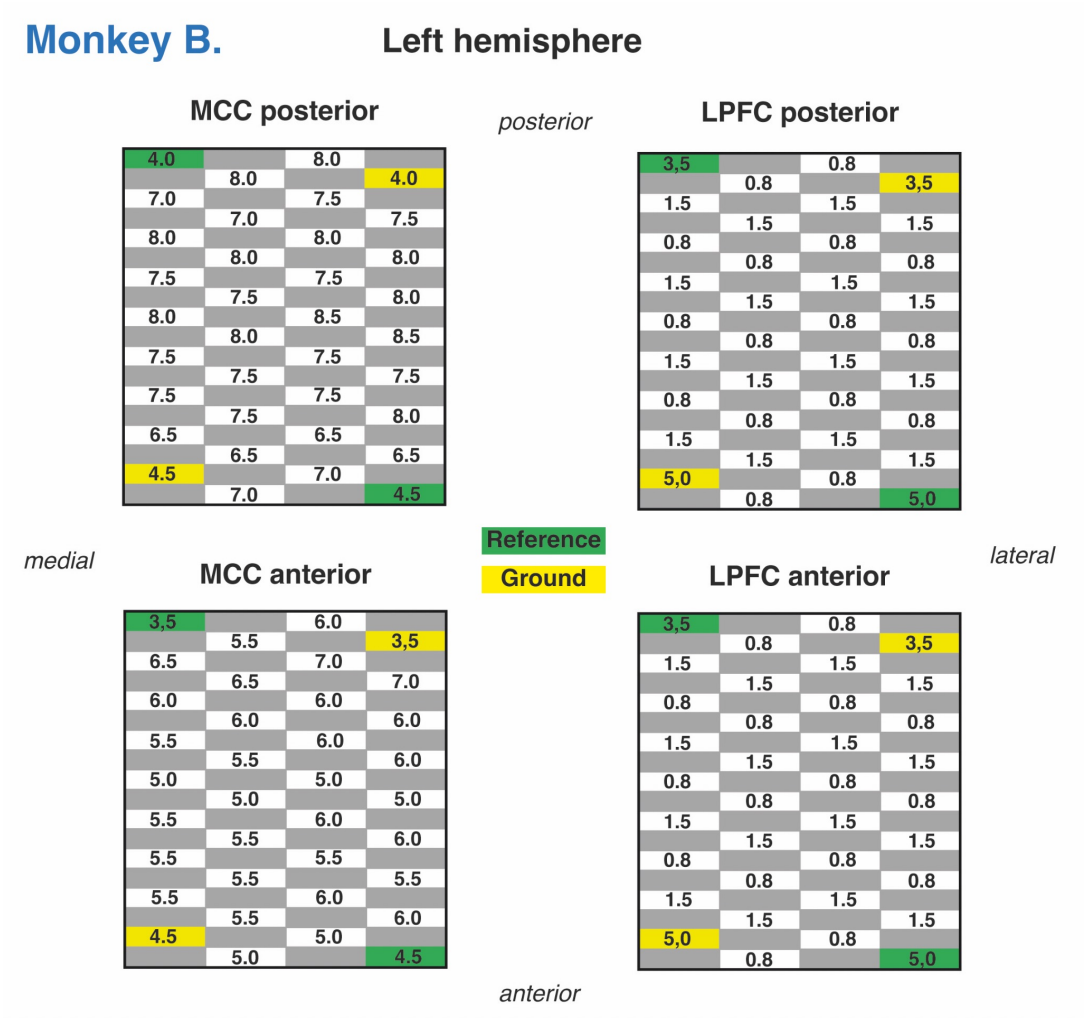

Figure 10. Electrodes depths in the contralateral hemisphere. Grid of electrodes with their specific depth. There are two different depths for the LPFC (1.5 and 0.8). For the MCC, the depth was adapted to the specific brain morphology of each subject. Numbers are in millimetres.

EXPERIMENTAL STUDIES

Chapter 1. Functional connectivity of the MCC-LPFC network in rs-fMRI

In this project, we focused on two main regions, the MCC and the LPFC. They are anatomically and functionally connected but there was no fine-grained description of their functional connectivity (FC). The aim of this first study was to define more precisely this FC with a differentiation between antero-posterior parts and sulcus parts. This study led to a scientific article published in Cerebral Cortex in August 2024 (Ducret et al., 2024).

I. Published paper

Medial to lateral frontal functional connectivity mapping reveals the organization of cingulate cortex

Authors: Ducret Marion[1], Giacometti Camille[1], Dirheimer Manon[2], Dureux Audrey[2], Autran-Clavagnier Delphine[3], Hadj-Bouziane Fadila[2], Verstraete Charles[1,4], Lamberton Franck [5,6], Wilson Charles R.E.[1], Amiez Céline[1*], Procyk Emmanuel[1*]

[1] Université Lyon 1, Inserm, Stem Cell and Brain Research Institute, INSERM U1208, 69500 Bron, France.

[2] Integrative Multisensory Perception Action and Cognition Team (ImpAct), INSERM U1028, CNRS UMR5292, Lyon Neuroscience Research Center (CRNL), Lyon, France; University of Lyon 1, Lyon, France.

[3] Inovarion, 75005 Paris, France

[4] Institut de neuromodulation, GHU Paris psychiatrie et neurosciences, Centre Hospitalier Sainte-Anne, pôle hospitalo-universitaire 15, Université Paris Cité, Paris, France

[5] CERMEP-Imaging Platform, Bron, France.

[6] SFR Lyon-Est, Université Lyon 1, CNRS UAR3453, INSERM US7, U69500, Lyon, France.

* The authors contributed equally to the article

Corresponding author:

Marion Ducret

18 avenue du Doyen Jean Lépine 69500 BRON

marion.ducret@inserm.fr
+33 6 62 56 42 91

Key words
prefrontal cortex, cingulate cortex, non-human primate, resting-state fMRI, functional connectivity

Abstract

The functional organization of the frontal lobe is a source of debate, focusing on broad functional subdivisions, large-scale networks, or local refined specificities. Multiple neurocognitive models have tried to explain how functional interactions between cingulate and lateral frontal regions contribute to decision making and cognitive control, but their neuroanatomical bases remain unclear. We provide a detailed description of the functional connectivity (FC) between cingulate and lateral frontal regions using resting-state functional MRI in rhesus macaques. The analysis focuses on the FC of the rostral part of the cingulate sulcus with the lateral frontal cortex. Data-driven and seed-based analysis revealed 3 clusters within the cingulate sulcus organized along the rostro-caudal axis: the anterior, mid, and posterior cluster display increased FC with, respectively, the anterior lateral prefrontal regions, face-eye lateral frontal motor cortical areas, and hand lateral frontal motor cortex. The location of these clusters can be predicted in individual subjects thanks to morphological landmarks. These results suggest that the anterior cluster corresponds to the anterior cingulate cortex, whereas the posterior clusters correspond to the face-eye and hand cingulate motor areas within the anterior midcingulate cortex. These data provide a comprehensive framework to identify cingulate subregions based on FC and local organization.

Introduction

The dynamics of cognitive processes rely both on intrinsic specificities of local neural microcircuits and on the structural properties of large-scale brain networks (Chaudhuri et al. 2015; Fontanier et al. 2022). While research has often focused on one aspect or the other,

both contribute to functional dynamics. In this context we studied the organizational principles of frontal brain networks devoted to action and cognitive control.

There are multiple hypotheses on how the functional organization of frontal networks and areal specificities contribute to the neurobiological bases of cognitive control (Dixon et al. 2014). While some propose that a large-scale network encompassing fronto-parietal and latero-medial (cingulate) frontal cortical areas are recruited as a non-specific network supporting ongoing task demands, others propose a rostro-caudal anatomo-functional organization contributing to a hierarchy of cognitive-motor controls (e.g. (Badre and D'Esposito 2009; Kouneiher et al. 2009; Duncan et al. 2020). These models are not exclusive, and both assign important functional roles to the anterior cingulate and/or anteriormidcingulate cortex (ACC and/or aMCC) and to its interaction with the lateral prefrontal cortex (LPFC). Several human functional brain imaging studies support a rostro-caudal functional organization of the lateral frontal cortex, but whether the cingulate cortex follows a similar principle remains unclear (Bush et al. 2000; Kouneiher et al. 2009).

Anatomically in primates, the most rostral region of the cingulate sulcus is subdivided in 2 parts: 1) the aMCC, the region extending from about the level of the anterior commissure to near the level of the rostral limit of the genu of the corpus callosum, and more anterior 2) the dorsal region of the Anterior Cingulate Cortex (ACC), the region located between the aMCC and the rostral end of the cingulate sulcus (CgS) (Vogt 2016; Amiez et al. 2019). The functional boundary between the ACC and the MCC remains unclear (Vogt 2016). Moreover, whereas the aMCC shows clear anatomo-functional homologies between humans and macaques (Amiez and Petrides 2014; Procyk et al. 2016; Amiez et al. 2019), this question is still unresolved for the ACC (Palomero-Gallagher et al. 2009; Amiez et al. 2019). The goal of the present paper is to shed new light on the functional organization of regions forming the rostral part of the CgS in the macaque brain by analyzing their connectivity with lateral frontal regions.

A primary characteristic of the aMCC is that it contains, within the CgS, the rostral Cingulate Motor Area (the so-called CMAr in macaques, and anterior Rostral Cingulate Zone -RCZa- in humans) which is somatotopically organized (i.e. it contains limb and face premotor representations) and projects weakly but directly to the spinal cord and primary motor cortices (for review see (Picard and Strick 1996; Dum and Strick 2002). Second, some neurons in the most rostral part of the CgS project to the dorsolateral prefrontal cortex (Borra et al. 2017).

These anatomical specificities, including connectivity with the frontal lobe, potentially confer to the aMCC a role in interfacing motor and cognitive controls (Paus 2001). Yet, the precise extent of CMAr across animals, its somatotopic organization, its precise interplay with the dorsolateral prefrontal cortex, and how it segregates from ACC remain to be elucidated.

Previous parcellations of the cingulate region in humans, macaques and marmosets have used either diffusion tractography or resting-state fMRI (rs-fMRI) (Beckmann et al. 2009; Hutchison et al. 2012). Most studies provided grand average mappings that provide important information and broad views of cingulate functional contributions but that might be difficult to use at the individual level, and hence to decipher precise anatomical and functional landmarks. So, because cingulate interactions with lateral frontal appear to be particularly relevant, we tested whether the connectivity between the two regions might enable identification of functional cingulate subdivisions even at the single subject level, hence revealing reliable principles of frontal cortex functional organization.

In the present investigation we first attempted to localize CMA subdivisions in macaque anterior regions of CgS at the single individual level. Second, we described the organization of functional connectivity (FC) between these cingulate regions and the lateral frontal cortex. We analyzed anesthetized rs-fMRI data from 15 rhesus macaques, to characterize the FC patterns of the aMCC and ACC regions with the lateral frontal cortex based on individual subject analysis allowing us to relate anatomical to functional features. Compared to previous studies we focused on the cortex lining the CgS, which has been the focus of most past recordings, and which contains CMAs. We also primarily restricted regions of interest to a finite list of frontal regions of interest considering regions with hand versus eye or face related functions, but confirmed our results using a non-supervised whole-brain analysis. Our results revealed that the CgS running anterior to the anterior commissure is composed of 3 main subregions aligned on the caudo-rostral axis: the hand motor/premotor field of CMAr, a face/eye premotor field, both putatively located in aMCC, and rostrally a subregion functionally connected to lateral prefrontal areas 46 and 10.

Materials and Methods

Subjects. Eighteen rhesus monkeys (*macaca mulatta*) were assessed in this study: 13 females (5-19 years old) and 5 males (10-17 years old) weighing from 5 to 13 kg. Three (2 females and 1 male, 11-12 years old) were excluded in the final analysis because of an unexplained lack of negative correlations in the functional connectivity data. All procedures followed the European Community Council Directive (directive 2010/63/UE) (Ministère de l'Agriculture et de la Forêt, Commission nationale de l'expérimentation animale) and were approved by the local ethical committee (Comité d'Ethique Lyonnais pour les Neurosciences Expérimentales, CELYNE, C2EA #42).

Animal preparation. Before anesthesia, monkeys were administered glycopyrrolate (Robinul: 0.06 mg/kg), an anticholinergic agent. After a 20-minute interval, anesthesia was induced with an intramuscular injection of tiletamine and zolazepam (Zoletil: 7 mg/kg). Subsequently, the animals were intubated and ventilated with oxygen-enriched air and different % Isoflurane depending on the monkeys (Table 1) throughout the entire scanning session. To minimize variability in measurements, an MRI-compatible stereotaxic frame (Kopf, CA, USA) secured the monkeys' heads in a sphinx position facing the back of the scanner. Breathing volume and frequency were adjusted based on the animals' weights. Physiological parameters, including heart rate and ventilation parameters (spO2 and CO2), were continuously monitored during the scan. Body temperature was maintained using warm air circulating blankets. Rs-fMRI data acquisitions were performed approximately 2 hours after anesthesia induction and at least 1 hour after the initial inhalation of isoflurane.

Monkey	% isoflurane	n slices	TR (s)	Spatial resolution	nb RUN
P	1%	28	1.8	1.7mm^3	5
K	1%	31	2	1.8mm^3	6
H	0.8%	31	1.9	1.7mm^3	5
O	1%	31	2	1.8mm^3	6
Po	1%	31	2	1.8mm^3	6
Y	1.2%	31	2	1.8mm^3	6
S	1%	25	1.7	1.7mm^3	5
V	0.8%	28	1.8	1.7mm^3	5

D	0.8%	28	1.8	1.7mm^3	5
A	1%	31	2.108	1.8mm^3	6
Ce	1.5%	31	2.108	1.8mm^3	6
Ci	1%	31	2.108	1.8mm^3	6
E	1%	31	2.108	1.8mm^3	6
Ge	1%	31	2.108	1.8mm^3	6
Gu	1%	31	2.108	1.8mm^3	6

Table 1. fMRI acquisition and anesthesia parameters for each monkey.

rs-fRMI data acquisition. Rs-fMRI data were acquired in anesthetized monkeys from a 3T Siemens Magnetom Prisma MRI scanner (Siemens Healthcare, Erlangen, Germany). Three Siemens loop coils were used: two L11 ring coils on each side of the monkey's head and one L7 above the monkey's head. A high-resolution T1-weighted anatomical scan (MPRAGE, 0.5mm^3 isotropic voxels, 144 slices, TR=3000ms, TE=366ms) was acquired for each of the 18 monkeys. rs-fMRI images covering the entire brain were obtained using a T2*-weighted gradient echo planar imaging (EPI) sequence. The acquisition parameters varied slightly for different groups of monkeys (Table 1). For each of the macaques, five or six runs of 400 volumes each were collected. Anatomical and functional data of each animal were acquired during the same session.

rs-fMRI data analysis. Rs-fMRI scans were preprocessed using SPM 12. The initial 5 volumes of each run were excluded to account for T1 equilibrium effects. Slice timing correction was performed with the time center of the volume as a reference, followed by rigid body realignment for head motion correction. Skull-stripping was executed using the bet tool from FSL software (Jenkinson et al. 2012). AFNI software (Cox 1996) was then employed for brain segmentation in both anesthetized and awake sessions on the previously skull-stripped brains. Temporal filtering extracted spontaneous slow fluctuating brain activity within the 0.01–0.1 Hz range. Linear regression removed nuisance variables, including cerebrospinal fluid and white matter signals from segmentation, as well as volumes with detected artifacts using the ART toolbox (https://www.nitrc.org/projects/artifact_detect/). The final step involved spatial smoothing with a 4-mm FWHM Gaussian kernel applied to the regression output.

Location of seeds in the prefrontal cingulate cortex. In each hemisphere of each monkey brain, we positioned spherical 2.5mm radius seeds in the dorsal bank, fundus, and ventral bank of the CgS from the anterior commissure (i.e. caudal limit of the aMCC, see (Amiez et al. 2019) to the rostral end of the CgS (i.e. the rostral end of the ACC, see (Amiez et al. 2019) with a spacing of 2.5mm between each seed (**Fig. 11**). The seed radius was chosen to achieve the finest-grained analysis possible, constrained by our data's spatial resolution (voxels of 1.8mm3^) and spatial smoothing (4mm). This radius has been previously validated for assessing functional connectivity in the MCC-lateral frontal and MCC-amygdala networks (Giacometti et al. 2023, 2024). Due to interindividual variability, the number of seeds differs across monkeys (see details in Table 2).

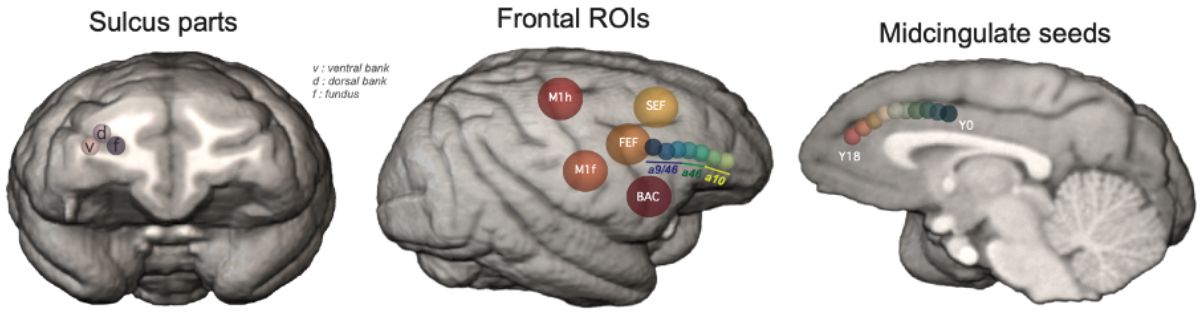

Figure 11. Position of ROIs and seeds in monkey Na in the right hemisphere. ROIs are located in the in frontal and prefrontal areas and seeds in the MCC. They are positioned in the principalis for the former and cingulate sulcus for the later and divided in three sub-regions located in the dorsal bank, the ventral bank and the fundus of their respective sulcl M1h: M1 hand, M1f: M1 face, FEF: frontal eye field, SEF: supplementary eye field, BAC: Broca's area complex.

Location of Regions of Interest (ROIs) in the lateral frontal cortex. We first aimed to identify the hand and the face premotor representations of CMAr. We expected a stronger FC between the hand premotor representation of CMAr with the primary hand motor cortex (M1Hand). By contrast, we anticipated a stronger FC between CMAr face representation and face/oculomotor-related areas (M1Face) in the lateral frontal cortex, which includes the primary face motor cortex, the Frontal (FEF) and Supplementary (SEF) Eye Fields, and

Broca's area complex (BAC). We thus positioned the following ROIs based on local sulcal morphology in each hemisphere of individual subjects (**Fig. 11**):

- M1Hand and M1Face positioned in the dorsal and the ventral part of the posterior part of the precentral gyrus respectively (He et al. 1993; Rizzolatti and Luppino 2001; Graziano et al. 2002; Giacometti et al. 2023).
- The FEF localized within the rostral bank of the genu of the arcuate sulcus (Bruce et al. 1985; Amiez and Petrides 2009).
- The SEF placed dorsally and caudally to the rostral limit of the superior part of the arcuate sulcus (Schlag and Schlag-Rey 1987).
- BAC within the fundus of the ventral part of the arcuate sulcus (Petrides et al. 2005).

Then, we aimed to examine the precise functional dialogue between the cingulate and the principal sulcus. We positioned ROIs along the entire principal sulcus, in its fundus as well as dorsal and ventral banks (**Fig. 11**). These ROIs correspond to 2.5mm radius spheres, spaced by 2.5mm. Due to interindividual variability, the number of principal sulcus ROIs differs across monkeys (see details in Table 2) All the other lateral frontal ROIs were 5mm radius spheres. We also identified morphological changes in the principal sulcus at 2 antero-posterior Y levels: the landmark 1 that corresponds to the rostral limit of the genu of the corpus callosum and the landmark 2 that corresponds to the fork at the end of the cingulate sulcus or to the rostral end if there is no fork. Interestingly, we show that these 2 landmarks delimitate anatomo-functional territories that correspond to, on the postero-anterior axis, the dorsolateral prefrontal area 9/46, area 46, and the frontopolar area 10 (Amiez, Sallet, et al. 2023). We thus also merged the ROIs described above in each of these territories to obtain a9/46, a46, and a10 ROIs.

In the dorsolateral prefrontal cortex (dlPFC):

- Area 9/46 (a9/46) corresponds to ROIs located in the posterior part of the principal sulcus, posterior to the first morphological change in this sulcus (Landmark 1), which also appears to be at the antero-posterior Y level whereof the rostral part of the genu of the corpus callosum is observed (Amiez, Sallet, et al. 2023).
- Area 46 (a46) corresponds to ROIs located in the middle part of the principal sulcus, between Landmark 1 the level of the rostral part of the genu of the corpus callosum and

the second morphological change in this sulcus (Landmark 2), which also appears to occur at the antero-posterior Y level where the rostral end of the CgS is found (Amiez, Sallet, et al. 2023).

- Area 10 (a10) corresponds to ROIs located in the rostral part of the principal sulcus, rostrally to the anteroposterior level where the rostral end of the CgS is found (Amiez, Sallet, et al. 2023).

Monkey	Seeds in CgS	ROIs in principal sulcus
P	10	7
K	11	10
H	10	7
O	10	7
Po	10	6
Y	10	7
S	10	5
V	10	5
D	10	6
A	10	7
Ce	9	6
Ci	10	5
E	10	6
Ge	10	6
Gu	10	6

Table 2. Number of seeds in Cgs and ROIs in principal sulcus for each monkey. These numbers are identical in both hemispheres.

Individual subject analyses. For each hemisphere of each animal, Pearson correlation coefficients between the filtered BOLD signal in the seeds with the filtered BOLD signal in the ROIs were computed and normalized using the Fisher's r-to-Z transform formula. The significant threshold at the individual subject level was set to $Z = 0.1$ ($p < 0.05$). These normalized correlation coefficients, which correspond to the FC strength between each seed and each ROI in individual brains, were subsequently processed with R software. Then, to

assess the location in the CgS where the strongest FC is observed, we extracted the peaks of correlation (positive and negative) for each monkey and hemisphere (**Fig. 12A**).

Group analyses.

The following analyses were realized with R software

ROI re-alignment

Because of the strong inter-hemispheric and inter-subject variabilities of the posterior extent of the prefrontal cortex (PFC) as marked by the genu of the arcuate sulcus on the lateral surface (Amiez, Sallet, et al. 2023), the antero-posterior Y values of the cingulate seeds were first all realigned on the antero-posterior Y values of the genu of the arcuate sulcus in each hemisphere of each individual. We chose this landmark as it was the one leading to the lowest inter-individual variance for each frontal ROI compared to the anterior commissure, the caudal and rostral limits of the genu of the corpus callosum and the fork at the rostral end of the cingulate sulcus (composed of the suprarostral sulcus ventrally and the sus-orbitalis sulcus dorsally, see Amiez et al. 2019). In addition, we spatially remapped all the seeds in the CgS according to 3 specific landmarks: 1) the anterior commissure (i.e., anteroposterior level in the caudal limit of aMCC), the genu of the arcuate sulcus, 2) the caudal (i.e., antero-posterior level of the caudal limit of the principal sulcus) and rostral genu of the corpus callosum and 3) the rostral end of the CgS (Amiez et al. 2019). To do so, we calculated the mean y axis coordinate for each landmark and scaled the seeds coordinates points to ensure consistency across all monkeys. We then performed a linear model (*model:* CgS *y coordinates ~ lateral frontal ROIs*) and extracted the r-squared value to describe the CgS FC peaks organization.

Parcellation

To test whether peaks of FC between cingulate seeds and ROIs in frontal areas were clustered in subregions of the cingulate cortex we computed a similarity matrix using the Gower distance via the 'daisy' function from the 'cluster' library (*https://cran.r-project.org/web/packages/cluster/index.html*) to capture intricate relationships between

observations. We then performed a hierarchical clustering using the “Ward.D2” method. To determine the optimal number of clusters, we applied K-means models with varying values of k and computed the within-cluster sum of squares (WCSS) to identify the point where the acceleration of successive differences in WCSS was maximal. Then we assigned clusters to the data using the 'cutree' function.

The seed based parcellation described above identified that the best number of clusters in the cingulate sulcus was 3 (see results). To identify whether this parcellation stood when assessing the whole-brain FC of the cingulate sulcus, we performed a data-driven parcellation of the cingulate sulcus using a clustering algorithm on the 3D matrix of FC to classify voxels composing the gray matter of the entire brain depending on their *z* score (see Amiez et al. 2023). We expected that voxels of the cingulate sulcus mask displaying similar connectivity profiles would be clustered together revealing a sulcal subregion associated with a specific whole-brain connectivity profile. To optimize inter-subject comparisons, we reprocessed the data after registration of anatomical and functional images to the CHARM common atlas space (Seidlitz et al. 2018; Jung et al. 2021). We applied spectral clustering algorithms (Cheng et al. 2021). From the 2D matrix representing the whole-brain connectivity profile of each voxel of the cingulate sulcus mask, we computed the adjacency matrix (correlation between rows) and used the *k*-nearest neighbor to extract the similarity matrix. From the latter, the Laplacian matrix and its spectral decomposition were computed, and a *K*-means algorithm on the eigenvalues matrix provided the clusters (von Luxburg 2007). Clustering procedures were run under Python 3.8.10 using scikit-learn (Pedregosa et al., 2011), pandas (McKinney 2010), numpy (Harris et al. 2020) and nibabel (Fanton and Thompson 2023). To select an optimal number of clusters we used silhouette index scores (ratio of the sum of between-cluster and within-cluster dispersions for all clusters (dispersion is the sum of distances squared).

Statistical analysis

To capture characteristics of the functional connectivity patterns between seeds and ROIs, we performed a general linear mixed-effect models: (*glmm: Z score ~ ROI + seed + hemisphere + interaction , with subject as random factor)*followed by post-hoc Tukey tests. To

precise this pattern, we further ran one-sample student tests to calculate the difference to zero and extract the p-value on which we applied a false discovery rate correction.

Finally, to assess the proportion of negative and positive Z score value between seeds and ROIs, we first used a Wilcoxon test and then performed Dunn post-hoc tests to highlight specificities between seeds and ROIs.

Results

General FC pattern between the aMCC/ACC seeds and lateral frontal ROIs

We first sought to identify whether aMCC subregions displayed a FC pattern suggesting the presence of a somatotopy as described for cingulate motor areas (Dum and Strick 2002; Procyk et al. 2016). We thus extracted a global map of FC (as assessed by the Z values, see Materials and Methods) between the seeds located along the CgS, and the different lateral frontal cortical ROIs (**Fig. 11**). Figure 12 shows the resulting FC pattern in 2 example subjects (**Fig. 12A**), where the x-axis has been re-scaled because of the different lengths of CgS in different subjects. These examples reveal important common properties across subjects. First, at the level of the genu of the arcuate sulcus, the cingulate FC with the M1hand region presents a peak located posteriorly to those observed with other ROIs. Anterior to this region displaying increased FC with the primary hand cortex, a peak of FC is observed with the primary face area (M1Face), FEF, SEF, BAC and 9/46. Third, from this latter region to the rostral end of the CgS, the more anterior the seed is in the CgS, the stronger its FC with the SEF and the lateral dorsolateral prefrontal and frontopolar regions (a9/46, a46, a10) is. Fourth, these FC peaks are also observed in different zones of the CgS (dorsal bank, ventral bank, fundus. **Fig. 12B**), with the positive and negative FC peaks predominantly detected in the fundus/dorsal bank and the dorsal/ventral banks of the CgS respectively.

Altogether, these individual data revealed the presence of a CMA containing hand and face motor representations and showed that the cortex lying in the CgS is organized along a rostro-caudal anatomo-functional organization captured at single subject level, with more rostral (putative ACC) seeds displaying stronger FC with anterior lateral frontal ROIs than posterior (putative aMCC) seeds.

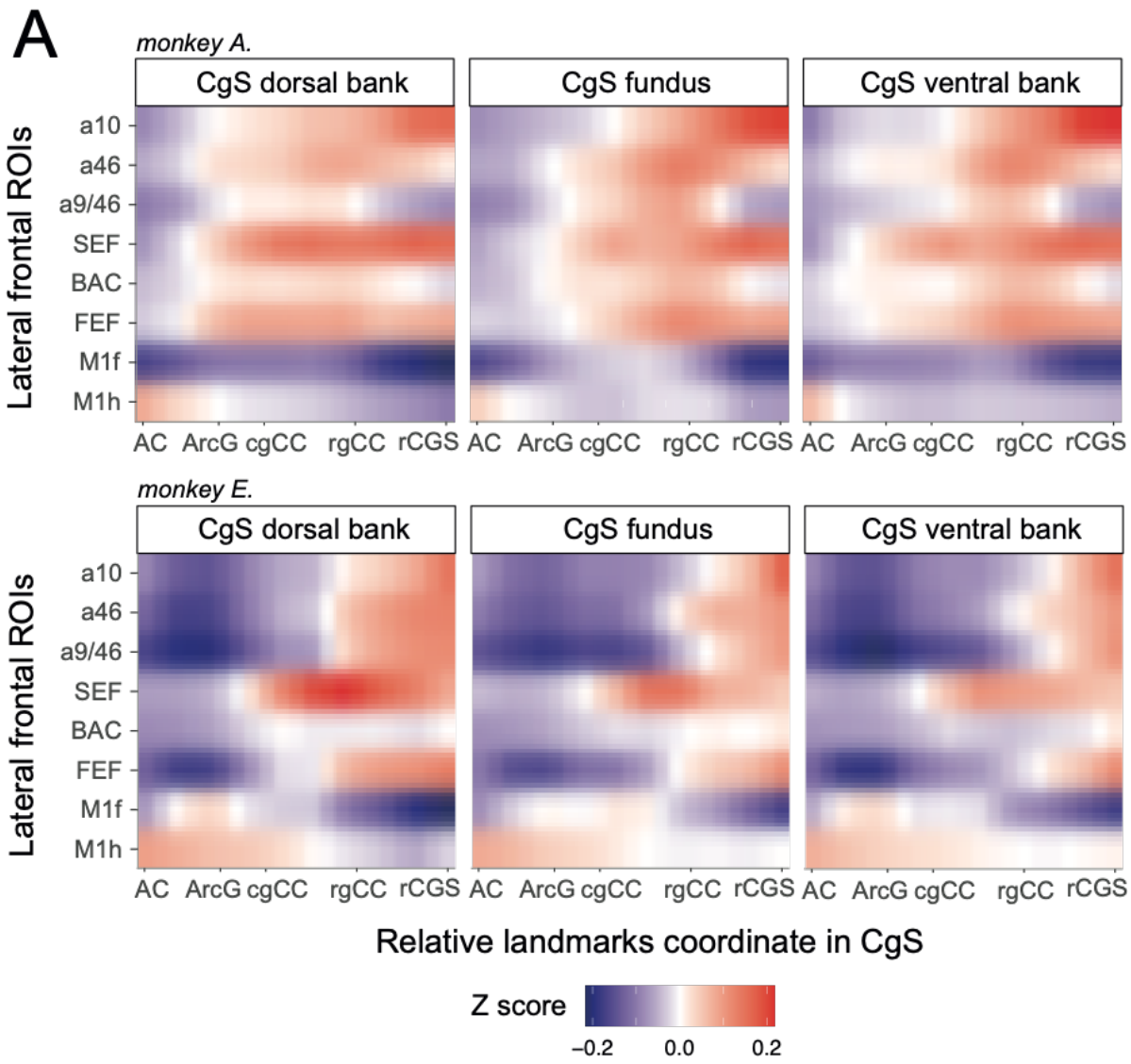
A
monkey A.
CgS dorsal bank
CgS fundus
CgS ventral bank
Lateral frontal ROIs
a10
a46
a9/46
SEF
BAC
FEF
M1f
M1h
AC ArcG cgCC rgCC rCGS
monkey E.
Relative landmarks coordinate in CgS
Z score
−0.2 0.0 0.2

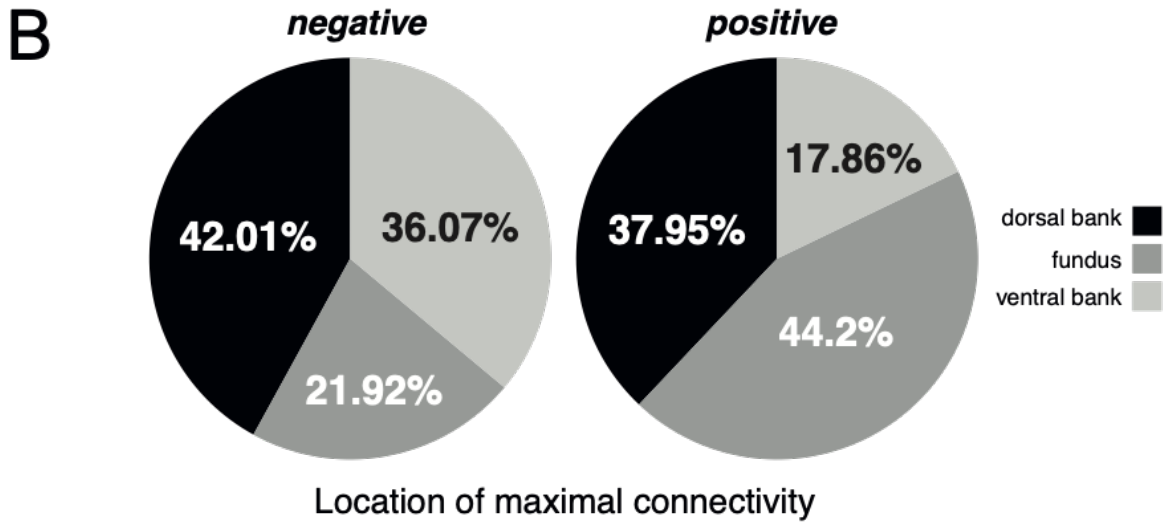
B
negative
positive
42.01%
36.07%
21.92%
37.95%
17.86%
44.2%
dorsal bank
fundus
ventral bank
Location of maximal connectivity

Figure 12. FC profiles between the cingulate seeds located in the dorsal bank, fundus and dorsal banks of the cingulate sulcus and lateral frontal ROIs in the left hemisphere. A. Heatmap displaying z-scores between lateral ROIs and cingulate seeds in 2 monkey subjects (top: monkey A and bottom: monkey E). In abscissa is represented the antero-posterior Y coordinate level of the cingulate seeds with the relative ant-posterior levels of key landmarks (AC = anterior commissure, ArcG = genu of the arcuate sulcus, cgCC/rgCC = caudal/rostral limits of genu of corpus callosum, rCGS = rostral end of cingulate sulcus) and in ordinate is represented the lateral ROIs. Within the tiles, Z score correlations between both are scaled from negative (blue) to positive (red). In all examples, on the caudo-rostral axis of cingulate seeds, we observed 1) a maxima of FC with the primary hand motor ROI (M1Hand) for seeds located posterior to the genu of the arcuate sulcus (ArcG), 2) a maxima of FC with the face premotor and motor ROIs (M1Face, FEF, BAC, SEF) for seeds located 5-10 mm anterior to the genu of the arcuate sulcus, and 3) increasing FC with the dorsolateral (a9/46, a46) and the frontopolar (a10) ROIs for the seeds located rostral to the cingulate face motor area. **B** Pie charts representing the percentages of cases where negative (left) and positive (right) peaks of FC between seeds and ROIs are located in the dorsal bank, the fundus and the ventral bank in our population (15 subjects).

The caudo-rostral cingulate organization.

A clear spatial distribution pattern of FC peaks was observed only for positive peaks of FC with the lateral frontal ROIs in both hemispheres (left hemisphere: R2=0.42, p=0.001, right hemisphere: R2=0.45, p=0.0015) but not for negative peaks of FC (left hemisphere: R2=0.2, p=0.65, right hemisphere: R2=0.21, p=0.67). (**Fig. 13A**). This confirms at the population level that anterior-to-posterior lateral frontal ROIs are positively correlated with anterior-to-posterior parts of the CgS cortex. It also confirms the presence of a rostral hand motor representation located posterior to a face motor representation (including FC connectivity with M1face, BAC, SEF, FEF). Specifically, the hand motor representation (connected with M1hand) appears to be, at the population level, located posterior to the level of the genu of the arcuate sulcus (Y median = -2.5 / interquartile range (IQR) = 3.75 in the left and Y median = -3 / IQR = 4.25 in the right hemisphere in 18 subjects), whereas the face motor representation is located anterior to it (Y median = 6.5 / IQR = 4.75 in the left and Y median = 6 / IQR = 5 in the right hemisphere).

Interestingly, positive FC peaks were more often located in the fundus for connections with M1face, a9/46, a46 and a10 areas, and in the dorsal bank for M1 hand and FEF, BAC and SEF (**Fig. 13B**). Regarding M1face these results corroborate with previous anatomical and functional studies (Morecraft et al. 2007; Cléry et al. 2018). Negative peaks were more often located in the dorsal bank for connectivity with M1 hand, a9-46, SEF, a46 and a10, and in the ventral bank for M1face and FEF. For BAC the proportions are equal in the dorsal and ventral

banks. Overall, the rostro-caudal FC organization was more pronounced for positive correlations with a significant slope (Fisher test, $p<0.01$) than for the negative ones, and the distinction between cingulate sub-regions was sharper.

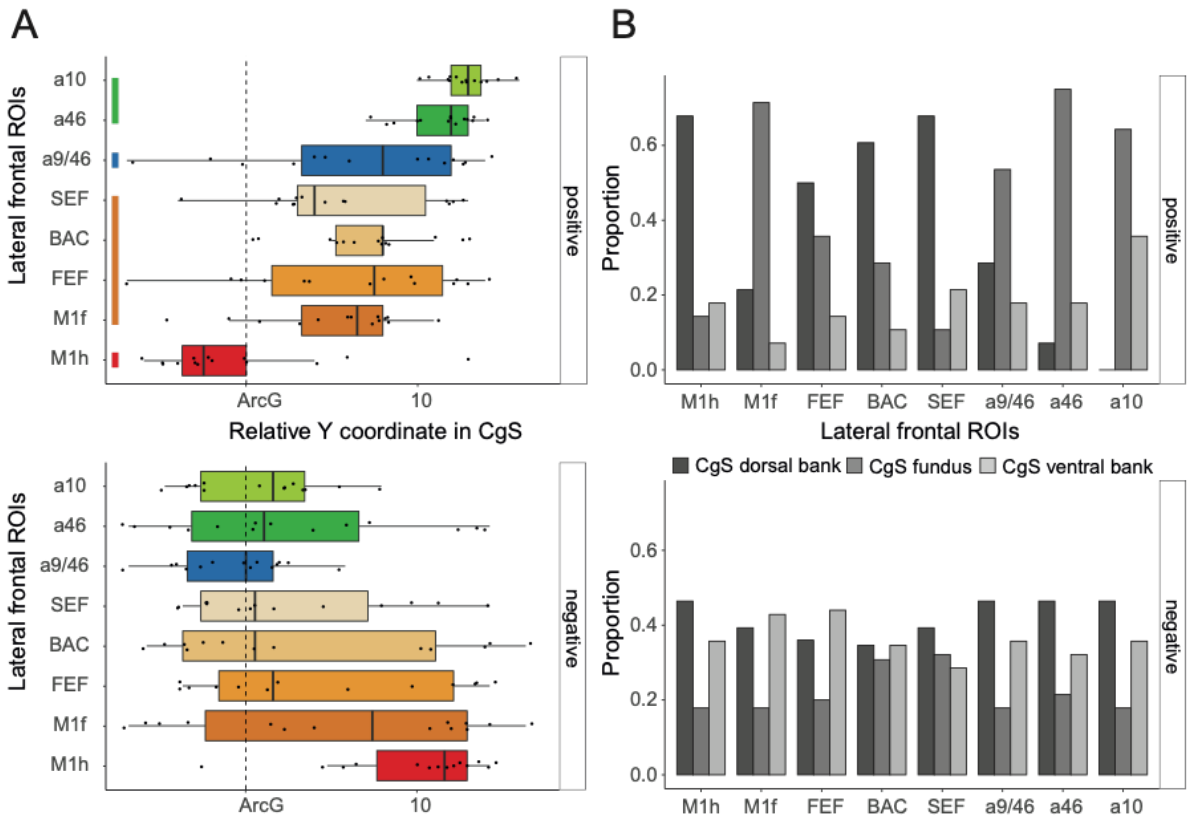

Figure 13. Rostro-caudal FC organization between the cingulate sulcal cortex and the lateral frontal ROIs. A. Antero-posterior locations of the cingulate region displaying the positive and negative FC peaks (top and bottom diagrams, respectively) with the lateral frontal ROIs in all individuals in the left hemisphere. ROIs are ordered based on their average Y coordinate. Each point represents the location of the FC peak in a given monkey. In each boxplot, the lower and upper hinges of the box correspond to the first and third quartiles respectively. Upper and lower whiskers extent from their corresponding hinges to the largest and lowest value respectively define as 1.5 x of the interquartile range. Individual data points are also represented for each boxplot. Colored lines represent the hierarchical clustering (see methods). M1h = M1 hand, M1f = M1 face. B Bar plots representing the percentage of cases where the positive and negative FC peaks are located in the ventral or dorsal banks, or in the fundus of the cingulate sulcus. The 2 hemispheres are combined to have a global view of this distribution.

CMAr somatomotor representations are likely to be within the aMCC region but the position of the face field and its relationship or limit with ACC is still unresolved (Vogt 2016). Figure 13 shows that positive FC peaks related to the M1face overlap at the population level with peaks linked to FEF, SEF, BAC, and a9/46, functional areas related to face, oculomotor controls,

and working memory (Constantinidis and Qi 2018). The overlap thus seems to reflect the presence of a functionally specific field that we named: the face field. One hypothesis is that the limit between aMCC and ACC within the cingulate sulcus is found around the level of the genu of the corpus callosum (CC). Although the FC peak data do not show a clear limit between the face field and a more rostral region, potentially ACC, it suggests that the rostral region displaying stronger FC with a46 and a10 is anatomically and functionally differentiated.

The dispersion of FC peaks along the CgS thus suggests partitions of the cingulate region of interest into multiple functional subdivisions. The positive FC peaks across monkeys could be clustered in 4 groups of connectivity with lateral frontal ROIs (**Fig. 13A**). Cluster 1, characterized by its FC with M1hand, is found posterior to the level of the genu of the arcuate sulcus. More anteriorly we can observe cluster 2 (M1 face, FEF, BAC, SEF), cluster 3 (a9/46) and cluster 4 (a46, a10).

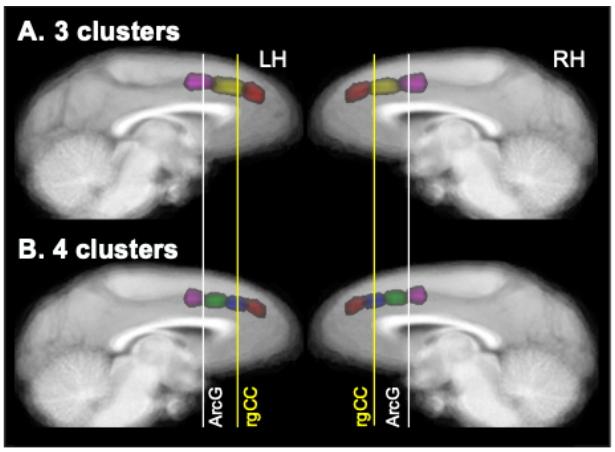

Figure 14. Whole brain data driven clustering. Clusters are defined on the group data (all monkeys). Data are displayed on the average T1 MRI volume. A. 3 cluster outcome. B 4 cluster outcome. Note that morphological landmarks (white and yellow lines) provide indications about the relative position of clusters (as observed for each hemisphere in supplementary figure 1 and 2). White line: antero-posterior level of the genu of the arcuate sulcus. Yellow line: antero posterior level of the rostral limit of the corpus callosum.

We confirmed clustering of the cingulate region of interest with an unsupervised approach applied on each run for each hemisphere of each brain and based on the whole brain connectivity matrices. The optimal number of clusters was 3 in 62 and 68 % of cases (for left and right hemispheres respectively) cases, and 4 in 27% and 17% of cases. The reconstruction of clusters on each MRI relative to key morphological landmarks (genu of the arcuate sulcus, and anterior end of the genu of the corpus callosum) revealed a first cluster

located posterior to or around the genu of the arcuate (white line in **Fig. 14A**). The most anterior cluster was anterior to the level of the genu of the corpus callosum (yellow line). Note that 3 and 4 cluster parcellations provided very coherent maps across monkeys in terms of cluster position relative to morphological landmarks (**Supplementary Fig. 1 & 2)**. In the 4-parcels schema (**Fig 14B**)**,** the mid subdivision is dissociated in 2 subdivisions. Note also that no clustering led to divisions of the dorsal versus ventral banks of the cingulate sulcus. Thus the cingulate region of interest is parceled in 3 or 4 functional subregions that are found in each hemisphere at reliable positions relative to brain morphological landmarks. Remarkably the whole-brain FC analysis showed clear dissociations between the cingulate subdivisions in terms of large-scale connectivity. In the 3-parcel schema of the cingulate sulcus (**Fig 15**), we first observed a caudo-rostral dissociation in which the i) posterior, ii) mid, and iii) anterior subdivision displays FC, respectively, with i) hand motor/premotor cortex (i.e. M1 Hand, PMd) and putamen, ii) face/eye motor/premotor (M1Face, BAC, FEF), caudal prefrontal cortex (a9/46, SEF), as well as putamen/caudate nucleus, and iii) anterior prefrontal cortex (a46, a10), the anterior insula, the amygdala, the caudate nucleus, the Posterior Cingulate Cortex (PCC), and the superior temporal sulcus (STS). In addition, we observed that the posterior and mid subdivisions share FC with the posterior parietal cortex (PPC), posterior insula, precuneus (PRC) and temporal cortex (TpT, and superior temporal gyrus - STG). Thus, the whole brain analysis revealed clear anatomo-functionnal dissociations between the large-scale networks centered on the different cingulate subdivisions.

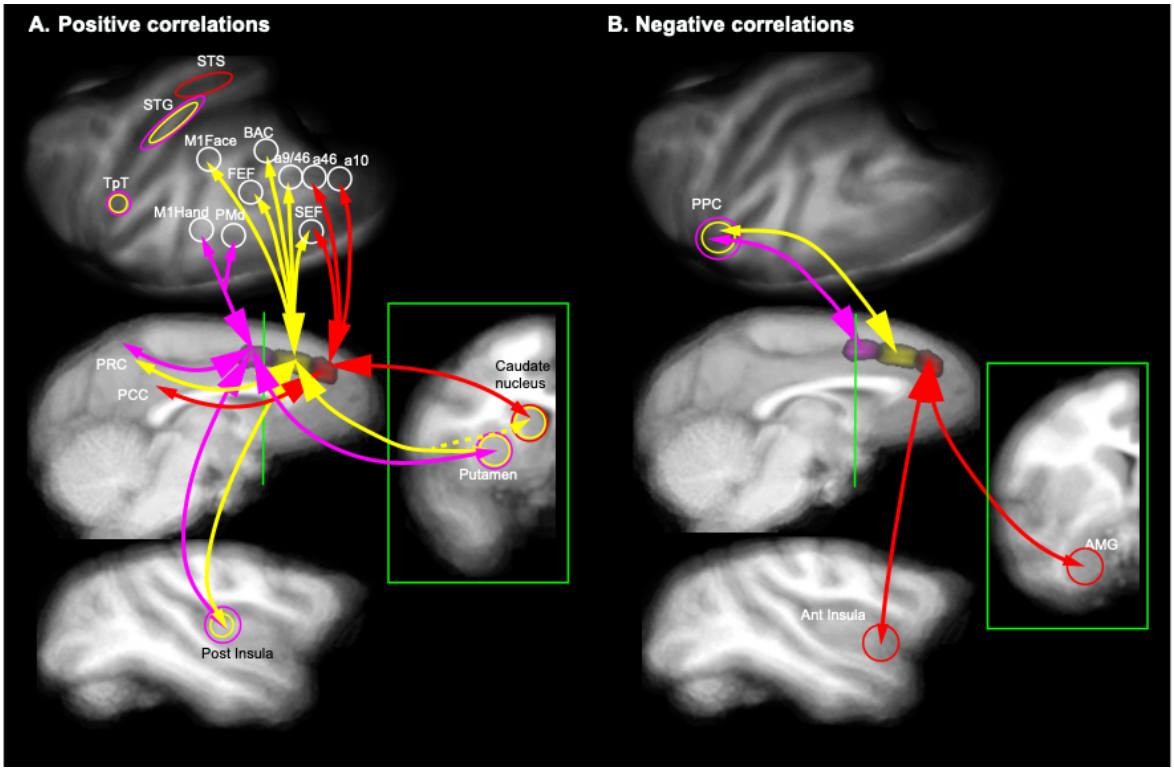

Figure 15. Whole-brain functional connectivity of the cingulate sulcus. A. Positive correlations. B Negative correlations. The green line indicates the location of the coronal section in green box. STS: superior temporal sulcus, STG: superior temporal gyrus, TpT: temporo-parietal cortex, PMd: dorsal premotor area, PRC: precuneus, PCC: posterior cingulate cortex, PPC: posterior parietal cortex, AMG: amygdala., Ant and Post Insula: anterior and posterior insula.

FC organization between the cingulate and principal sulci

Recordings in monkeys but also functional brain imaging studies in humans suggest that the aMCC and subregions of the dlPFC are co-activated for cognitive control regulation (Shenhav et al. 2013; Kolling et al. 2018). Whether such co-activations relate to specific anatomo-functional organizations is thus a central question. We assessed the fine-grained organization of the FC between seeds located in the various subdivisions and along the CgS and the ROIs located along the principal sulcus (*in* dorsal and ventral banks and fundus subdivisions). The analyses provided 2D maps of FC between these different subdivisions (**Fig. 16**).

The pattern of FC followed a rostro-caudal organization with stronger positive correlations between the BOLD signals in the rostral part of the CgS and the anterior most part of the principal sulcus (**Fig. 16**). The increased FC involved more reliably the dorsal bank and the fundus, and less the ventral bank, of the sulcus principalis located anterior to landmark 2 in both hemispheres (*i.e.,* anterior to the level of the rostral end of the CgS. See Materiel and

Methods, *student test, p<0.001.* **Supplementary Fig.3**). This is of great interest because previous studies have shown that morphological landmarks within the principal sulcus could be landmarks of cytoarchitectonic areas, landmark 2 noted here being related to the transition between area 46 and area 10 (Amiez, Sallet, et al. 2023). Note, however, that the FC pattern between the cingulate and the principal sulci differed significantly between the 2 hemispheres (*see model in methods, Main effect of Principal-Sulcus_ROI: p<2.2e-16, Main effect of Cingulate-Sulcus_SEED: p<2.2e-16; Main effect of Hemisphere: p<2.2e-16*). The FC pattern varied also according to the sulcus subdivisions - dorsal, ventral and fundus. In the left hemisphere, the patterns of FC differed between all cingulate parts (*Tukey multiple comparisons test: p<0.0001*) and all principal sulcus parts (*Tukey multiple comparisons test: p<0.0001*). In the right hemisphere, the FC patterns differed when comparing data for the dorsal bank and the fundus of the principal sulcus (*Tukey multiple comparisons test: p<0.002*). From the point of view of the CgS, the FC patterns differed between the dorsal and the ventral banks (*Tukey multiple comparisons test: p<0.04*) and between the fundus and ventral bank (*Tukey multiple comparisons test: p<0.004*). **Supplementary figure 3** shows at what level, and for which sulci parts, the cingulate-principalis connectivity differed from 0. It shows that the FC between Cgs and PS was more pronounced between the fundus parts in both hemispheres.

Finally, negative correlations were more pronounced in the left hemisphere than in the right hemisphere (*Wilcoxon test, p<0.005*) and more specifically in the ventral bank of the principal sulcus (*Dunn tests, p<0.00001*).

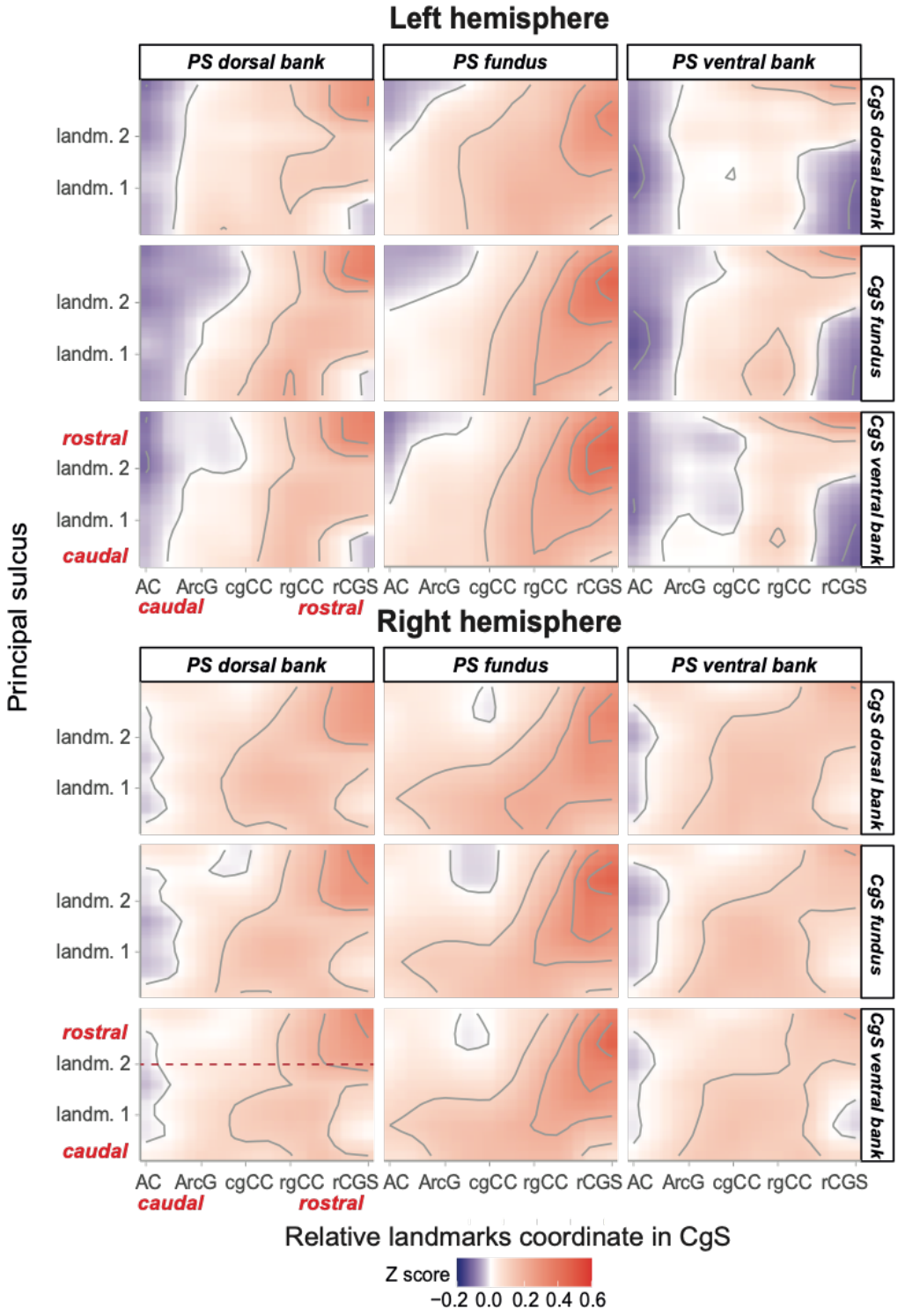

Figure 16. Rostro-caudal organization of the FC between the ventral bank, fundus et dorsal bank of the principal and the cingulate sulci in the left and right hemispheres across the population. Correlation map of the FC between principalis sulcus and cingulate sulcus, represented by the Z-value (red to blue gradient for positive to negative correlations respectively). Data are realigned on specific landmarks for each monkey. AC = anterior commissure, ArcG = genu of the arcuate sulcus, cgCC/rgCC = caudal/rostral limits of genu of corpus callosum, rCGS = rostral end of cingulate sulcus.

Discussion

The present study revealed that cingulo-lateral frontal cortical networks in the macaque brain are organized along a caudo-rostral axis. Using precise and reliable anatomical landmarks, we described a fine-grained anatomo-functional organization. Specifically, in the caudal most CgS seeds, we identified across individual subjects that the hand-related premotor representations of CMAr were located more often in the dorsal bank of the CgS and caudal to the level of the genu of the arcuate sulcus, whereas the face-related representation were located more often in the fundus of the CgS and rostral to the genu of the arcuate. In addition, more rostral parts of the CgS were more strongly functionally connected with more rostral parts of the principal sulcus. Overall, the study revealed a tripartition of the CgS in the frontal lobe shedding new light on the organization of the cingulo-lateral frontal network in non-human primates (**Fig. 15**).

Our results also revealed the presence of a rostro-caudal FC organization between the CgS and the principal sulcus. Although this organization involves the dorsal/ventral banks and fundus of sulci, it appears stronger when considering the fundus of the principal sulcus in both hemispheres (**Fig. 13**). These results fit with the known tract-tracing data between these two regions (Barbas and Pandya 1989; Joyce et al. 2020). By contrast, the most caudal part of the CgS studied here, that includes a CMAr hand motor representation, appears mostly negatively correlated with the principal sulcus, thus reinforcing the existence of anticorrelated networks, here between a motor and a cognitive network.

Somatotopy in CMAr and cingulate functional organization

The respective locations of CMAr hand- and face-related fields in the CgS, detected with FC peaks with M1, are consistent with the literature. Anatomical and functional studies showed that these fields are respectively located in the dorsal bank and fundus of the CgS, with the face-related field located rostral to the hand-related one (**Fig. 12**) (Dum and Strick 2002; Morecraft et al. 2007; Procyk et al. 2016; Cléry et al. 2018). The hand-related subdivision (as represented by FC peaks, **Fig. 12**) was located in the CgS between the level of the anterior commissure and the level of the genu of the arcuate sulcus (ArcG). The core of the face-

related representation was located on average 6mm anterior to the level of ArcG. The known cytoarchitectonic organization suggests that both the hand and face fields of CMAr belong to the aMCC region (Vogt 2005; Amiez et al. 2019). The caudal and rostral limits of aMCC are presumably at the level of, respectively, the anterior commissure and the rostral limit of the genu of the corpus callosum (rgCC) (Vogt et al. 2003; Vogt et al. 2006; Palomero-Gallagher et al. 2009; Amiez et al. 2019).

The data suggest that more caudal versus rostral cingulate seeds displayed positive FC with respectively more caudal versus rostral frontal ROIs (**Fig. 12**). This aligns with previous studies in human and non-human primates (Loh et al. 2018; Giacometti et al. 2022). However, our study reveals a more intricate relationship. Indeed, our clustering suggests that the CgS part under study is subdivided in 3 or in some cases 4 functional sectors: a caudal sector involved with hand-related motor and premotor regions, a middle sector displaying functional connectivity with frontal areas involved with oral and oculomotor/attentional functions (M1face, BAC, FEF, SEF, a9/46), and a more rostral sector connected to anterior prefrontal areas (a46 and a10). The middle face field sector supposedly corresponds to the region the most recorded in neurophysiological studies displaying neural activity related to outcome processing, behavioral shifting, and exploratory decisions (Procyk et al. 2016). This region might even be subdivided in two parts, one related to the oral domain and one to the oculomotor domain. This additional subdivision would further explain why 4 cluster subdivisions was observed in more than 15% of cases among our monkey population. However, the limited spatial resolution of our fMRI data prevents us from clarifying any further. The rostral limit of the face field sector within the CgS is located at the rostro-caudal level of the genu of the corpus callosum. This might represent the limit between aMCC and ACC in the cingulate sulcus, which is also suggested by the clustering method. The whole-brain FC is also showing a shift in large scale connectivity between the 2 posterior and the most anterior cingulate subregion, the anterior part of the CgS being more functionally connected with limbic regions (amygdala and anterior insula) and anterior lateral prefrontal regions (a46, a10) (**Fig. 15**). However, a definitive description of this aMCC-ACC limit will require a devoted cytoarchitectonic and connectivity analysis.

Importantly, the parcellation results, whether the whole-brain data-driven parcellation or the unsupervised clustering within our network of interest, fit perfectly with previous analyses in

macaques showing 3 sectors in the cingulate cortex associated with somato-motor (CMAr hand), attention-orienting (face/eye) and executive networks (Hutchison et al. 2012). The network embedding the attention-orienting sector delineated by Hutchison and colleagues overlaps with a similar frontal anatomical network encompassing regions involved with oral/face motor control and proposed to play a role in communication/emotions and reward processing (Ferrari et al. 2017). We proposed that the mere existence of a CMAr face-related network involved in information-/reward- seeking, shifting and decision making reflects a principle by which such functions are embodied, i.e. that their root mechanisms, and potentially computational principle, are intimately related to effector specificities, the functions being ecologically bounded to these effectors (Procyk et al. 2016).

Parcellations of the cingulate cortex in humans based on connectivity have shown multiple clusters that, for the most anterior ones at least, fit with our observations in macaques in terms of rostro-caudal organization (Beckmann et al. 2009). Beckman and colleagues, using diffusion tractography, found that a caudal cingulate cluster had major premotor connectivity while a more rostral cluster had more prefrontal connectivity. Comparative functional network analyses between humans and macaques have shown good homologies between cingulate subdivisions (Neubert et al. 2015). Interestingly, functional connectivity clustering of the homolog cingulate region in marmosets led to a clear separation at the level of the genu of the corpus callosum, the more caudal cluster being connected to premotor regions, and the anterior ones to prefrontal regions (Schaeffer et al. 2018). Finally, human and marmoset cingulate parcellations showed important similarity regarding their functional connectivity with lateral frontal regions (Schaeffer et al. 2020). Human, macaque and marmoset have thus very conserved subdivisions of the cingulate region although no direct comparisons have been done between the three species.

Brain morphology landmarks and functional connectivity

Cingulate subregions were consistently observed in particular locations relative to morphological landmarks. This converges with a growing body of evidence suggesting tight relationships between gross morphology, sulcal organization, cytoarchitectonic organization, functional organization, and behavior in macaques (Morecraft et al. 2007; García-Cabezas

and Barbas 2014; Procyk et al. 2016; Cléry et al. 2018), chimpanzees (Keller et al. 2009; Amiez et al. 2021), in humans (Vogt et al. 1995; White 1997; Amiez et al. 2006; Amiez and Petrides 2007; Amiez et al. 2013; Loh et al. 2018; Lopez-Persem et al. 2019; Loh et al. 2020) and even in primate comparatives studies (Amiez et al. 2019; Amiez, Sallet, et al. 2023; Amiez, Verstraete, et al. 2023). Such relationships are to be expected given that the cytoarchitectonic organization might constrain the connectivity of a given area (Passingham et al. 2002) and that the protomap tightly links sulcal pits with cytoarchitectonic organization (Rakic 1988; Régis et al. 2005; Fischl et al. 2008), see also (Amiez, Sallet, et al. 2023) for more details about the possible foundations of such relationships). Anatomo-functional maps and morphological landmarks may thus serve as additional indices to locate specific functional subregions. This would be particularly relevant for targeted approaches such as anatomical tracer injections, electrophysiological recordings, or transcranial ultrasound stimulation. Complemented with human-macaque comparative studies of frontal sulcal organizations, these maps could be transposed to humans.

From a clinical point of view, prefrontal to cingulate networks are proposed to play a role in the etiology and manifestations of various neurological and psychiatric disorders. Dysfunctional connectivity between these regions have been observed in a range of conditions including attention deficit hyperactivity disorder (Bush et al. 2005), obsessive-compulsive disorder (Menzies et al. 2008), schizophrenia (Fornito et al. 2009), and mood disorders (Phillips et al. 2003). Thus, characterizing the precise functional connectivity patterns between cingulate and lateral frontal areas could provide markers to quantify pathological connectivity as well as to define targets for potential focused treatments.

Dorso-ventral heterogeneity in the principal sulcus

In our study, we focused on the functional connectivity and data-driven parcellation of the principal sulcus, which revealed a clear rostro-caudal segmentation into three distinct regions. However, we acknowledge the existing evidence for dorsoventral heterogeneity in this area, as detailed by Barbas and Pandya (1989), Morecraft et al. (2015), and Rapan et al. (2023). These studies underscore cytoarchitectonic differences between the dorsal and ventral banks

of the principal sulcus, which our approach did not detect. There are several reasons for this discrepancy. First, our whole-brain functional connectivity analysis might lack the sensitivity to detect subtle dorsoventral differences. Such differences could be specific to particular networks and not broadly reflected across the entire brain, making them challenging to identify with the broad scope of our analysis. Second, the limitations of rsfMRI may also play a role. While rsfMRI is a powerful tool for mapping functional connectivity, its spatial resolution might not be fine enough to capture the detailed cytoarchitectonic distinctions between the dorsal and ventral banks of the principal sulcus. These subtle differences likely require more precise imaging techniques or targeted, high-resolution analyses beyond the capabilities of conventional rsfMRI Furthermore, a comprehensive cytoarchitectonic study that maps the precise boundaries between Areas 10, 46, and 9/46 along the entire extent of the principal sulcus is essential for future research. Such a study would provide a definitive anatomical framework to complement and refine our functional connectivity findings, ensuring that both the functional and structural nuances of this region are thoroughly understood.

Negative functional connectivity

Interestingly, a marginal (non-significant) reverse rostro-caudal organization was captured by the distribution of negative FC peaks (more caudal cingulate seeds display a negative FC peak with more rostral frontal ROIs; **Fig. 12**). For example, the FC between the CgS and M1hand is characterized by a positive FC peak located in the posterior part of aMCC and a negative FC peak in the ACC (**Fig 12**). The interpretation and relevance of negative correlations in BOLD signal in general is still misunderstood and disputed (Biswal et al. 1995; Chang and Glover 2009; Giove et al. 2009; Murphy et al. 2009; Weissenbacher et al. 2009) and often neglected (Chen and Calhoun 2011). However, recent hypotheses suggest that two anticorrelated systems such as the Default Mode Network (DMN, involved in some introspection activity at rest, see (Gusnard et al. 2001; Raichle et al. 2001) and the Dorsal Attentional Network (DAN, involved in the performance of cognitive tasks, are competitive networks that cannot act at the same time and are thus “inhibiting” each other depending on the context (Fransson 2005; Kelly et al. 2008; Chai et al. 2012; Chai et al. 2014). Such a process appears critical to obtain a dynamic but stable system (Saberi et al. 2021), its

disruption being observed in numerous neurological and psychiatric disorders (Wang and Fan 2007; Sun et al. 2012; Patriat et al. 2016; Posner et al. 2016; Whitfield-Gabrieli et al. 2018). Anterior versus posterior subdivisions of the cingulate region devoted to respectively emotional and cognitive processing have been proposed in humans, with a putative reciprocal suppression (Bush et al. 2000). Based on this literature, our results might suggest that the recruitment of CMAr, which is located in the aMCC, is associated with the deactivation of ACC regions, or rather that regions involved with motor control (through links with the primary motor cortex) are naturally in opposition with regions involved with the lateral prefrontal regions. Note however that our data were obtained from anesthetized states (see Limitations).

Limitation

Our results were fairly reliable across our 15 monkeys despite the fact that they were acquired under isoflurane anesthesia, which is known to affect FC (Hutchison et al. 2014; Barttfeld et al. 2015; Lv et al. 2016) In particular, anesthesia reduces FC strength in general and reduces negative correlations (at least in frontal networks) (Hori et al. 2020; Giacometti et al. 2022). We have also shown that it prevents the assessment of posterior cingulate motor areas (CMAc) as they are strongly connected with the primary motor areas (as opposed to CMAr) and these latter regions are shut down by anesthesia (Giacometti et al. 2022). However, we excluded here the assessment of the FC of CMAc. Thus, although anesthesia decreases globally the FC strength in our network of interest, it does not change its overall pattern (Giacometti et al. 2022). Furthermore, it allowed us to perform our subject-by-subject analysis in a larger dataset (18 monkeys), and importantly our results demonstrated the reliability of the use of sulcal individual morphological patterns to extract fine-grained FC patterns in the frontal cortex.

Conclusion

The present study revealed that the cingulate organization can be captured in individual monkey brains based on the functional connectivity pattern of the CgS and the lateral frontal cortex. We identified the fine-grained FC interplay between the cingulate and the principal

sulci that might sustain the functional dialogue between these regions. Importantly, this organization can also be predicted from local morphological features that all individuals possess, thus providing a framework usable with short resting-state MRI scans to precisely target cingulate or lateral frontal cortical regions. Finally, subdivisions of the cingulate region of interest are characterized by their embedding in dissociated functional networks, whose specificity should be considered in order to understand the computational bases of cingulate functions.

Authors' contributions

E.P. and C.A. organized the project. F.L. defined and optimized neuroimaging acquisition protocols. C.G., D.A-C., A.D., C.W., M.DI, and F.H.-B acquired neuroimaging data. C.V. did the clusterisation algorithm. M.Du., E.P., and C.A. analyzed and interpreted data. M.Du., E.P., C.A. and C.W. wrote the article. The authors thank V Vezoli, N. Ferroukhi, and C Nay for administrative help and support, and A. Bellemin-Menard, F. Da Silva Couto, J Lachaud, G Gardechaux, and M Filiptchenko for help and support with animal welfare and care.

Funding

This work was supported by Fondation pour la Recherche Médicale, by the ANR-19-CE37-0008-01, ANR-18-CE37-0016 and ANR-18-CE37-0012, and was performed within the framework of the LABEX CORTEX (ANR-11-LABX-0042) of Université de Lyon operated by the French National Research Agency (ANR). E.P. and C.A. are employed by the Centre National de la Recherche Scientifique.

Supplementary figures

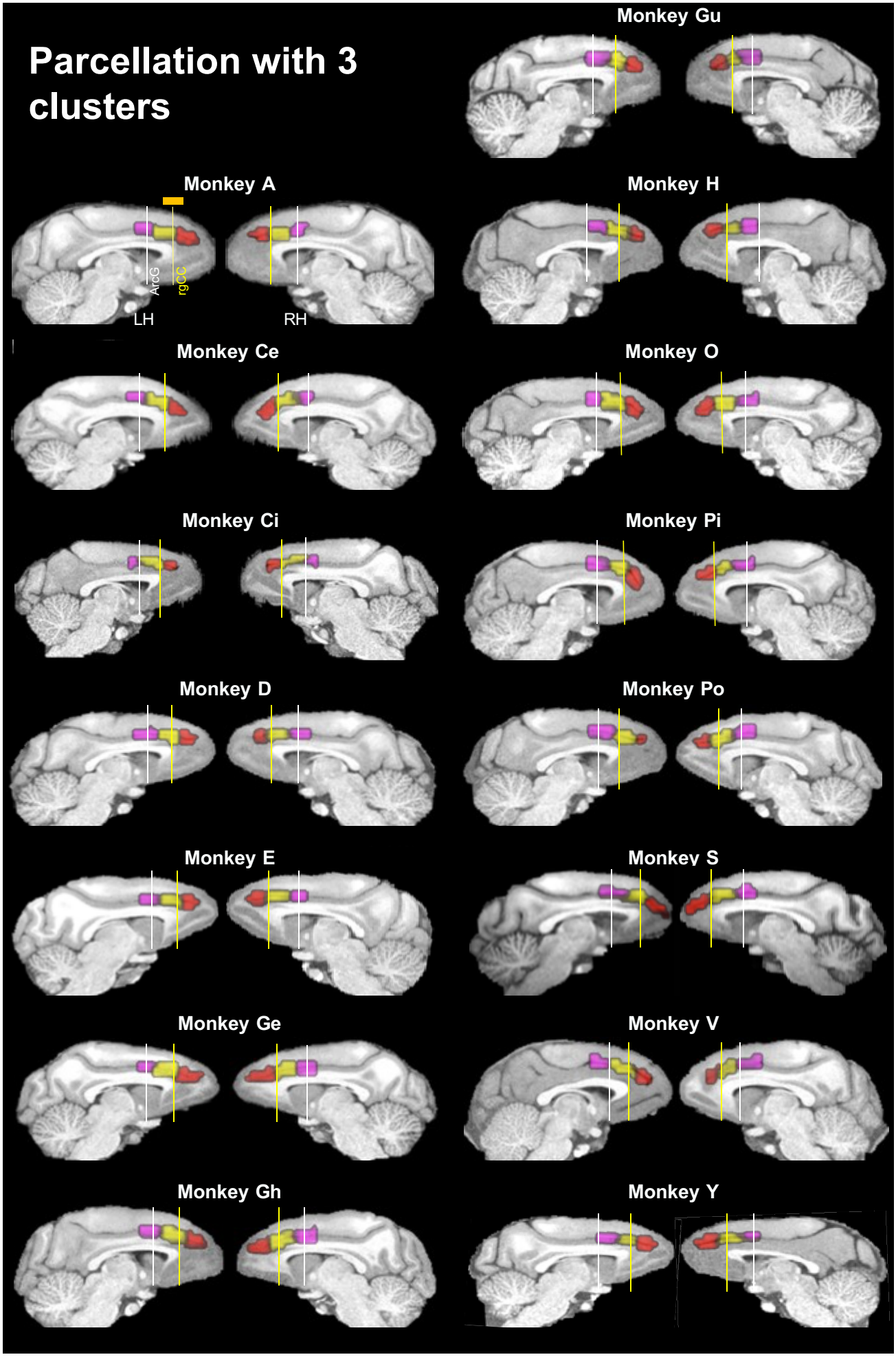

Supplementary figure 1. 3 clusters parcellation for each hemisphere. Data are displayed on the MRI volume of each animal. Note that morphological landmarks (white and yellow lines) provide indications about the relative position of clusters. White line: antero-posterior level of the genu of the arcuate sulcus. Yellow line: antero posterior level of the rostral limit of the corpus callosum.

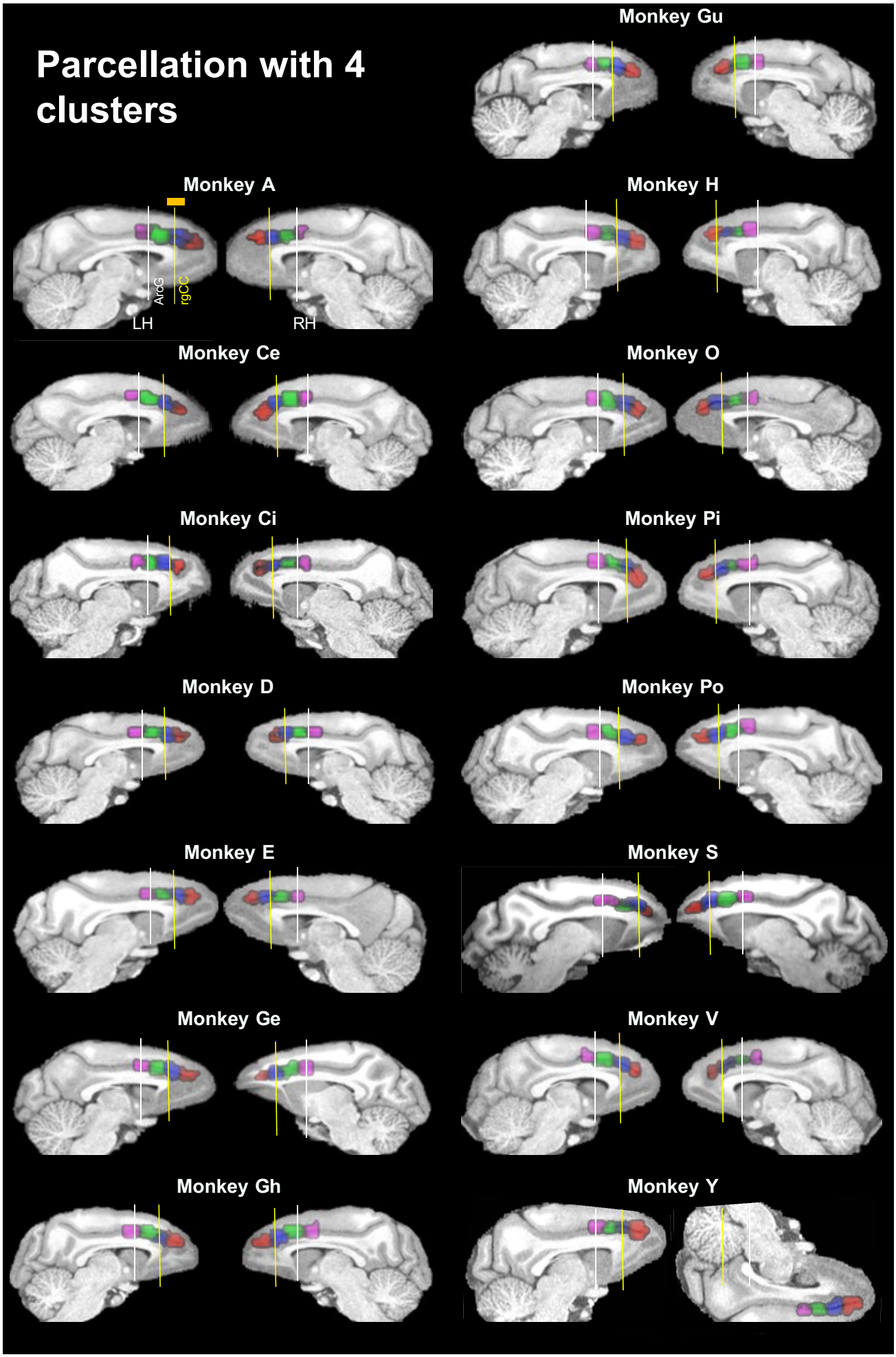

Supplementary figure 2. 4 clusters parcellation for each hemisphere. Data are displayed on the MRI volume of each animal. White line: antero-posterior level of the genu of the arcuate sulcus. Yellow line: antero posterior level of the rostral limit of the corpus callosum.

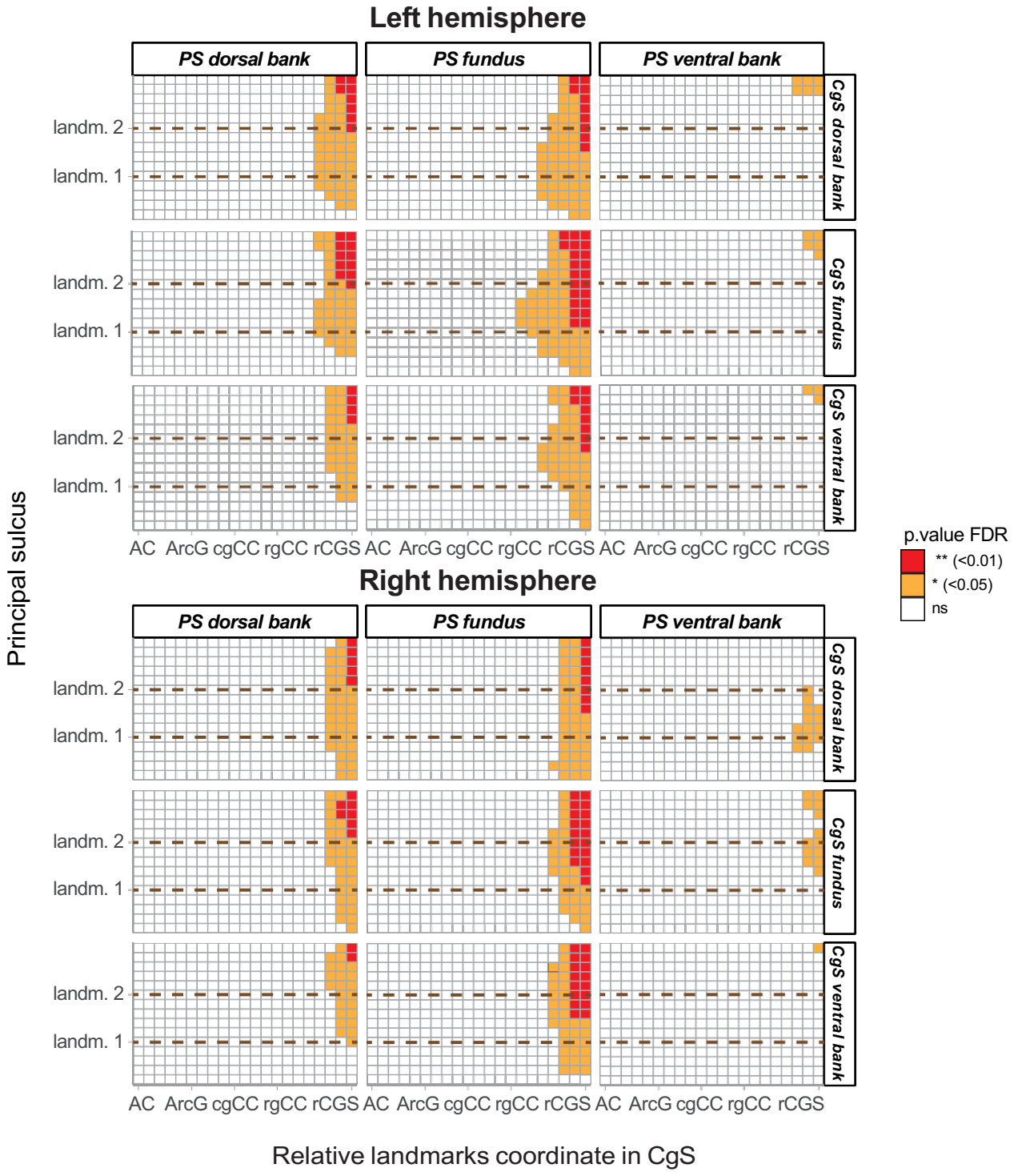

Supplementary figure 3. Statistical map of the functional connectivity between the ventral bank, fundus, and dorsal bank of the principal and the cingulate sulci in the left and right hemispheres across the population, represented by the FDR (false discovery rate) p-value of difference to zero t-tests. Data are realigned on specific landmarks for each monkey. AC = anterior commissure,, ArcG = arcuate genu, cgCC/rgCC = caudal/rostral genu of corpus callosum, rCGS = rostral end of cingulate sulcus.

References

Amiez C, Joseph JP, Procyk E. 2006. Reward Encoding in the Monkey Anterior Cingulate Cortex. Cerebral Cortex. 16(7):1040–1055. doi:10.1093/cercor/bhj046.

Amiez C, Neveu R, Warrot D, Petrides M, Knoblauch K, Procyk E. 2013. The Location of Feedback-Related Activity in the Midcingulate Cortex Is Predicted by Local Morphology. J Neurosci 33(5):2217–2228. doi:10.1523/JNEUROSCI2779-12.2013.

Amiez C, Petrides M. 2007. Selective involvement of the mid-dorsolateral prefrontal cortex in the coding of the serial order of visual stimuli in working memory. Proc Natl Acad Sci USA. 104(34):13786–13791. doi:10.1073/pnas.0706220104.

Amiez C, Petrides M. 2009. Anatomical organization of the eye fields in the human and non-human primate frontal cortex. Progress in Neurobiology. 89(2):220–230. doi:10.1016/j.pneurobio.2009.07.010.

Amiez C, Petrides M. 2014. Neuroimaging Evidence of the Anatomo-Functional Organization of the Human Cingulate Motor Areas. Cerebral Cortex. 24(3):563–578. doi:10.1093/cercor/bhs329.

Amiez C, Sallet J, Giacometti C, Verstraete C, Gandaux C, Morel-Latour V, Meguerditchian A, Hadj-Bouziane F, Ben Hamed S, Hopkins WD, et al. 2023. A revised perspective on the evolution of the lateral frontal cortex in primates. Sci Adv. 9(20):eadf9445. doi:10.1126/sciadv.adf9445.

Amiez C, Sallet J, Hopkins WD, Meguerditchian A, Hadj-Bouziane F, Ben Hamed S, Wilson CRE, Procyk E, Petrides M. 2019. Sulcal organization in the medial frontal cortex provides insights into primate brain evolution. Nat Commun. 10(1):3437. doi:10.1038/s41467-019-11347-x.

Amiez C, Sallet J, Novek J, Hadj-Bouziane F, Giacometti C, Andersson J, Hopkins WD, Petrides M. 2021. Chimpanzee histology and functional brain imaging show that the paracingulate sulcus is not human-specific. Commun Biol. 4(1):54. doi:10.1038/s42003-020-01571-3.

Amiez C, Verstraete C, Sallet J, Hadj-Bouziane F, Ben Hamed S, Meguerditchian A, Procyk E, Wilson CRE, Petrides M, Sherwood CC, et al. 2023. The relevance of the unique anatomy of the human prefrontal operculum to the emergence of speech. Commun Biol. 6(1):693. doi:10.1038/s42003-023-05066-9.

Badre D, D'Esposito M. 2009. Is the rostro-caudal axis of the frontal lobe hierarchical? Nat Rev Neurosci 10(9):659–669. doi:10.1038/nrn2667.

Barbas H, Pandya DN. 1989. Architecture and intrinsic connections of the prefrontal cortex in the rhesus monkey. J of Comparative Neurology. 286(3):353–375. doi:10.1002/cne.902860306.

Barttfeld P, Uhrig L, Sitt JD, Sigman M, Jarraya B, Dehaene S. 2015. Signature of consciousness in the dynamics of resting-state brain activity. Proc Natl Acad Sci USA. 112(3):887–892. doi:10.1073/pnas.1418031112.

Beckmann M, Johansen-Berg H, Rushworth MFS. 2009. Connectivity-Based Parcellation of Human Cingulate Cortex and Its Relation to Functional Specialization. J Neurosci 29(4):1175–1190. doi:10.1523/JNEUROSCI3328-08.2009.

Biswal B, Zerrin Yetkin F, Haughton VM, Hyde JS. 1995. Functional connectivity in the motor cortex of resting human brain using echo-planar mrI Magnetic Resonance in Med. 34(4):537–541. doi:10.1002/mrm.1910340409.

Borra E, Ferroni CG, Gerbella M, Giorgetti V, Mangiaracina C, Rozzi S, Luppino G. 2017. Rostro-caudal Connectional Heterogeneity of the Dorsal Part of the Macaque Prefrontal Area 46. Cerebral Cortex. 29(2):485–504. doi:10.1093/cercor/bhx332.

Bruce CJ, Goldberg ME, Bushnell MC, Stanton GB 1985. Primate frontal eye fields. II Physiological and anatomical correlates of electrically evoked eye movements. Journal of Neurophysiology. 54(3):714–734. doi:10.1152/jn.1985.54.3.714.

Bush G, Luu P, Posner MI 2000. Cognitive and emotional influences in anterior cingulate cortex. Trends in Cognitive Sciences. 4(6):215–222. doi:10.1016/S1364-6613(00)01483-2.

Bush G, Valera EM, Seidman LJ. 2005. Functional Neuroimaging of Attention-Deficit/Hyperactivity Disorder: A Review and Suggested Future Directions. Biological Psychiatry. 57(11):1273–1284. doi:10.1016/j.biopsych.2005.01.034.

Chai XJ, Castañón AN, Öngür D, Whitfield-Gabrieli S. 2012. Anticorrelations in resting state networks without global signal regression. NeuroImage. 59(2):1420–1428. doi:10.1016/j.neuroimage.2011.08.048.

Chai XJ, Ofen N, Gabrieli JDE, Whitfield-Gabrieli S. 2014. Selective Development of Anticorrelated Networks in the Intrinsic Functional Organization of the Human Brain. Journal of Cognitive Neuroscience. 26(3):501–513. doi:10.1162/jocn_a_00517.

Chang C, Glover GH. 2009. Relationship between respiration, end-tidal CO2, and BOLD signals in resting-state fMRI NeuroImage. 47(4):1381–1393. doi:10.1016/j.neuroimage.2009.04.048.

Chaudhuri R, Knoblauch K, Gariel M-A, Kennedy H, Wang X-J. 2015. A Large-Scale Circuit Mechanism for Hierarchical Dynamical Processing in the Primate Cortex. Neuron. 88(2):419–431. doi:10.1016/j.neuron.2015.09.008.

Chen Z, Calhoun VD. 2011. Two pitfalls of BOLD fMRI magnitude-based neuroimage analysis: Non-negativity and edge effect. Journal of Neuroscience Methods. 199(2):363–369. doi:10.1016/j.jneumeth.2011.05.018.

Cheng L, Zhang Y, Li G, Wang J, Sherwood C, Gong G, Fan L, Jiang T. 2021. Connectional asymmetry of the inferior parietal lobule shapes hemispheric specialization in humans, chimpanzees, and rhesus macaques. eLife. 10:e67600. doi:10.7554/eLife.67600.

Cléry J, Amiez C, Guipponi O, Wardak C, Procyk E, Ben Hamed S. 2018. Reward activations and face fields in monkey cingulate motor areas. Journal of Neurophysiology. 119(3):1037–1044. doi:10.1152/jn.00749.2017.

Constantinidis C, Qi X-L. 2018. Representation of Spatial and Feature Information in the Monkey Dorsal and Ventral Prefrontal Cortex. Front Integr Neurosci 12:31. doi:10.3389/fnint.2018.00031.

Cox RW. 1996. AFNI: Software for Analysis and Visualization of Functional Magnetic Resonance Neuroimages. Computers and Biomedical Research. 29(3):162–173. doi:10.1006/cbmr.1996.0014.

Dixon ML, Fox KCR, Christoff K. 2014. Evidence for rostro-caudal functional organization in multiple brain areas related to goal-directed behavior. Brain Research. 1572:26–39. doi:10.1016/j.brainres.2014.05.012.

Dum R, Strick P. 2002. Motor areas in the frontal lobe of the primate. Physiology & Behavior. 77(4–5):677–682. doi:10.1016/S0031-9384(02)00929-0.

Duncan J, Assem M, Shashidhara S. 2020. Integrated Intelligence from Distributed Brain Activity. Trends in Cognitive Sciences. 24(10):838–852. doi:10.1016/j.tics.2020.06.012.

Fanton S, Thompson WH. 2023. *NetPlotBrain* : A Python package for visualizing networks and brains. Network Neuroscience. 7(2):461–477. doi:10.1162/netn_a_00313.

Ferrari PF, Gerbella M, Coudé G, Rozzi S. 2017. Two different mirror neuron networks: The sensorimotor (hand) and limbic (face) pathways. Neuroscience. 358:300–315. doi:10.1016/j.neuroscience.2017.06.052.

Fischl B, Rajendran N, Busa E, Augustinack J, Hinds O, Yeo BTT, Mohlberg H, Amunts K, Zilles K. 2008. Cortical Folding Patterns and Predicting Cytoarchitecture. Cerebral Cortex. 18(8):1973–1980. doi:10.1093/cercor/bhm225.

Fontanier V, Sarazin M, Stoll FM, Delord B, Procyk E. 2022. Inhibitory control of frontal metastability sets the temporal signature of cognition. eLife. 11:e63795. doi:10.7554/eLife.63795.

Fornito A, Yücel M, Patti J, Wood SJ, Pantelis C. 2009. Mapping grey matter reductions in schizophrenia: An anatomical likelihood estimation analysis of voxel-based morphometry studies. Schizophrenia Research. 108(1–3):104–113. doi:10.1016/j.schres.2008.12.011.

Fransson P. 2005. Spontaneous low-frequency BOLD signal fluctuations: An fMRI investigation of the resting-state default mode of brain function hypothesis. Human Brain Mapping. 26(1):15–29. doi:10.1002/hbm.20113.

García-Cabezas MÁ, Barbas H. 2014. A direct anterior cingulate pathway to the primate primary olfactory cortex may control attention to olfaction. Brain Struct Funct. 219(5):1735–1754. doi:10.1007/s00429-013-0598-3.

Giacometti C, Amiez C, Hadj-Bouziane F. 2023. Multiple routes of communication within the amygdala-mPFC network: A comparative approach in humans and macaques. Current Research in Neurobiology. 5:100103. doi:10.1016/j.crneur.2023.100103.

Giacometti C, Dureux A, Autran-Clavagnier D, Wilson CRE, Sallet J, Dirheimer M, Procyk E, Hadj-Bouziane F, Amiez C. 2022. Frontal cortical functional connectivity is impacted by anaesthesia in macaques. Cerebral Cortex. 32(18):4050–4067. doi:10.1093/cercor/bhab465.

Giove F, Gili T, Iacovella V, Macaluso E, Maraviglia B 2009. Images-based suppression of unwanted global signals in resting-state functional connectivity studies. Magnetic Resonance Imaging. 27(8):1058–1064. doi:10.1016/j.mrI2009.06.004.

Graziano MSA, Taylor CSR, Moore T. 2002. Complex Movements Evoked by Microstimulation of Precentral Cortex.

Gusnard DA, Akbudak E, Shulman GL, Raichle ME. 2001. Medial prefrontal cortex and self-referential mental activity: Relation to a default mode of brain function. Proc Natl Acad Sci USA. 98(7):4259–4264. doi:10.1073/pnas.071043098.

Harris CR, Millman KJ, Van Der Walt SJ, Gommers R, Virtanen P, Cournapeau D, Wieser E, Taylor J, Berg S, Smith NJ, et al. 2020. Array programming with NumPy. Nature. 585(7825):357–362. doi:10.1038/s41586-020-2649-2.

He S, Dum R, Strick P. 1993. Topographic organization of corticospinal projections from the frontal lobe: motor areas on the lateral surface of the hemisphere. J Neuroscl 13(3):952–980. doi:10.1523/JNEUROSCI13-03-00952.1993.

Hori Y, Schaeffer DJ, Gilbert KM, Hayrynen LK, Cléry JC, Gati JS, Menon RS, Everling S. 2020. Altered Resting-State Functional Connectivity Between Awake and Isoflurane Anesthetized Marmosets. Cerebral Cortex. 30(11):5943–5959. doi:10.1093/cercor/bhaa168.

Hutchison RM, Hutchison M, Manning KY, Menon RS, Everling S. 2014. Isoflurane induces dose-dependent alterations in the cortical connectivity profiles and dynamic properties of the brain's functional architecture: Dose-Dependent Isoflurane Effects. Hum Brain Mapp. 35(12):5754–5775. doi:10.1002/hbm.22583.

Hutchison RM, Womelsdorf T, Gati JS, Leung LS, Menon RS, Everling S. 2012. Resting-State Connectivity Identifies Distinct Functional Networks in Macaque Cingulate Cortex. Cerebral Cortex. 22(6):1294–1308. doi:10.1093/cercor/bhr181.

Jenkinson M, Beckmann CF, Behrens TEJ, Woolrich MW, Smith SM. 2012. FSL. NeuroImage. 62(2):782–790. doi:10.1016/j.neuroimage.2011.09.015.

Joyce MKP, García-Cabezas MÁ, John YJ, Barbas H. 2020. Serial Prefrontal Pathways Are Positioned to Balance Cognition and Emotion in Primates. J Neurosci 40(43):8306–8328. doi:10.1523/JNEUROSCI0860-20.2020.

Jung B, Taylor PA, Seidlitz J, Sponheim C, Perkins P, Ungerleider LG, Glen D, Messinger A. 2021. A comprehensive macaque fMRI pipeline and hierarchical atlas. NeuroImage. 235:117997. doi:10.1016/j.neuroimage.2021.117997.

Keller SS, Crow T, Foundas A, Amunts K, Roberts N. 2009. Broca's area: Nomenclature, anatomy, typology and asymmetry. Brain and Language. 109(1):29–48. doi:10.1016/j.bandl.2008.11.005.

Kelly AMC, Uddin LQ, Biswal BB, Castellanos FX, Milham MP. 2008. Competition between functional brain networks mediates behavioral variability. NeuroImage. 39(1):527–537. doi:10.1016/j.neuroimage.2007.08.008.

Kolling N, Scholl J, Chekroud A, Trier HA, Rushworth MFS. 2018. Prospection, Perseverance, and Insight in Sequential Behavior. Neuron. 99(5):1069-1082.e7. doi:10.1016/j.neuron.2018.08.018.

Kouneiher F, Charron S, Koechlin E. 2009. Motivation and cognitive control in the human prefrontal cortex. Nat Neurosci 12(7):939–945. doi:10.1038/nn.2321.

Loh KK, Hadj-Bouziane F, Petrides M, Procyk E, Amiez C. 2018. Rostro-Caudal Organization of Connectivity between Cingulate Motor Areas and Lateral Frontal Regions. Front Neurosci 11:753. doi:10.3389/fnins.2017.00753.

Loh KK, Procyk E, Neveu R, Lamberton F, Hopkins WD, Petrides M, Amiez C. 2020. Cognitive control of orofacial motor and vocal responses in the ventrolateral and dorsomedial human frontal cortex. Proc Natl Acad Sci USA. 117(9):4994–5005. doi:10.1073/pnas.1916459117.

Lopez-Persem A, Verhagen L, Amiez C, Petrides M, Sallet J. 2019. The Human Ventromedial Prefrontal Cortex: Sulcal Morphology and Its Influence on Functional Organization. J Neurosci 39(19):3627–3639. doi:10.1523/JNEUROSCI2060-18.2019.

von Luxburg U. 2007. A Tutorial on Spectral Clustering. [accessed 2024 Feb 26]. http://arxiv.org/abs/0711.0189.

Lv P, Xiao Y, Liu B, Wang Y, Zhang X, Sun H, Li F, Yao L, Zhang W, Liu L, et al. 2016. Dose-dependent effects of isoflurane on regional activity and neural network function: A resting-state fMRI study of 14 rhesus monkeys. Neuroscience Letters. 611:116–122. doi:10.1016/j.neulet.2015.11.037.

McKinney W. 2010. Data Structures for Statistical Computing in Python. Austin, Texas. p. 56–61. [accessed 2024 Feb 26]. https://conference.scipy.org/proceedings/scipy2010/mckinney.html.

Menzies L, Chamberlain SR, Laird AR, Thelen SM, Sahakian BJ, Bullmore ET. 2008. Integrating evidence from neuroimaging and neuropsychological studies of obsessive-compulsive disorder: The orbitofronto-striatal model revisited. Neuroscience & Biobehavioral Reviews. 32(3):525–549. doi:10.1016/j.neubiorev.2007.09.005.

Morecraft RJ, McNeal DW, Stilwell-Morecraft KS, Gedney M, Ge J, Schroeder CM, Van Hoesen GW. 2007. Amygdala interconnections with the cingulate motor cortex in the rhesus monkey. J of Comparative Neurology. 500(1):134–165. doi:10.1002/cne.21165.

Murphy K, Birn RM, Handwerker DA, Jones TB, Bandettini PA. 2009. The impact of global signal regression on resting state correlations: Are anti-correlated networks introduced? NeuroImage. 44(3):893–905. doi:10.1016/j.neuroimage.2008.09.036.

Neubert F-X, Mars RB, Sallet J, Rushworth MFS. 2015. Connectivity reveals relationship of brain areas for reward-guided learning and decision making in human and monkey frontal cortex. Proc Natl Acad Sci USA. 112(20). doi:10.1073/pnas.1410767112. [accessed 2024 Feb 26]. https://pnas.org/doi/full/10.1073/pnas.1410767112.

Palomero-Gallagher N, Mohlberg H, Zilles K, Vogt B 2009. Cytology and receptor architecture of human anterior cingulate cortex. J of Comparative Neurology. 508(6):906–926. doi:10.1002/cne.21684.

Passingham RE, Stephan KE, Kötter R. 2002. The anatomical basis of functional localization in the cortex. Nat Rev Neuroscl 3(8):606–616. doi:10.1038/nrn893.

Patriat R, Birn RM, Keding TJ, Herringa RJ. 2016. Default-Mode Network Abnormalities in Pediatric Posttraumatic Stress Disorder. Journal of the American Academy of Child & Adolescent Psychiatry. 55(4):319–327. doi:10.1016/j.jaac.2016.01.010.

Paus T. 2001. Primate anterior cingulate cortex: Where motor control, drive and cognition interface. Nat Rev Neuroscl 2(6):417–424. doi:10.1038/35077500.

Pedregosa F, Varoquaux G, Gramfort A, Michel V, Thirion B, Grisel O, Blondel M, Prettenhofer P, Weiss R, Dubourg V, et al. Scikit-learn: Machine Learning in Python. MACHINE LEARNING IN PYTHON.

Petrides M, Cadoret G, Mackey S. 2005. Orofacial somatomotor responses in the macaque monkey homologue of Broca's area. Nature. 435(7046):1235–1238. doi:10.1038/nature03628.

Phillips ML, Drevets WC, Rauch SL, Lane R. 2003. Neurobiology of emotion perception II: implications for major psychiatric disorders. Biological Psychiatry. 54(5):515–528. doi:10.1016/S0006-3223(03)00171-9.

Picard N, Strick PL. 1996. Motor Areas of the Medial Wall: A Review of Their Location and Functional Activation. Cereb Cortex. 6(3):342–353. doi:10.1093/cercor/6.3.342.

Posner J, Song I, Lee S, Rodriguez CI, Moore H, Marsh R, Blair Simpson H. 2016. Increased functional connectivity between the default mode and salience networks in unmedicated adults with obsessive-compulsive disorder: Default Mode and Salience Networks in OCD. Hum Brain Mapp. 38(2):678–687. doi:10.1002/hbm.23408.

Procyk E, Wilson CRE, Stoll FM, Faraut MCM, Petrides M, Amiez C. 2016. Midcingulate Motor Map and Feedback Detection: Converging Data from Humans and Monkeys. Cereb Cortex.:bhu213. doi:10.1093/cercor/bhu213.

Raichle ME, MacLeod AM, Snyder AZ, Powers WJ, Gusnard DA, Shulman GL. 2001. A default mode of brain function. Proc Natl Acad Sci USA. 98(2):676–682. doi:10.1073/pnas.98.2.676.

Rakic P. 1988. Specification of Cerebral Cortical Areas. Science. 241(4862):170–176. doi:10.1126/science.3291116.

Régis J, Mangin J-F, Ochiai T, Frouin V, Riviére D, Cachia A, Tamura M, Samson Y. 2005. "Sulcal Root" Generic Model: a Hypothesis to Overcome the Variability of the Human Cortex Folding Patterns. Neurol Med Chir(Tokyo). 45(1):1–17. doi:10.2176/nmc.45.1.

Rizzolatti G, Luppino G. 2001. The Cortical Motor System. Neuron. 31(6):889–901. doi:10.1016/S0896-6273(01)00423-8.

Saberi M, Khosrowabadi R, Khatibi A, Misic B, Jafari G. 2021. Topological impact of negative links on the stability of resting-state brain network. Sci Rep. 11(1):2176. doi:10.1038/s41598-021-81767-7.

Schaeffer DJ, Gilbert KM, Ghahremani M, Gati JS, Menon RS, Everling S. 2018. Intrinsic functional clustering of anterior cingulate cortex in the common marmoset. NeuroImage. 186:301–307. doi:10.1016/j.neuroimage.2018.11.005.

Schaeffer DJ, Hori Y, Gilbert KM, Gati JS, Menon RS, Everling S. 2020. Divergence of rodent and primate medial frontal cortex functional connectivity. Proc Natl Acad Sci USA. 117(35):21681–21689. doi:10.1073/pnas.2003181117.

Schlag J, Schlag-Rey M. 1987. Evidence for a supplementary eye field. Journal of Neurophysiology. 57(1):179–200. doi:10.1152/jn.1987.57.1.179.

Seidlitz J, Sponheim C, Glen D, Ye FQ, Saleem KS, Leopold DA, Ungerleider L, Messinger A. 2018. A population MRI brain template and analysis tools for the macaque. NeuroImage. 170:121–131. doi:10.1016/j.neuroimage.2017.04.063.

Shenhav A, Botvinick MM, Cohen JD. 2013. The Expected Value of Control: An Integrative Theory of Anterior Cingulate Cortex Function. Neuron. 79(2):217–240. doi:10.1016/j.neuron.2013.07.007.

Sun L, Cao Q, Long X, Sui M, Cao X, Zhu C, Zuo X, An L, Song Y, Zang Y, et al. 2012. Abnormal functional connectivity between the anterior cingulate and the default mode network in drug-naïve boys with attention deficit hyperactivity disorder. Psychiatry Research: Neuroimaging. 201(2):120–127. doi:10.1016/j.pscychresns.2011.07.001.

Vogt BA. 2005. Pain and emotion interactions in subregions of the cingulate gyrus. Nat Rev Neurosci 6(7):533–544. doi:10.1038/nrn1704.

Vogt BA. 2016. Midcingulate cortex: Structure, connections, homologies, functions and diseases. Journal of Chemical Neuroanatomy. 74:28–46. doi:10.1016/j.jchemneu.2016.01.010.

Vogt BA, Berger GR, Derbyshire SWG. 2003. Structural and Functional Dichotomy of Human Midcingulate Cortex. Eur J Neurosci 18(11):3134–3144.

Vogt BA, Nimchinsky EA, Vogt LJ, Hof PR. 1995. Human cingulate cortex: Surface features, flat maps, and cytoarchitecture. J of Comparative Neurology. 359(3):490–506. doi:10.1002/cne.903590310.

Vogt BA, Vogt L, Laureys S. 2006. Cytology and functionally correlated circuits of human posterior cingulate areas. NeuroImage. 29(2):452–466. doi:10.1016/j.neuroimage.2005.07.048.

Wang H, Fan J. 2007. Human Attentional Networks: A Connectionist Model. Journal of Cognitive Neuroscience. 19(10):1678–1689. doi:10.1162/jocn.2007.19.10.1678.

Weissenbacher A, Kasess C, Gerstl F, Lanzenberger R, Moser E, Windischberger C. 2009. Correlations and anticorrelations in resting-state functional connectivity MRI: A quantitative comparison of preprocessing strategies. NeuroImage. 47(4):1408–1416. doi:10.1016/j.neuroimage.2009.05.005.

White L. 1997. Structure of the human sensorimotor system. I: Morphology and cytoarchitecture of the central sulcus. Cerebral Cortex. 7(1):18–30. doi:10.1093/cercor/7.1.18.

Whitfield-Gabrieli S, Fischer AS, Henricks AM, Khokhar JY, Roth RM, Brunette MF, Green AI 2018. Understanding marijuana's effects on functional connectivity of the default mode network in patients with schizophrenia and co-occurring cannabis use disorder: A pilot investigation. Schizophrenia Research. 194:70–77. doi:10.1016/j.schres.2017.07.029.

II. Conclusion

This study highlighted the importance of considering the antero-posterior gradient connectivity pattern in the MCC and the LPFC instead of studying each area as a whole. We decided to separate our FMAs in 6 antero-posterior groups following this work to fine-tune our analysis and take into account the antero-posterior level.

Chapter 2. Behavioural strategy in discrimination learning (DL) task

I. Introduction

The discrimination learning (DL) task is a classic tool in neuroscience (Harlow, 1949). Its simplicity, well-documented nature, and extensive study make it invaluable for evaluating both basic learning processes and the learning to learn strategies (Beran et al., 2008; Izquierdo et al., 2004). Whilst a very simple task, DL has the benefit that the task permits clear separation between individual problem learning, which must occur for every problem as stimuli are always novel, and overall task acquisition to an expert level demonstrated by a gradual reduction in the errors required to reach a criterion on successive problems. Specifically, Harlow characterised this latter process as the acquisition of a learning set (Harlow, 1949), a process considered one of task-specific strategy acquisition that does not rely on the same cognitive processes (or it turns out neural systems) as the gradual learning of individual problems. This task therefore allows researchers to identify theoretical stages of learning that serve as foundational benchmarks for further investigation.

In addition to studying overall learning approaches, focusing on the behaviour of monkeys in neuroscience is crucial because, like any individual, they exhibit interpersonal differences (Gosling, 2001). These differences manifest in various ways, such as unique characteristics, motivations, levels of fatigue, and working styles (Schapiro et al., 1996). Understanding these variations is essential as they lead to specific work strategies that must be clearly identified before examining the neuronal correlates of learning (Kalcher-Sommersguter et al., 2015). By recognizing and analysing the individual behavioural strategies of each monkey, we can better understand the underlying neural mechanisms. This approach ensures that we account for the personal nuances that influence learning and performance, thereby providing a more comprehensive and accurate picture of cognitive processes (McGonigle & Chalmers, 2006).

II. Specific materials and methods

The two subjects performed the DL task daily (see general methods) until they reached a "plateau" in their learning curve. This "plateau" was defined as ten successive problems under 10 errors to criterion and we considered it as a marker that the monkey has learned to learn in the task. The total number of sessions was 78 for monkey I and 94 for monkey B The duration of each session was defined by the number of rewards requested: 350 for monkey I and 200 for monkey B We adapted the parameters for each monkey to maintain around one hour of work. At the end of each session, if the monkey reached the requested number of rewards, it received what we called a 'green circle': a large bonus of juice obtained by a simple touch of a large green circle stimulus. As such monkeys received a supplementary motivation to finish the sessions well, in addition to the trial-by-trial rewards.

A correct answer was reinforced with 0.8 ml of 50% diluted apple juice, and an incorrect one was followed by a latency time: 7000 ms for monkey I and 5000 ms for monkey B The latency was longer for monkey I as she appeared to make more compulsive and rapid responses, and the delay had a positive impact on the learning. Notably, because she worked particularly fast, she received a lot of reward even by responding randomly, given random responding elicited a reward every 2 trials on average. Hence slowing her trial rate after errors improved her behaviour.

We chose the stimuli from a pool of random/abstract images and paired them based on colour and shape similarity criteria. One pair represents a problem, with monkey I completing 122 problems and monkey B completing 76 problems.

The statistical analysis was performed using R Studio software with CSV files from EventIDE software.

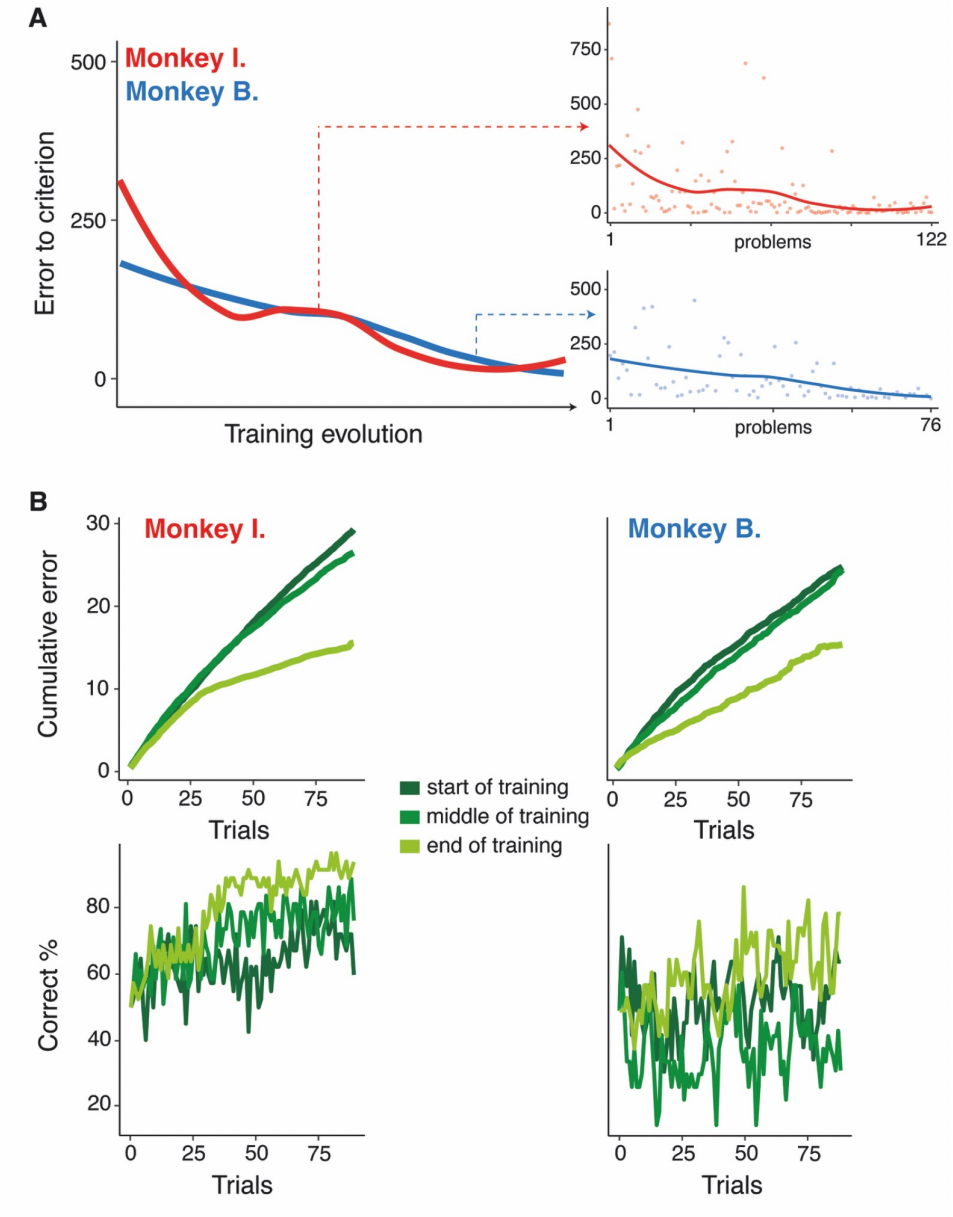

Figure 17. Learning curve in discrimination learning task for both monkeys. A) Training evolution across problems represented by the number of errors to reach the criterion. Left panel: The coloured line represents the LOESS (Locally Estimated Scatterplot Smoothing) fit, a non-parametric regression method that creates a smooth line through the data points by fitting multiple regressions in localised subsets of the data. Right panel: The coloured points represent the real data. B) Performance evolution inside sessions represented by the number of errors (upper panels) and the percentage of correct responses (lower panels). Start, middle and end of training represent the total number of sessions divided in three equal groups. We showed only the first 90 trials as it was the minimum to reach the criterion of a problem.

Monkeys were able to learn problems correctly and attain the behavioural criterion, across a large number of problems. In the task as proposed here and with these monkeys, error rates were high compared to previous implementations of this task (Faraut et al., 2016; Harlow, 1949; Wilson & Gaffan, 2008). Beyond error rates on individual problems, we looked at their “error-to-criterion” curve and showed that both reduced their errors to criterion progressively over task acquisition, and eventually both reached the plateau of 10 sessions under 10 errors, our definition of the learning to learn step (**Fig. 17A**). The shape of this curve was similar between monkeys even if Monkey I started with a really high number of errors (869) while Monkey B made fewer errors at the beginning (197).

A key question around this apparent learning to learn is to study how monkeys improved their behaviour to reach this plateau. Work on learning set acquisition from Harlow (1959) and subsequent laboratories (e.g. Browning et al 2007) has suggested that learning set in the DL task emerges through acquisition of a prospective performance strategy - for example Win Stay, Lose Shift - that permits more efficient choice. As such we had the hypothesis that reaching the learning to learn plateau could be represented by a drastic change of performance directly in the second trial of a problem, where the prospective strategy can be implemented, and as originally demonstrated by Harlow. We observed the within-problem learning curves to identify changes in the cinetic across training. We showed an acceleration of the learning curves across problems, which explains the reduction in errors to criterion. But contrary to our hypothesis, there was no drastic change in the second trial and the reach of the learning to learn plateau was represented by a diminution of late errors and so a late increase of performance. The change appeared around 30 trials for Monkey I and around 15 trials for Monkey B (**Fig. 17B**). These results were not expected as it differed from the previous theories of Harlow associating the learning to learn level with a drastic change of performance in the second trial of a problem. This showed that the acquisition of a learning set could be a more progressive process not only based on the prospective theory.

We used the error as a reference of performance to describe the learning and learning to learn curves. Thus, it was important to describe the possible bias that could impact the performance of monkeys such as persistent behaviours. We defined two distinct forms of persistent pattern - side persistence and incorrect persistence. Side persistence represents a laterality bias in which the monkey keeps choosing the side of its preferred hand, irrespective

of the (randomised) localisation of the rewarded stimulus. The incorrect bias corresponds to the case where the monkey keeps choosing the unrewarded target, irrespective of the side on which it appears. This latter case may seem to describe very counterintuitive behaviour, but we identified this pattern by watching Monkey I working. At the beginning of the training, half of the completed pattern presented a side persistence for both monkeys in the side of their preferred hand. Monkey I reduced this persistence across training to 12% of completed trials whereas Monkey B kept it around 40% until the end of the training. Monkey B was then more sensible to laterality bias. The incorrect persistence did not reflect what we saw during the work of Monkey I as it stayed low (around 10% of completed trials) during the whole training for both monkeys. However, we can see a little increase in the last part of the training for Monkey I (**Fig. 18**).

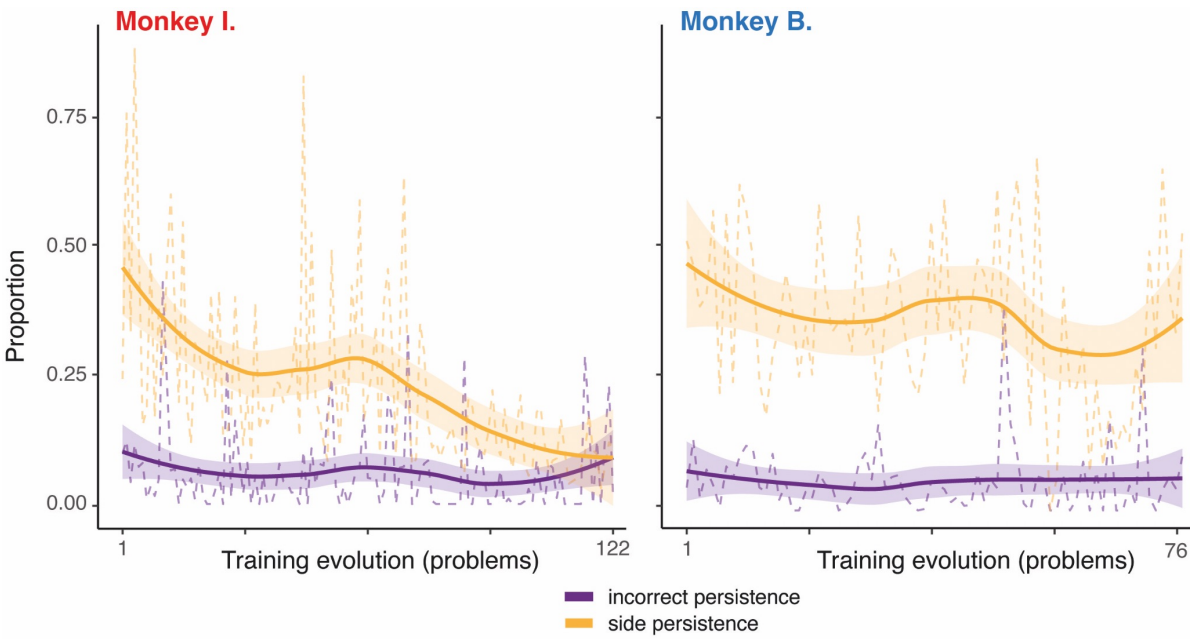

Figure 18. Proportion of persistence pattern on completed trials across training. Side persistence refers to a series of trials in a row in the preferred-hand side (left side for Monkey I and right side for Monkey B). Incorrect persistence represents a series of incorrect trials in a row. Dashed lines represent real data and continuous lines represent the LOESS (Locally Estimated Scatterplot Smoothing) fit, a non-parametric regression method that creates a smooth line through the data points by fitting multiple regressions in localised subsets of the data.

We also had the hypothesis that some uncompleted trials could help us quantify motivation and fatigue in the session or in the task as they represent a lack of efficiency for the monkey. In fact, different types of bias could exist in this task and impact the performance

but these analyses were still performed on completed trials in which the monkey tried to succeed. We could find two types of uncompleted trials: aborted trials and not-engaged trials. In the first case monkeys started a trial by validating a lever but abandoned and did not validate a target. The not engaged trial is when the monkey did not validate the lever within the 15 seconds made available for a given trial, and thus did not start the trial at all. As a reminder monkeys were provided with the opportunity to engage new trials immediately after the ITI but were freely able to not engage if they wanted. A period of 15000ms was considered a trial offer, after which 1500ms happened before another trial was proposed. We looked at their evolution throughout training to define their impact on the learning process.

Monkey I worked consistently with a weak proportion of not engaged trials that reduced over sessions (between 0.3 and 0.1) and almost no aborted trials in the whole training (below 0.1). Monkey B showed a very different willingness to engage trials during the session and so had a high proportion of not engaged trials. Her proportion of aborted trials was low but increased over training (**Fig. 19 - upper panels).** Overall Monkey I seemed to improve her working behaviour to be more efficient whereas Monkey B could be less motivated.

We described above that monkeys could have different types of errors and different types of uncompleted trials showing different reasons for a lack of efficiency. Nevertheless, we showed at the beginning of this section that monkeys learned the task well. In addition to errors and incomplete trials, we observed a further behaviour, made possible by the constraints of the task, that might have been contributing to their improving efficiency. We found trials in which the monkey first briefly touched one target then touched and validated the other one, and we called these hesitation trials (**Fig. 19 - lower panels**). This kind of trial existed because the monkey needed to hold the target for 700ms to validate it. Both monkeys increased this type of trials in the first part of the training. We looked at the proportion of hesitation trials that were actually correction trials, meaning that the monkey validated the rewarded target at the end of the hesitation trial. Almost all hesitation trials were indeed correction trials for both monkeys (85% for Monkey I and 84% for Monkey B). This suggests that monkeys learned in the beginning of the training to quickly correct their choice. We tested a hypothesis that hesitation trials were the consequence of an overly rapid response movement to the same side as the previous response in cases where there was a switch of

side of the rewarded target. Yet given only 50% of the hesitation trials followed a switch of side of the rewarded stimulus for both monkeys, we were able to rule out this hypothesis.

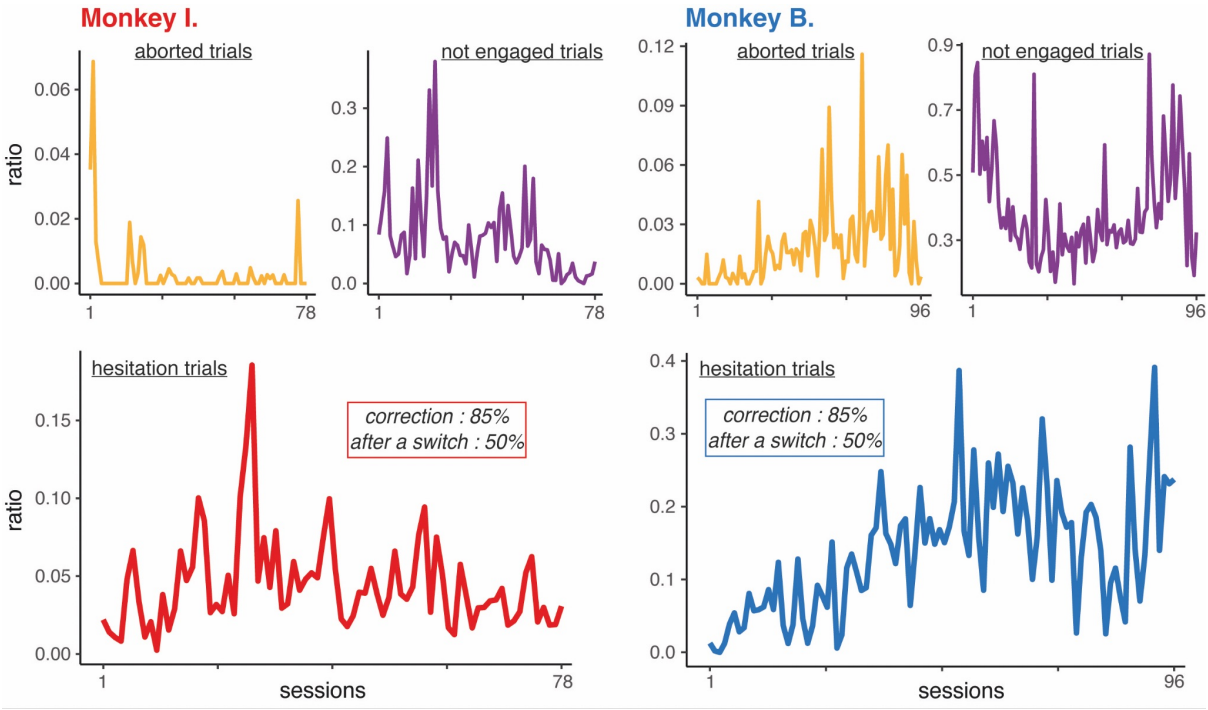

Figure 19. Trial type evolution across sessions. Upper panels: Evolution of uncompleted trials across sessions. Aborted trials correspond to trials in which the monkey validates the lever but not the target. Not engaged trials represent trials in which the monkey does not start the trial, in other words it does not validate the lever. Lower panels: Evolution of hesitation trials across sessions. The hesitation trial corresponds to when the monkey starts by touching a target then validates the other one in the same trial. Values in the squares provide specific information on these hesitation trials: the percentage of hesitation trials that corresponds to correction trials (when the validated target is the rewarded one) and the percentage of hesitation trials that follow a switch (when the rewarded target changes side). The ratio value in all panels represents the proportion of specific trial type to all trials.

The main objective of this study was to describe the evolution of specific behavioural markers across learning that can be linked to electrophysiological signals. To follow these evolutions throughout the training we needed to define different steps of learning. We divided the problems in 3 equal groups thanks to the tertile values (**Fig. 20**). The first group represents the naive state and the beginning of the learning, the second one is the middle of the learning and the last one represents the learning to learn success. The switch between these 3 steps is represented by a significant diminution of the error proportion and a significant augmentation of the correct one (Wilcoxon test, error: $p<0.0001$ - correct: $p<0.0001$ for Monkey I and $p<0.05$

for Monkey B) for both monkeys which confirms an improvement of learning (**Fig. 21**). The evolution of uncompleted trials - aborted and not engaged - vary between steps and monkeys supporting the fact that these variables are not directly linked with learning.

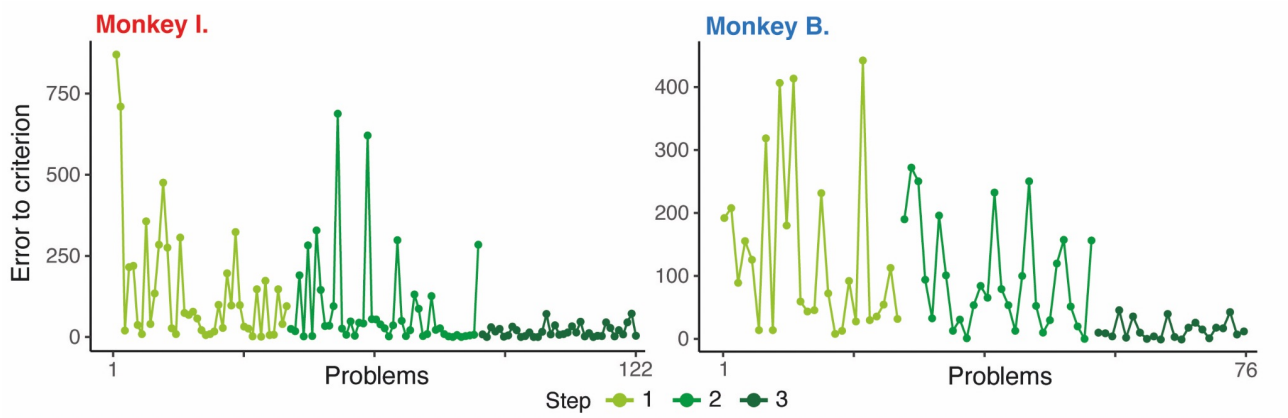

Figure 20. Learning steps in discrimination learning task. The learning to learn curve is divided into three groups based on training evolution. The division is based on tertile values.

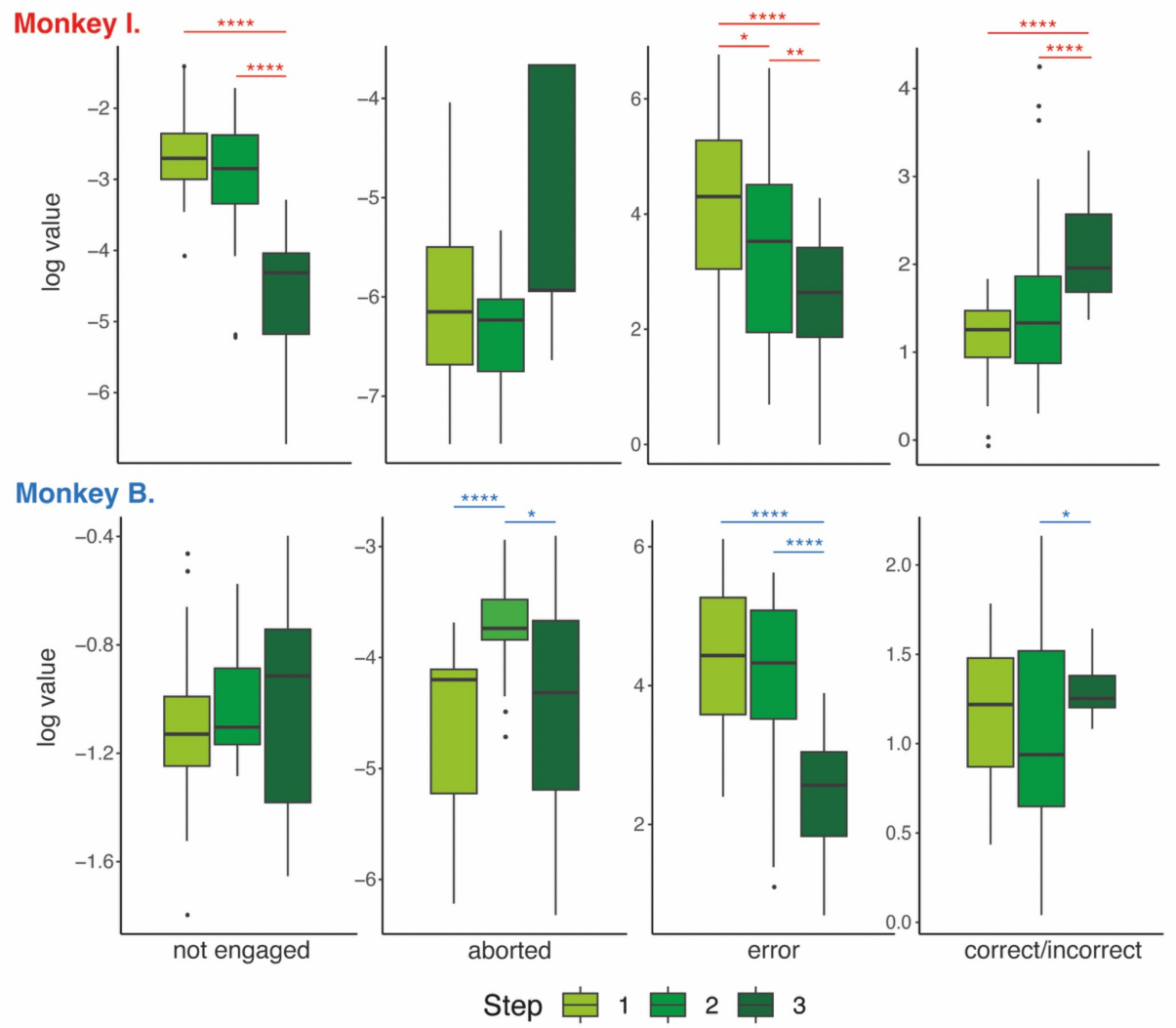

Figure 21. Descriptive parameters of learning steps description. The number of aborted and not engaged (no go) trials and also the number of error and correct responses in each learning step. The value is normalised with the logarithm. The stars represent the significance of Wilcoxon tests between learning steps. * = p-value<0.05, ** = p-value<0.01, *** = p-value<0.001, **** = p-value<0.0001.

Finally, an important question in this behavioural approach was can we identify factors that had impact on learning and how to quantify them to isolate the learning process as much as possible. Both monkeys learned the task correctly and reached the learning to learn plateau, however the analyses above show different patterns in error and trial types. These results point out two important factors: the motivation and the difficulty, well-known to have an impact on learning processes (Bjork & Bjork, 2014; Deci & Ryan, 2000; Sweller, 1988).

Because it was a visual discrimination task, the difficulty was defined as a degree of similarity between the two images of a pair. To assess this similarity objectively, we combined

multiple approaches: two algorithms and an online survey. First, we used the VGG-19 (Simonyan & Zisserman, 2015), a pre-trained deep convolutional neural network (DNN) with 19 layers which capture high-level image features. This DNN assessed a similarity value to each pair: the higher the value, the stronger the similarity. Secondly, we used the Structural Similarity Index Measure (SSIM) (Z. Wang et al., 2004), a perception-based model that incorporates important structural information, including both luminance and contrast terms. With this measure, a low value is associated with a high similarity. Finally, we used an online survey to have a sample of human perception. We showed them the pairs and asked them to rate the difficulty of differentiation between 1 and 10. In that case, as for SSIM, a low value is associated with a high similarity. We assessed the difficulty for the first 50 problems and then correlated it with the performance represented by the number of errors to criterion (**Fig. 22**). None of the three approaches revealed any correlation between the difficulty and the performance (Pearson test, p>0.05).

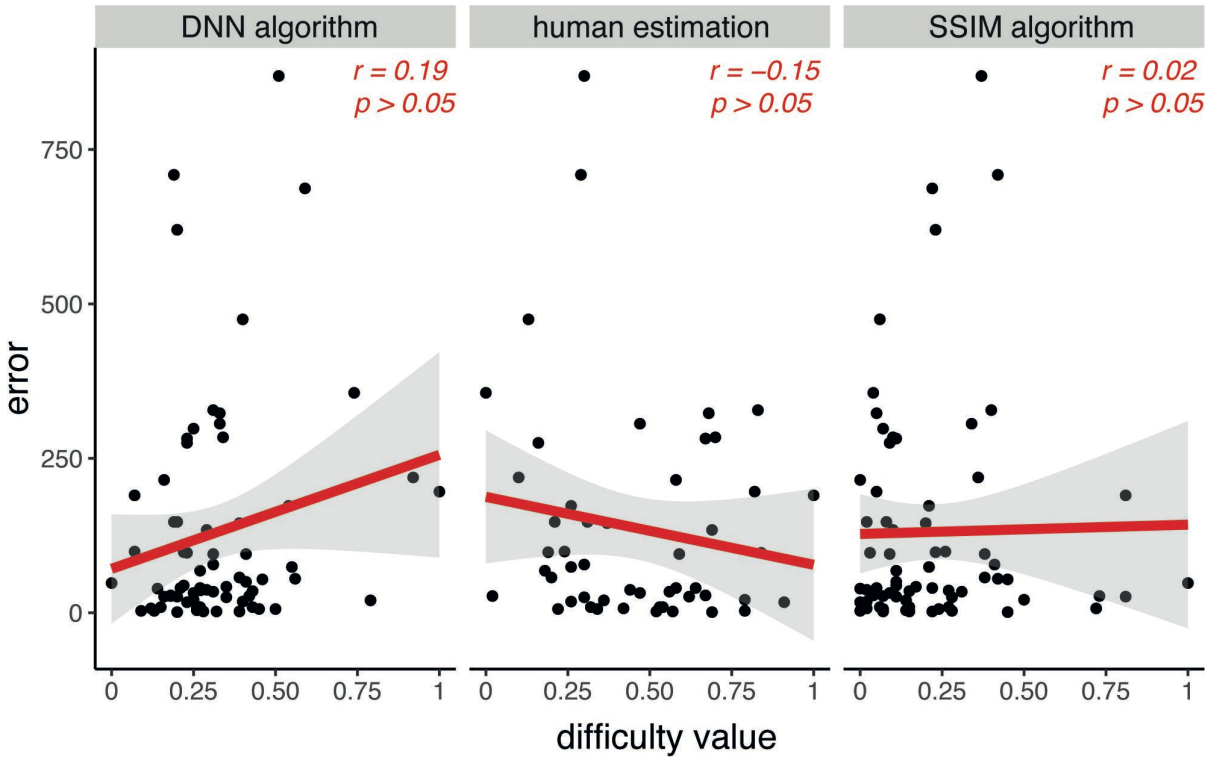

Figure 22. Correlation between performance and difficulty. The difficulty corresponds to the degree of similarity between paired targets. The difficulty of each pair has been defined with 3 distinct methods: a pre-trained deep convolutional network (VGG-19) known to capture high-level image features (DNN), a measure of the perceptual similarity taking into account the structural information, luminance and contrast differences (SSIM) and an online

survey of 52 human subjects. For DNN a higher value corresponds to a higher similarity, for SSIM and human estimation a higher value corresponds to a lower similarity. Only the first 50 problems are included in this analysis. Red lines correspond to a linear fit and the statistic corresponds to a correlation Pearson test.

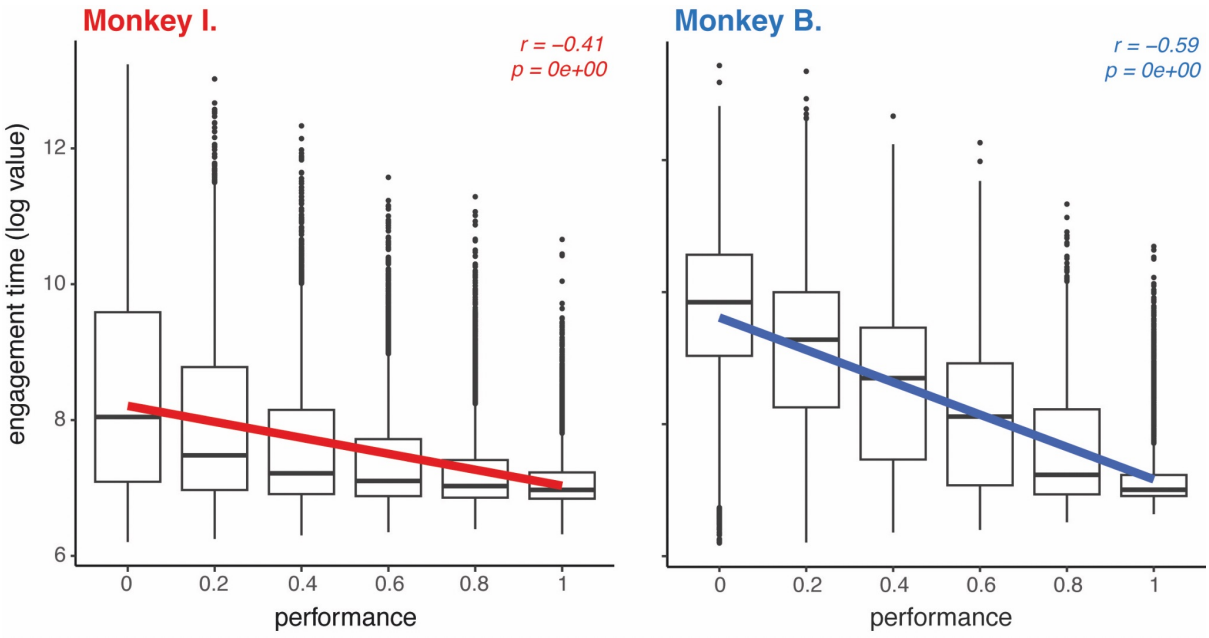

Figure 23. Correlation between performance and motivation. The motivation value corresponds to the log of the engagement time in ms (time between the lever apparition and the lever validation). The performance value is calculated on a sliding window of 5 trials. Red lines correspond to a linear fit and the statistic corresponds to a correlation Pearson test.

To define a motivation value, we searched for a marker of the willingness of the monkey to work. As a reminder, monkeys had an imposed inter-trial time but after that they were freely able to engage in trials when they wanted so we decided to use the engagement time (i.e. the time between the onset of the lever at the beginning of a trial and the time when the monkey validates the lever) as a quantification of the motivation. In fact, a rapid succession of trials may be a sign that the monkey is motivated to progress in the session whereas a long delay in starting a trial could show that the monkey preferred/needed to take a break.

We correlated this motivation value with the performance and highlighted a significant correlation for both monkeys (*p value<0.001, Pearson test*) (**Fig. 23**).

The performance of monkeys in the task is impacted by motivation more than by the difference of difficulty between problems.

Taking the engagement time as a motivation value engendered a dichotomy between being motivated and getting back to the task quickly or taking a more or less long break before starting again. We saw that this motivation had an impact on the performance thus to go further in this analysis, we focused on the period when the monkey decided to take a break during the session. We defined two types of pauses: short ones that last between 20 and 60 seconds; and long ones, lasting longer than 60 seconds. These time periods were defined by looking at and analysing the distribution of pause times. We looked at the proportion of these two types across learning steps for each monkey (**Fig. 24**). We showed that for both monkeys, there are more short pauses than long ones. There is also a gap between monkeys, with a higher number of pauses for Monkey B than Monkey I. For both monkeys, short pauses remained quite stable during learning, but long pauses evolved, with a progressive diminution across learning steps for Monkey I and an augmentation in the last step for Monkey B.

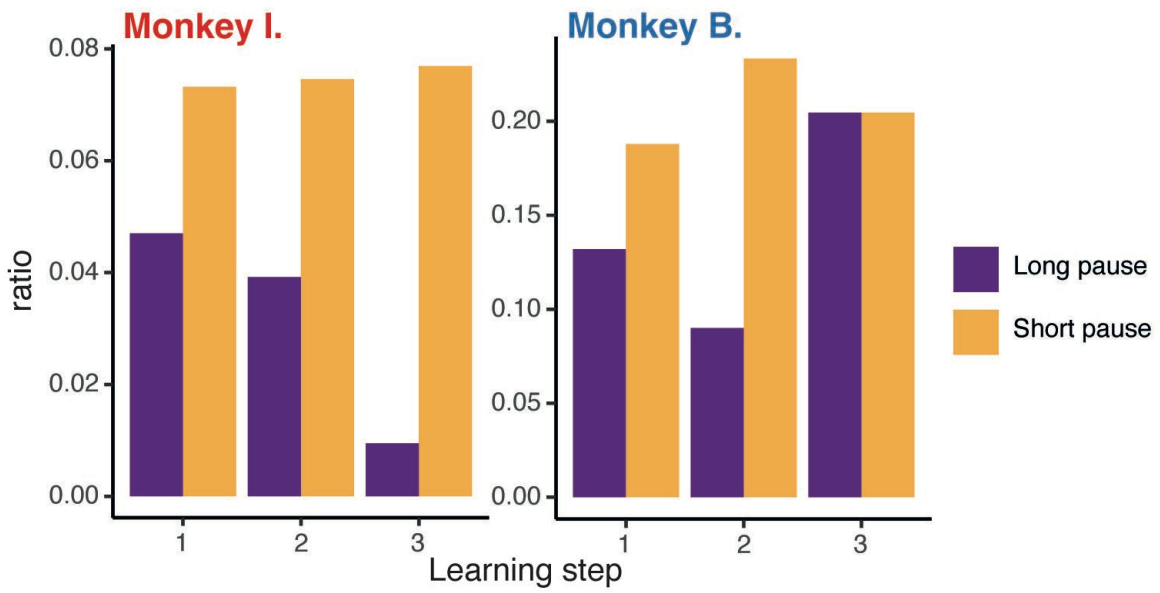

Figure 24. Pause type across learning step. The ratio value represents the proportion of pause type to all trials. Long pause corresponds to a pause of more than 60 seconds, short pause corresponds to a pause between 20 and 60 seconds.

Even if we first looked at the pause as a lack of motivation marker, we hypothesised that it could be associated with different behaviours and have opposite impacts on the learning depending on the context. We wondered if the short and the long pauses could have different roles and if it represented a lack of motivation or a general fatigue of the subject, or an

integration of information necessary for the learning. We looked at the distribution of the pause during the session. We defined three groups of sessions (start, middle and end of training) to observe a possible change in this distribution (**Fig. 25**). We hypothesised that if the pauses were representative of a lack of motivation or fatigue, they should be condensed in specific parts of the session, whereas if they were linked to a learning or consolidation process, they should be distributed more or less equally along the session, or at least more dispersed.

For Monkey B, the pattern was similar for both pause types with no change across the training. There was a higher proportion of pauses at the beginning of the session that could represent a lack of motivation at the beginning of the session. We saw an exception in the last part of training for short pauses where the distribution seemed to be more dispersed across the session. For Monkey I, we saw changes across training for both types. In the start of training, the higher proportion of long pauses were at the beginning and at the end of the session, which can be associated with a lack of motivation at the beginning and fatigue at the end. Then across training the proportion of long pauses decreased in all the session and in the last part it remained only a few at the beginning of the session. For short pauses, the distribution was more equally distributed throughout the session except a little concentration at the beginning of the session. And in the last part of the training, the distribution was more dispersed across the session. This could support the hypothesis that short pauses could be linked with the learning process and allowed an integration of information.

To sum up, the distribution of pauses across the session seemed to link long and short pauses with a lack of motivation. But the training could have an effect and the monkeys could start to use the short pauses in a positive way to integrate information in the second and the last part of training.

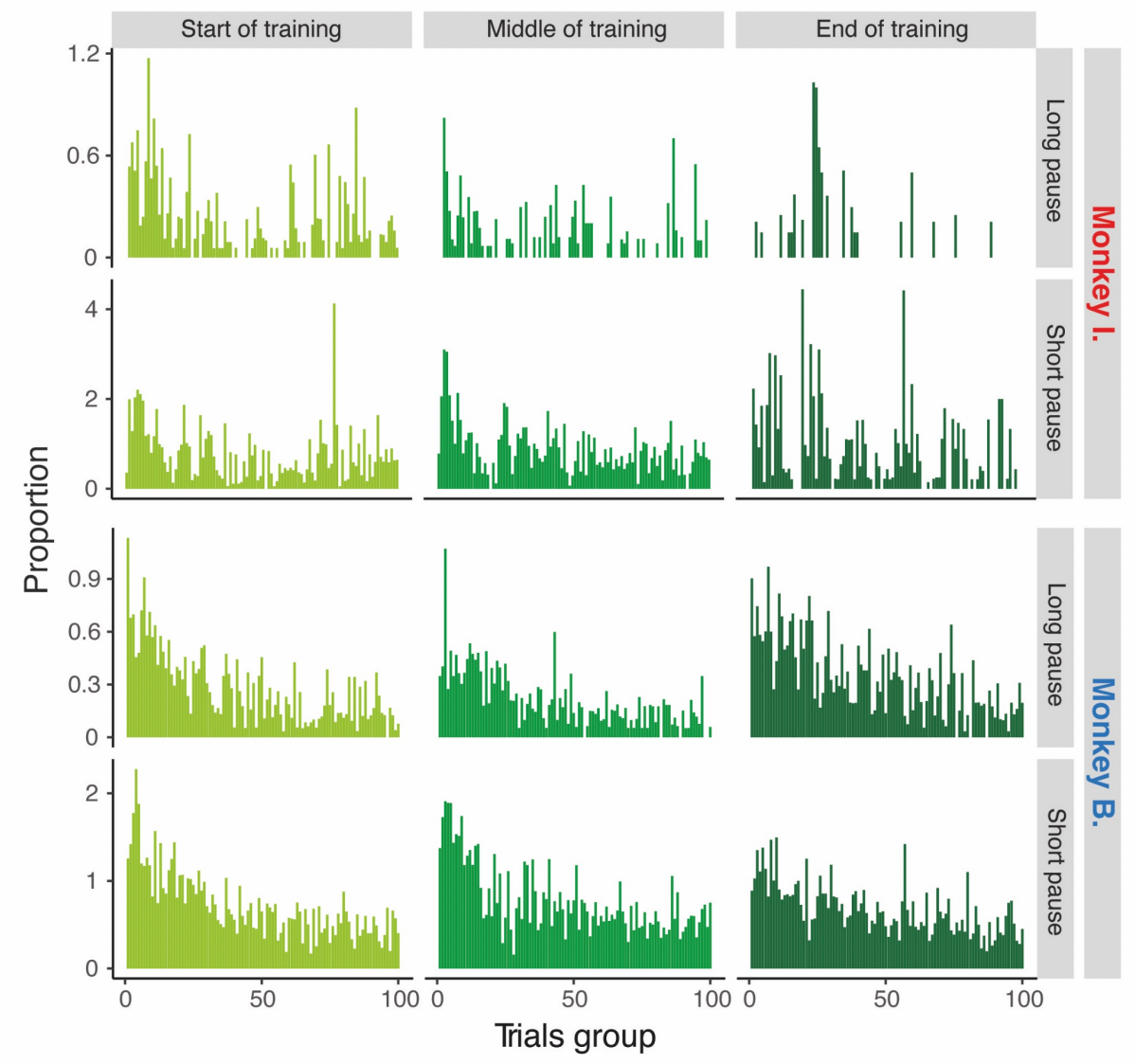

Figure 25. Pause distribution in session. Graph shows the proportions of pauses present in a specific group over total pauses number. For each session trials were divided in 100 equal groups. Long pauses correspond to pauses of more than 60 seconds, short pauses correspond to pauses between 20 and 60 seconds. Start, middle and end of training represent the total number of sessions divided in three equal groups.

The distribution of the type of pause in the session showed a different pattern for short and long pauses meaning that they could have separated functions. We linked the long pauses with a lack of motivation whereas short pauses could be used to learn efficiently.

A key manner to determine whether pauses in general, or a specific type of pause, had a role in the cognitive performance of the task is to directly link short and long pause occurrence with performance. Two hypotheses of particular interest were whether pauses

were induced by incorrect performance, or whether performance was improved following a pause. We looked at the proportion of incorrect trials before the pause and correct trials after the pause by taking a window of three trials each time and studied the evolution of these two proportions across training (**Fig. 26**).

For Monkey I, we showed that trials before both types of pauses were incorrect in less than 50% of cases except before a long pause in the last part of training (around 65%). Moreover, trials after the long pauses were correct in 50% of cases except again the last part of training in which the proportion is lower but it is important to note that there was more variance in the last part of training for Monkey I. Trials after the short pauses were correct in more than half the cases and this proportion seemed to increase across training even if no statistically significant result was found (Wilcoxon test, $p>0.05$).

For Monkey B, both types of pauses arrived after incorrect trials only in approximately 25% of cases and no significant change across training was found (Wilcoxon test, $p>0.05$). After both types of pauses, there were correct trials in 50% of cases in the start of training, then there was a significant increase of this proportion (Wilcoxon test, $p<0.01$) between the beginning and the middle of training. Overall, it seemed that short pauses were followed mainly by correct trials for both monkeys with an increase of this proportion across training, supporting the hypothesis that pauses, specifically the short ones, improved the performance. Long pauses had also an effect on the performance for Monkey B but not for Monkey I. However, we didn't make the link between a series of incorrect trials and the need to take a break afterwards, no matter how long the pause was. On the contrary, for Monkey B, both types of pauses followed mainly correct trials. Thus, it seemed that monkeys decided to do a pause, whatever their performance at the time, but that these breaks were beneficial for improving their performance later on.

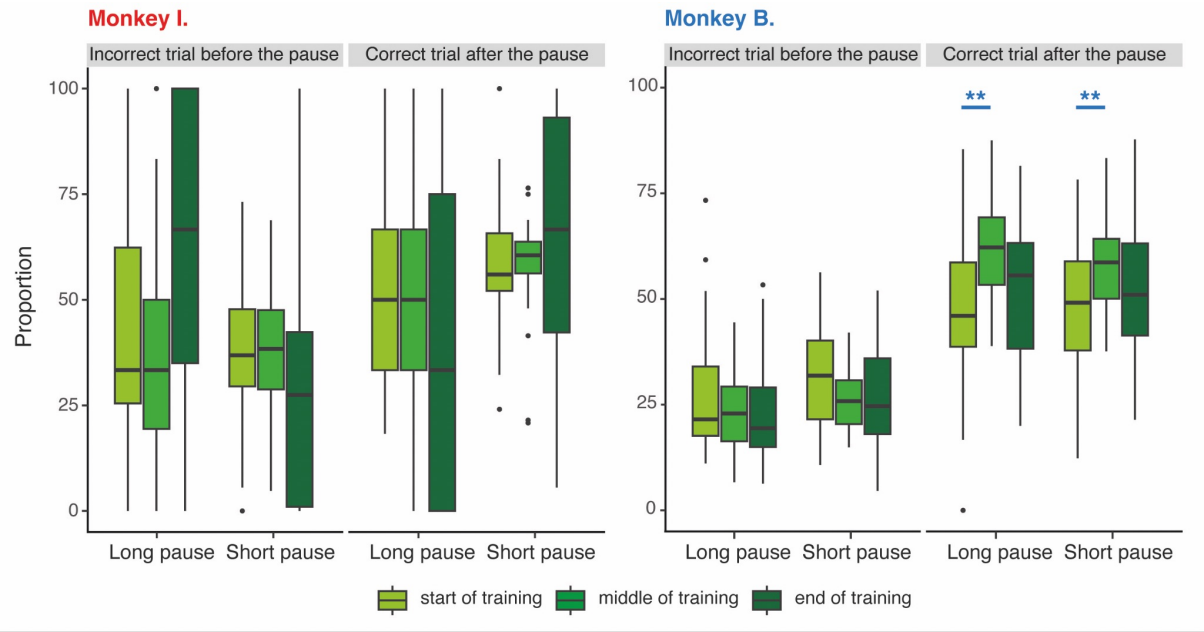

Figure 26. Relation between pauses and performance throughout learning. The boxplots represent the proportion of incorrect and correct trials among completed trials. We calculated the proportion on a window of three trials before and after the pause. Long pause corresponds to a pause of more than 60 seconds, short pause corresponds to a pause between 20 and 60 seconds. Start, middle and end of training represent the total number of sessions divided in three equal groups. Start, middle and end of training represent the total number of sessions divided in three equal groups. The stars represent the significance of Wilcoxon tests between training periods., ** = p-value<0.01.

IV. Conclusion

Both monkeys succeeded in learning the task and reached the learning to learn plateau of performance. The way in which they learned to learn differed from previous studies in terms of timing. In fact, the learning set described by Harlow and others elicited a difference between the learning and the learning to learn level directly in the second trials of the problem. In our case the differentiation between the two levels was slower, around 15-30 trials depending on the monkey. This means that reaching the learning to learn level could be more progressive with a less drastic change than described in previous studies using the same cognitive paradigm. This result was not expected and different hypotheses could be drawn, based on the difference of protocols. The first one was the possible difficulty brought by the highly similar pairs of abstract images but we assessed the link between the difficulty and the performance and found no effect. The second one was linked to the reward design of the task. In fact, liquid

rewards could be less motivating for the monkeys than food rewards. Moreover, monkeys received a small quantity of reward for each correct trial but at the scale of the session, as they performed a lot of trials in one session, missing a trial had no big effect. This could mean that they had less need to be effective at the trial scale.

In any case, we defined three learning steps that will be used to analyse longitudinal learning progress in the electrophysiological analysis below and describe their specific learning performance and behavioural components. In fact, in addition to this common learning pattern, each monkey learned with specific strategy differences in their persistence pattern and timing dynamic. Monkey I privileged the constancy and the rapidity with fewer pauses and fewer uncompleted trials while Monkey B alternated periods of work and periods of pause. This could mean that Monkey I favoured finishing her session as quickly as possible while maximising her performance whereas Monkey B chose to maximise her performance by taking the necessary breaks without worrying about the overall time of the session.

We also identified motivation as an important parameter of learning as it has a major impact on learning behaviour. In particular in this study we have two subjects with different behavioural strategies and also different motivational levels, and these differences provide us with a wealth of data to assess this motivation question.

This behavioural study showed that reaching the learning to learn level could be achieved in a more progressive way than the drastic one described before. Also, that the behavioural specificities of the subject have an impact that must be considered. To sum up, this study will be used as the basis of all the electrophysiological studies below.

Chapter 3. Positive and negative feedback processing

I. Introduction

The DL task brought to the monkeys the notion of choice for the first time. The necessity of making a choice will help the monkey to understand that there is something to learn and then increases the importance of extracting information from feedback (Walton et al., 2003). Thus, the processing of the positive and the negative feedbacks is a key step for learning. The main interest of this study was to define precisely how the identification of the feedback type took place from scratch and how it evolved during learning to reach the higher level of learning to learn. Our task used the reward as positive feedback. It is one of the most common positive feedbacks in cognitive tasks. Nevertheless, little is known about how the neural response to reward takes shape when we are confronted with it as informational feedback for the first time.

II. Specific materials and methods

The electrophysiological data were recorded during the DL and the RL task. The DL task represents the task of interest to compare different steps of learning (as seen in the previous chapter). The RL task is used to test the generalisation of the learning to learn across tasks. To focus on the feedback part of trials, we used epochs of the local-field potentials (LFP) pre-processed data aligned on the positive or the negative feedback. As said earlier, the positive feedback was represented by a reward so data were aligned on the deliverance of the reward. The negative one was represented by the absence of reward and a latency time before the next trial so data were aligned to the time where monkeys should have received a reward if it was not an incorrect trial. Doing so, we have the same time between the target validation and the "feedback time" in both cases. We took a time window of 600ms with 200ms before the feedback and 400ms after. We also used single-unit activity (SUA) data, sorted with Kilosort2 (Pachitariu et al., 2016) and curated manually. We aligned data on feedback (positive or negative) and took a time window of 600 ms with 100 ms before the feedback and 500 ms

after. Bad electrodes were removed during the manual curation. As a reminder, the sampling rate was at 1kHz for LFP data and 30kHz for SUA data.

We used the antero-posterior groups presented in part II of this manuscript to group the electrodes in the analyses of this chapter.

LFP data statistical analyses were performed with Python and visualisation with Python and RStudio. Statistical analyses of SUA and visualisations were done with RStudio. We performed statistical analyses by using Kruskal-Wallis tests with Bonferroni corrections and Mann-Whitney post-hoc tests.

III. Results

a) Signal stability

Working with longitudinal chronic recordings, and with data derived from FMA electrodes as here, requires us to assess signal stability across days, in order to consider the extent to which different periods of analysis are directly comparable. The FMA electrodes are “floating”, in that they are inserted into the brain but not directly fixed to any rigid structure like the skull. As such, electrodes could move slightly with the natural movements of the brain under the skull, and because of some phenomenon such as immune factors or gliosis that might change electrode position within the tissue (Griffith & Humphrey, 2006; Hermann & Capadona, 2018). Quantifying this loss allows the possible changes in the signal in the analyses to be associated with a real neurophysiology phenomenon.

To do so, we used two different methods to make our stability assessment more robust. First, we performed an analysis of the aperiodic offset of power spectra using the “fitting of oscillations and one-over f noise” (FOOOF) model (Donoghue et al., 2020) which enables certain characteristics of brain activity to be quantified, particularly in terms of background noise and aperiodic fluctuations. If the aperiodic offset increases significantly over the sessions, this may indicate an increase in background noise, potentially due to the degradation of recording conditions. Secondly, the signal to noise ratio (SNR) (Suarez-Perez et al., 2018) which is defined as the dimensionless ratio of the signal power to the noise power contained

in a recording. We performed the analysis between 1 and 48Hz as our main interest was in frequency bands from delta to low gamma. Results with both approaches showed no signal loss for Monkey I whereas Monkey B had a significant increase of the aperiodic offset (Pearson test, p-value = 0.01) and of the SNR (Pearson test, p-value = 0.001) (**Fig. 27**). Thus, the signal seemed quite stable for Monkey I and we will be able to remove this factor in further analyses. However, Monkey B had a clear loss of signal across training and it will be important to keep it in mind to interpret observed changes of signal. It should be noted that the loss of signal for Monkey B was mainly driven by the last 8 sessions whereas it seemed quite stable before that.

Here we highlighted signal loss and kept it in mind for the interpretation of all the electrophysiological analysis below. However, a next step will be to quantify this loss in order to take it into account in all the electrophysiological analysis. Also, to also assess the signal stability in the single-units by looking at the number of units sorted across sessions.

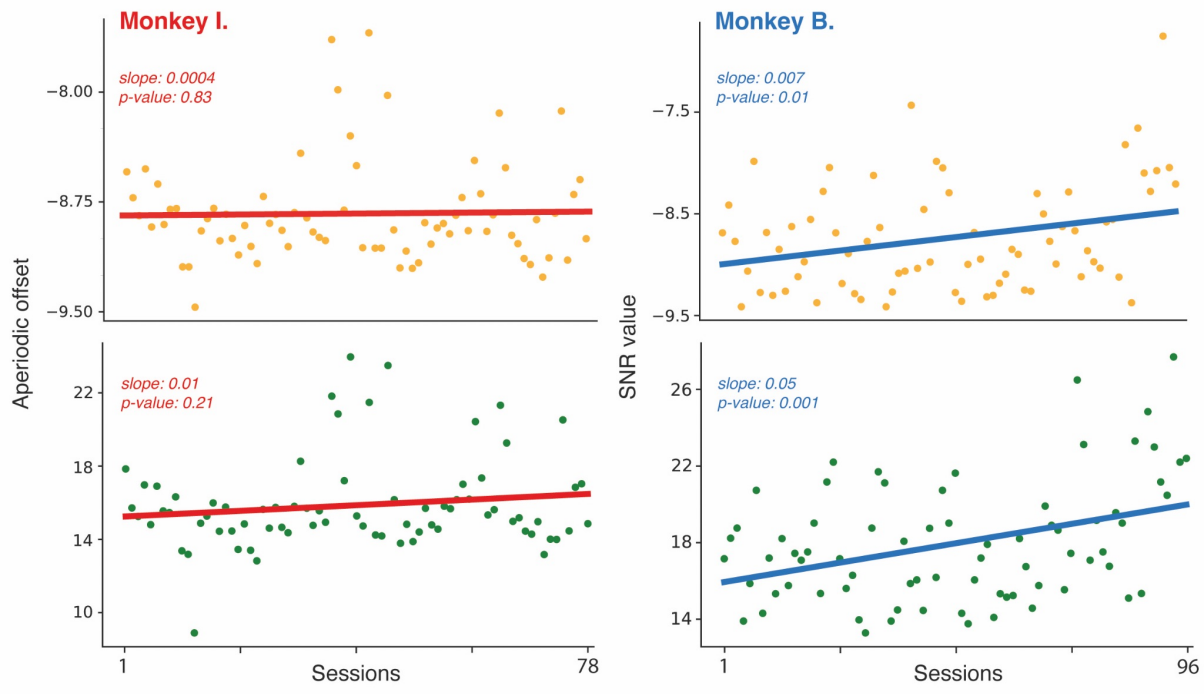

Figure 27. Measure of signal stability across sessions. Upper panels: Aperiodic offset of power-spectrum density (FOOOF model). Lower panels: SNR. Points represent real data and lines the linear fit. Slope and p-value were extracted from a Pearson correlation test.

b) Evoked-potentials in local field potential

Feedback types differentiation

Our main objective in this analysis was to describe how the feedback was processed throughout learning and especially to elucidate how monkeys learned to distinguish between the positive and the negative feedback when they faced feedback for the first time. We wondered how this distinction was reflected in the evoked responses to feedback so we defined the critical period in which positive and negative feedback elicited a different response in each area and across the antero-posterior groups (see Part II General material and methods) of the controlateral hemisphere for both monkeys. We calculated the difference between the raw pre-processed signal aligned on the positive feedback and the one centred on negative feedback. We choose a time window of 100ms before the feedback and 400ms after to capture feedback response without overlapping with other elements of the task. The 100ms before the feedback were used as a baseline to remove from the signal. We also filtered data by removing specific problems in which the signal was superior to the mean of all problems plus five times the standard deviation. To define the limits of our time window of interest - that we will call the peak window - we calculated changes in signal between time points and we highlighted those higher than the standard deviation of all time points changes of all problems and extracted the maximum and minimum limits of these changes (**Fig. 28 & 29**).

We replicated this analysis on all combinations of areas and antero-posterior groups (called area-groups in the following analyses) to have a peak window specific for each area-groups for each monkey. The peak windows were between 150ms and 400ms post-feedback in the LPFC and in the MCC for Monkey I. For Monkey B, it was between 154ms and 399ms in the LPFC and between 150ms and 400ms for the MCC.

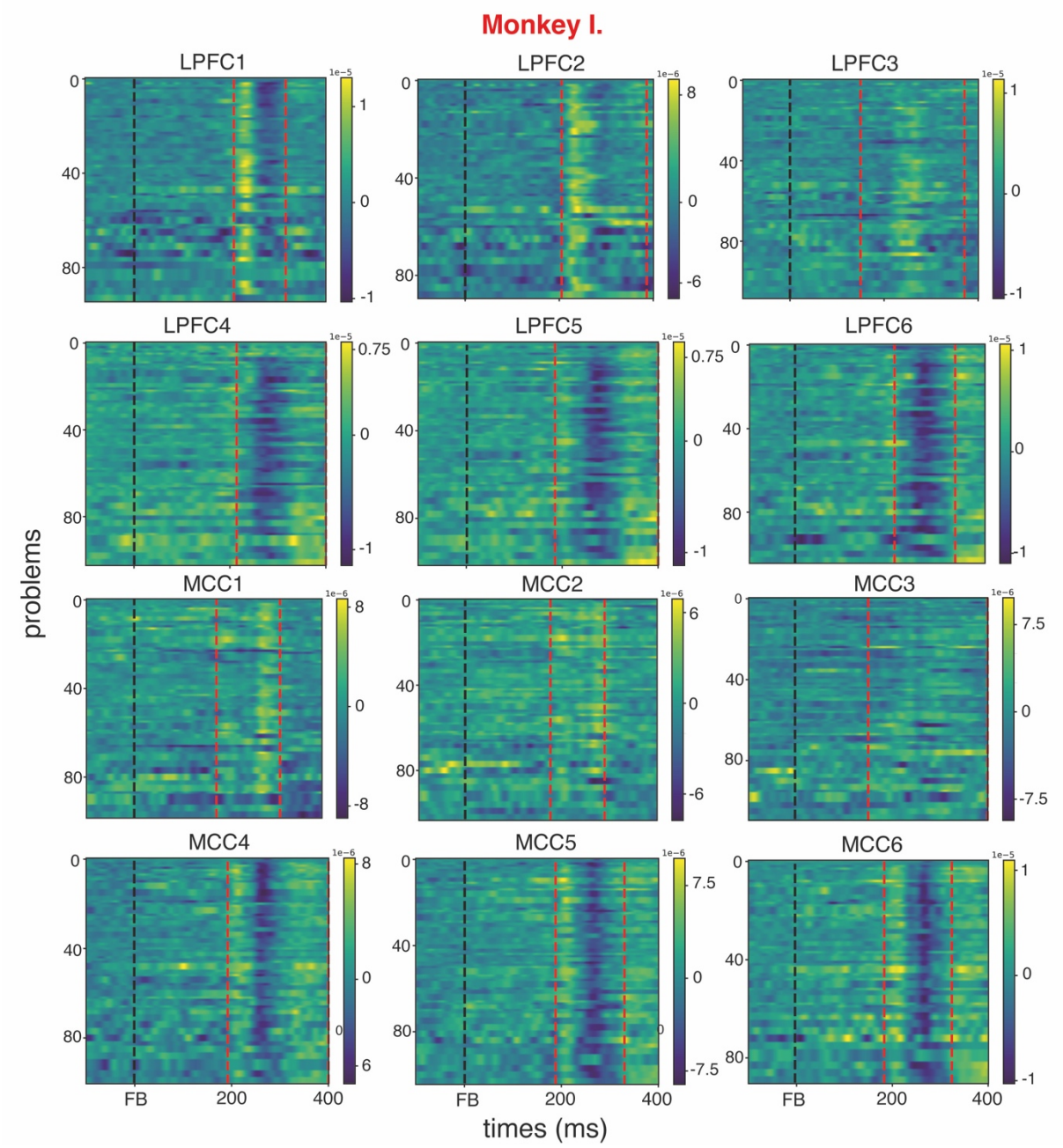

Figure 28. Peak time window definition of Monkey I. Positive negative difference (POS-NEG) signals for each problem. Time window of 100ms before the feedback and 400ms after. Black dashed line represents the feedback at time 0. Red dashed lines represent the limit of the peaks window. FB = feedback.

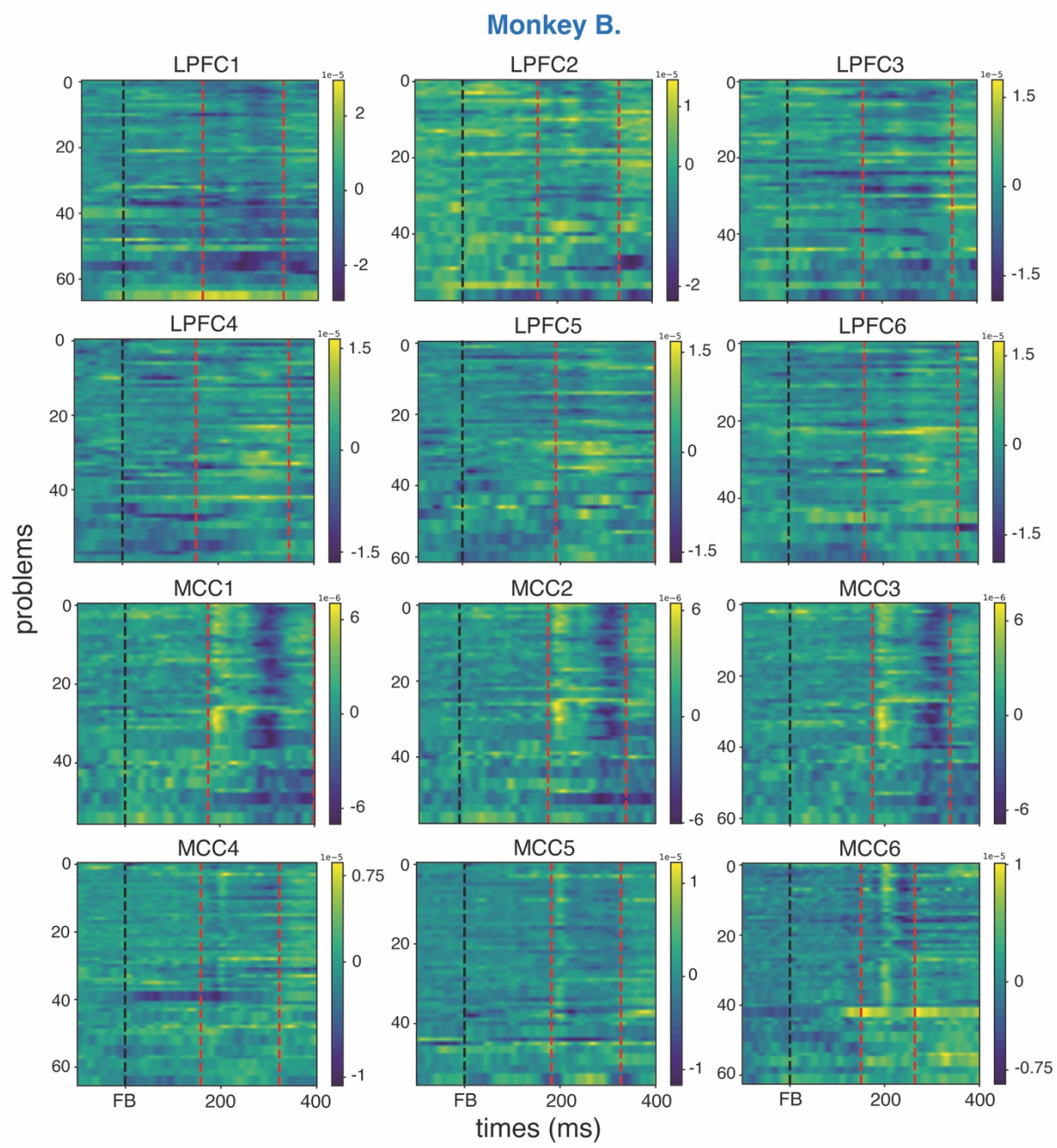

Figure 29. Peak time window definition of Monkey B. Positive negative difference (POS-NEG) signals for each problem. Time window of 100ms before the feedback and 400ms after. Black dashed line represents the feedback at time 0. Red dashed lines represent the limit of the peaks window. FB = feedback.

We noted that the difference between the positive and the negative feedbacks (we will call it the 'POS-NEG signal' in the following analysis) was more pronounced in the MCC anterior part (1-3) for Monkey I and in the MCC and LPFC posterior parts (4-6) for Monkey B. We also found that for some specific area-groups, the POS-NEG signal showed no difference at the beginning of the training. For example, we showed that this difference is constant only

starting from problem number 9 for Monkey I in LPFC group 5 (**Fig. 30**). However, this result was not consistent across all area-groups, it started around 10 problems for LPFC3, 7 problems for LPFC4 and 9 problems for LPFC6. We saw no such effect in the MCC. For Monkey B, there was a less clear difference between feedbacks so this effect was not visible. This raised the need to specify how each type of feedback was processed at the beginning of learning - in the naive state - and how the distinction between the two was established/arised. And also, to specifically address this question on each area-group independently.

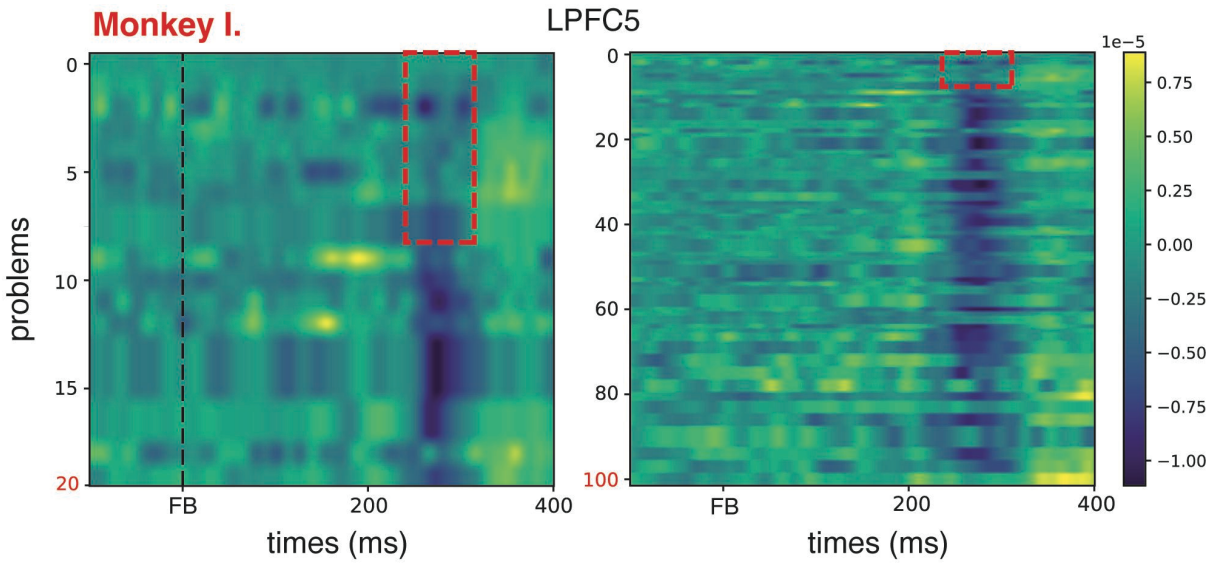

Figure 30. Feedback differences in beginning of training. Left panel: POS-NEG signal for each 20 first problems. Right panel: POS-NEG signal for all problems. Time window of 100ms before the feedback and 400ms after. Black dashed line represents the feedback at time 0. The red dashed square highlights the same part in both panels. FB = feedback.

We looked at the POS-NEG signals across the three learning steps in each area-groups, using the same time window (-100 to 400ms). There was a waveform difference between anterior (groups 1 to 3) and posterior parts (groups 4 to 6) in the MCC and in the LPFC for both monkeys (**Fig. 31 & 32**). For Monkey B, as shown in the previous heatmap, the differences were less clear than Monkey I, so peaks were less visible and the signals in step 3 were often noisy. As it was the last part of the training it could be due to the signal loss identified above.

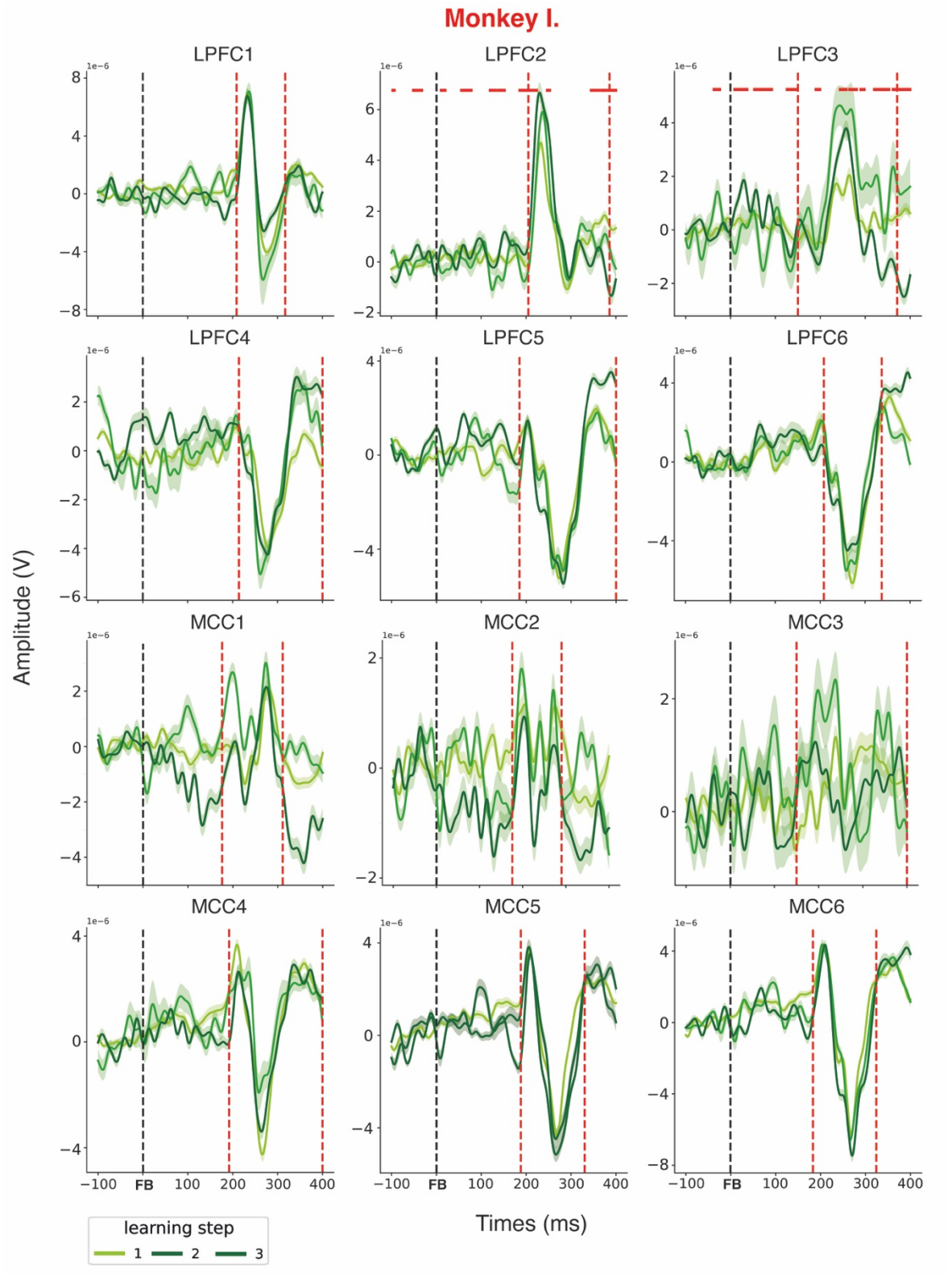

Figure 31. POS-NEG signals across training for Monkey I. The POS-NEG signal represents the response of positive feedback minus the response of negative feedback. Time window of 100ms before the feedback and 400ms after. Black dashed line represents the feedback at time 0. Red dashed lines represent the limit of the peaks window. Red horizontal segments indicate a significant p-value of the Kruskal-Wallis test between learning steps for each time point. FB = feedback.

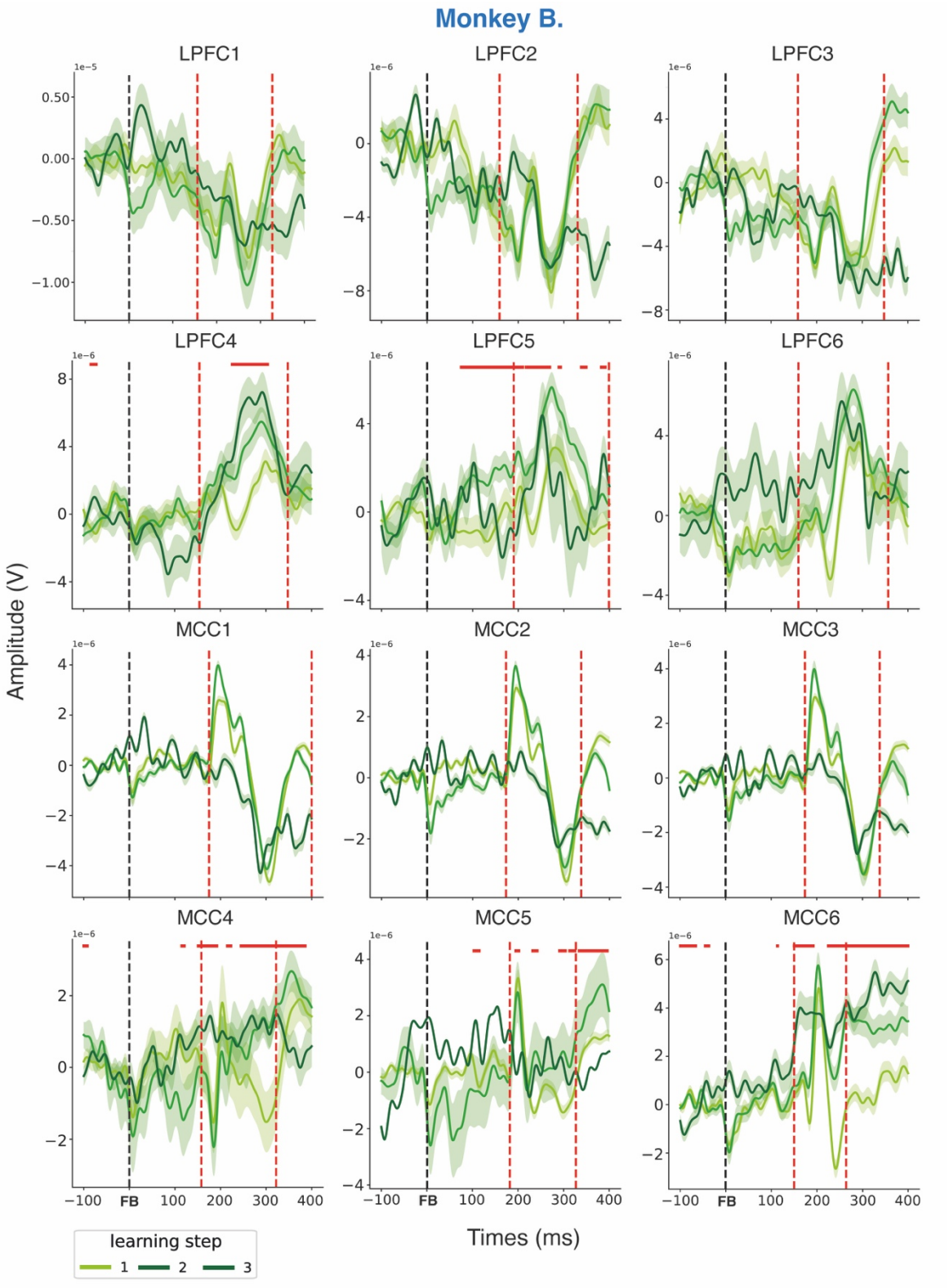

Figure 32. POS-NEG signals across training for Monkey B. The POS-NEG signal represents the response of positive feedback minus the response of negative feedback. Time window of 100ms before the feedback and 400ms after. Black dashed line represents the feedback at time 0. Red dashed lines represent the limit of the peaks window. Red horizontal segments indicate a significant p-value of the Kruskal-Wallis test between learning steps for each time point. FB = feedback.

Statistical analysis of evoked response

The next step was to extract specific parameters to compare the POS-NEG signals across area-groups and learning steps in the most objective way possible. We focused on the peak window defined above for each area-group. We applied a peak detection function ("*find_peaks" from scipy.signal Python toolbox*) on all the signals and kept those present in the specific peak window of each area-group. We chose the appropriate parameters (height = mean+std, width = 5 time points and distance = 5 time points) by testing different parameters and visually checking the peak detection on the data. We presented the peak detection for each monkey to illustrate the process (**Fig. 33 & 34**). We extracted the time of the positive peak in the peak window of step 1. There was only one peak in the majority of cases but if many were present we kept the first one. Then, for step 2 and step 3, if more than one peak was present we chose the one that was the nearest to the time of the peak in step 1. Depending on the shape of the signal, some area-groups had no peak at all. We focused on positive peaks as they were well detected, negative ones were less detected and more work on the detection method will be necessary in the future to study them.

We hypothesised that changes in the feedback processing could be represented by a change in the amplitude and in the temporality of the response. The peak detection allowed us to extract these two values for the positive peak in each problem. We had problems in which we had no peak for some area-groups but this case was rare and, as we had a big number of problems, it did not impact the statistical analysis.

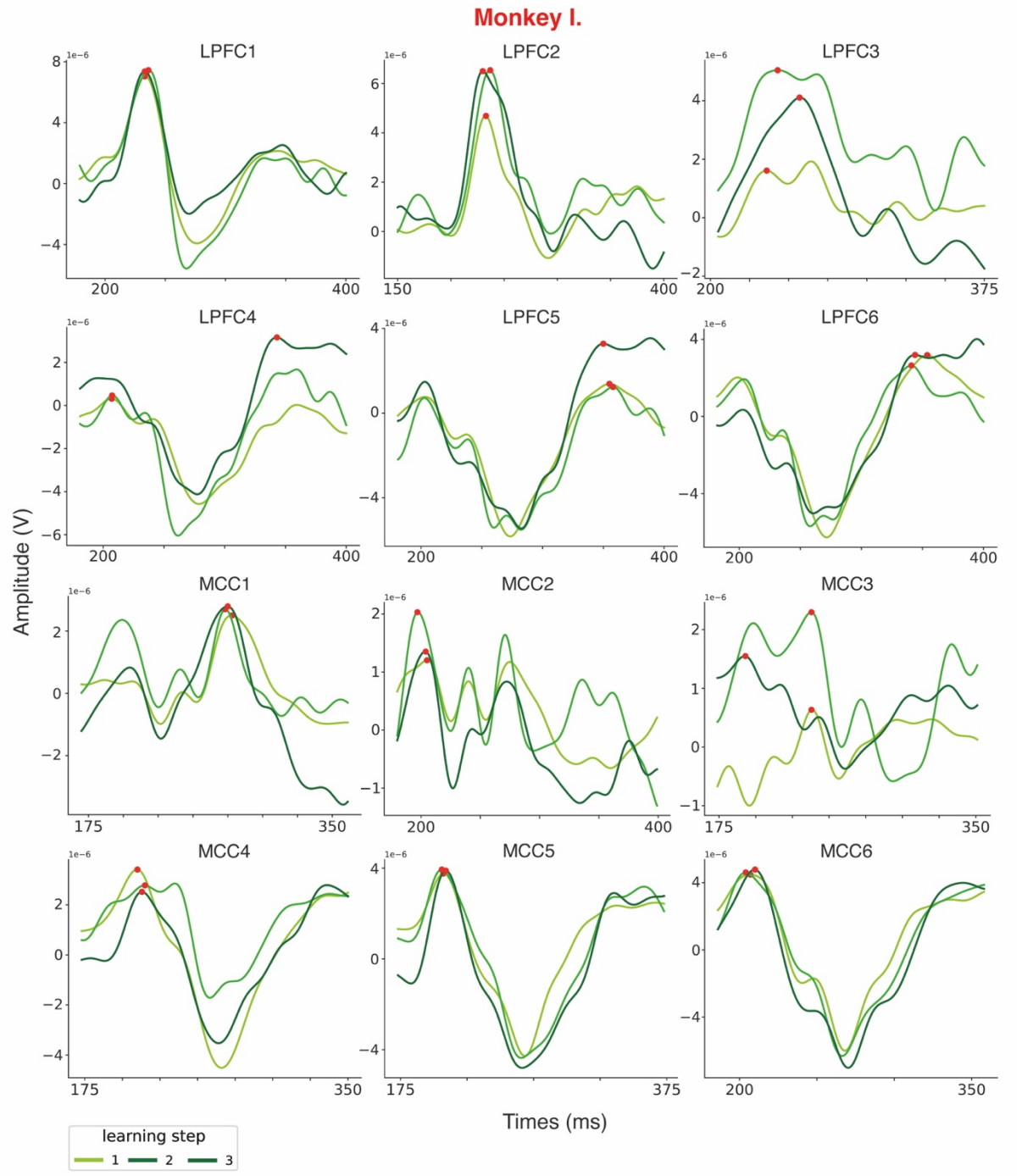

Figure 33. Peaks detection across learning steps for Monkey I. The time window represents the peak window of each combination of areas and antero-posterior groups. Detection parameters: height = mean of the data + standard deviation of the data, width = 5 time points and distance = 5 time points. The points represent the positive peaks detected.

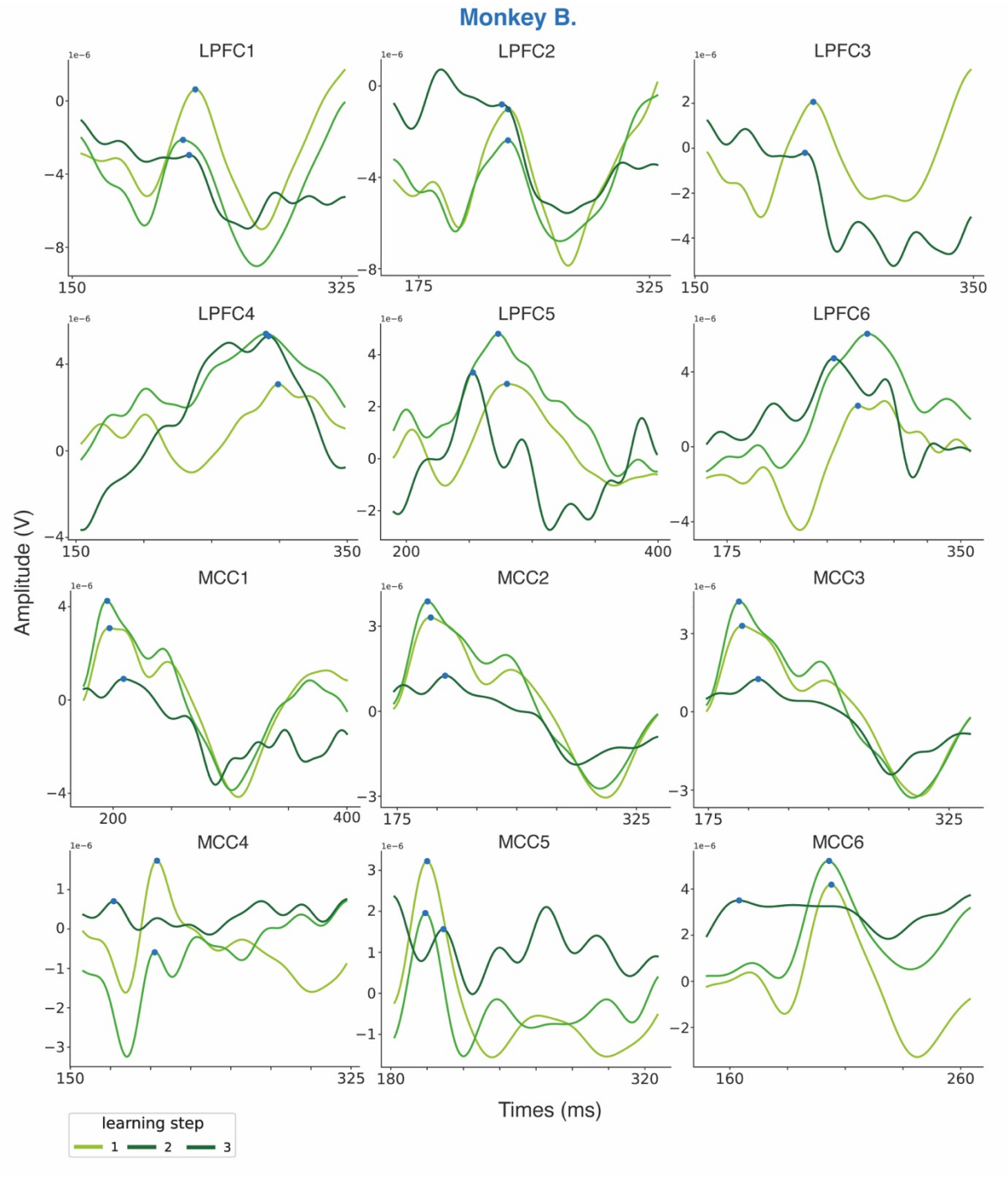

Figure 34. Peaks detection across learning steps for Monkey B. The time window represents the peak window of each combination of areas and antero-posterior groups. Detection parameters: height = mean of the data + standard deviation of the data, width = 5 time points and distance = 5 time points. The points represent the positive peaks detected.

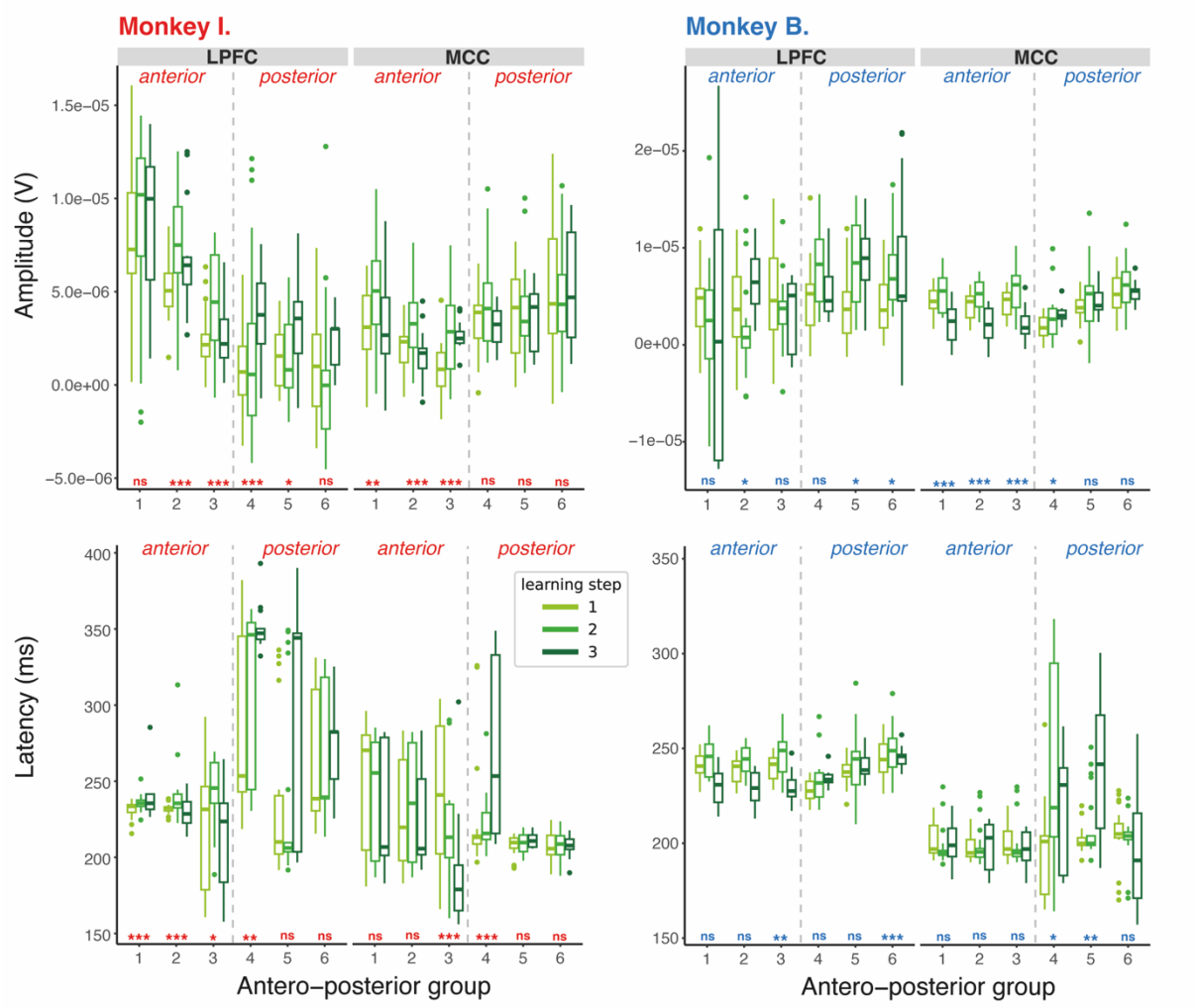

Figure 35. Evolution of amplitude and latency of POS-NEG signals across training. The boxplots represent the amplitude and the latency of all the peaks extracted in each problem of each learning step.
Kruskal-Wallis test between learning steps. ns = no significant, * = p<0.05, ** = p<0.001, *** = p<0.0001.

We tested the changes in amplitude and latency with a Kruskal-Wallis test between learning steps for each area-group and applied a Bonferroni correction on the p-values to be more robust. We showed significant changes of amplitude and latency between learning steps in specific area-groups for both monkeys (**Fig. 35**). There were also antero-posterior and area patterns. The amplitude decreased in the anterior part for the LPFC of Monkey I, from anterior to posterior and it had more variability in the LPFC compared to the MCC for Monkey B. Also, the latency was higher in the LPFC compared to the MCC for Monkey B and there was a big increase of it between group 3 and group 4, so between anterior and posterior parts, in the LPFC of Monkey I.

Post-hoc Mann-Whitney tests on each significant area-group helped describe the direction of the change of amplitude (**Fig. 36**). We observed different patterns regarding the area-groups: some had a change of direction with an increase between steps 1 and 2 and a decrease between steps 2 and 3. Or, in contrary, a decrease between steps 1 and 2 and an increase between steps 2 and 3. Others had a gradual increase or a gradual decrease across learning steps. Thus, changes of amplitude across learning differed depending on the area-group.

Monkey I.

Area	comparison	statistic	p-value	significance	direction
LPFC_2	1 vs 2	4.20e+02	1.21e-04	***	increase
LPFC_2	1 vs 3	4.59e+02	1.49e-02	*	increase
LPFC_2	2 vs 3	9.78e+02	1.76e-01	ns	decrease
LPFC_3	1 vs 2	4.78e+02	5.87e-04	***	increase
LPFC_3	1 vs 3	6.46e+02	5.49e-01	ns	increase
LPFC_3	2 vs 3	1.15e+03	2.77e-03	**	decrease
LPFC_4	1 vs 2	7.80e+02	6.25e-01	ns	increase
LPFC_4	1 vs 3	2.49e+02	2.53e-06	***	increase
LPFC_4	2 vs 3	5.32e+02	5.16e-03	**	increase
LPFC_5	1 vs 2	8.16e+02	7.28e-01	ns	decrease
LPFC_5	1 vs 3	4.41e+02	5.56e-03	**	increase
LPFC_5	2 vs 3	6.13e+02	4.12e-02	*	increase
MCC_1	1 vs 2	5.24e+02	2.48e-03	**	increase
MCC_1	1 vs 3	7.23e+02	8.36e-01	ns	decrease
MCC_1	2 vs 3	1.15e+03	3.03e-03	**	decrease
MCC_2	1 vs 2	5.08e+02	1.22e-02	*	increase
MCC_2	1 vs 3	7.67e+02	1.13e-01	ns	decrease
MCC_2	2 vs 3	1.03e+03	3.99e-04	***	decrease
MCC_3	1 vs 2	4.02e+02	3.59e-05	***	increase
MCC_3	1 vs 3	1.32e+02	1.46e-09	***	increase
MCC_3	2 vs 3	8.57e+02	8.23e-01	ns	decrease

Monkey B.

Area	comparison	statistic	p-value	significance	direction
LPFC_2	1 vs 2	3.45e+02	1.38e-01	ns	decrease
LPFC_2	1 vs 3	2.21e+02	2.54e-01	ns	increase
LPFC_2	2 vs 3	1.38e+02	1.50e-02	*	increase
LPFC_5	1 vs 2	1.77e+02	1.43e-02	*	increase
LPFC_5	1 vs 3	1.72e+02	2.88e-02	*	increase
LPFC_5	2 vs 3	2.60e+02	9.39e-01	ns	increase
LPFC_6	1 vs 2	1.52e+02	1.90e-03	**	increase
LPFC_6	1 vs 3	1.99e+02	1.07e-01	ns	increase
LPFC_6	2 vs 3	3.14e+02	4.11e-01	ns	decrease
MCC_1	1 vs 2	2.18e+02	1.03e-01	ns	increase
MCC_1	1 vs 3	4.37e+02	1.47e-04	***	decrease
MCC_1	2 vs 3	4.80e+02	1.28e-05	***	decrease
MCC_2	1 vs 2	2.14e+02	5.72e-02	ns	increase
MCC_2	1 vs 3	4.24e+02	1.53e-03	**	decrease
MCC_2	2 vs 3	4.74e+02	2.28e-05	***	decrease
MCC_3	1 vs 2	2.01e+02	3.12e-02	*	increase
MCC_3	1 vs 3	4.39e+02	4.87e-04	***	decrease
MCC_3	2 vs 3	4.64e+02	5.77e-05	***	decrease
MCC_4	1 vs 2	2.42e+02	2.50e-01	ns	increase
MCC_4	1 vs 3	1.23e+02	1.99e-03	**	increase
MCC_4	2 vs 3	2.36e+02	4.11e-01	ns	increase

Figure 36. Statistical results of the amplitudes of the POS-NEG signals between learning steps. Mann-Whitney U post-hoc tests for each comparison of each area. ns = no significant, * = $p<0.05$, ** = $p<0.001$, *** = $p<0.0001$.

We did the same post-hoc tests on each significant area-group to describe the direction of the change of latency (**Fig. 37**). We saw that less post-hoc tests were significant for the latency compared to the amplitude. For Monkey I, 12 tests on 21 for the amplitude and 5 tests on 15 for the latency were significant and for Monkey B, 12 tests on 18 for the amplitude and 8 tests on 18 for the latency. This could mean that learning steps had a smaller effect on the peak's latency than on the amplitude. Here again, we highlighted different patterns regarding the area-groups. It can be noted that area-groups with significant changes of amplitude and latency had the same direction for both, meaning that a higher amplitude in POS-NEG signals was associated with a longer latency.

Monkey I.

Area	comparison	statistic	p-value	significance	direction
LPFC_1	1 vs 2	4.34e+02	1.10e-04	***	increase
LPFC_1	1 vs 3	4.54e+02	8.24e-03	**	increase
LPFC_1	2 vs 3	8.38e+02	9.59e-01	ns	increase
LPFC_2	1 vs 2	3.84e+02	2.78e-05	***	increase
LPFC_2	1 vs 3	8.01e+02	2.09e-01	ns	decrease
LPFC_2	2 vs 3	1.25e+03	1.08e-04	***	decrease
LPFC_3	1 vs 2	6.12e+02	2.65e-02	*	increase
LPFC_3	1 vs 3	7.47e+02	6.45e-01	ns	decrease
LPFC_3	2 vs 3	1.14e+03	4.77e-03	**	decrease
LPFC_4	1 vs 2	6.08e+02	3.63e-02	*	increase
LPFC_4	1 vs 3	3.70e+02	6.69e-04	***	increase
LPFC_4	2 vs 3	7.69e+02	5.57e-01	ns	increase
MCC_3	1 vs 2	1.02e+03	1.24e-01	ns	decrease
MCC_3	1 vs 3	9.87e+02	2.64e-03	**	decrease
MCC_3	2 vs 3	1.18e+03	1.30e-03	**	decrease
MCC_4	1 vs 2	6.26e+02	3.63e-02	*	increase
MCC_4	1 vs 3	3.96e+02	1.16e-03	**	increase
MCC_4	2 vs 3	5.56e+02	1.00e-02	*	increase

Monkey B.

Area	comparison	statistic	p-value	significance	direction
LPFC_3	1 vs 2	2.79e+02	7.50e-01	ns	decrease
LPFC_3	1 vs 3	4.44e+02	7.41e-05	***	decrease
LPFC_3	2 vs 3	2.92e+02	2.50e-01	ns	decrease
LPFC_6	1 vs 2	3.52e+02	4.49e-01	ns	decrease
LPFC_6	1 vs 3	4.60e+02	7.85e-05	***	decrease
LPFC_6	2 vs 3	4.62e+02	7.19e-05	***	decrease
MCC_4	1 vs 2	1.56e+02	4.06e-03	**	increase
MCC_4	1 vs 3	1.87e+02	9.22e-02	ns	increase
MCC_4	2 vs 3	3.46e+02	1.30e-01	ns	increase
MCC_5	1 vs 2	2.54e+02	4.97e-01	ns	decrease
MCC_5	1 vs 3	1.02e+02	2.49e-03	**	increase
MCC_5	2 vs 3	1.22e+02	2.68e-02	*	increase

Figure 37. Statistical results of the latencies of POS-NEG signals between learning steps. Mann-Whitney U post-hoc tests for each comparison of each area. ns = no significant, * = p<0.05, ** = p<0.001, *** = p<0.0001.

By focusing on the POS-NEG signals we showed changes occurring during the learning steps. These changes were not linear/gradual and depended on the area-groups concerned. The variability of these changes could have different possible explanations, one could be that changes could take place in the individual processing of positive and negative

feedback and that these changes may not take place in the same area-group at the same time. Thus, to understand precisely how the differentiation between positive and negative feedback took place, we studied the processing of each type of feedback individually.

Positive feedback

We focused first on the positive feedback brought by the reward in the DL task. At the beginning of the training, so of the DL task, monkeys were familiar with reward as they had done multiple baseline task sessions before. However, until the DL task the reward brought no information to the monkey about future action or learning, beyond learning to touch the single stimulus available. They received it in all trials without other conditions than touching the screen. Thus, the reward became positive feedback by bringing useful information only in the DL task where the task requires an explicit choice between two options. In the baseline task, rewards elicited an evoked response (**Fig. 38**). There were differences between antero-posterior levels with a clear distinction between anterior (1-3) and posterior (4-6) parts for both monkeys in both areas (MCC and LPFC). However, this distinction was not the same in each monkey as the evoked potential by the reward had a higher amplitude in anterior parts for Monkey I whereas it was in posterior parts for Monkey B.

Even if there were some variations, the reward elicited a response in both LPFC and MCC in the baseline task with an antero-posterior differentiation. This will be used as a comparison for the real aim of this part, which was to describe any changes in the evoked response when the reward gained informational value (in that it also became a feedback), and to describe how it evolved throughout training.

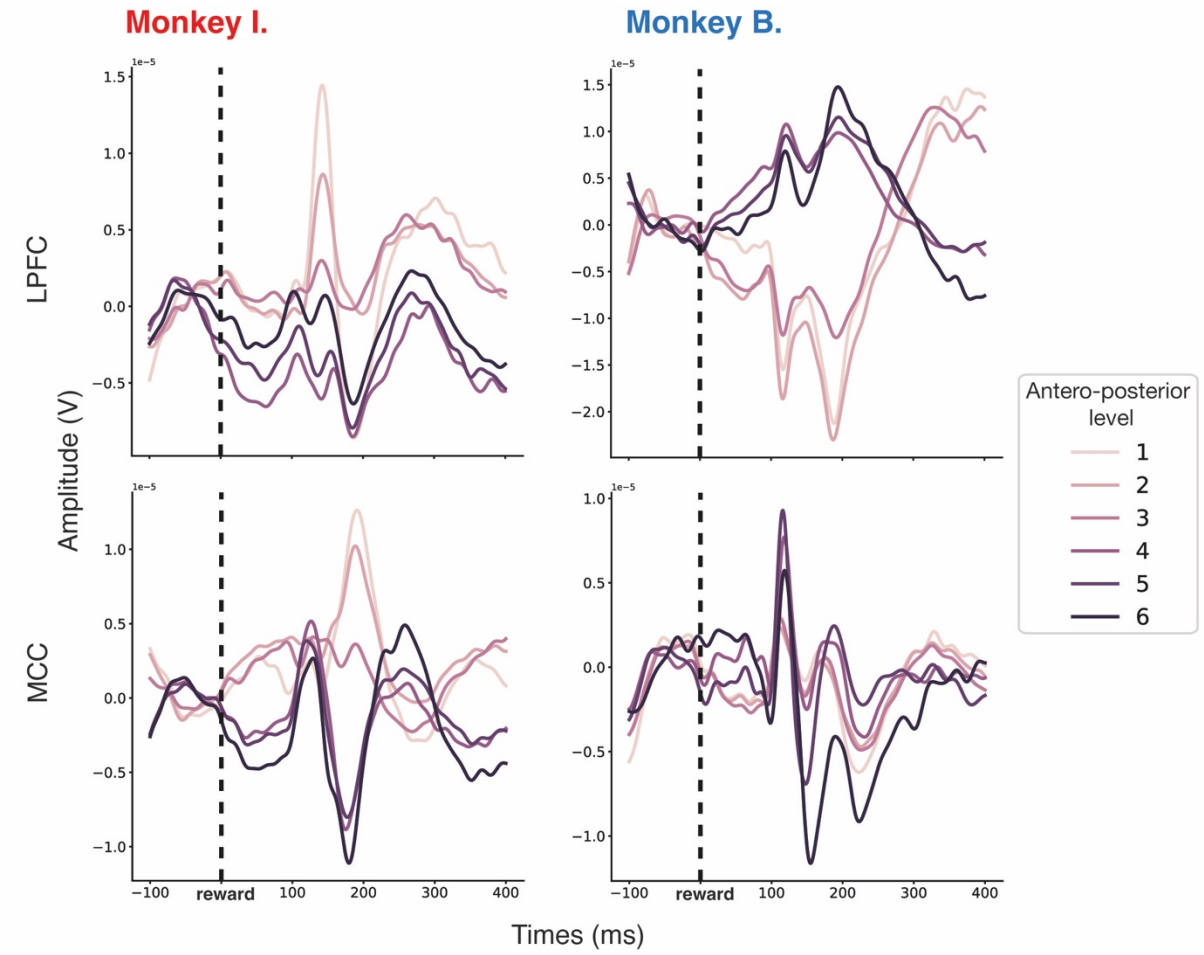

Figure 38. Evoked potentials by reward in the baseline task. Time window of 100 ms before the feedback and 400 ms after. Black dashed line represents the reward onset at time 0. In antero-posterior level, 1 is the most anterior and 6 the most posterior.

We looked at the potential evoked by the positive feedback for each learning step, with still the same time window as previously (-100 to 400ms) (**Fig. 39 & 40**). The signal after the feedback was significantly different between the learning steps (Kruskal-Wallis test, $p<0.05$) in all area-groups for both monkeys (except LPFC5 and LPFC6 of Monkey B) showing that learning elicited a modulation of the positive feedback response. We noted in Monkey I LPFC and MCC signals and in Monkey B MCC signal that there was only one clear positive peak evoked by the reward in the baseline task between 100 and 200 ms of latency, as the second one, if present, was very large and with little variations.

In contrast, there were two clear positive peaks evoked by the positive feedback brought by the reward in the DL task for Monkey I LPFC and posterior MCC. Importantly, the peak present in the peak window was the second one so the one which was less clear in the

baseline task. For Monkey B, we remarked again that steps 1 and 2 had a more stable signal in which we can identify peaks whereas step 3 had more little variations, making it noisier. Some peaks in Monkey I could be associated with specific ERP components. For example, all MCC groups and the posterior part of the LPFC (4 to 6) elicited a negative peak around 250-300 ms post-feedback which could correspond to a fERN component, supporting a feedback detection. Posterior parts of the MCC and the LPFC also elicited a positive deflection after 300 ms that could be associated with a P300 component, linked to feedback evaluation. These observations highlight the potential associations to well-known ERP components. The presence of the fERN in the 250-300 ms range, followed by a positive deflection that could represent a P300 component, suggests that these brain regions are involved in both detecting feedback and evaluating it. This supports the idea that MCC and LPFC are key players in feedback processing, with distinct roles in feedback detection and evaluation during learning tasks, particularly when processing positive reinforcement.

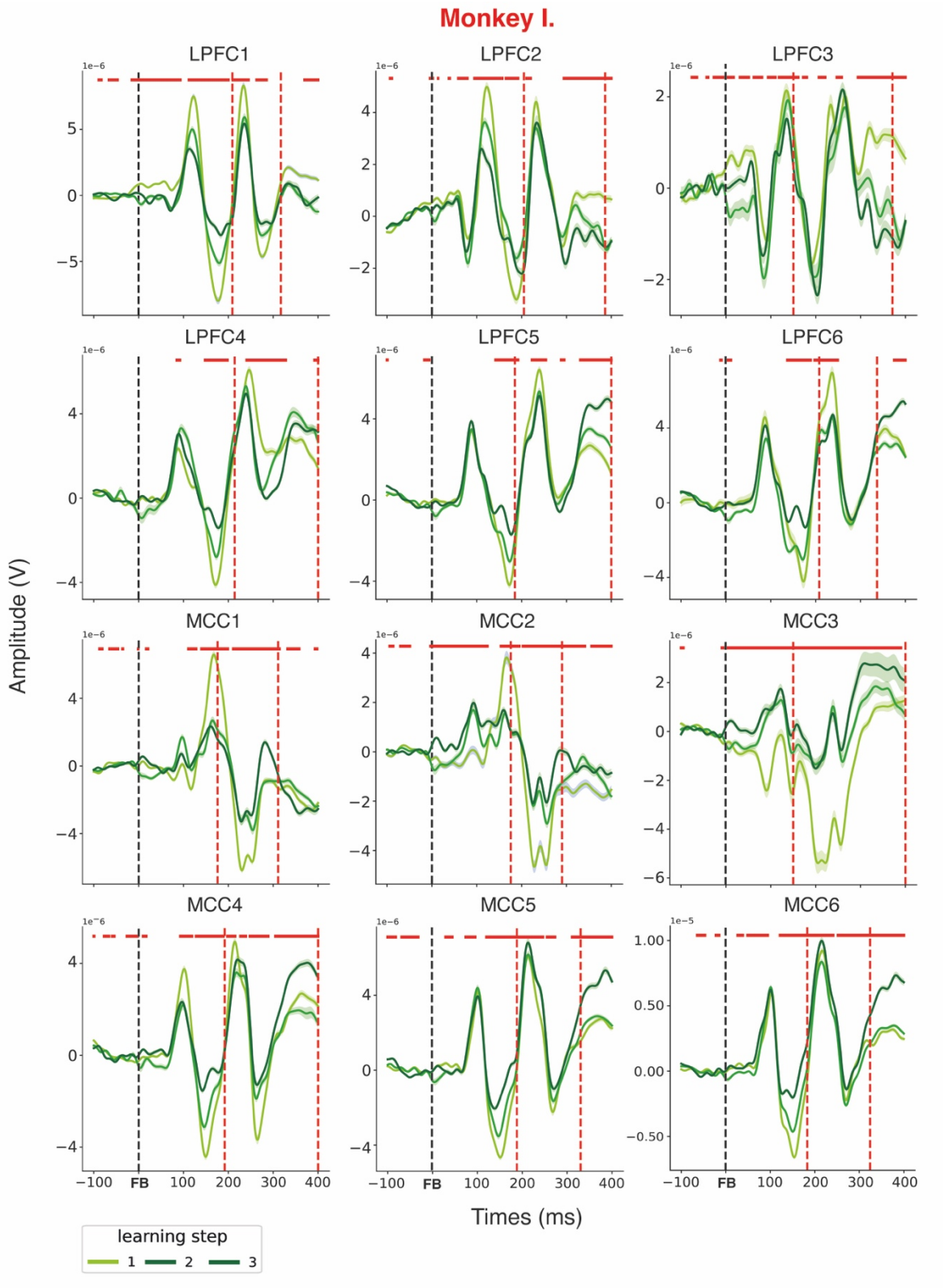

Figure 39. Evoked potentials by positive feedback across learning steps for Monkey I. Time window of 100ms before the feedback and 400ms after. Black dashed line represents the feedback at time 0. Red dashed lines represent the limit of the peaks window. Red horizontal segments indicate a significant p-value of the Kruskal-Wallis test between learning steps for each time point. FB = feedback.

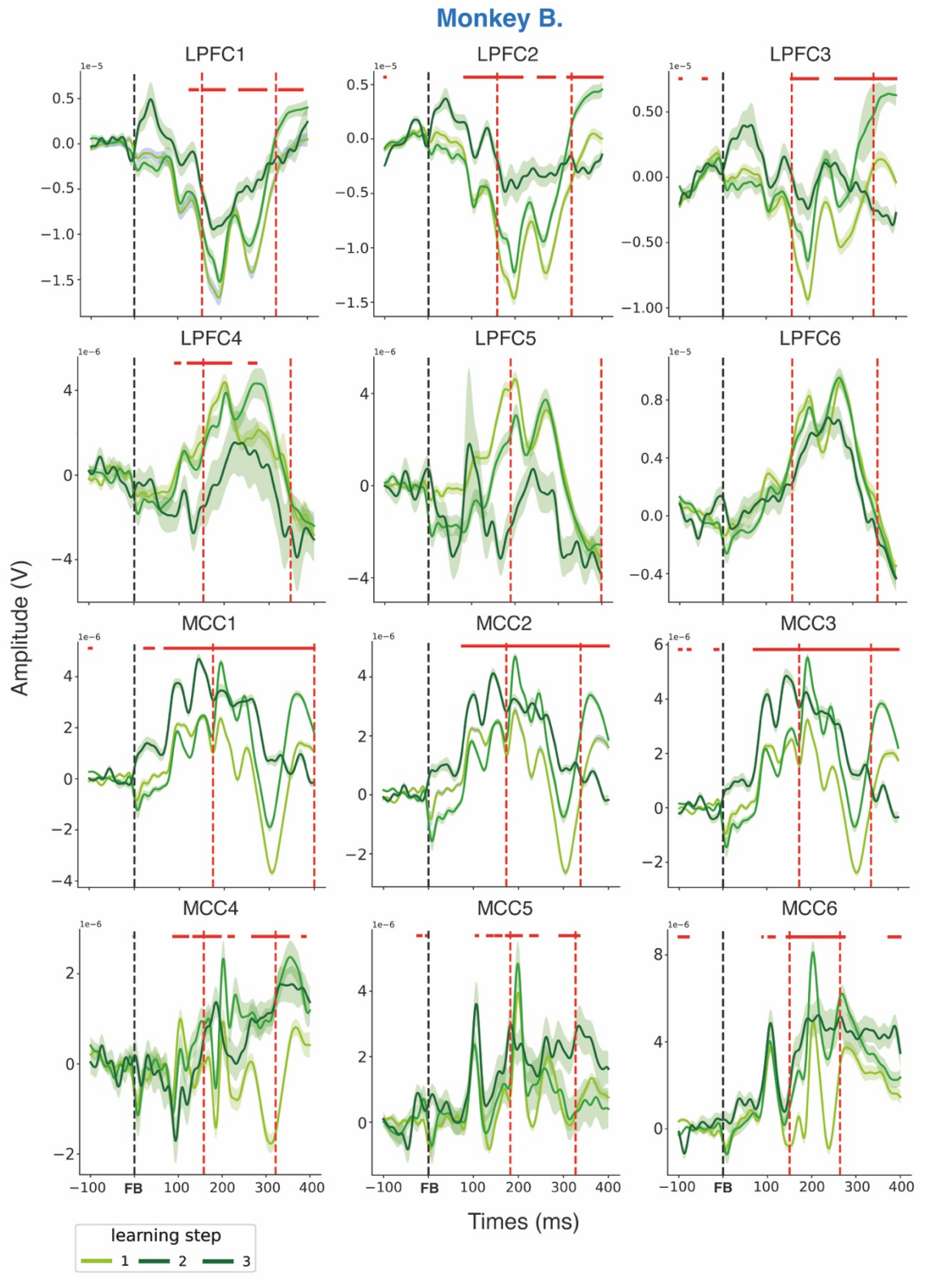

Figure 40. Evoked potentials by positive feedback across learning steps for Monkey B. Time window of 100ms before the feedback and 400ms after. Black dashed line represents the feedback at time 0. Red dashed lines represent the limit of the peaks window. Red horizontal segments indicate a significant p-value of the Kruskal-Wallis test between learning steps for each time point. FB = feedback.

Statistical analysis of evoked response

Then, we performed the same peak detection analysis that we described above. We tested the changes in amplitude and latency with a Kruskal-Wallis test between learning steps for each area-group and applied a Bonferroni correction on the p-values. There were significant changes of amplitude and latency across learning steps depending on the area-groups for both monkeys in the positive peak evoked by the positive feedback (**Fig. 41**). Amplitude decreased from anterior to posterior in the anterior part of the LPFC of Monkey I. Otherwise it increased from anterior to posterior in MCC posterior parts for Monkey I, in all the LPFC parts and in MCC posterior parts of Monkey B.

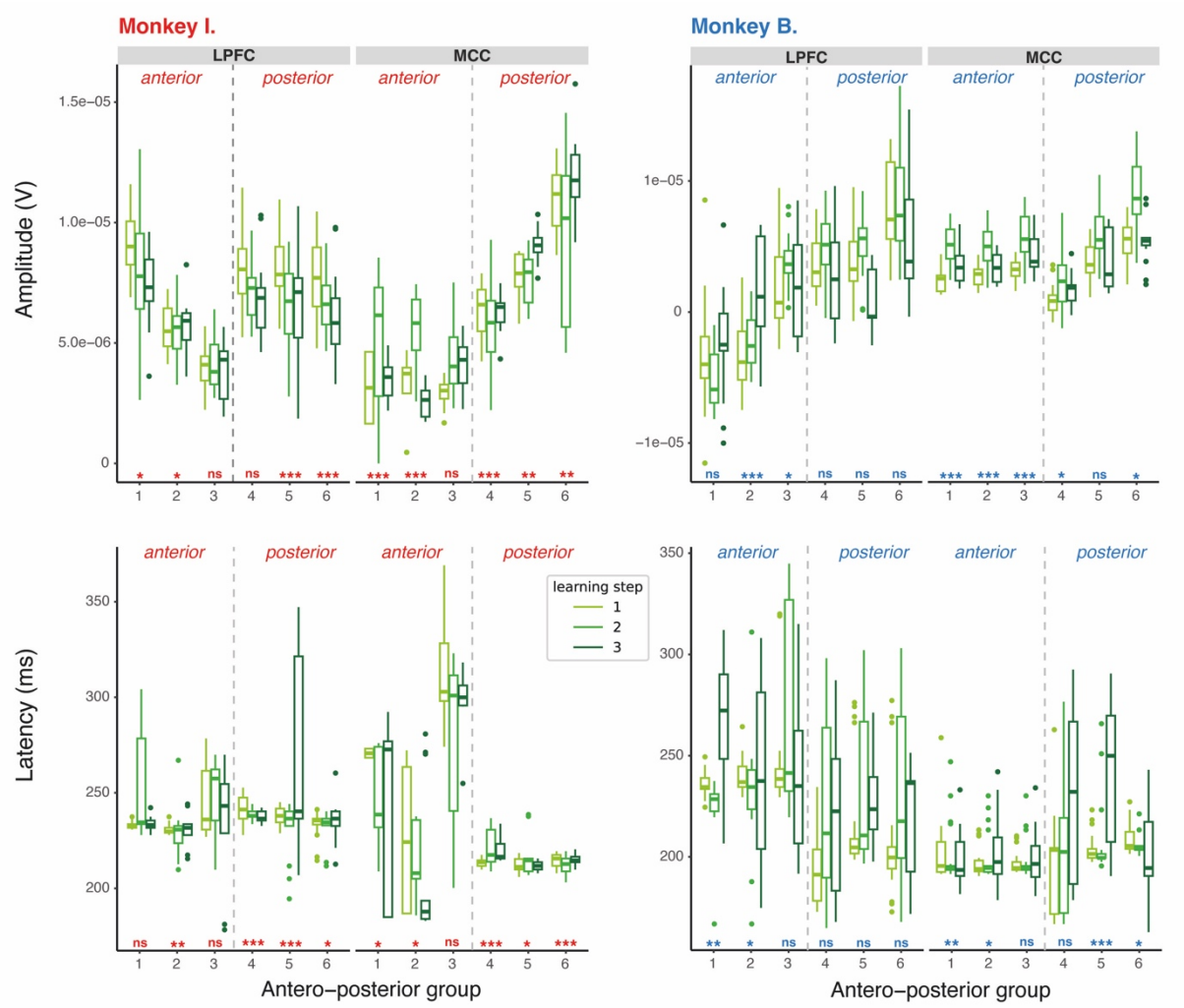

Figure 41. Evolution of amplitude and latency of potentials evoked by positive feedback across training. Kruskal-Wallis test between learning steps. ns = no significant, * = p<0.05, ** = p<0.001, *** = p<0.0001.

We did post-hoc Mann-Whitney tests on each significant area-group to describe the direction of the change (**Fig. 42 & 43**). There were different patterns of evolution between monkeys. Amplitude changes had always been in the same direction for Monkey I with a decrease across learning steps whereas results were more variable for Monkey B. Most of the area-groups showed an increase but some had an increase then a decrease across learning steps. The latencies elicited more mixed results for both monkeys.

Monkey I.

Area	comparison	statistic	p-value	significance	direction
LPFC_1	1 vs 2	1.12e+03	1.54e-02	*	decrease
LPFC_1	1 vs 3	1.13e+03	5.00e-06	***	decrease
LPFC_1	2 vs 3	9.75e+02	1.86e-01	ns	decrease
LPFC_4	1 vs 2	1.16e+03	5.44e-03	**	decrease
LPFC_4	1 vs 3	1.04e+03	4.40e-04	***	decrease
LPFC_4	2 vs 3	1.00e+03	1.17e-01	ns	decrease
LPFC_5	1 vs 2	1.17e+03	6.65e-04	***	decrease
LPFC_5	1 vs 3	9.28e+02	3.89e-03	**	decrease
LPFC_5	2 vs 3	7.93e+02	7.16e-01	ns	increase
LPFC_6	1 vs 2	1.03e+03	5.93e-04	***	decrease
LPFC_6	1 vs 3	1.06e+03	1.71e-04	***	decrease
LPFC_6	2 vs 3	7.32e+02	6.11e-01	ns	decrease
MCC_2	1 vs 2	3.00e+01	1.53e-02	*	increase
MCC_2	1 vs 3	1.50e+02	1.52e-01	ns	decrease
MCC_2	2 vs 3	4.04e+02	2.82e-03	**	decrease
MCC_3	1 vs 2	2.42e+02	2.09e-08	***	increase
MCC_3	1 vs 3	2.13e+02	2.10e-07	***	increase
MCC_3	2 vs 3	7.60e+02	5.02e-01	ns	increase
MCC_5	1 vs 2	7.90e+02	8.49e-01	ns	increase
MCC_5	1 vs 3	2.67e+02	1.08e-05	***	increase
MCC_5	2 vs 3	4.89e+02	1.38e-03	**	increase

Monkey B.

Area	comparison	statistic	p-value	significance	direction
LPFC_2	1 vs 2	9.10e+01	1.44e-01	ns	increase
LPFC_2	1 vs 3	6.00e+01	1.22e-03	**	increase
LPFC_2	2 vs 3	5.00e+01	5.36e-02	ns	increase
LPFC_4	1 vs 2	2.02e+02	5.12e-02	ns	increase
LPFC_4	1 vs 3	3.22e+02	2.06e-01	ns	decrease
LPFC_4	2 vs 3	3.96e+02	1.02e-02	*	decrease
LPFC_5	1 vs 2	1.84e+02	5.15e-02	ns	increase
LPFC_5	1 vs 3	3.70e+02	2.03e-02	*	decrease
LPFC_5	2 vs 3	4.15e+02	2.44e-04	***	decrease
MCC_1	1 vs 2	8.10e+01	1.24e-05	***	increase
MCC_1	1 vs 3	1.72e+02	2.88e-02	*	increase
MCC_1	2 vs 3	3.88e+02	6.59e-03	**	decrease
MCC_2	1 vs 2	8.20e+01	1.36e-05	***	increase
MCC_2	1 vs 3	1.78e+02	6.00e-02	ns	increase
MCC_2	2 vs 3	3.99e+02	8.43e-03	**	decrease
MCC_3	1 vs 2	7.20e+01	5.36e-06	***	increase
MCC_3	1 vs 3	1.48e+02	1.11e-02	*	increase
MCC_3	2 vs 3	3.83e+02	2.18e-02	*	decrease
MCC_4	1 vs 2	1.88e+02	1.61e-02	*	increase
MCC_4	1 vs 3	1.64e+02	1.84e-02	*	increase
MCC_4	2 vs 3	3.08e+02	4.88e-01	ns	decrease
MCC_5	1 vs 2	1.98e+02	2.70e-02	*	increase
MCC_5	1 vs 3	3.02e+02	3.90e-01	ns	decrease
MCC_5	2 vs 3	3.59e+02	3.42e-02	*	decrease
MCC_6	1 vs 2	7.90e+01	1.76e-05	***	increase
MCC_6	1 vs 3	2.25e+02	2.91e-01	ns	increase
MCC_6	2 vs 3	3.73e+02	6.63e-03	**	decrease

Figure 42. Statistical results of positive feedback amplitude across learning steps. Mann-Whitney U post-hoc tests for each comparison of each area. ns = no significant, * = p<0.05, ** = p<0.001, *** = p<0.0001.

Monkey I.

Area	comparison	statistic	p-value	significance	direction
LPFC_1	1 vs 2	5.28e+02	2.67e-03	**	increase
LPFC_1	1 vs 3	6.12e+02	3.32e-01	ns	increase
LPFC_1	2 vs 3	1.03e+03	6.04e-02	ns	decrease
LPFC_3	1 vs 2	6.17e+02	2.98e-02	*	increase
LPFC_3	1 vs 3	7.28e+02	7.99e-01	ns	increase
LPFC_3	2 vs 3	1.15e+03	3.50e-03	**	decrease
LPFC_4	1 vs 2	8.82e+02	8.08e-01	ns	decrease
LPFC_4	1 vs 3	9.74e+02	3.95e-03	**	decrease
LPFC_4	2 vs 3	1.16e+03	2.05e-03	**	decrease
LPFC_5	1 vs 2	8.22e+02	9.13e-01	ns	decrease
LPFC_5	1 vs 3	3.96e+02	2.75e-03	**	increase
LPFC_5	2 vs 3	5.06e+02	2.27e-03	**	increase
MCC_4	1 vs 2	5.17e+02	3.14e-03	**	increase
MCC_4	1 vs 3	1.99e+02	1.36e-07	***	increase
MCC_4	2 vs 3	6.18e+02	4.56e-02	*	decrease
MCC_5	1 vs 2	6.30e+02	8.78e-02	ns	increase
MCC_5	1 vs 3	7.22e+02	5.42e-01	ns	decrease
MCC_5	2 vs 3	1.10e+03	1.10e-02	*	decrease

Monkey B.

Area	comparison	statistic	p-value	significance	direction
LPFC_1	1 vs 2	1.45e+02	2.31e-02	*	decrease
LPFC_1	1 vs 3	5.80e+01	4.11e-04	***	increase
LPFC_1	2 vs 3	3.10e+01	1.51e-02	*	increase
LPFC_4	1 vs 2	1.66e+02	7.34e-03	**	increase
LPFC_4	1 vs 3	1.67e+02	3.37e-02	*	increase
LPFC_4	2 vs 3	2.89e+02	7.73e-01	ns	decrease
MCC_5	1 vs 2	3.69e+02	2.67e-01	ns	decrease
MCC_5	1 vs 3	9.00e+01	1.43e-04	***	increase
MCC_5	2 vs 3	1.15e+02	1.11e-03	**	increase

Figure 43. Statistical results of positive feedback latency across learning steps. Mann-Whitney U post-hoc tests for each comparison of each area. ns = no significant, * = p<0.05, ** = p<0.001, *** = p<0.0001.

We showed that changes occurred in peak amplitude and latency of each area-group across learning with a majority of decrease for Monkey I and increase for Monkey B. Thus, learning had an impact on the evoked response to positive feedback but interestingly this impact was in the opposite direction between monkeys.

Temporality between areas

We also studied the nature of the relations *between* area-groups. As described above, the LPFC and the MCC form an interconnected network linked to many cognitive functions. We hypothesised that the physiological relation between these areas could change across learning, potentially reflecting the network state once learning or learning to learn are achieved. We studied the temporality of the reward response by comparing the latency in the LPFC to the latency in the MCC (**Fig. 44**). There are 6 antero-posterior groups of electrodes in both MCC and LPFC. We directly compared the timing in the most anterior of each and so

on in a posterior direction. A strong overall pattern was clear that the reward response was significant in the MCC before the LPFC for both monkeys, aligning with previous literature (Hayden & Platt, 2010), but whilst there were significant changes across learning steps, these changes did not form a consistently interpretable pattern across the antero-posterior groups (**Fig. 45**). This would therefore seem to rule out any generalised shift in the MCC-LPFC hierarchy for this particular measure over learning. An exception to the general pattern was noted for Monkey I within group 3 showing the opposite pattern (responses arrived first in the LPFC then in the MCC).

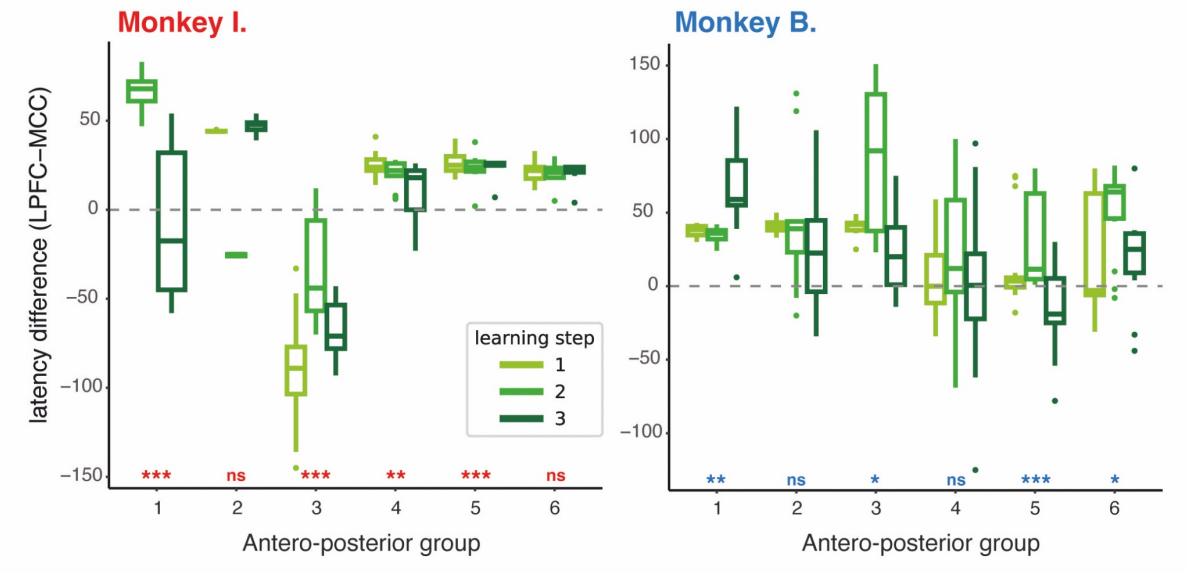

Figure 44. Difference of evoked potentials by positive feedback latency between LPFC and MCC across learning steps. LPFC > MCC means that response arrived first in MCC then in LPFC. LFPC < MCC means that response arrived first in LPFC then in MCC. Kruskal-Wallis test between learning steps. ns = no significant, * = p<0.05, ** = p<0.001, *** = p<0.0001.

Monkey I.

ant-posterior	comparison	statistic	p-value	significance	direction
gp1	1 vs 2	0.00e+00	2.85e-02	*	increase
gp1	1 vs 3	4.60e+01	4.25e-01	ns	decrease
gp1	2 vs 3	5.00e+02	1.11e-07	***	decrease
gp3	1 vs 2	1.34e+02	2.82e-09	***	increase
gp3	1 vs 3	2.84e+02	9.20e-04	***	increase
gp3	2 vs 3	1.02e+03	8.43e-07	***	decrease
gp4	1 vs 2	7.10e+02	4.55e-01	ns	decrease
gp4	1 vs 3	8.23e+02	1.02e-03	**	decrease
gp4	2 vs 3	9.38e+02	2.35e-03	**	decrease
gp5	1 vs 2	8.30e+02	5.97e-02	ns	decrease
gp5	1 vs 3	4.11e+02	4.08e-02	*	increase
gp5	2 vs 3	3.26e+02	6.83e-05	***	increase

Monkey B.

ant-posterior	comparison	statistic	p-value	significance	direction
gp1	1 vs 2	9.05e+01	1.99e-01	ns	decrease
gp1	1 vs 3	4.35e+01	8.99e-04	***	increase
gp1	2 vs 3	2.30e+01	1.29e-02	*	increase
gp3	1 vs 2	6.25e+01	7.17e-02	ns	increase
gp3	1 vs 3	2.28e+02	1.31e-01	ns	decrease
gp3	2 vs 3	2.15e+02	1.45e-02	*	decrease
gp5	1 vs 2	1.05e+02	6.35e-03	**	increase
gp5	1 vs 3	2.72e+02	7.07e-03	**	decrease
gp5	2 vs 3	3.13e+02	4.97e-04	***	decrease
gp6	1 vs 2	1.79e+02	6.70e-02	ns	increase
gp6	1 vs 3	2.35e+02	9.62e-01	ns	increase
gp6	2 vs 3	2.91e+02	1.36e-02	*	decrease

Figure 45. Statistical results of difference of positive feedback latency between LPFC and MCC. Mann-Whitney U post-hoc tests for each comparison of each area. ns = no significant, * = $p<0.05$, ** = $p<0.001$, *** = $p<0.0001$.

Overall, the responses to positive feedback showed a significant evolution of peak parameters throughout the learning steps highlighting a real impact of the training. It should be noted that here again, monkeys elicited an opposite pattern of changes showing that the training effect could be materialised in different ways. Moreover, contrary to our hypothesis, the training did not impact on the temporality between areas.

To go further on the evolution from reward responses to positive feedback responses, it would be interesting to assess changes in the first peak as it was present in both tasks. It arrived at a shorter latency, linking it with a more sensorial detection but it could add interesting information on how the transition between reward only and reward used as a positive feedback information appeared.

Negative feedback

Unlike the reward, there was no notion of error in the baseline task as, as a reminder, monkeys received a reward in all trials where there was a successful touch. Thus, they faced the notion of choice errors for the very first time when they started the DL task. In the start of the DL task, monkeys would not have the concept of a choice error, but they experienced an absence of reward and a latency time before the next trial, which they needed to learn to interpret as a negative feedback. Our aim was to study the evoked response to this negative feedback when they faced it for the first time and how it evolved throughout training.

We looked at the potential evoked by the negative feedback for each learning step, with still the same time window as previously (-100 to 400ms). Parts of the signal after the feedback were significantly different between the learning steps (Kruskal-Wallis test, $p<0.05$) for both monkeys, except in MCC2 and MCC3 for Monkey I and MCC4 and MCC5 for Monkey B (**Fig. 46 & 47**).

We noted the presence of a similar peak as in reward and positive feedback responses around 100-150 ms after the feedback for Monkey I LPFC and posterior part of MCC. Monkey B signals presented a lot more variance for each learning step than Monkey I, except in the MCC anterior parts. This could be linked to the signal loss but it could also mean that negative feedback response was less stable/clear for Monkey B.

Here again, we could identify specific ERP components. Posterior parts of the MCC and the LPFC of Monkey I showed a positive peak between 200 and 300 ms and, in the case of negative feedback, this could be associated with the Pe which indicates a conscious awareness of the error. Negative deflections between 200 and 300 ms could be associated with the fERN in MCC anterior parts of Monkey I and LPFC anterior part of Monkey B. In the posterior parts of both areas of Monkey I we also saw a negative deflection but before 200 ms, making it unclear between the ERN, associated with the error made, and the fERN. The identified ERP components suggest that both error detection and feedback evaluation processes are engaged differently across areas during negative feedback.

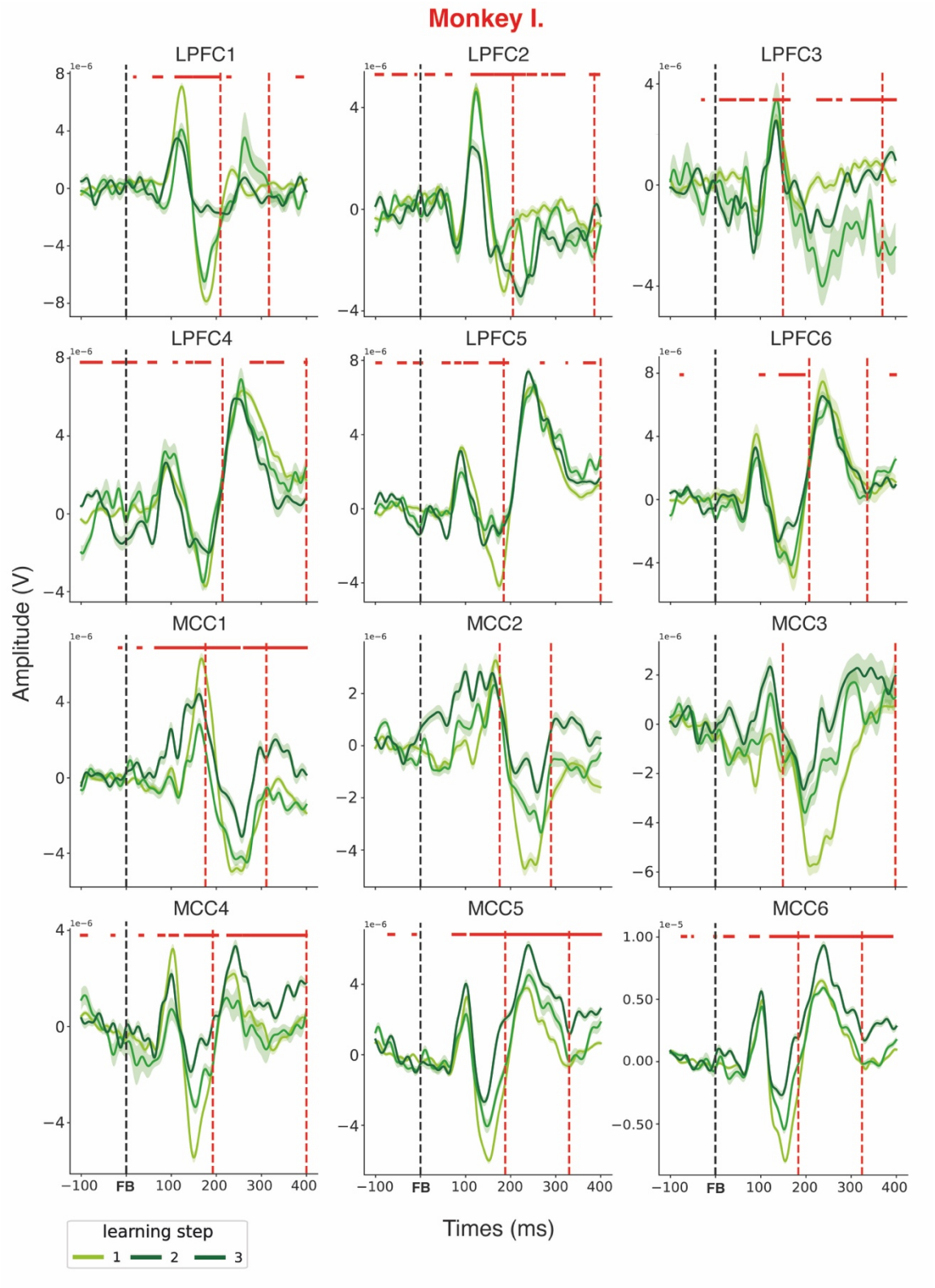

Figure 46. Evoked potentials by negative feedback across learning steps for Monkey I. Time window of 100ms before the feedback and 400ms after. Black dashed line represents the feedback at time 0. Red dashed lines represent the limit of the peaks window. Red horizontal segments indicate a significant p-value of the Kruskal-Wallis test between learning steps for each time point. FB = feedback.

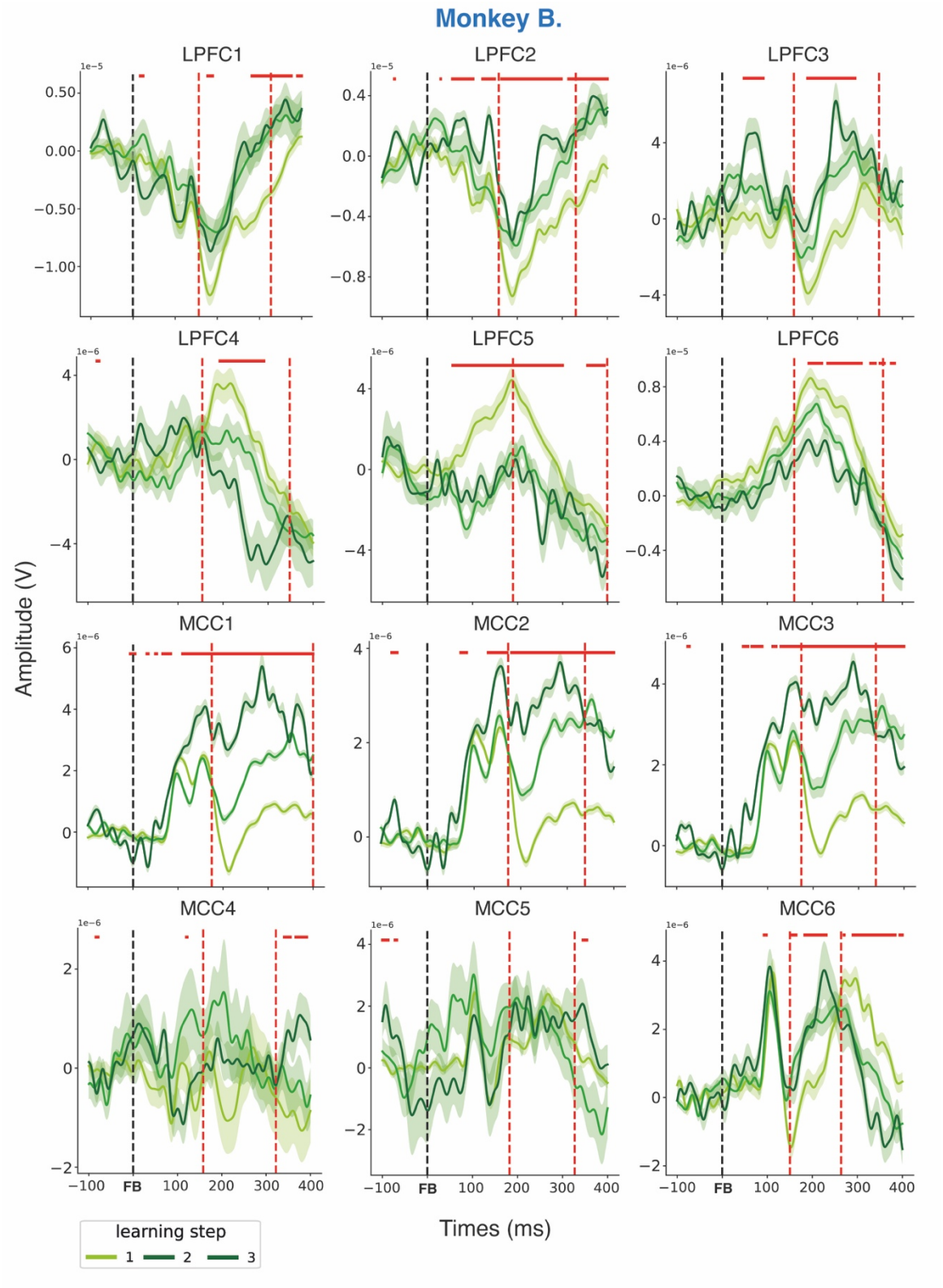

Figure 47. Evoked potentials by negative feedback across learning steps for Monkey B. Time window of 100ms before the feedback and 400ms after. Black dashed line represents the feedback at time 0. Red dashed lines represent the limit of the peaks window. Red horizontal segments indicate a significant p-value of the Kruskal-Wallis test between learning steps for each time point. FB = feedback.

Statistical analysis of evoked response

We did the same peak analysis as for positive feedback to describe the evolution of the latency and the amplitude of these responses. We used the same approach as described above to detect peaks and extract parameters.

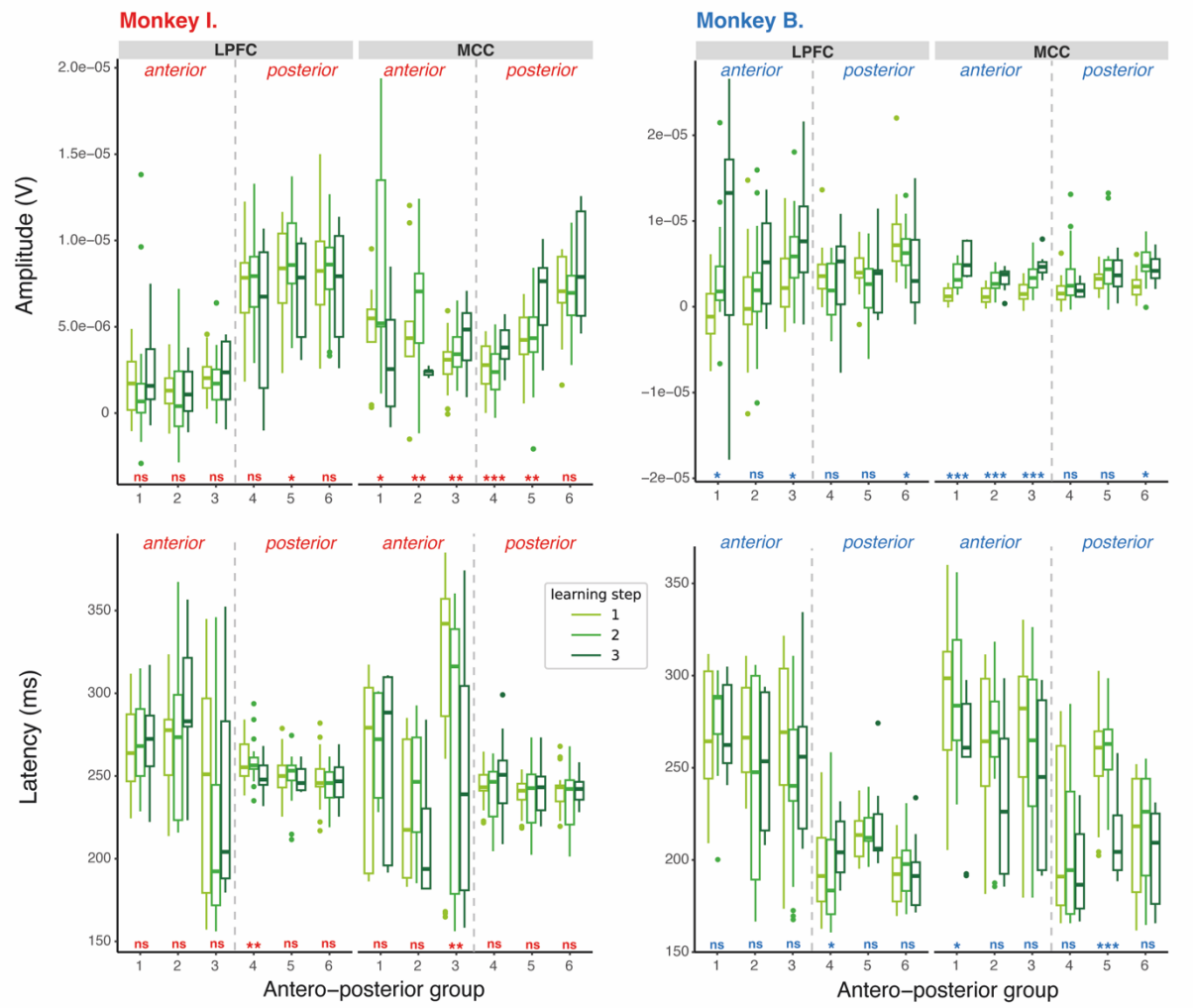

Figure 48. Evolution of amplitude and latency of potentials evoked by negative feedback across training. Kruskal-Wallis test between learning steps. ns = no significant, * = p<0.05, ** = p<0.001, *** = p<0.0001.

We tested changes in amplitude and latency with a Kruskal-Wallis test between learning steps for each area-group and applied a Bonferroni correction on the p-values. There were significant differences of amplitude and latency between learning steps for both monkeys (**Fig. 48**). However, there was no effect in latency for Monkey B in the MCC and no effect of amplitude in LPFC for Monkey I. Amplitudes were higher in the posterior part than in the

anterior part for Monkey I and it also increased from anterior to posterior in the MCC posterior part. There was also more amplitude variations in the LPFC compared to the MCC for Monkey B. The latencies had more variation in the anterior part compared to posterior parts in both the LPFC and the MCC for Monkey I and in the LPFC for Monkey B.

Overall, the learning course had less impact on the evoked response to negative feedback than the evoked response to positive feedback because we showed less significant effects between learning steps in area-groups.

Then we did post-hoc Mann-Whitney tests on each significant area to describe the direction of the change (**Fig. 49 & 50**). Monkeys had different patterns, with a majority of increases of amplitude across learning steps for Monkey B and only decreases for Monkey I.

Monkey I.

Area	comparison	statistic	p-value	significance	direction
LPFC_5	1 vs 2	8.36e+02	8.69e-01	ns	decrease
LPFC_5	1 vs 3	9.07e+02	3.10e-02	*	decrease
LPFC_5	2 vs 3	1.07e+03	2.59e-02	*	decrease
MCC_1	1 vs 2	6.40e+01	6.76e-01	ns	decrease
MCC_1	1 vs 3	1.72e+02	1.40e-01	ns	decrease
MCC_1	2 vs 3	4.27e+02	5.04e-03	**	decrease
MCC_2	1 vs 2	6.60e+01	2.67e-01	ns	increase
MCC_2	1 vs 3	1.18e+02	2.62e-02	*	decrease
MCC_2	2 vs 3	2.79e+02	9.07e-04	***	decrease
MCC_3	1 vs 2	6.26e+02	3.63e-02	*	increase
MCC_3	1 vs 3	3.76e+02	5.37e-04	***	increase
MCC_3	2 vs 3	6.42e+02	7.65e-02	ns	increase
MCC_4	1 vs 2	9.00e+02	5.35e-01	ns	decrease
MCC_4	1 vs 3	3.94e+02	1.71e-03	**	increase
MCC_4	2 vs 3	4.34e+02	2.07e-04	***	increase
MCC_5	1 vs 2	7.30e+02	2.57e-01	ns	increase
MCC_5	1 vs 3	3.88e+02	8.54e-04	***	increase
MCC_5	2 vs 3	6.12e+02	4.03e-02	*	increase

Monkey B.

Area	comparison	statistic	p-value	significance	direction
LPFC_1	1 vs 2	1.33e+02	2.93e-02	*	increase
LPFC_1	1 vs 3	1.22e+02	1.40e-02	*	increase
LPFC_1	2 vs 3	1.50e+02	1.80e-01	ns	increase
LPFC_3	1 vs 2	1.58e+02	2.18e-02	*	increase
LPFC_3	1 vs 3	1.26e+02	1.11e-02	*	increase
LPFC_3	2 vs 3	2.38e+02	4.36e-01	ns	increase
LPFC_6	1 vs 2	3.98e+02	9.91e-02	ns	decrease
LPFC_6	1 vs 3	3.91e+02	1.37e-02	*	decrease
LPFC_6	2 vs 3	3.52e+02	1.03e-01	ns	decrease
MCC_1	1 vs 2	9.00e+01	1.65e-05	***	increase
MCC_1	1 vs 3	2.80e+01	1.45e-07	***	increase
MCC_1	2 vs 3	1.52e+02	8.96e-03	**	increase
MCC_2	1 vs 2	1.32e+02	8.07e-04	***	increase
MCC_2	1 vs 3	7.90e+01	4.91e-05	***	increase
MCC_2	2 vs 3	1.90e+02	7.14e-02	ns	increase
MCC_3	1 vs 2	1.42e+02	9.71e-04	***	increase
MCC_3	1 vs 3	5.30e+01	2.30e-06	***	increase
MCC_3	2 vs 3	1.65e+02	1.95e-02	*	increase
MCC_6	1 vs 2	9.50e+01	4.02e-02	*	increase
MCC_6	1 vs 3	6.70e+01	4.94e-03	**	increase
MCC_6	2 vs 3	2.42e+02	8.11e-01	ns	decrease

Figure 49. Statistical results of negative feedback amplitude across learning steps. Mann-Whitney U post-hoc tests for each comparison of each area. ns = no significant, * = p<0.05, ** = p<0.001, *** = p<0.0001.

Monkey I.

Area	comparison	statistic	p-value	significance	direction
LPFC_4	1 vs 2	7.78e+02	4.87e-01	ns	increase
LPFC_4	1 vs 3	9.48e+02	9.30e-03	**	decrease
LPFC_4	2 vs 3	1.21e+03	4.10e-04	***	decrease
MCC_3	1 vs 2	1.10e+03	2.47e-02	*	decrease
MCC_3	1 vs 3	9.80e+02	3.30e-03	**	decrease
MCC_3	2 vs 3	9.62e+02	2.29e-01	ns	decrease

Monkey B.

Area	comparison	statistic	p-value	significance	direction
LPFC_4	1 vs 2	3.33e+02	5.16e-01	ns	decrease
LPFC_4	1 vs 3	1.52e+02	4.26e-02	*	increase
LPFC_4	2 vs 3	1.38e+02	2.93e-02	*	increase
MCC_1	1 vs 2	2.84e+02	5.80e-01	ns	decrease
MCC_1	1 vs 3	3.78e+02	2.79e-02	*	decrease
MCC_1	2 vs 3	4.00e+02	7.89e-03	**	decrease
MCC_5	1 vs 2	2.63e+02	6.20e-01	ns	increase
MCC_5	1 vs 3	4.70e+02	3.28e-05	***	decrease
MCC_5	2 vs 3	4.40e+02	2.34e-05	***	decrease

Figure 50. Statistical results of negative feedback latency across learning steps. Mann-Whitney U post-hoc tests for each comparison of each area. ns = no significant, * = p<0.05, ** = p<0.001, *** = p<0.0001.

For the latency, we showed a mix of decreases and increases across learning steps for Monkey I. For Monkey B, we showed an increase of latency across learning steps in LPFC1 and a decrease in LPFC2.

The evolution of the negative feedback response was more variable depending on the area-groups and the monkey. As a reminder, monkeys faced the notion of negative feedback for the very first time in the DL task and its definition was less evident as they should have also learned the meaning of errors for the first time. This could explain why the potential evoked by the negative feedback is less stable than the positive one. One aspect of the negative feedback was the lack of reward, but other trial types were associated with a lack of reward and could be associated with an error: the aborted trials. In fact, aborted trials resulted in an absence of target validation which could be due to a work stop but also to a bad holding of the target. This bad holding could be considered as a behavioural error for the monkey. Therefore, it will be interesting in future analysis to study evoked potentials by aborted trials to compare it with the negative feedback responses. In that sense, we could try to separate general behavioural errors and choice errors and see if the lack of reward had a different impact according to the trial context.

Temporality between areas

We did the same analysis than above on the temporality differences between areas. We showed no significant difference between learning steps for Monkey I with responses arriving first in the MCC then in the LPFC in all antero-posterior groups except group 3. Nevertheless, it should be noted that in posterior parts (group 4 to group6), the responses emerged almost at the same time in the LPFC and the MCC. For Monkey B, the response arrived almost always in the MCC then in the LPFC with an increase across learning steps for groups 1, 4 and 5 (**Fig. 51**). Here we showed almost no effect of the learning steps on the response temporality meaning that the training did not affect the organisation between the MCC and the LPFC (**Fig. 52**). This could mean that learning how to use the negative feedback would not necessarily be associated with the establishment of a temporal hierarchy between the areas.

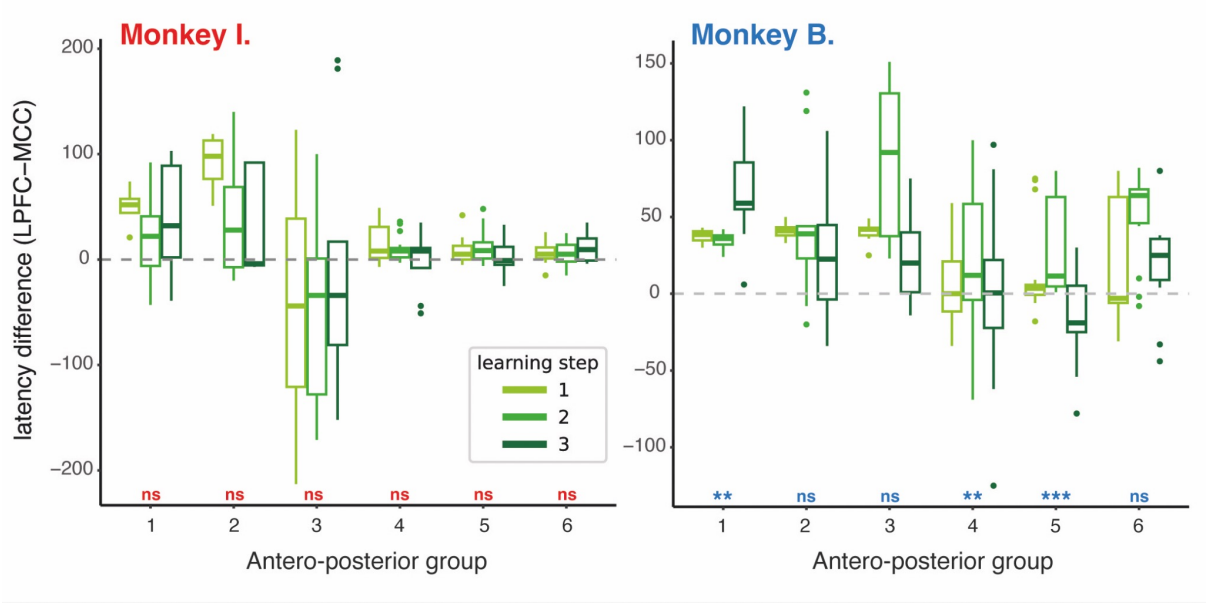

Figure 51. Difference of evoked potentials by negative feedback latency between LPFC and MCC across learning steps. LPFC > MCC means that response arrived first in MCC then in LPFC. LFPC < MCC means that response arrived first in LPFC then in MCC. Kruskal-Wallis test between learning steps. ns = no significant, * = p<0.05, ** = p<0.001, *** = p<0.0001.

Monkey B.

ant-posterior	comparison	statistic	p-value	significance	direction
gp1	1 vs 2	2.09e+02	7.75e-01	ns	decrease
gp1	1 vs 3	1.29e+02	3.75e-02	*	increase
gp1	2 vs 3	6.50e+01	1.32e-03	**	increase
gp4	1 vs 2	2.20e+02	3.28e-01	ns	increase
gp4	1 vs 3	8.25e+01	3.88e-03	**	increase
gp4	2 vs 3	7.35e+01	1.65e-03	**	increase
gp5	1 vs 2	2.20e+02	1.00e+00	ns	increase
gp5	1 vs 3	6.55e+01	2.95e-04	***	increase
gp5	2 vs 3	7.25e+01	6.00e-04	***	increase

Figure 52. Statistical results of difference of negative feedback latency between LPFC and MCC. Mann-Whitney U post-hoc tests for each comparison of each area. No significant difference for Monkey I. ns = no significant, * = p<0.05, ** = p<0.001, *** = p<0.0001.

Intermediate conclusion

The processing of the reward as a positive feedback once the task requires choices involves an evolution of the initial reward response with the appearance of a clearer second later peak and an evolution of the amplitude and the latency of this peak across the training. The evolution of the negative feedback response processing is more variable and could be linked to a more abstract notion of the negative aspect as it could take a few sessions for the monkey to understand that the absence of reward and the latency time are in fact feedback information.

The validation of this statement will need further analysis of the negative feedback responses. We focused on the period where the differentiation between positive and negative feedback was made but it could be possible that negative feedback response processing elicits changes in other parts of the trial, like the inter-trial part. Also, for both feedback types, we could miss some specific information by looking only at the positive component of the peak. Detailing the same type of analysis on the negative component could add precious information. In both feedback types, we saw that MCC responses generally preceded LPFC responses, from the start of learning. This hierarchy between areas is therefore already present before any learning process in these tasks, and although we see changes across learning we do not see a systematic change in this hierarchy. Nevertheless, comparing the temporality of evoked responses to feedback between areas is not sufficient to make assumptions about the link between the MCC and the LPFC. Linking it with the assessment

of the functional connectivity will add more valuable information and this will be our focus in the next chapter.

In any case, we showed that the evoked responses to positive and negative feedback had some evolution throughout learning and that the learning step had an impact on specific parameters of the response, such as the amplitude and the latency. This highlighted the fact that monkeys constructed and optimised their responses to feedback during learning to increase their performance.

Generalisation across tasks

We hypothesised that reaching the learning to learn plateau would be associated with a stabilisation of the responses shown previously, meaning that evoked potentials by both feedbacks should stay stable and no difference should be found with other similar tasks. We compared the evoked potentials during the last learning step in the DL task (step 3) with those evoked in the next RL task that followed. The nature of stimuli, responses, and outcomes in this task were identical, but the rule at problem switch was different (a reversal). As previously shown discrimination learning usually provides a learning set which permits rapid shifting to, for example, reversal tasks, where some common performance rules can be applied. As such an open question in these cases is whether the feedback responses remain identical despite a task shift.

We showed that positive feedback elicited a response with similar shape in all area-groups of step 3 and RL task, with some differences of amplitude (**Fig. 53 & 54**). There were amplitude changes in the peak window for all areas of Monkey I but only in the MCC for Monkey B. However, we saw a bigger variance in RL task signals of Monkey B. The RL task was the very last part of the training, meaning that the loss of signal identified in Monkey B was at its maximum. Thus, it would be difficult to conclude on the reasons for this variation.

Overall, the evoked responses to the positive feedback seemed to stay similar in areas and antero-posterior groups after reaching the learning to learn plateau, but unexpectedly there were still changes of amplitude between the tasks, refuting our theories of a stabilisation of the positive feedback responses.

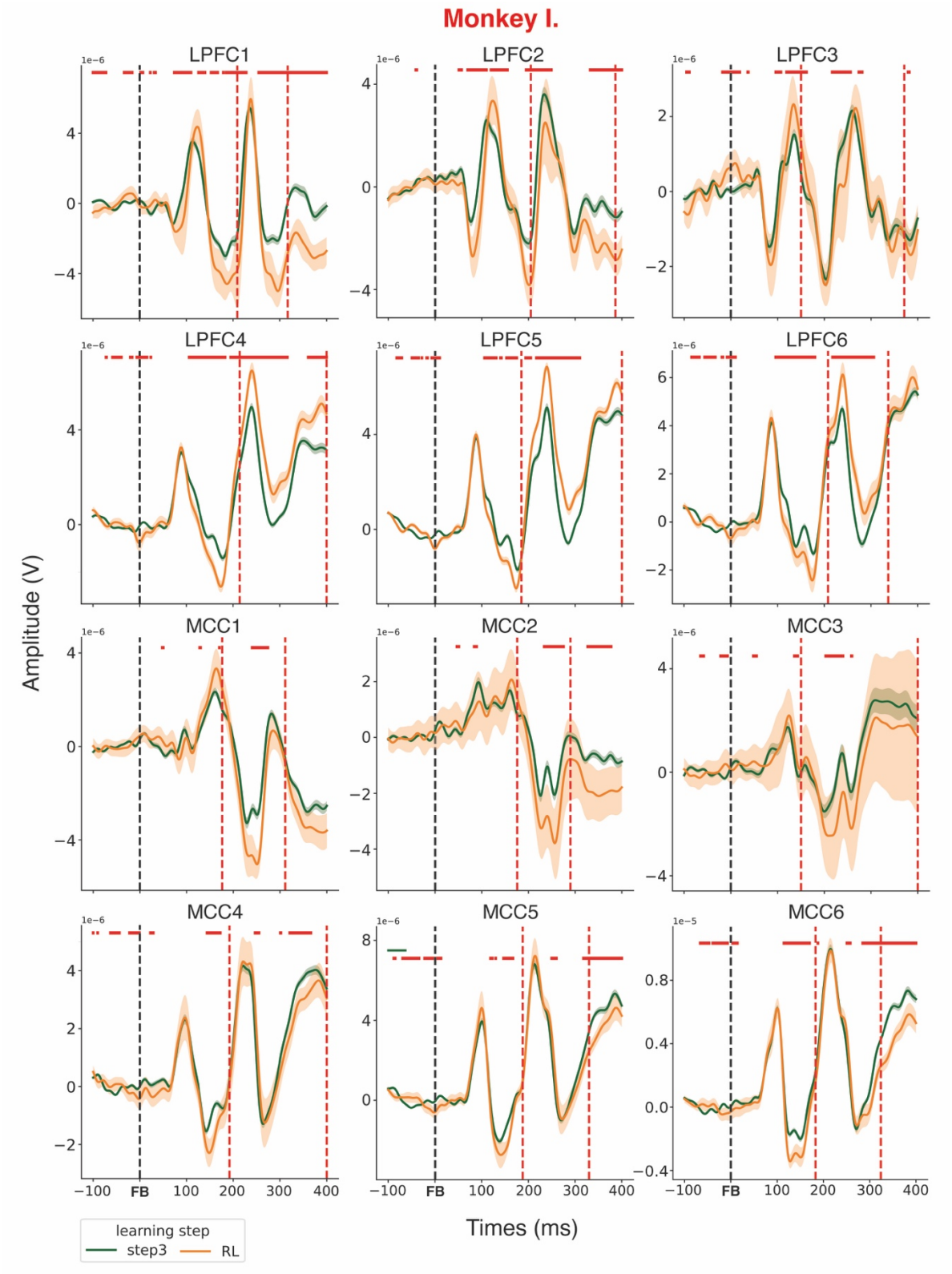

Figure 53. Evoked potentials by positive feedback in learning step 3 and RL task for Monkey I. Time window of 100ms before the feedback and 400ms after. Black dashed line represents the feedback at time 0. Red dashed lines represent the limit of the peaks window. Red dashed lines represent the limit of the peaks window. Red horizontal segments indicate a significant p-value of the Mann-Whitney U test between learning steps for each time point. FB = feedback.

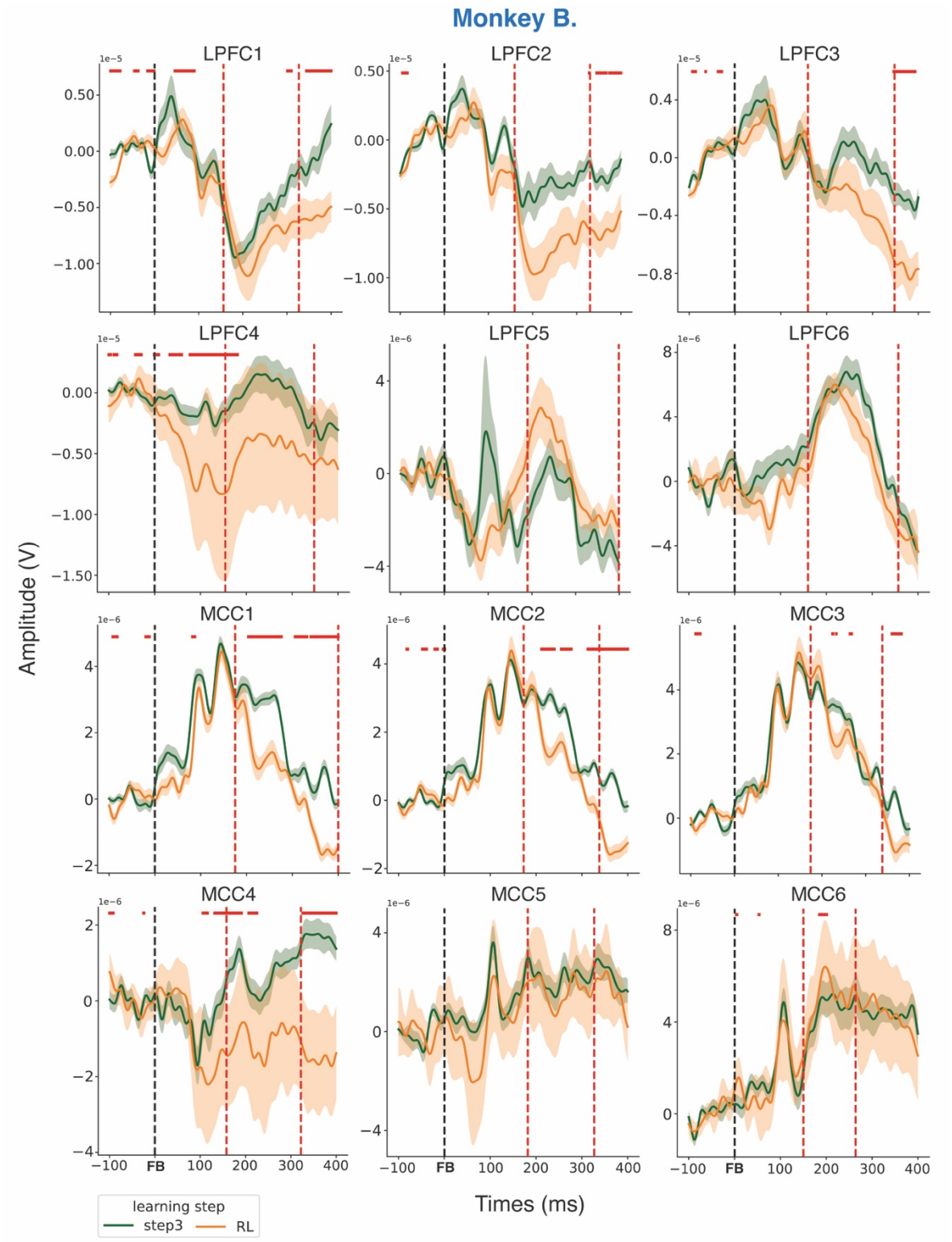

Figure 54. Evoked potentials by positive feedback in learning step 3 and RL task for Monkey B. Time window of 100ms before the feedback and 400ms after. Black dashed line represents the feedback at time 0. Red dashed lines represent the limit of the peaks window. Red horizontal segments indicate a significant p-value of the Mann-Whitney U test between learning steps for each time point. FB = feedback.

We did the exact same thing for the evoked response by the negative feedback (**Fig. 55 & 56**). There were differences between the tasks in the peak window for anterior parts of LPFC and MCC for Monkey I and only in LPFC3, LPFC4, MCC1 and MCC4 for Monkey B. Again, it should be noted that there was a lot more variance in the RL task that could impact these results.

Even if changes were still present and that our hypothesis was not validated neither in positive or negative feedback responses, it should be noted that these changes were present in less area-groups than during training.

In any case, as we could not prove a stabilisation of the feedback processing after reaching the learning to learn level, it will be necessary to focus future analysis on other parts of the session. For example, the inter-trial or the period between the apparition of the target and its validation that could represent the anticipation of the next action. In fact, as we could not identify a stabilisation of feedback processing, it could mean that learning to learn could reside in higher cognitive processes.

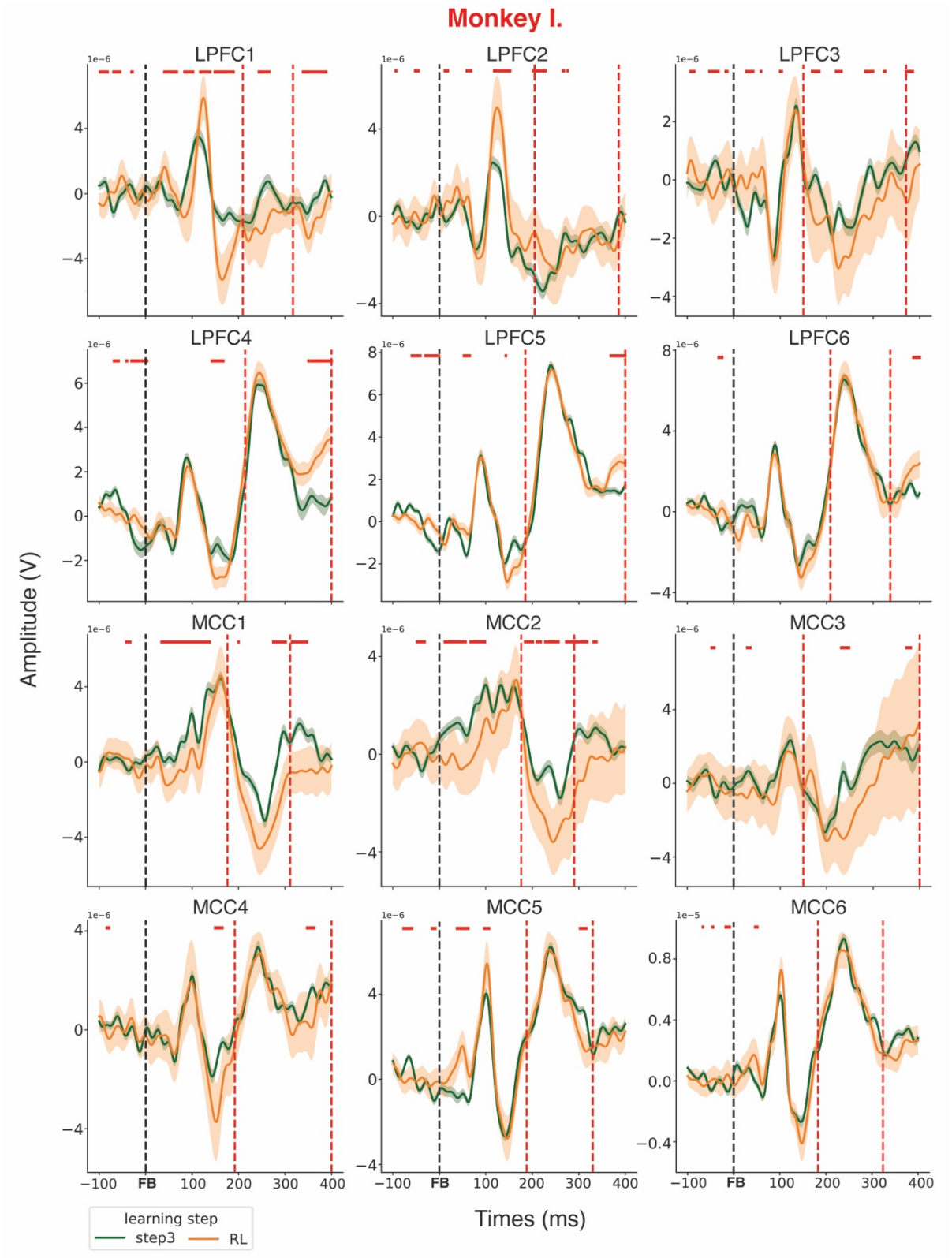

Figure 55. Evoked potentials by negative feedback in learning step 3 and RL task for Monkey I. Time window of 100ms before the feedback and 400ms after. Black dashed line represents the feedback at time 0. Red dashed lines represent the limit of the peaks window. Red horizontal segments indicate a significant p-value of the Mann-Whitney U test between learning steps for each time point. FB = feedback.

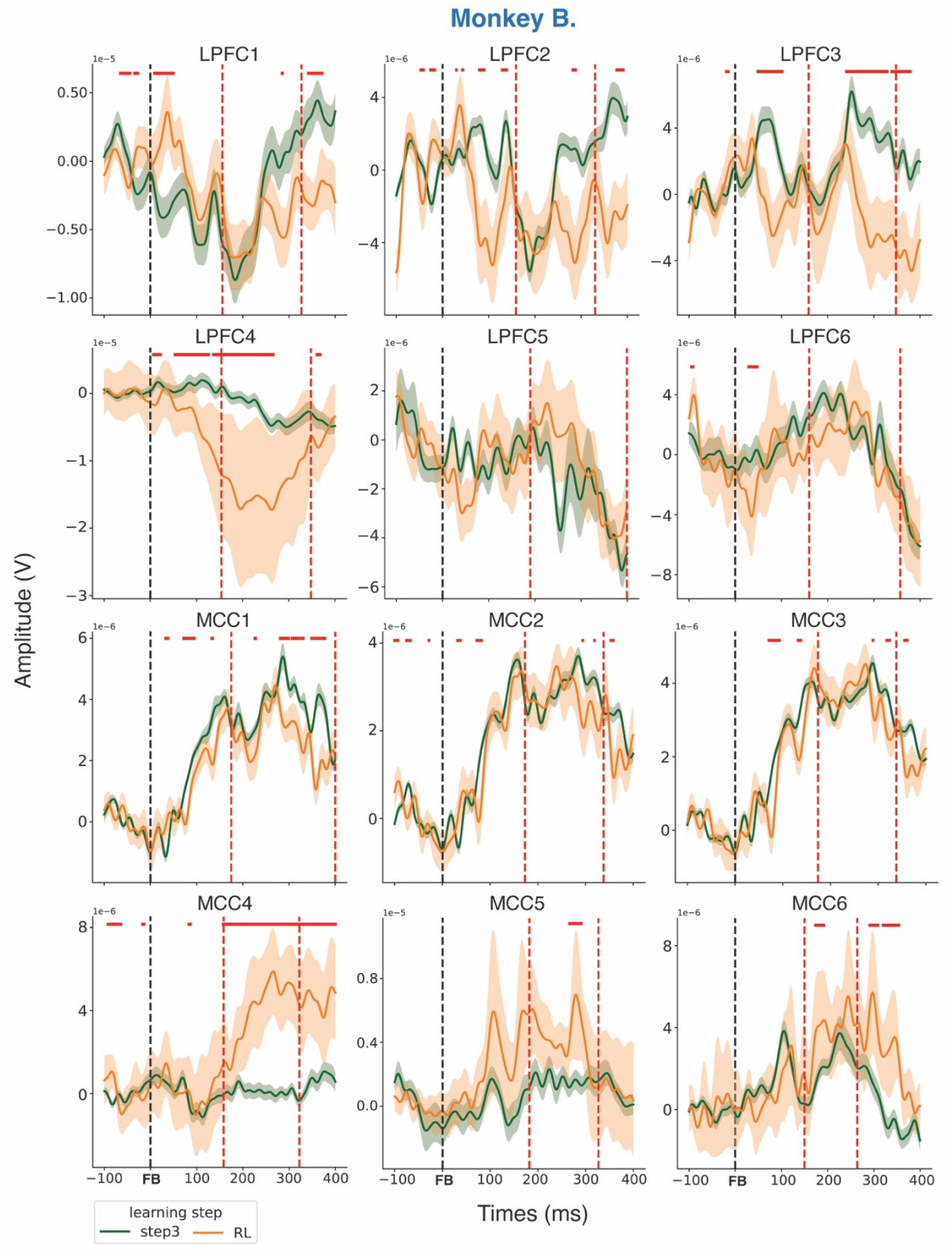

Figure 56. Evoked potentials by negative feedback in learning step 3 and RL task for Monkey B. Time window of 100ms before the feedback and 400ms after. Black dashed line represents the feedback at time 0. Red dashed lines represent the limit of the peaks window. Red horizontal segments indicate a significant p-value of the Mann-Whitney U test between learning steps for each time point. FB = feedback.

c) Single unit activity

We described in detail the evoked responses to positive and negative feedbacks at the local field potentials scale and showed that the learning course had an impact on them. This highlighted the fact that the learning process shapes the response to perform better and that reaching the learning to learn plateau level could be associated with a diminution of responses changes in some way. Importantly, our chronic recordings also allowed us to record single-unit activity. We hypothesized that changes in the evoked responses to feedbacks could relate to changes in positive and negative feedback encoding at the single neuron level. We looked at the proportion of units that responded for each feedback and grouped our single-units in area-groups in the same way as for local-field potentials (**Fig. 57**). We called 'responsive unit' a neuron that had a spike rate significantly different from the baseline. The baseline was calculated on the 400ms before the feedback.

We showed that for both feedbacks, there was a higher proportion of responsive neurons in the MCC than in the LPFC. More precisely, in the anterior part of the MCC for Monkey I and in the posterior part for Monkey B where the proportion went beyond 50%. These results fit with what we highlighted in POS-NEG signals in LFP analysis as well as with previous published data of our team (Goussi-Denjean et al., 2023).

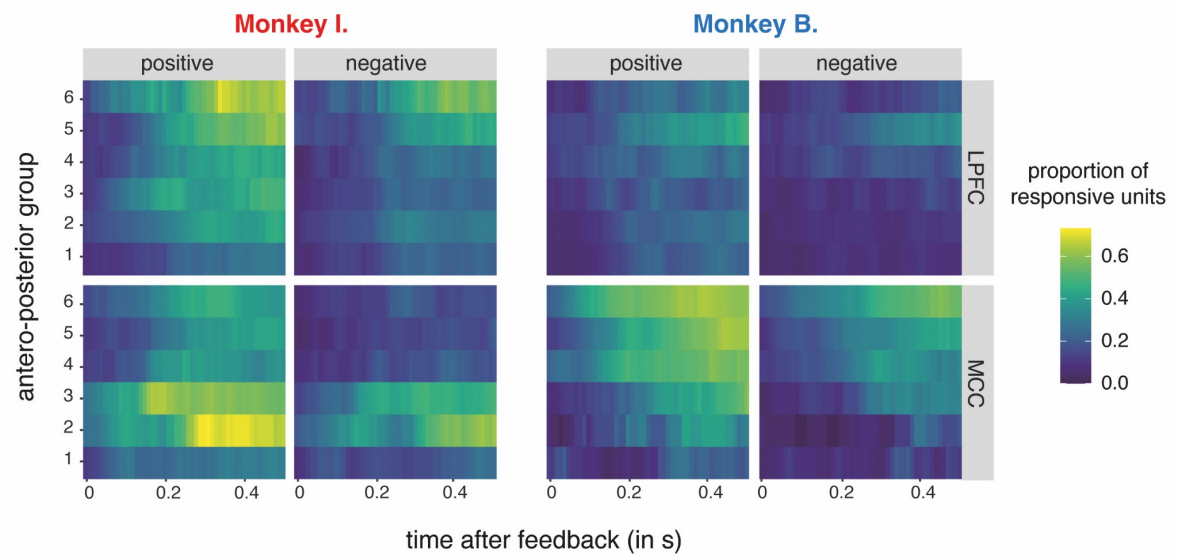

Figure 57. Time-resolved proportion of responsive units to positive and negative feedback according to the antero-posterior group in the DL task. Time window of 500 ms after the feedback. In the antero-posterior groups, a smaller number corresponds to the most anterior part. Controlateral hemisphere for each monkey: right for Monkey I and left for Monkey B.

Local-field potential analyses revealed that the evoked response to feedback evolved across training so we hypothesised that the proportion of responsive neurons should also change throughout the sessions. The main question was could the change in evoked potentials be explained by a change in the responsive units of a same area-group?

We looked at the evolution of responsive neurons to each feedback across sessions (**Fig. 58-61**). There were changes across sessions that were specific for each area-groups. MCC2 in Monkey I was particularly responsive to positive and negative feedback.

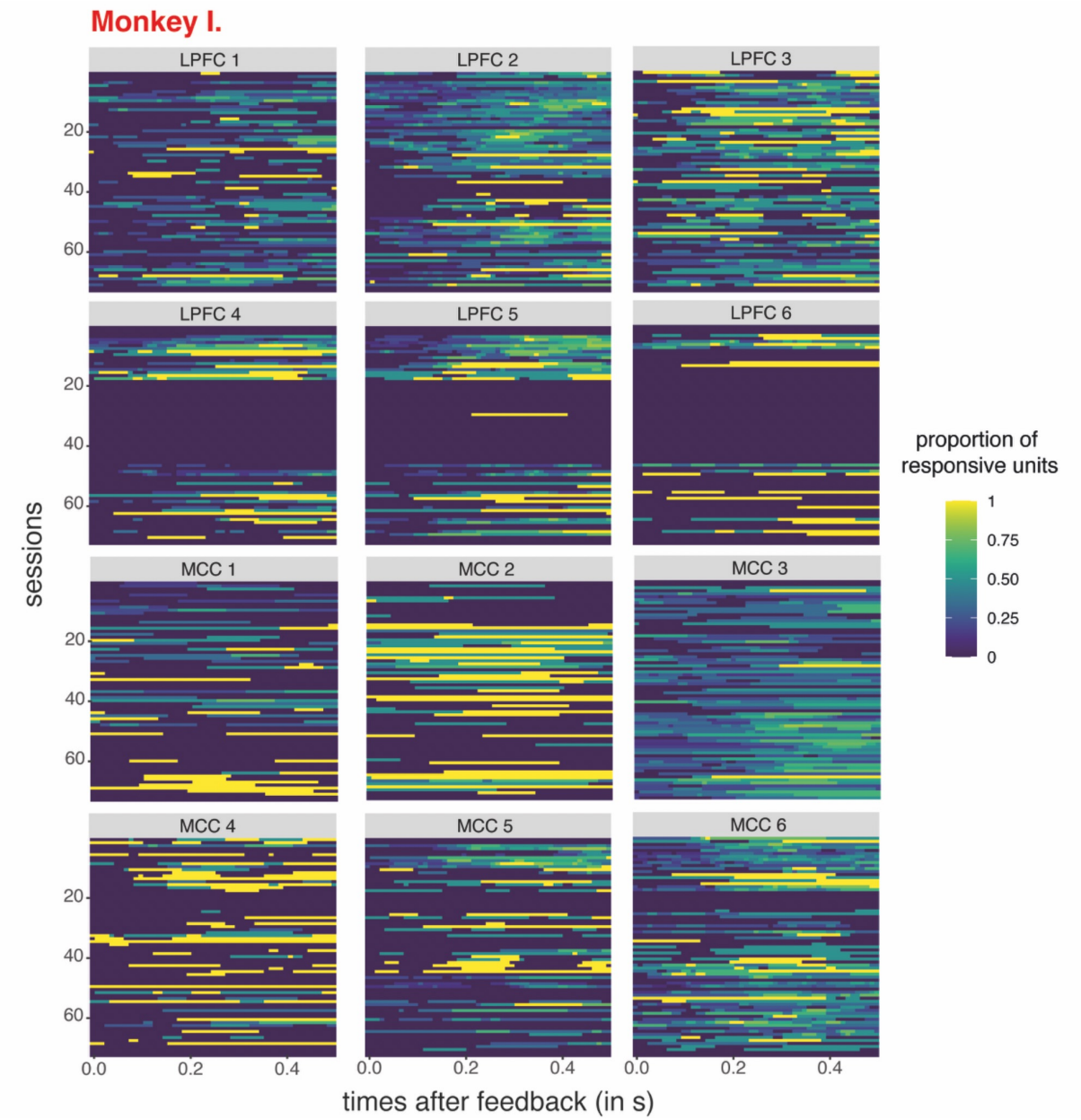

Figure 58. Proportion of responsive units to positive feedback across sessions for Monkey I. Time window of 500 ms after the feedback. Controlateral hemisphere: right for Monkey I.

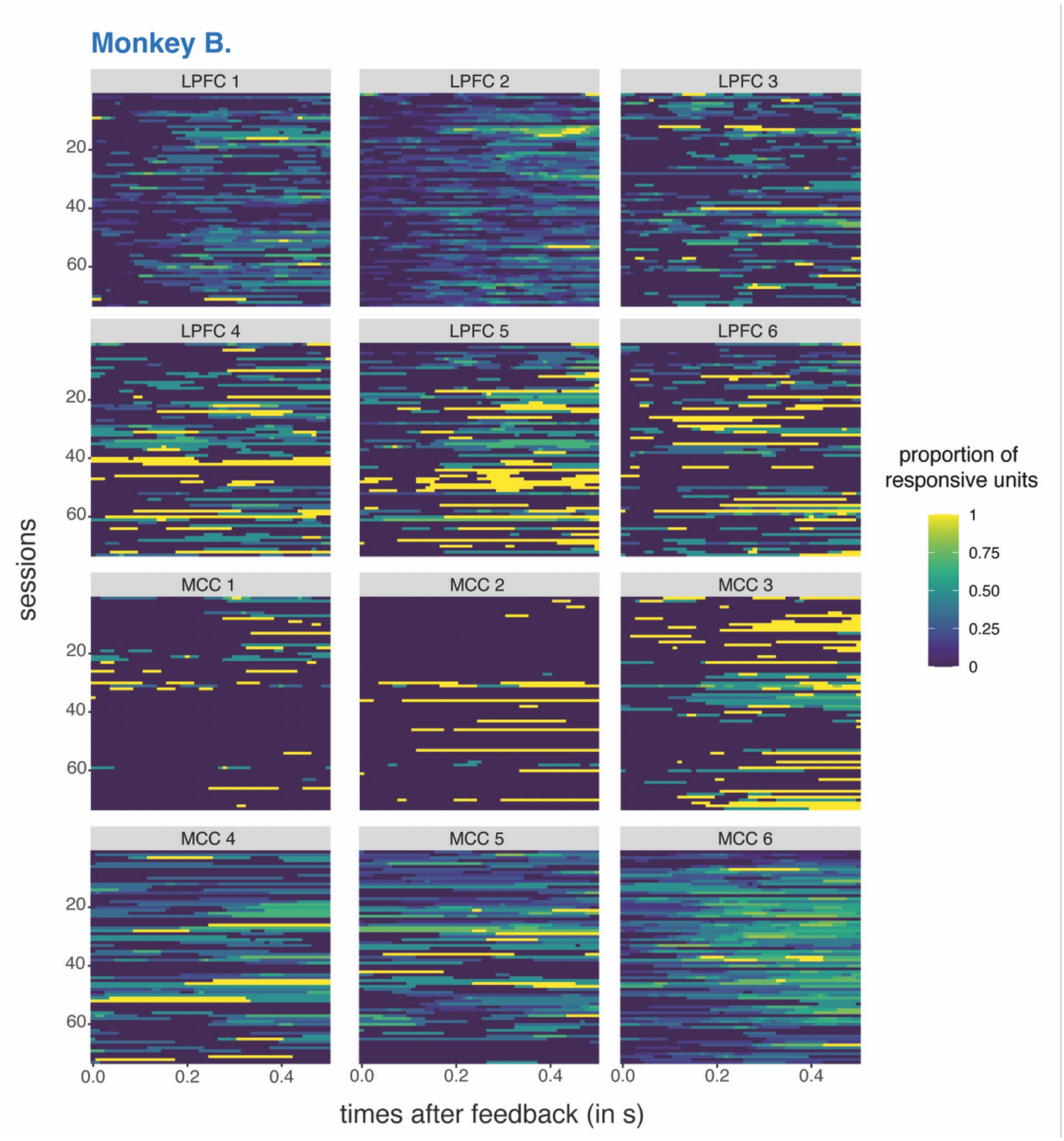

Figure 59. Proportion of responsive units to positive feedback across sessions for Monkey B. Time window of 500 ms after the feedback. Controlateral hemisphere: left for Monkey B.

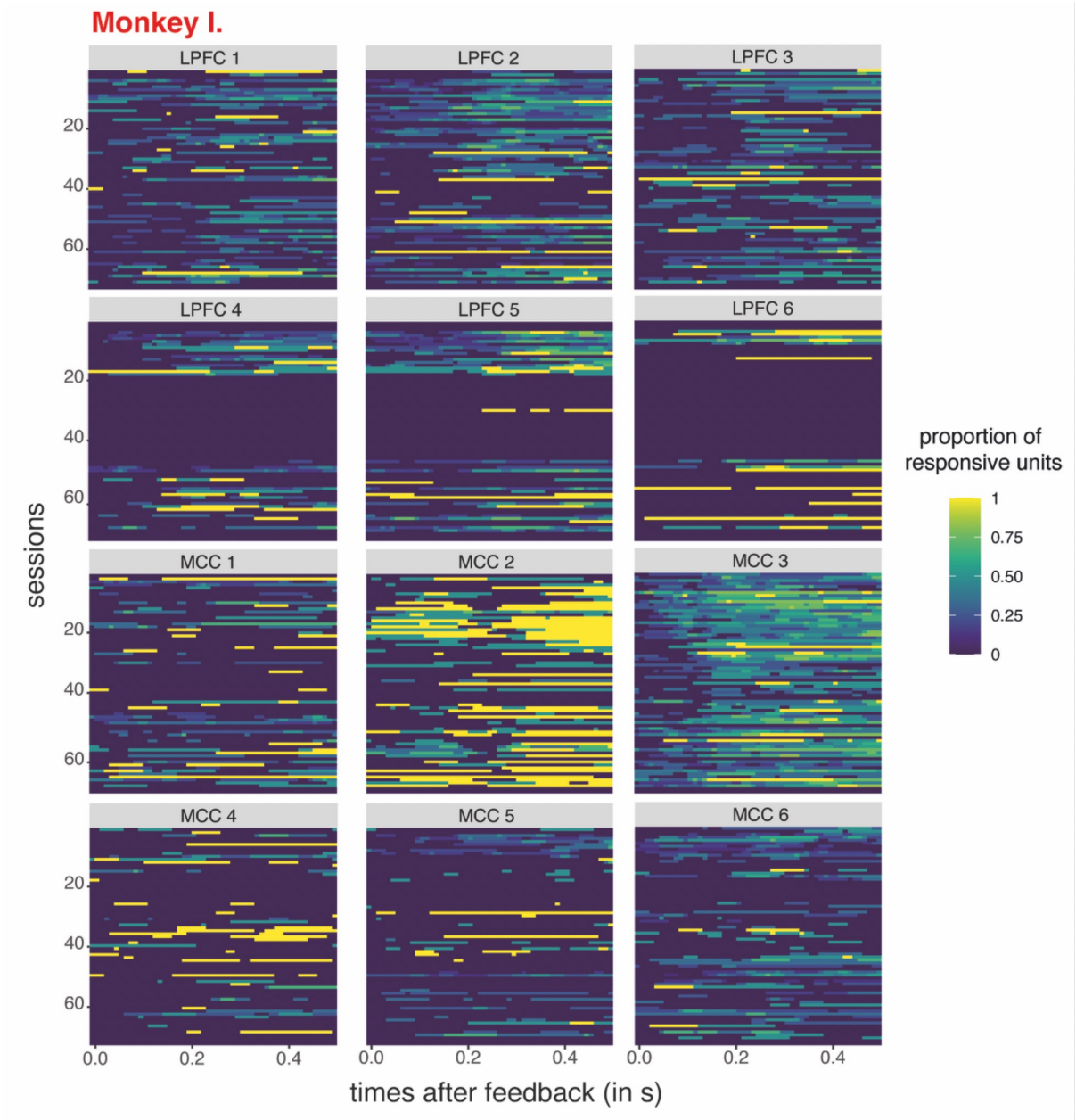

Figure 60. Proportion of responsive units to negative feedback across sessions for Monkey I. Time window of 500 ms after the feedback. Controlateral hemisphere: right for Monkey I.

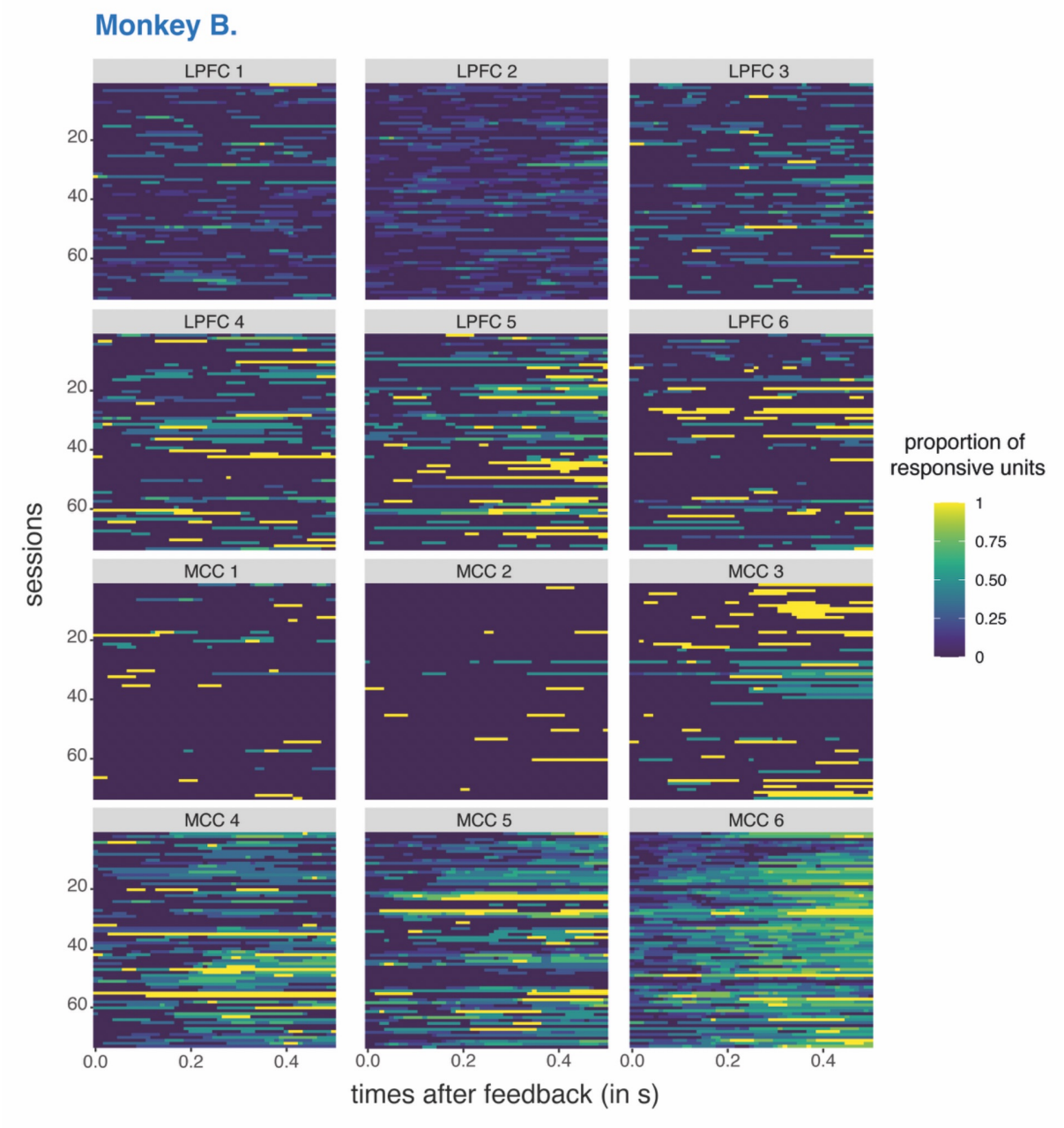

Figure 61. Proportion of responsive units to negative feedback across sessions for Monkey B. Time window of 500 ms after the feedback. Controlateral hemisphere: left for Monkey B.

Overall, LPFC and MCC both had neurons responsive to each kind of feedback but the proportion was higher in the MCC. We showed that area-groups had different evolutions across sessions but we highlighted no general increase or decrease pattern. Thus, it seems that the pattern observed in the evoked response by feedback cannot be explained only by a change in the proportion of responsive neurons.

The second hypothesis was that if changes could not be explained only by a proportion of responsive neurons for each feedback then maybe it was linked to the encoding of the feedback type. This means that there were not a higher number of neurons which responded but more an evolution of the neuron population and distributed code itself which learned to differentiate between positive and negative feedbacks. Thus, we looked at the proportion of neurons distinguishing between specific feedbacks (**Fig. 62**) - meaning that they responded differently for positive and negative feedback. Again, neurons which differentiate between feedback types were more present in the MCC than in the LPFC. It was even more pronounced in the posterior part of MCC for Monkey B and in the anterior one for Monkey I.

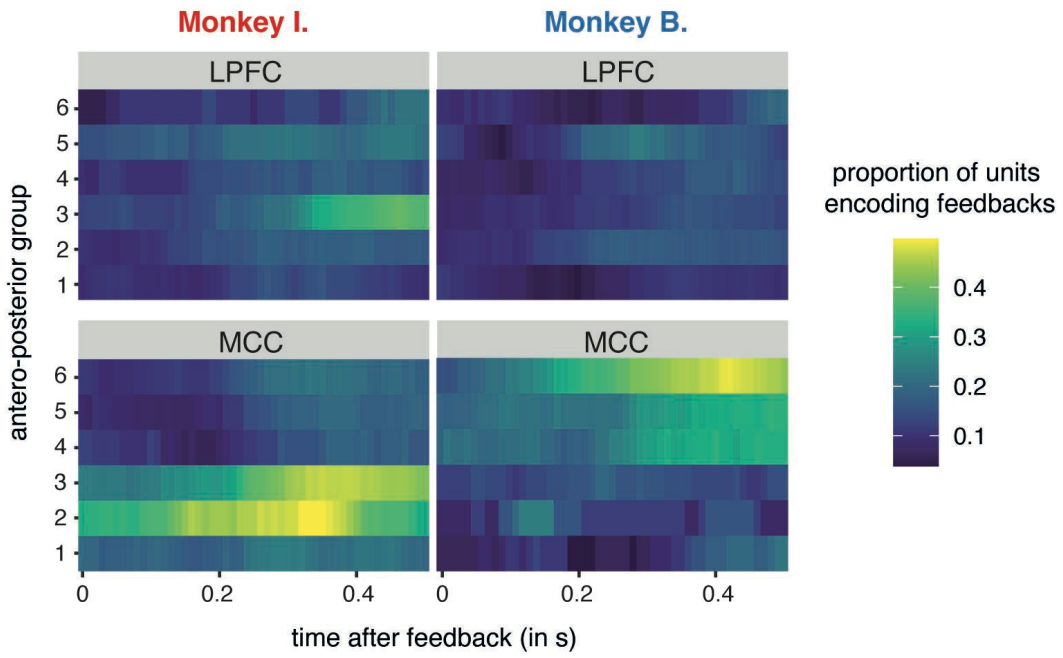

Figure 62. Proportion of units distinguishing between specific feedbacks in the DL task. Time window of 500 ms after the feedback. Controlateral hemisphere for each monkey: right for Monkey I and left for Monkey B.

Then we did the same thing as for responsive neurons and looked at the evolution of this proportion across sessions (**Fig. 63 & 64**). Again, we could not highlight a pattern of evolution across training.

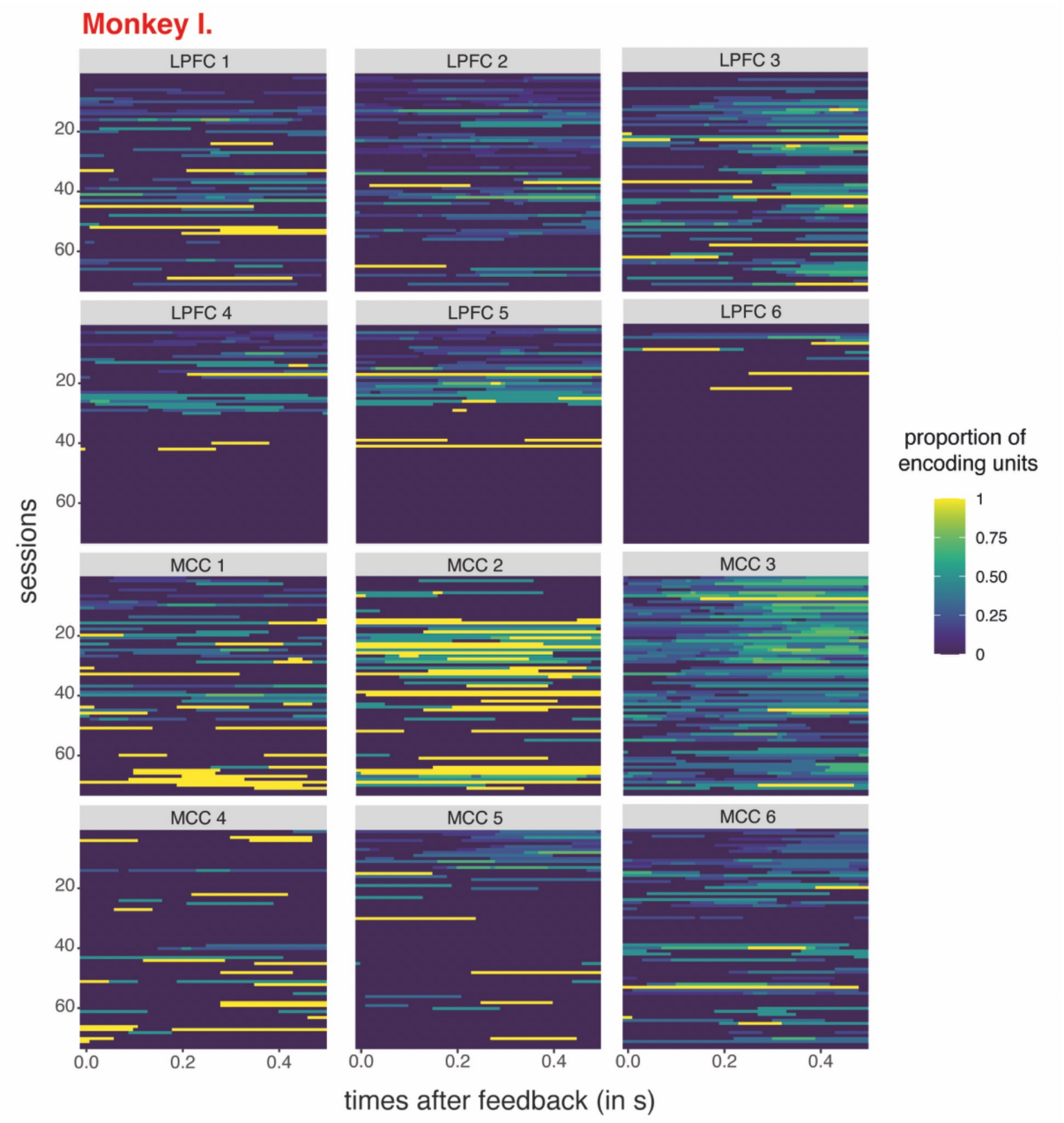

Figure 63. Proportion of units distinguishing between specific feedbacks across sessions for Monkey I. Time window of 500 ms after the feedback. Controlateral hemisphere: right for Monkey I.

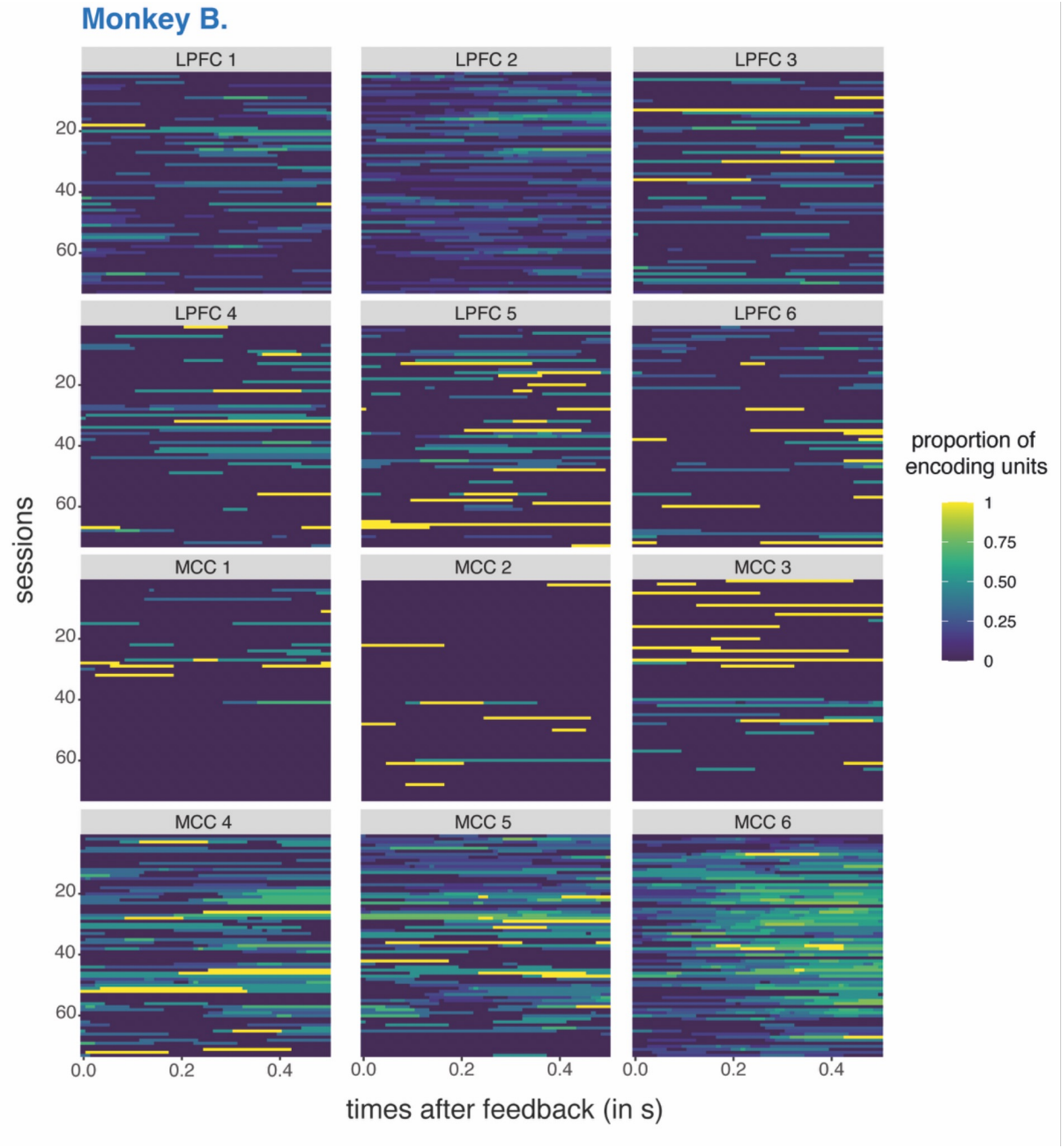

Figure 64. Proportion of units distinguishing between specific feedbacks across sessions for Monkey B. Time window of 500 ms after the feedback. Controlateral hemisphere: left for Monkey B.

IV. Conclusion

The training had a real impact on the two different types of feedback processing showing changes on peak amplitude and latency and on responsive and encoding unit's proportion. The evolution of the positive feedback was clearer, starting with the comparison with the reward in the baseline task. The major result of this analysis is that each monkey elicited a specific pattern of changes (increase or decrease) that was not similar between each other. These differences were found in all levels of analysis, from the LFP to the single units. To conclude, learning to learn did not elicit a clear evolution in one way of feedback processing. In contrary, it was reflected by changes specific to each individual, showing that there is not only one universal way of learning.

Chapter 4. Functional connectivity of the MCC-LPFC network in electrophysiology

I. Introduction

The MCC and the LPFC are functionally and anatomically connected areas as we saw in chapter 1. There is also evidence of network dynamics for cognitive functions such as decision-making (Procyk et al., 2021; Stoll et al., 2016). Moreover, we explained in the general introduction how they are both essential for the learning and the learning to learn processes. All of this points out the fact that these two regions work together in many functions and have a strong connection. However, we do not know whether or how this communication is modified by learning in cognitive tasks, or how the connectivity between the MCC and the LPFC develops as an animal goes from cognitive task naïve to expert. In this study, we aimed to describe the communication of this network throughout the learning and to highlight if a specific state of this network could be linked to the learning to learn step.

II. Specific materials and methods

The electrophysiological data were recorded during the DL and the RL task. The DL task represents the task of interest to compare different steps of learning (as seen in previous chapter). The RL task is used to test the generalisation of the learning to learn across tasks. To assess the functional connectivity (FC), we used three different variables: the coherence, the phase-locking value (PLV) and the envelope of amplitude correlation (ENVA).

Coherence was calculated using the '*spectral_connectivity'* function from the *'mne_connectivity'* Python toolbox, which computes coherence by normalizing the cross-spectral density by the power spectral densities of the two signals. This measure provides insight into the phase and amplitude synchrony between brain areas across different frequency bands. PLV was also computed using the *'spectral_connectivity'* function. This metric evaluates the consistency of phase differences between two signals across multiple

trials, focusing purely on phase synchrony without regard to amplitude. ENVA was calculated using functions from the *'scipy*.signal' toolbox. It measures the correlation between the amplitude envelopes of two signals, highlighting synchrony in amplitude modulation. The analytic signal was first computed using the Hilbert transform, from which the amplitude envelope was extracted. The correlation between these envelopes provided the ENVA metric.

Combining these three values allows a more robust quantification of the FC. We calculated the three at the session scale and the coherence and the ENVA at the trial scale. We used epoch data centred on the positive feedback and used the antero-posterior groups presented in the part II of this manuscript to group the electrodes in the analyses of this chapter.

FC statistical analyses were done with Python ("*mne_connectivity*" and "*scipy.signal*" toolboxes) and visualisation was done with Python and RStudio. We performed model analyses by using general-linear-mixed models with Bonferroni corrections and Dunn post-hoc tests.

III. Results

a) Functional connectivity

Our first aim was to define if the changes in feedback responses highlighted in the LFP and single-unit analyses were due to a re-organization in the communication between the areas, so linked to a change of connectivity. We had two hypotheses, first that these changes could be associated with an increase of communication between the MCC and the LPFC as we saw in the introduction that these regions form a network involved in feedback and learning processes. Secondly, changes in communication could also occur inside the area, between anterior and posterior parts, as we saw in the chapter 1 of this experimental part that areas could have different implications/functions according to the antero-posterior level. We looked at the connectivity in these two levels: intra-area - with different antero-posterior groups in the same area (LPFC or MCC) - and extra-area, between antero-posterior groups of different areas (LPFC and MCC). We also wondered if a specific frequency band could be more

implicated in the functional connectivity during the feedback processing. We defined our 4 frequency bands of interest (delta, alpha, beta, low gamma) by looking at peaks in the power-spectrum density.

We had the hypothesis that different measures of connectivity could bring different information depending on the learning level. For example, an increase of functional connectivity could be represented by an increase of the amplitude correlation at the beginning of learning and by an increase of phase correlation at the end. Thus, we decided to combine different measures of connectivity implying phase and amplitude correlations: the coherence, the amplitude envelope correlation (ENVA) and the phase-locking value (PLV).

Learning to learn scale

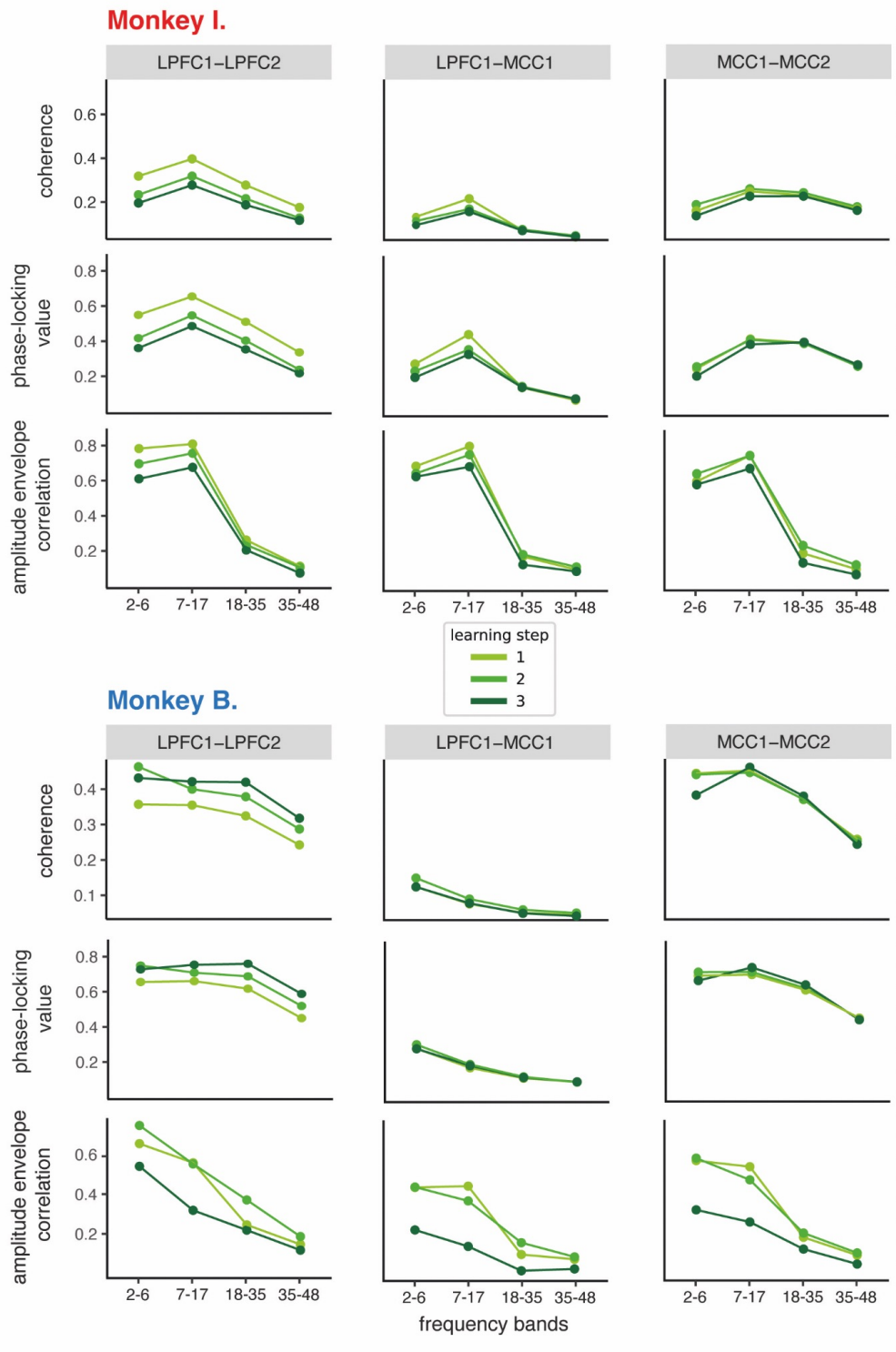

Figure 65. Example pairs of functional connectivity measures across learning steps and frequency bands. Frequency bands are in Hertz. Area-group pairs are indicated in the grey frame: left and right columns show examples of intra-area connectivity and middle column shows an example of extra-area connectivity.

We calculated these connectivity measures at the session level for each pair intra and extra-area, averaged it for each learning step and looked at the difference between frequency bands and learning steps for each pair (**Fig. 65**).

The coherence and the PLV had the same pattern of evolution whereas the ENVA was different. The PLV is based on the phase correlation, the ENVA on the amplitude correlation and the coherence on the phase and the amplitude correlation. According to this result, it seemed that the coherence was more driven by the phase correlation. Also, because the pattern was identical between coherence and PLV we could focus on coherence and ENVA only. Functional connectivity measures were higher in intra-area pairs than in extra-area pairs for both monkeys supporting the fact that these measures are dependent on spatial proximity.

Moreover, as we expected by separating the analyses in different frequency bands, we showed differences between them with higher connectivity measures in all intra and extra pairs in the alpha band (7-17Hz) for Monkey I. For Monkey B, the predominant frequency band was the delta band (2-6Hz) but it depended on the pairs, the connectivity measure used and the learning step. For example, the delta band was predominant in the extra-area pairs with the coherence whereas it was the alpha band in specifics extra-area pairs such as LPFC1-MCC1 with the ENVA in learning step 3. We also saw changes between learning steps for both monkeys, with an increase of connectivity across learning steps for some pairs and a decrease for others. The direction of change was the same in the different connectivity measures for Monkey I while Monkey B showed different patterns according to the measure.

As we had a lot of conditions, we resumed all statistical effects in **Fig. 66**. There was a global increase of coherence value in intra and extra pairs for Monkey I whereas there was a global decrease for Monkey B. For the ENVA value, statistical results were less significant but those that were significant had the same direction than the coherence. Thus, the training enhanced the functional connectivity of the MCC and the LPFC for Monkey I while it reduced it for Monkey B.

Overall, we saw that using different connectivity measures could be redundant in some cases (like the coherence and the PLV) but could also bring important information in another case, as it could even have a totally different evolution pattern (coherence and ENVA for Monkey B).

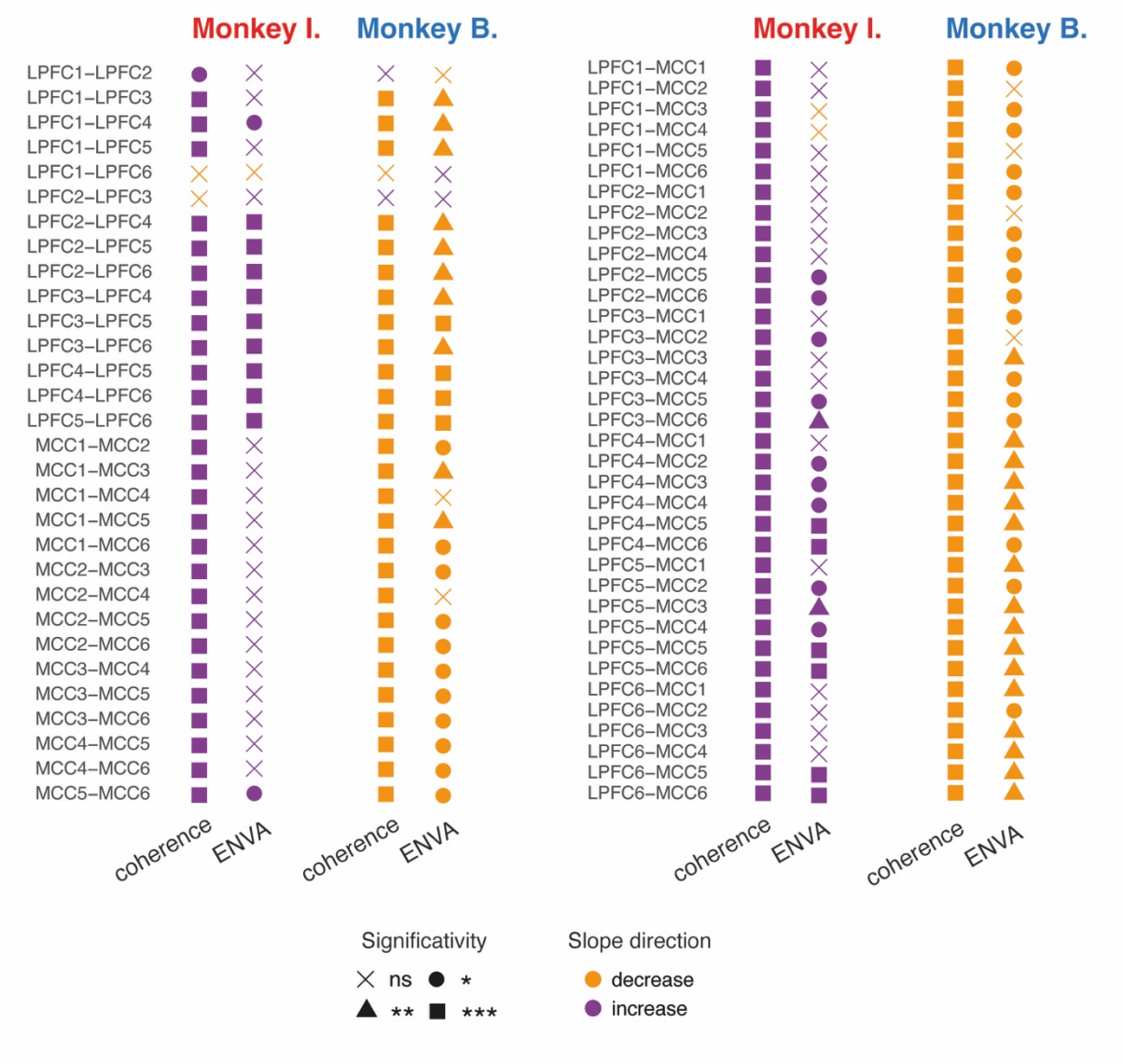

Figure 66. Statistical results of linear models: coherence/ENVA ~ learning steps*pairs. ns = no significant, * = p<0.05, ** = p<0.001, *** = p<0.0001.

Learning scale

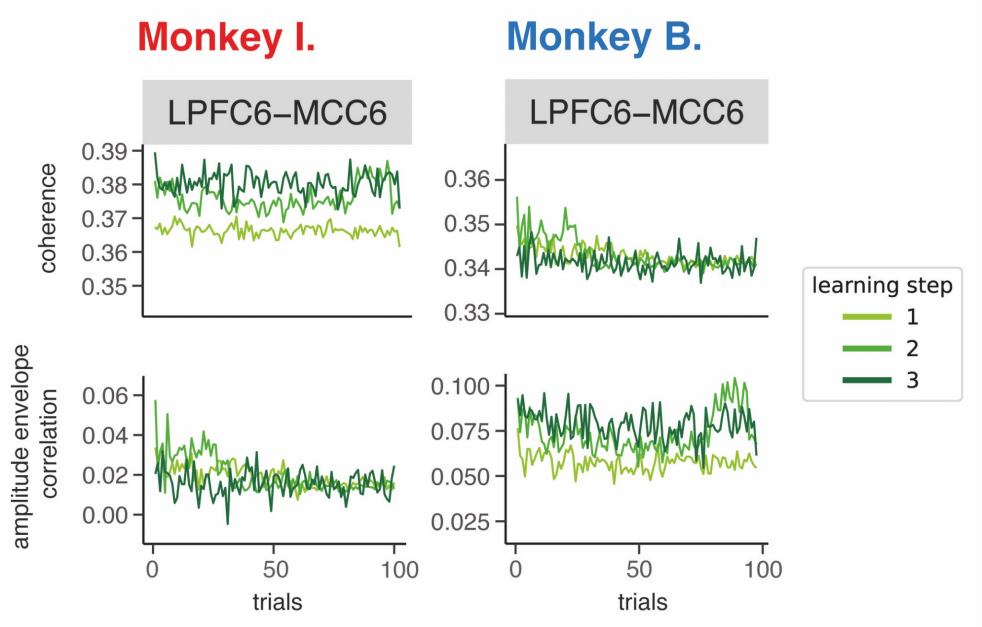

Figure 67. Example of functional connectivity measures across trials for frequency band 7-17Hz.

We showed changes across the training but we also supposed that functional connectivity changes could occur inside a session with for example an increase throughout the session. We looked at the functional connectivity at the trial level and we normalised trial numbers between 0 and 100 to have comparable lengths. We again grouped data in learning steps and looked at the change across training of the evolution of functional connectivity inside the session. For this analysis, we presented only the coherence and the ENVA measures as we have seen that PLV had the same pattern as the coherence (example of one pair in **Fig. 67**). We focused the statistical analysis on the major frequency bands of each monkey (2-6 Hz for Monkey B and 7-17 Hz for Monkey I) and on the coherence only as the training effect was higher in coherence than ENVA. We applied a linear model assessing the link between the coherence and the trials for each pair. There was mostly a decrease of the coherence value inside the session for both monkeys. The decrease was present in learning steps 1 and 2 but less present in step 3 (**Fig. 68**). Overall, it seemed that the decreased effect of the functional connectivity observed in the beginning of learning disappeared in the learning to learn level, meaning that the evolution of functional connectivity could be useful only during the learning part.

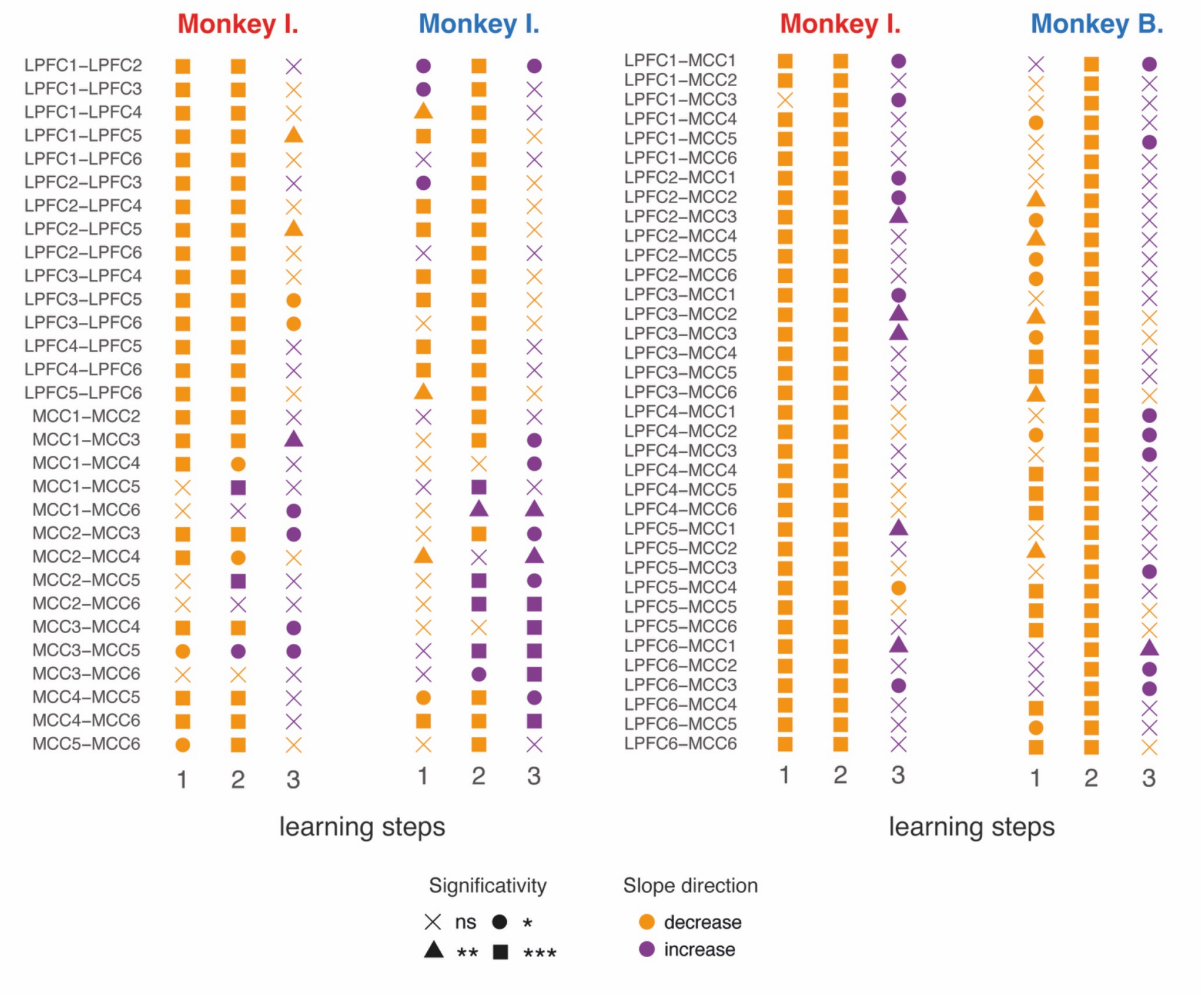

Figure 68. Statistical results of linear models: coherence ~ trials*pairs. Specific frequency bands: 2-6 Hz for Monkey B and 7-17 Hz for Monkey I. ns = no significant, * = p<0.05, ** = p<0.001, *** = p<0.0001.

b) Granger causality

Finally, following our hypothesis from the previous chapter, we proposed that the difference between the learning and learning-to-learn stages could be linked to changes in communication between the LPFC and the MCC. Although the timing of evoked responses to feedback in these regions did not show any noticeable change during learning, we hypothesized that the difference might lie in the connectivity between these areas. To test this hypothesis, we used Granger causality (GC) analysis to measure directed interactions between the MCC and LPFC, dividing our analysis into two regions: anterior and posterior (**Fig. 69**). Two approaches were used to assess GC: the classical Granger method and the

time-reversed version. The latter involves reversing the time series before applying the GC analysis. The purpose of the time-reversed method is to check whether temporal order plays a crucial role in the relationships observed. As Haufe and colleagues suggest, weak asymmetries in the data can bias traditional GC methods, leading to false detections (Haufe et al., 2012). By comparing the results from original and time-reversed data, we can better distinguish genuine relationships from artefacts caused by noise or other factors. This approach is particularly effective at rejecting misleading results caused by mixed signals, such as those typically encountered in neuroimaging studies. Similarly, Vinck and colleagues also highlight the robustness of the time-reversed method in distinguishing true interactions from spurious ones caused by noise and volume conduction (Vinck et al., 2015).

By combining these two approaches, we aim to strengthen the robustness of our findings and ensure that the observed interactions reflect true physiological connections, while minimizing the effects of temporal biases and artefacts.

The comparison between classic and time-reversed GC revealed different patterns for both monkeys. For Monkey I, the GC values dropped significantly when using the time-reversed method, especially in the LPFC to MCC direction. This indicates that the causal connection between LPFC and MCC is strongly dependent on the temporal order of the events in the data. In other words, the interaction we observed in the original data might disappear or change when the sequence of events is reversed, suggesting that this connection is likely real and directional, rather than being a random or spurious relationship. On the other hand, Monkey B showed much more stable GC values between the original and time-reversed data, meaning that the connections are not influenced by whether time flows forward or backward. This could indicate that the observed interaction is less about a true directional influence from one region to the other, and more likely to be a reflection of shared external influences affecting both regions simultaneously. In such cases, the activity in LPFC and MCC might be driven by a third factor, such as another brain region or a task-related input, rather than one region directly causing changes in the other. This is why the results appear stable, even when the time order is reversed.

Notably, for both monkeys, GC was higher in the MCC to LPFC direction, especially in the posterior part, with peaks found in the higher frequency range (20-40 Hz). In the LPFC to

MCC direction, Monkey I showed stronger GC in the anterior part, with peaks in the 10-20 Hz range, while in the posterior part, two peaks emerged (10-20 Hz and around 30 Hz).
In terms of learning steps, for Monkey I, GC was generally higher in steps 1 and 2, particularly in the MCC to LPFC direction, with a peak between 5-10 Hz. For Monkey B, GC was higher in step 3, suggesting a later development of stronger connectivity, with the most prominent peak also occurring between 5-10 Hz.

Overall, these results suggest that the GC interactions predominantly flow from the MCC to the LPFC, particularly in the alpha and beta frequency bands, with learning influencing the strength of the connectivity but not its overall directionality or pattern. This indicates that while learning affects the intensity of the connections, it does not alter the fundamental connectivity pathways between these regions.

.

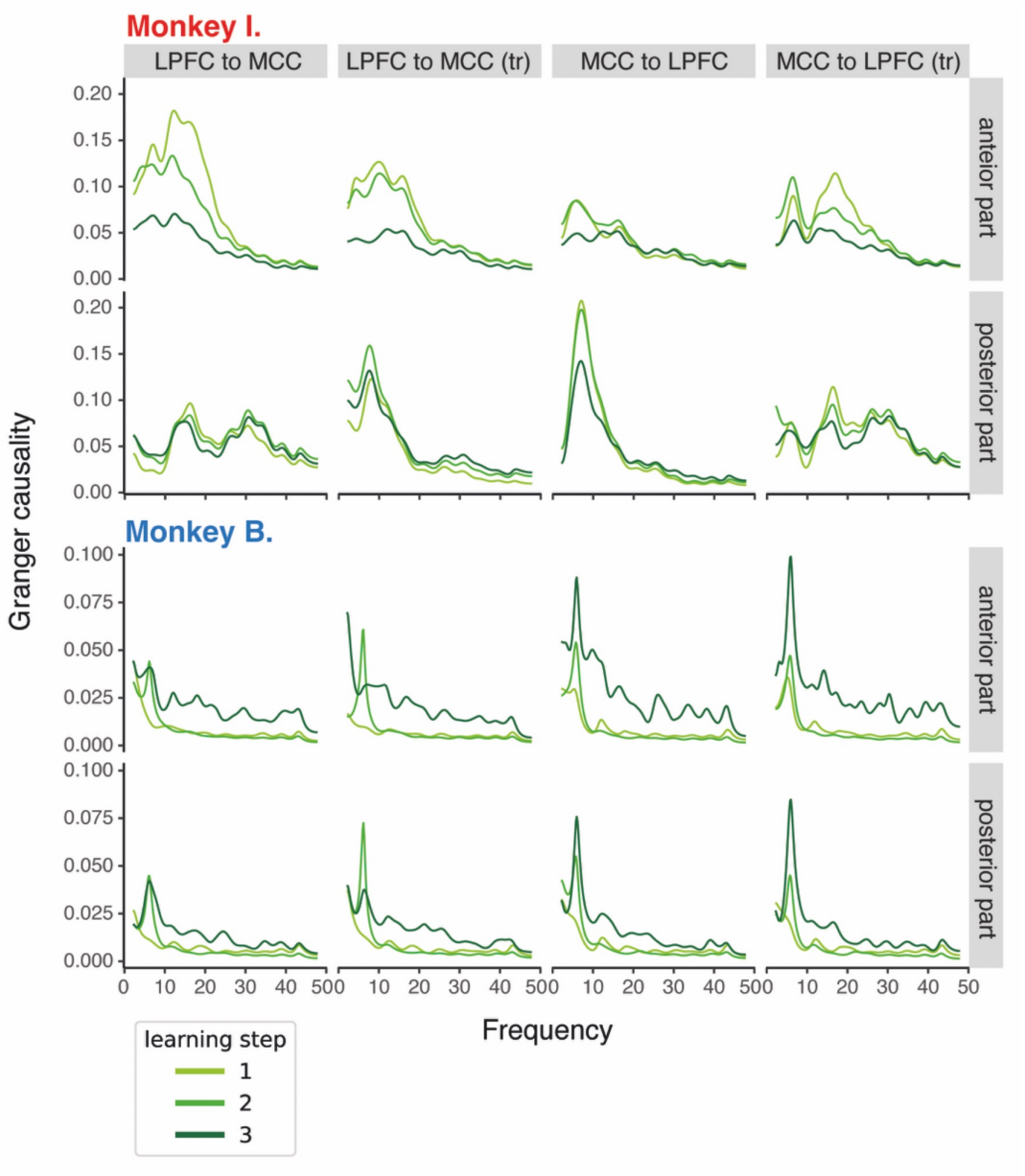

Figure 69. Granger causality between the LPFC and the MCC across learning steps. The 'tr' represents the reversed-time granger causality, others are classical granger causality.

IV. Conclusion

Overall, as for evoked potential analysis (chapter 3), FC and GC across training revealed an opposite pattern between monkeys. In contrast, FC inside the session showed a decrease across trials for both monkeys. This means that changes across training and changes inside the session did not highlight the same process and further work will be necessary to clarify to what each one is linked.

If we link the results of this chapter with those in chapter 3, this could mean that a decrease of the evoked response amplitude is linked to an increase of FC and a decrease of granger causality whereas an increase of amplitude could be linked to a decrease of FC and an increase of granger causality.

Furthermore, this FC analysis was focused on data centred on positive feedback as the evoked potentials results were clearer with it but in the future, it would be interesting to reproduce this analysis on data centred on negative feedback.

Chapter 5. Motivation impact on feedback processing

I. Introduction

The motivation is a difficult concept because of its abstract nature, and the fact that it necessarily interacts with other processes that we are measuring in cognitive tasks, the clear example in our context here being learning. The definitions are multiple depending on the context (Braver et al., 2014). In our task, we defined it as the willingness of the monkey to reach the end of a session in the fastest way possible. Because the duration of each session was based on the number of trials received, being fast also meant being as efficient as possible. We showed in the behavioural chapter (chapter 2) that our subjects had different ways of apprehending the task with clear differences in levels of motivation. Nevertheless, they both learned the task and reached the level of learning to learn with an error to criterion curve with similar shapes. We therefore have overall comparable patterns of learning between the monkeys, but different levels of motivation between the two individuals. It should be noted that this is an extremely common phenomenon in monkey neurophysiological studies, though rarely studied explicitly. In any case this outcome allowed us to study the possible effects of the level of motivation on learning. This study aimed to compare motivation levels and described its impact on the feedback processing described in the previous chapter (chapter 3).

II. Specific materials and methods

We focused on the DL task only in this part as we wanted to assess the learning part and separated the problems into two groups: high motivation and low motivation. We defined a motivation score based on a combination of several behavioural measures that together would describe whether an animal was motivated in a given session. We combined a measure of the number of aborted trials, the number of not-engaged trials, and the proportion of long pauses

made by the animals. We combined the motivation groups with the learning steps defined in chapter 2 (**Fig. 70**). We saw that the distribution of the type of motivation was different between monkeys. Monkey I had more low motivation at the beginning of the training and almost only high motivation at the end. Monkey B had a more dispersed distribution with a majority of low motivation (66%) compared to Monkey I (33%).

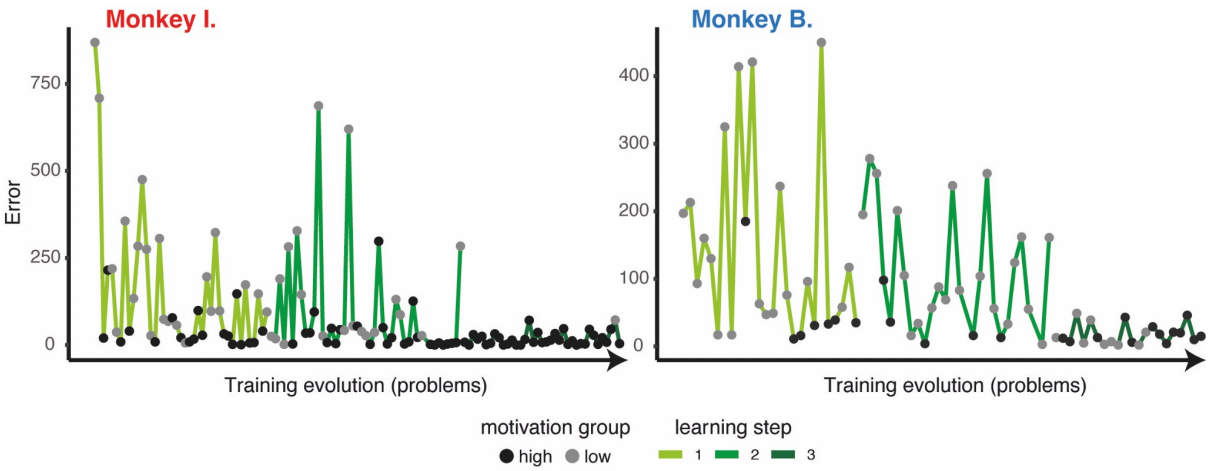

Figure 70. Evolution of motivation level across training. Error represents the number of errors to criterion.

We performed statistical analyses by using Kruskal-Wallis tests with Bonferroni corrections and Mann-Whitney post-hoc tests.

III. Results

We highlighted in chapter 2 of this experimental part that motivation is a key factor in cognitive tasks and that its impact on the learning process should be considered. Our aim in this study was to assess the impact of the motivation level on the electrophysiological results highlighted in the previous chapters.

a) Motivation groups

First, as we saw with Monkey I, motivation clusters could be linked to the learning steps (low motivation at the beginning of the training and high at the end). Then it was important to

dissociate them and avoid inferring a motivational effect which would in fact be due to learning steps. We looked at the evoked responses to positive feedback depending on the motivation level without taking the learning step into account (**Fig. 71 & 72**). We showed that the motivation level elicited differences, also during the peak window. Monkeys had opposite effects. Monkey I's evoked response to positive feedback in the LPFC had higher amplitude in the peak window with low motivation than with high motivation. In the MCC, differences were more mixed. Monkey B had no significant difference in all LPFC groups and a significant difference in the peak window for all MCC groups, with a higher amplitude for the high motivation level than the low motivation level.

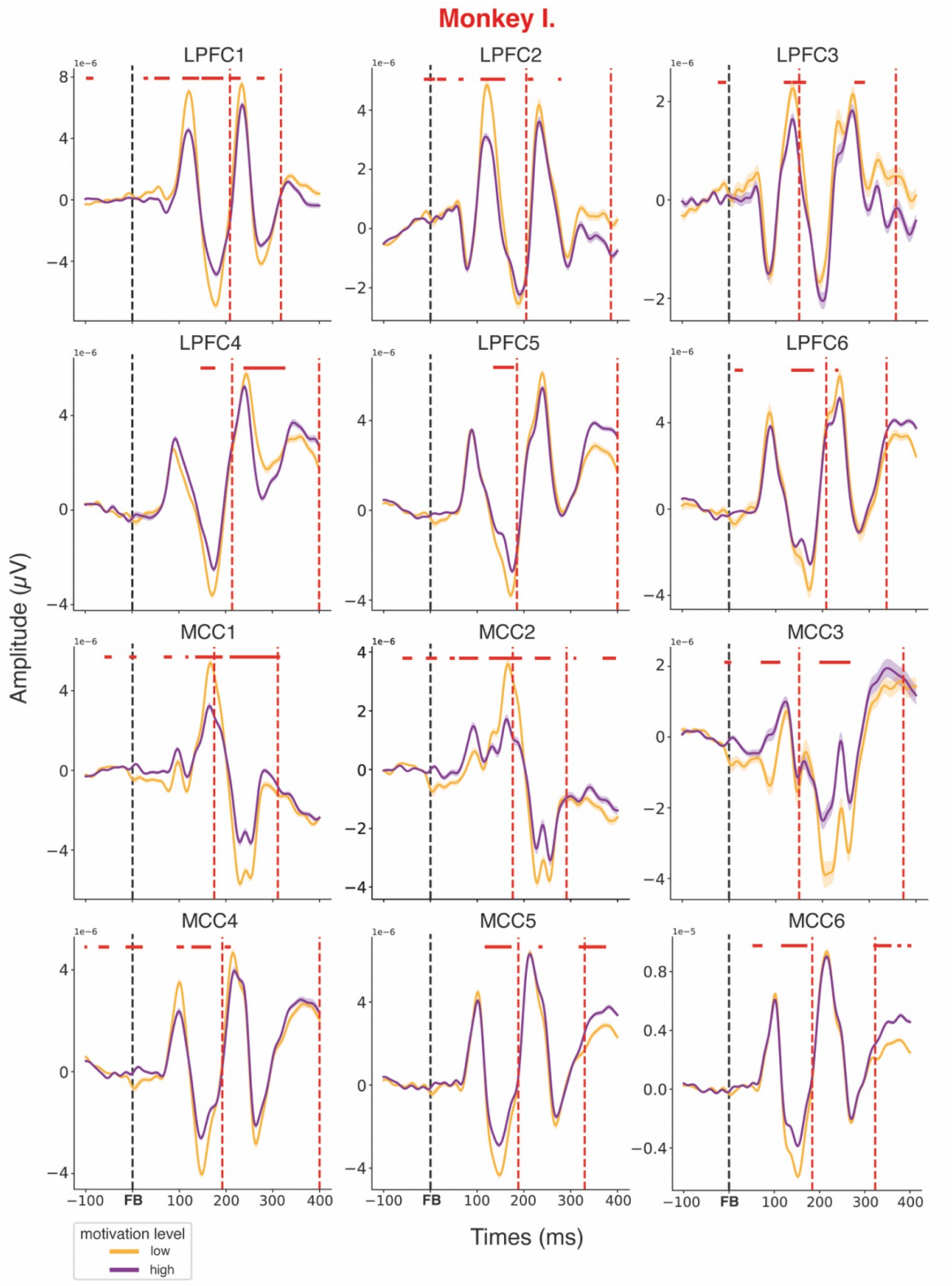

Figure 71. Evoked potentials by positive feedback across motivation levels for Monkey I. Time window of 100ms before the feedback and 400ms after. Black dashed line represents the feedback at time 0. Red dashed lines represent the limit of the peaks window. Red horizontal segments indicate a significant p-value of the Kruskal-Wallis test between learning steps for each time point. FB = feedback.

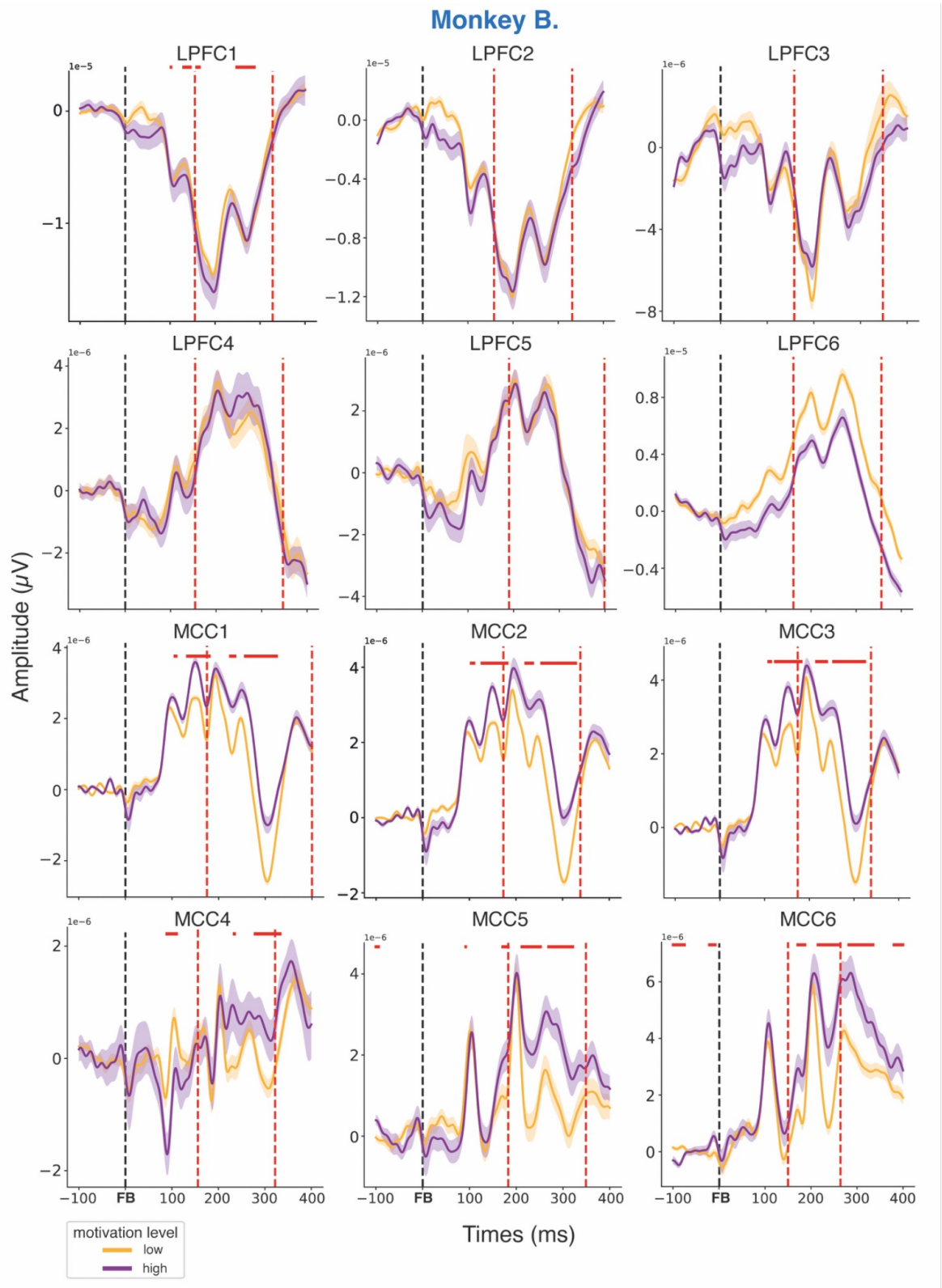

Figure 72. Evoked potentials by positive feedback across motivation levels for Monkey B. Time window of 100ms before the feedback and 400ms after. Black dashed line represents the feedback at time 0. Red dashed lines represent the limit of the peaks window. Red horizontal segments indicate a significant p-value of the Kruskal-Wallis test between learning steps for each time point. FB = feedback.

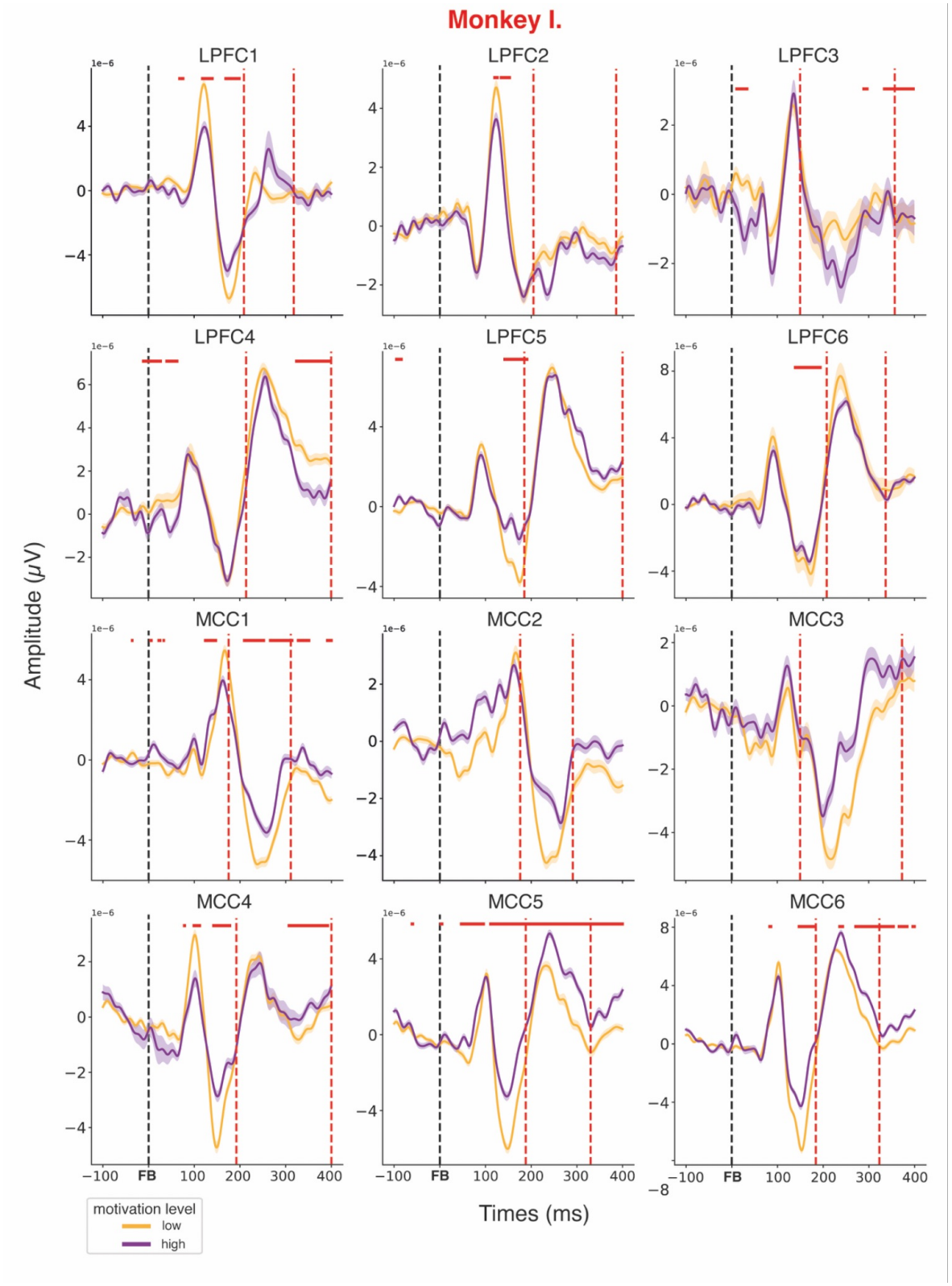

Figure 73. Evoked potentials by negative feedback across motivation levels for Monkey I. Time window of 100ms before the feedback and 400ms after. Black dashed line represents the feedback at time 0. Red dashed lines represent the limit of the peaks window. Red horizontal segments indicate a significant p-value of the Kruskal-Wallis test between learning steps for each time point. FB = feedback.

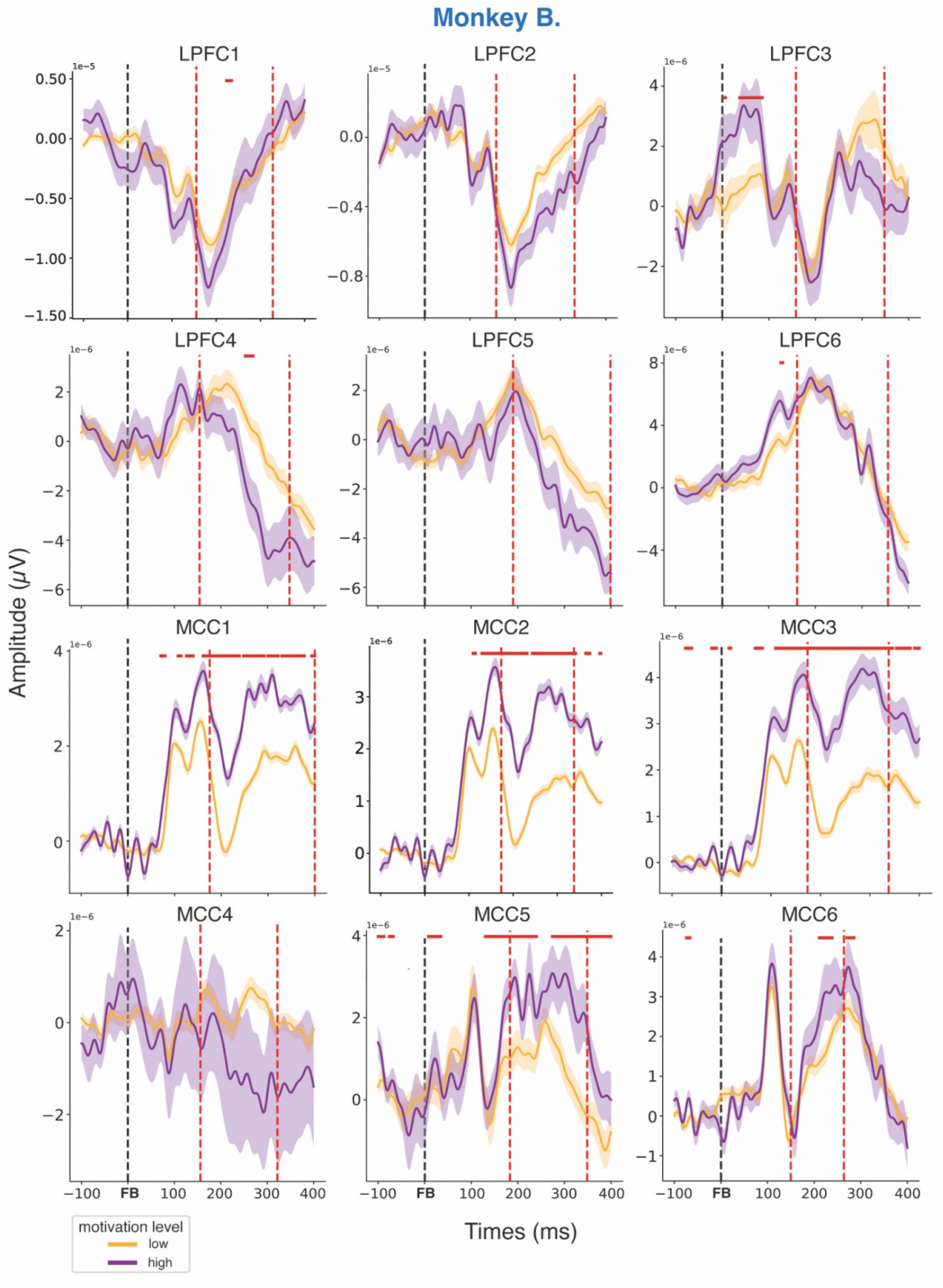

Figure 74. Evoked potentials by negative feedback across motivation levels for Monkey B. Time window of 100ms before the feedback and 400ms after. Black dashed line represents the feedback at time 0. Red dashed lines represent the limit of the peaks window. Red horizontal segments indicate a significant p-value of the Kruskal-Wallis test between learning steps for each time point. FB = feedback.

Then we did the same approach to the evoked responses to negative feedback (**Fig. 73 & 74**) and showed that for both monkeys there was no significant difference in the LPFC during the peak window except in the LPFC4 where the low motivation level had a higher amplitude than the high motivation level. In the MCC, in both monkeys, ERP amplitudes increased with a higher motivation level. This

Overall, the level of motivation showed a significant impact on the evoked response to both types of feedback. In the LPFC, a low motivation seemed to reduce the response to positive feedback for Monkey I whereas there was no effect for Monkey B. There was also no effect of motivation on the response to negative feedback in the LPFC for both monkeys. In the MCC, a high motivation increased the response to positive feedback in the anterior parts (MCC1 to MCC3) for Monkey I and in all parts for Monkey B. It also increased the response to negative feedback for both monkeys. These effects were found without taking the step of learning in consideration and we showed that motivation levels and learning steps were closely linked for Monkey I meaning that the effect could also be attributed to the learning step. However, Monkey B had not the same pattern with a more distributed repartition of the motivation levels across the learning step meaning that the effect raised here could be attributed to the motivation level alone. One should note that this statistical analysis was done time point per time point, thus ignoring offset and peak effects. A deeper peak analysis will be necessary to confirm or precise this motivation effect.

b) Motivation and learning groups

To sum up, motivation did have an impact on the feedback responses and this first approach allowed us to assess its effect alone but we wondered how this effect could have evolved throughout the training. We were particularly interested in the impact of the motivation during the learning phase, thus we focused on the learning steps 1 and 2 and combined it with the motivational level. We looked first at the evoked response to positive feedback (**Fig. 75 & 76**). We showed that when we separated the responses in learning steps and motivation level, we found no significant effect for Monkey I except two small effects in LPFC1 step 2 and LPFC3 step1. For Monkey B, we also found no effect in the LPFC however we saw a tendency in the MCC with again a higher amplitude for high motivation level in both steps.

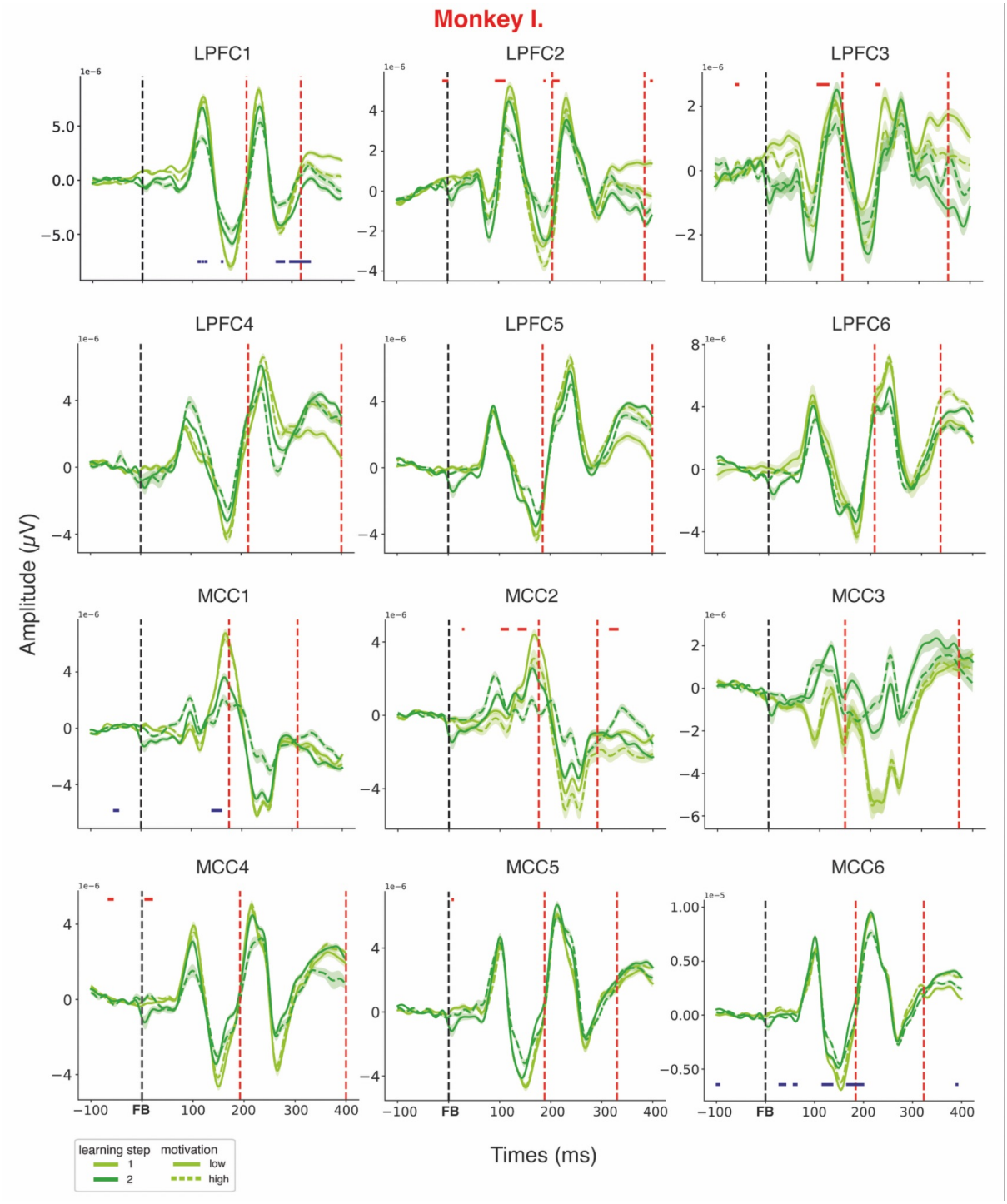

Figure 75. Evoked potentials by positive feedback across learning steps and motivation levels for Monkey I. Time window of 100ms before the feedback and 400ms after. Black dashed line represents the feedback at time 0. Red dashed lines represent the limit of the peaks window. Red horizontal segments indicate a significant p-value of the Kruskal-Wallis test between motivation level in step 1 and blue one in step 2. FB = feedback.

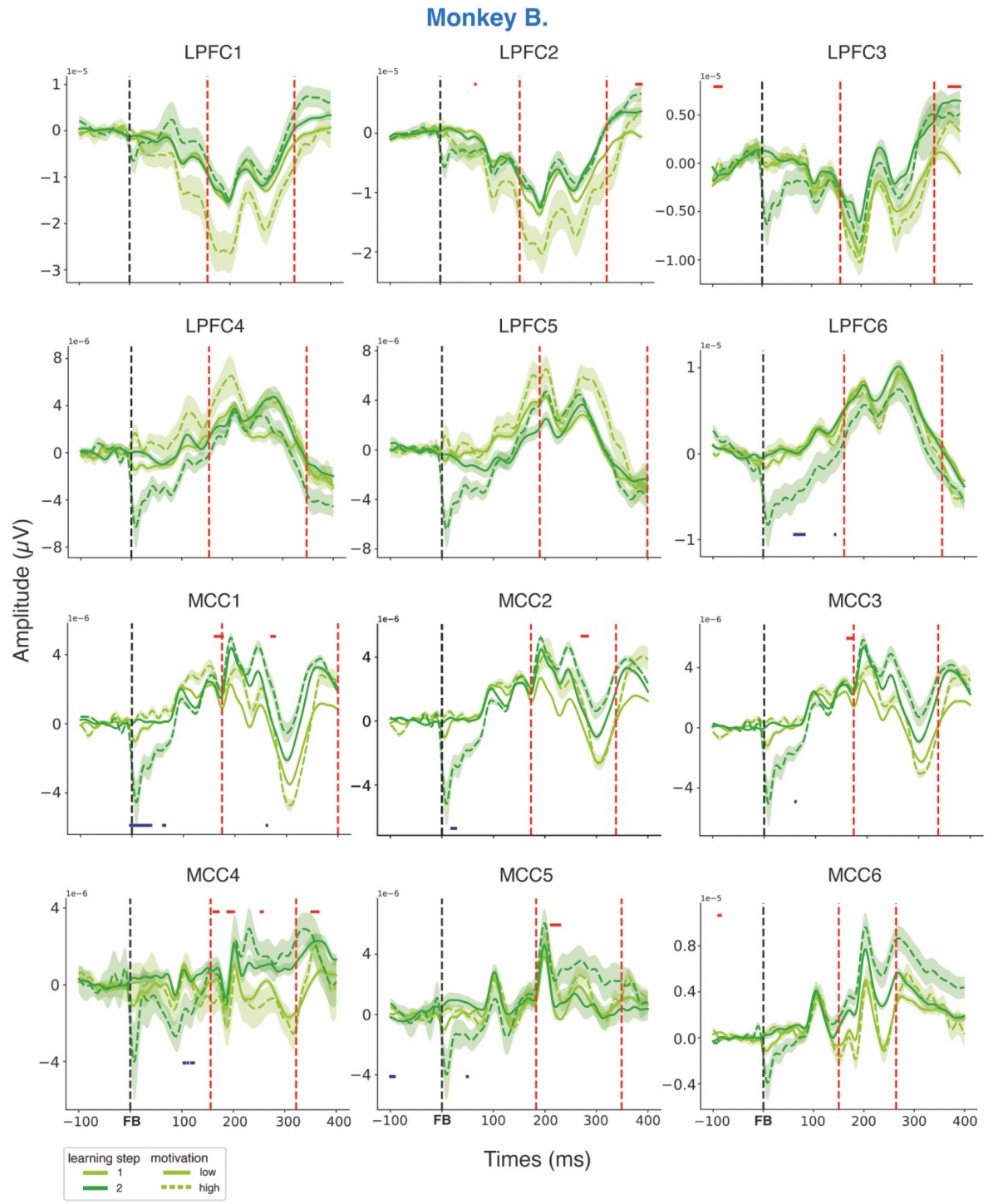

Figure 76. Evoked potentials by positive feedback across learning steps and motivation levels for Monkey B. Time window of 100ms before the feedback and 400ms after. Black dashed line represents the feedback at time 0. Red dashed lines represent the limit of the peaks window. Red horizontal segments indicate a significant p-value of the Kruskal-Wallis test between motivation level in step 1 and blue one in step 2. FB = feedback.

Then we did the same thing with negative feedback (**Fig. 77 & 78**). There were varied effects, different between monkeys. Step 1 had almost no significant effect between motivation levels in the peak window for Monkey I. Step 2 elicited significant differences between motivation levels for Monkey I but no difference in the MCC for Monkey B.

Overall, we showed that for the positive feedback there was also no effect in any step in the LPFC of both monkeys. There was also no effect in the MCC for Monkey I however we saw a higher response in high motivation level in step 1 for Monkey B. Results were different for the negative feedback, with varied effects but concentrated in step 2 for Monkey I. There was less effect for Monkey B, with no effect at all in MCC step 2. Finally, this could mean that the motivation had more impact on the positive feedback processing in step 1 for Monkey B whereas it had an impact only on the negative feedback processing and principally in step 2 for Monkey I.

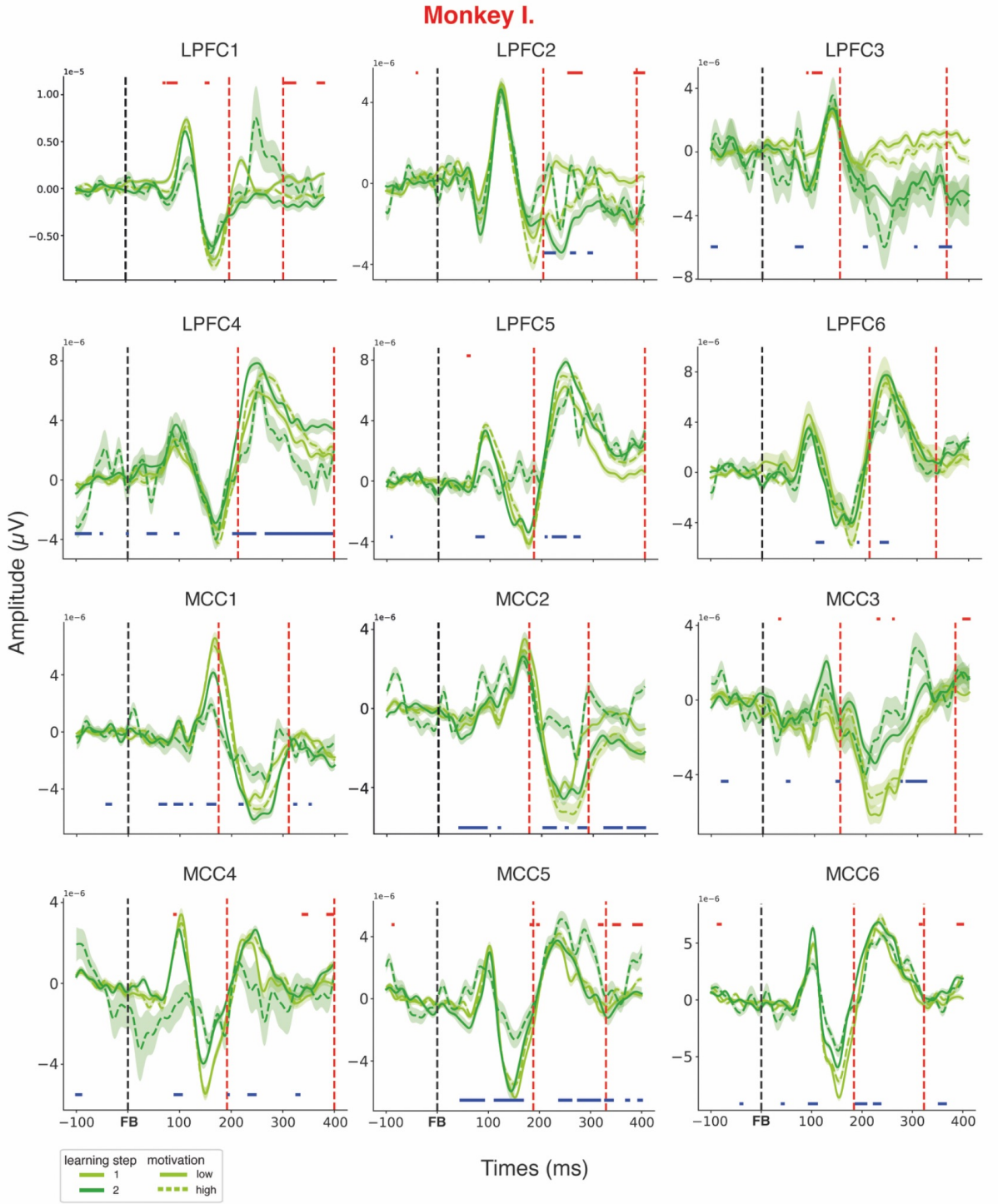

Figure 77. Evoked potentials by negative feedback across learning steps and motivation levels for Monkey I. Time window of 100ms before the feedback and 400ms after. Black dashed line represents the feedback at time 0. Red dashed lines represent the limit of the peaks window. Red horizontal segments indicate a significant p-value of the Kruskal-Wallis test between motivation level in step 1 and blue one in step 2. FB = feedback.

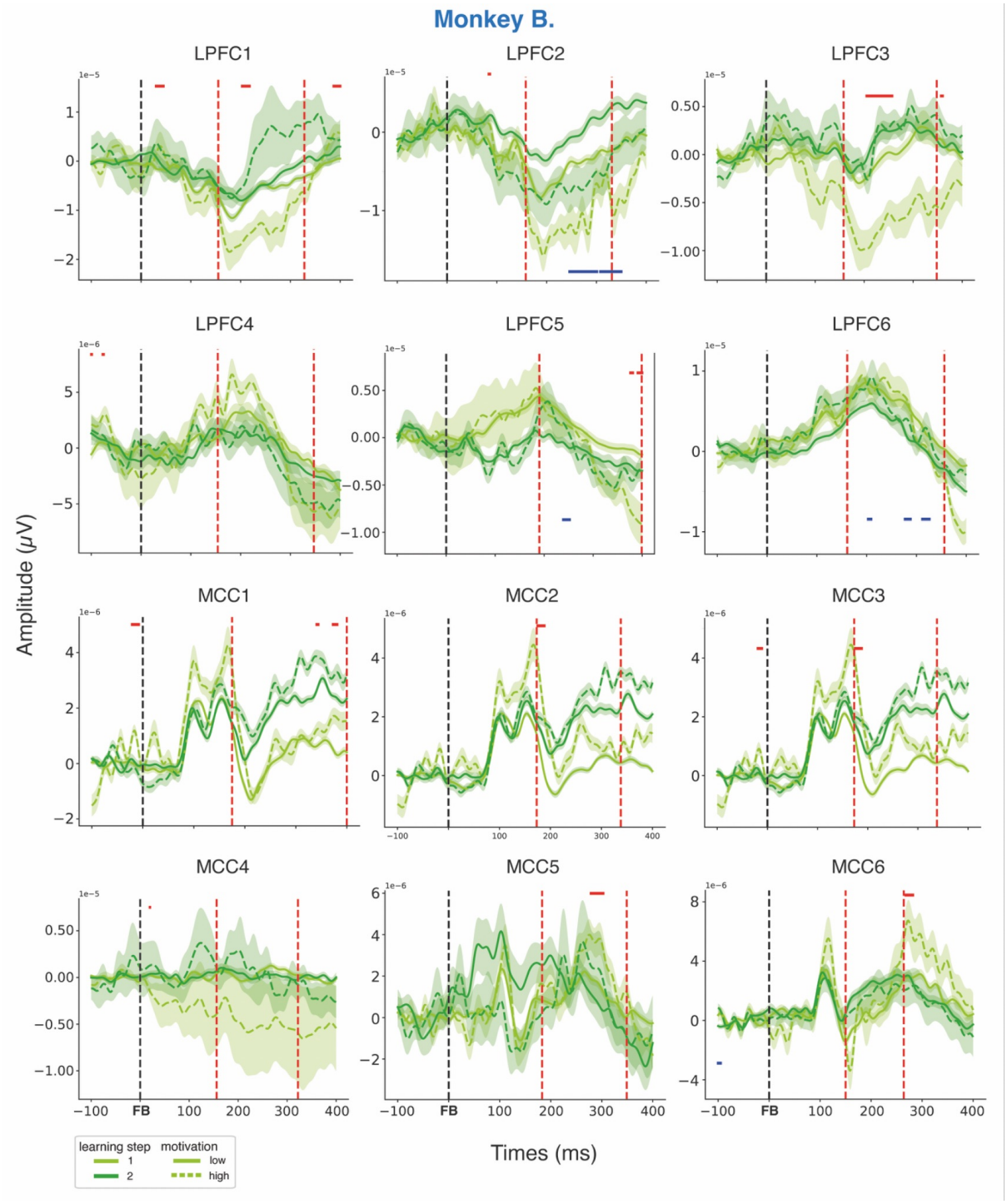

Figure 78. Evoked potentials by negative feedback across learning steps and motivation levels for Monkey B. Time window of 100ms before the feedback and 400ms after. Black dashed line represents the feedback at time 0. Red dashed lines represent the limit of the peaks window. Red horizontal segments indicate a significant p-value of the Kruskal-Wallis test between motivation level in step 1 and blue one in step 2. FB = feedback.

IV. Conclusion

Overall, the motivation really had an impact on feedback evoked response. This was even more true for Monkey B for whom we could separate learning and motivation more easily and who seemed to have more behavioural motivation impact (chapter 2). Interestingly, the motivation impact was not at the same learning step for both monkeys. It has more effect on the first step for Monkey B whereas it was the second step for Monkey I.

However, one should keep in mind that separating motivation and learning in cognitive tasks is really difficult and that we could not be sure that the effect highlighted here was totally due to motivation level only.

Further analyses will be necessary to dig on this motivation concept, starting by assessing the motivation level impact on the functional connectivity results presented in chapter 4. Also, it will be interesting to measure motivation inside the session, trial by trial. And finally, to apply statistical models that will explicitly compare the effects of learning and motivation.

GENERAL DISCUSSION

Chapter 1. Findings overview

Our different ways of assessing the impact of the training on positive and negative feedback processing showed that differentiation between them appeared quickly after the beginning of learning and stayed marked until the end of training. However, both types of feedback had different evolutions across the learning steps with a clearer pattern for the positive one than the negative one. These evolutions were reflected in significant evoked potential peak amplitude and latency changes, also in changes of proportion of responsive and encoding sorted units, as well as in FC and granger causality changes across training and inside sessions. We showed that these changes were present in both areas (MCC and LPFC) but to a greater or lesser extent according to the parameters and the monkeys studied. Importantly, monkeys had opposite patterns in all different scales of analysis, from the behavioural analysis to the electrophysiological ones.

Monkey I demonstrated a faster adaptation to the task, with fewer errors over sessions, indicative of a more efficient learning process. In contrast, Monkey B showed greater variability in performance, particularly during the initial stages of learning, indicating a slower integration of feedback and refinement of strategies.

At the neural level, Monkey I exhibited more consistent changes in LFP dynamics in response to feedback across problems, reflecting stable feedback processing throughout learning. Monkey B, on the other hand, displayed more fluctuating LFP activity in response to feedback, suggesting a more exploratory phase before stabilizing its learning strategy. Regarding the FC, Monkey I showed stronger and more consistent connectivity between the LPFC and the MCC during the learning process, indicating a more integrated and efficient neural network for processing feedback and adjusting behaviour accordingly. In contrast, Monkey B exhibited more variable connectivity, especially in the early learning stages, which stabilized as its performance improved.

Motivational differences were also evident, with Monkey I displaying higher engagement and quicker response times, particularly in reward-related trials, as indicated by neural markers of motivation. Monkey B, while more exploratory and slower in initial responses, particularly to negative feedback, gradually adapted its behaviour, showing that

both motivational and feedback-processing strategies can vary substantially between subjects. These results pointed out the fact that learning optimization could be achieved by different paths and that reaching the learning to learn level is not linked to one specific immutable pattern. This work was part of a large-scale project and further analyses on other specific components of the learning will help to describe the learning to learn process.

Chapter 2. Why did our monkeys learn differently compared to previous similar studies?

In previous studies describing the acquisition of learning to learn capacities, the acquired learning strategy was expressed in abrupt changes of performance on the second trial or problems presented at the end of learning to learn, showing that monkeys had extracted general performance rules to near-optimise performance on the task (Faraut et al., 2016; Harlow, 1949; Wilson & Gaffan, 2008). Our experimental paradigm aimed to reproduce this effect, but it is fair to say that in this study monkeys did not acquire this simple task in the same way as previous versions. Whilst our monkeys showed learning across training, leading to a plateau defined as the learning to learn level, this took more problems than previous studies, and the performance plateau achieved was not the near optimal level seen in other studies. For example, learning set acquisition on a very similar task in Wilson & Gaffan (2008) led to a plateau after 30-50 problems with performance around 3-5 errors per problem (Fig 6 of that study). In contrast, monkeys here plateaued after 60-70 problems at around 10 errors per problem (**Fig. 17**). Furthermore, the within-problem learning from trial 2 onwards was much less evident in the current animals. The change of performance evidenced in later well learned problems was slower to emerge after exposure to a new problem, arriving after around 10 and 30 trials depending on the monkey. The upshot of this is that whilst our animals in this study clearly learned to learn through a significant improvement of the errors made to criterion over problems, they did not do so to the extent and with the pattern that has been previously recognised as being the expression of a discrimination learning set as laid out by Harlow (1949).

Several reasons could explain the difference between our study and the previous ones. First, we had the hypothesis that our chosen image pairs were too similar and could have brought visual perceptual difficulty to the discrimination over and above the difficulty of learning to make feedback driven discriminations. However, even if a deeper work on the difficulty assessment remains to be done, our first analysis on the subject did not highlight an impact of the difficulty on the motivation. Secondly, we hypothesised that the format of our sessions

of work and the difference in reward number and size could be responsible. Monkeys performed between 200 and 400 trials per day and worked for small ~1ml juice rewards, as is customary in electrophysiology preps. In order to fully motivate late session work they received a big reward bonus at the end of each finished session. This raised the reward to a high quantity each day. This means that if we consider the relative size of a single juice reward on a given single trial, the quantity of reward is small, and so for any given trial the reward driven incentive is small. This contrasts with many of the previous studies we have been comparing with, which were performed out of the electrophysiology prep in which tasks are designed to maximise within-session trial numbers for recording reasons. For example, Wilson & Gaffan (2008) used pellet rewards 190mg each, so with a larger calorific content per reward, and monkeys worked for 100-200 problems at most per day. Thus, in our study the incentive brought by a given individual reward at each trial was significantly less, and therefore rapid behavioural adjustment might have been less incentivised for the monkey. Another way of saying this is that this meant that our design did not push monkeys to perform optimally at every trial, and so they were slow to adapt and did not develop a prospective strategy in the same way as evidenced in other studies.

Linked to this of course is the possible effect of the type of reward. In our experiment, monkeys received liquid rewards as described above. Other studies used food reward in non-headfixed preps. We can hypothesise that food and liquid rewards did not elicit the same interest in monkeys, or that differences in either objective (calorific) or subjective reward size impacted their motivation to be as efficient as possible.

Chapter 3. Is the motivation and the learning really dissociable?

Trying to clearly separate learning and motivation in cognitive tasks not designed for this purpose is a challenge as they are often closely linked. However, one can ask if this dissociation is really informative as these processes are also not always dissociable in the daily life. However, even if our focus is not on separating them perfectly, it is now well-known and we confirmed it in our results, that motivation has a real impact that should be considered. The traditional working set-up for monkeys in neuroscience uses a box in which the experimenters need to bring the monkey. Because of evident technical limits, this means that the monkey works during defined periods in one block. However, this approach either leads to an uncertain motivational state at the start of work as the monkey is not choosing to work, or more frequently as here it is coupled with a motivation control paradigm (here water control) which means that motivation levels are increased and controlled by the experimenter.

Recently, laboratories developed free-access facilities that allow monkeys to decide periods when they want to work (Ferrari & Baldi, 2024; Voloh et al., 2023). This ecological approach allowed scientists to refine works with monkeys but also to leave more space for intrinsic motivation. Developing these structures will be a game-changer for the learning field as it will permit electrophysiological recordings in more ecological conditions and to assess the real motivation of monkeys.

Chapter 4. The longitudinal approach in electrophysiology

The longitudinal approach in neurosciences, particularly in electrophysiology, offers unique insights into the evolution of neural and behavioural correlates over time. In this thesis, tracking changes throughout different stages of learning provided crucial data on how prefrontal areas, such as the LPFC and MCC, adapt with training. The choice to use a longitudinal design allowed us to study the subtle, progressive changes in neural dynamics that would otherwise be overlooked in cross-sectional or acute studies. In contrast to many previous studies, which focus on pre- and post-training comparisons, the longitudinal approach allowed us to capture the dynamic evolution of neural activity during the learning process itself. Studies like those by Meyer et al. (2011) and Qi et al. (2011) have identified task-relevant changes in the PFC after training, but they did not track how these changes developed over time. By observing how the neural activity changes across multiple stages of training in real-time, we gained a more detailed understanding of the neural adjustments involved in learning and learning to learn processes.

Despite its advantages, using a longitudinal approach in chronic electrophysiology poses significant technical challenges. Although modern chronic implants have improved, ensuring the stability of recorded signals over long periods remains difficult due to factors like tissue reactions or electrode movements. In our study, we maintained stable recordings for much of the duration, but there were some fluctuations in signal quality, especially during the latter sessions of Monkey B. Signal drift, which may have been caused by gliosis or micro-movements of electrodes within the tissue (Griffith & Humphrey, 2006; Hermann & Capadona, 2018), underscores the need for further technological advancements to improve electrode design and mitigate these issues.

By combining LFP and single-unit recordings across different stages of training, we were able to assess functional connectivity and local field potentials, providing a broader picture of how different brain regions coordinate during learning. The ability to track these changes continuously over time offers deeper insights into how regions like the LPFC and MCC adapt not just in response to feedback but across the entire training process.

Looking ahead, continued advancements in implant stability, data analysis techniques, and signal processing will make longitudinal studies even more valuable in cognitive neuroscience. This approach will enable researchers to more effectively capture the neural correlates of complex learning processes, providing a clearer understanding of how adaptive changes occur in the brain over time.

FUTURE PERSPECTIVES

This work was part of a bigger project that aimed to describe changes in neural correlates of the LPFC and MCC across different learning steps, from the task naïve state up to a state where learning is optimised through learning to learn. We focused the analyses of this manuscript on the processing of positive and negative feedback, but several other parts of the task could bring essential information on the learning process. One next step would be to focus on the inter-trial interval (ITI) to assess processes like planning and anticipation of the future actions based on the last feedback. As discussed, one possible implementation of the learning strategies that emerge is to render decisions more prospective and planned, rather than reactive to stimulus presentation. A possible neural implementation of this would be the emergence of anticipatory choice-related activity in the ITI or pre-trial delay period. A further effect that might link to this would be changes in beta bands during this period, where the team has already shown such prospective choice-based activity in the pre-trial delay, albeit in a different task with over-trained monkeys (Stoll et al., 2016). One prediction might be the emergence of such beta responses over the course of training. Stoll and colleagues also linked this beta band activity to cognitive effort changes over the course of the sessions, and this could further be linked to the motivation responses described here (Stoll et al., 2016).

Much of the work here focused on event-related potentials and combined it with LFP functional connectivity assessment. A full picture of the neural dynamics at play across the long learning period of the task requires combination of these results with analysis of the oscillatory activity through time-frequency analysis, and also further in-depth analysis of the roles of the single neurons and the population responses of those neurons. Further, assessment of the connectivity between the single-unit signal and the LFP would complete the neural dynamic description across different scales.

Another way to take this work further would be to add more descriptive variables of the signal. We had different depths of electrodes in both areas, reaching a superficial and a deep layer and previous works showed that LFP power varies with laminar depth in a manner that reflects cortical layer makeup and potentially the local oscillatory generator (Bastos et al., 2018). As we move to a more complete picture of the neural dynamical changes across learning, adding this depth information would permit us to ground any noted changes in the laminar makeup of cortex.

We could also add behavioural precision. We talked about the two-way impact of the difficulty and assessed it in the first 50 problems of the DL task with algorithms and human perception scores. However, we could think of a more robust way of defining an objective difficulty component usable in all problems and tasks. For example, we could link algorithm results with behavioural data such as reaction time, hesitation and aborted trials.

Finally, we focused on simple well-known cognitive tasks (DL and RL) to have an easy experimental design to follow in our longitudinal approach. However, we also recorded one monkey in a more complex task at the end of the training - the problem-solving task. Adding this comparison in this work could be used to assess the learning to learn effect in a task with more cognitive demand.

Overall, the data collected in this project will allow us to explore many aspects of the learning to learn process and to expand on the initial results presented in this manuscript.

BIBLIOGRAPHY

Amiez, C., Joseph, J. P., & Procyk, E. (2006). Reward Encoding in the Monkey Anterior Cingulate Cortex. *Cerebral Cortex*, *16*(7), 1040-1055. https://doi.org/10.1093/cercor/bhj046

Amiez, C., & Petrides, M. (2014). Neuroimaging Evidence of the Anatomo-Functional Organization of the Human Cingulate Motor Areas. *Cerebral Cortex*, *24*(3), 563-578. https://doi.org/10.1093/cercor/bhs329

Amiez, C., Sallet, J., Hopkins, W. D., Meguerditchian, A., Hadj-Bouziane, F., Ben Hamed, S., Wilson, C. R. E., Procyk, E., & Petrides, M. (2019). Sulcal organization in the medial frontal cortex provides insights into primate brain evolution. *Nature Communications*, *10*(1), 3437. https://doi.org/10.1038/s41467-019-11347-x

Amiez, C., Verstraete, C., Sallet, J., Hadj-Bouziane, F., Ben Hamed, S., Meguerditchian, A., Procyk, E., Wilson, C. R. E., Petrides, M., Sherwood, C. C., & Hopkins, W. D. (2023). The relevance of the unique anatomy of the human prefrontal operculum to the emergence of speech. *Communications Biology*, *6*(1), 693. https://doi.org/10.1038/s42003-023-05066-9

Andersen, R. A., & Cui, H. (2009). Intention, Action Planning, and Decision Making in Parietal-Frontal Circuits. *Neuron*, *63*(5), 568-583. https://doi.org/10.1016/j.neuron.2009.08.028

Ashby, W. R. (1956). An Introduction to Cybernetics. *Chapman & Hall*.

Badre, D., & D'Esposito, M. (2009). Is the rostro-caudal axis of the frontal lobe hierarchical? *Nature Reviews Neuroscience*, *10*(9), 659-669. https://doi.org/10.1038/nrn2667

Ball, K., Berch, D. B., Helmers, K. F., Jobe, J. B., Leveck, M. D., Marsiske, M., Morris, J. N., Rebok, G. W., Smith, D. M., Tennstedt, S. L., Unverzagt, F. W., Willis, S. L., & For The Active Study Group. (2002). Effects of Cognitive Training Interventions With Older Adults : A Randomized Controlled Trial. *JAMA*, *288*(18), 2271. https://doi.org/10.1001/jama.288.18.2271

Bandura, A. (1986). Social foundations of thought and action. *Englewood Cliffs, NJ*, 23-28.

Barkley, R. A., Cunningham, C. E., Gordon, M., Faraone, S. V., Lewandowski, L., & Murphy, K. R. (2006). ADHD Symptoms vs. Impairment : Revisited. *The ADHD Report*, *14*(2), 1-9. https://doi.org/10.1521/adhd.2006.14.2.1

Baron–Cohen, S. (2000). Is Asperger syndrome/high-functioning autism necessarily a disability? *Development and Psychopathology*, *12*(3), 489-500. https://doi.org/10.1017/S0954579400003126

Bastos, A. M., Loonis, R., Kornblith, S., Lundqvist, M., & Miller, E. K. (2018). Laminar recordings in frontal cortex suggest distinct layers for maintenance and control of working memory. *Proceedings of the National Academy of Sciences*, *115*(5), 1117-1122. https://doi.org/10.1073/pnas.1710323115

Bechara, A., Tranel, D., & Damasio, H. (2000). Characterization of the decision-making deficit of patients with ventromedial prefrontal cortex lesions. *Brain*, *123*(11), 2189-2202. https://doi.org/10.1093/brain/123.11.2189

Beran, M. J., Klein, E. D., Evans, T. A., Chan, B., Flemming, T. M., Harris, E. H., Washburn, D. A., & Rumbaugh, D. M. (2008). Discrimination Reversal Learning in Capuchin Monkeys (Cebus Apella). *The Psychological Record*, *58*(1), 3-14. https://doi.org/10.1007/BF03395599

Berridge, K. C., & Robinson, T. E. (1998). What is the role of dopamine in reward : Hedonic impact, reward learning, or incentive salience? *Brain Research Reviews*, *28*(3), 309-369. https://doi.org/10.1016/S0165-0173(98)00019-8

Berridge, K. C., & Robinson, T. E. (2003). Parsing reward. *Trends in Neurosciences*, *26*(9), 507-513. https://doi.org/10.1016/S0166-2236(03)00233-9

Bjork, E. L., & Bjork, R. (2014). Making Things Hard on Yourself, But in a Good Way : Creating Desirable Difficulties to Enhance Learning. *Psychology and the Real World: Essays Illustrating Fundamental Contributions to Society (2nd Edition)*.

Bliss, T. V. P., & Collingridge, G. L. (1993). A synaptic model of memory : Long-term potentiation in the hippocampus. *Nature*, 31-39.

Bonini, F., Burle, B., Liégeois-Chauvel, C., Régis, J., Chauvel, P., & Vidal, F. (2014). Action Monitoring and Medial Frontal Cortex : Leading Role of Supplementary Motor Area. *Science*, *343*(6173), 888-891. https://doi.org/10.1126/science.1247412

Borra, E., Belmalih, A., Calzavara, R., Gerbella, M., Murata, A., Rozzi, S., & Luppino, G. (2008). Cortical Connections of the Macaque Anterior Intraparietal (AIP) Area. *Cerebral Cortex*, *18*(5), 1094-1111. https://doi.org/10.1093/cercor/bhm146

Braver, T. S., Krug, M. K., Chiew, K. S., Kool, W., Westbrook, J. A., Clement, N. J., Adcock, R. A., Barch, D. M., Botvinick, M. M., Carver, C. S., Cools, R., Custers, R., Dickinson, A., Dweck, C. S., Fishbach, A., Gollwitzer, P. M., Hess, T. M., Isaacowitz, D. M., Mather, M., … for the MOMCAI group. (2014). Mechanisms of motivation–cognition interaction : Challenges and opportunities. *Cognitive, Affective, & Behavioral Neuroscience*, *14*(2), 443-472. https://doi.org/10.3758/s13415-014-0300-0

Browning, P. G. F., Easton, A., & Gaffan, D. (2007). Frontal-Temporal Disconnection Abolishes Object Discrimination Learning Set in Macaque Monkeys. *Cerebral Cortex*, *17*(4), 859-864. https://doi.org/10.1093/cercor/bhk039

Burle, B., Roger, C., Allain, S., Vidal, F., & Hasbroucq, T. (2008). Error Negativity Does Not Reflect Conflict : A Reappraisal of Conflict Monitoring and Anterior Cingulate Cortex Activity. *Journal of Cognitive Neuroscience*, *20*(9), 1637-1655. https://doi.org/10.1162/jocn.2008.20110

Butterworth, B. (2010). Foundational numerical capacities and the origins of dyscalculia. *Trends in Cognitive Sciences*, *14*(12), 534-541. https://doi.org/10.1016/j.tics.2010.09.007

Carmichael, S. T., & Price, J. L. (1995). Sensory and premotor connections of the orbital and medial prefrontal cortex of macaque monkeys. *Journal of Comparative Neurology*, *363*(4), 642-664. https://doi.org/10.1002/cne.903630409

Carroll, J. B. (1963). A model of school learning. *Teachers college record*, *64*(8), 1-9.

Cepeda, N. J., Pashler, H., Vul, E., Wixted, J. T., & Rohrer, D. (2006). Distributed practice in verbal recall tasks : A review and quantitative synthesis. *Psychological Bulletin*, *132*(3), 354-380. https://doi.org/10.1037/0033-2909.132.3.354

Chatila, R., Renaudo, E., Andries, M., Chavez-Garcia, R.-O., Luce-Vayrac, P., Gottstein, R., Alami, R., Clodic, A., Devin, S., Girard, B., & Khamassi, M. (2018). Toward Self-Aware Robots. *Frontiers in Robotics and AI*, *5*, 88. https://doi.org/10.3389/frobt.2018.00088

Collins, A., & Koechlin, E. (2012). Reasoning, Learning, and Creativity : Frontal Lobe Function and Human Decision-Making. *PLoS Biology*, *10*(3), e1001293. https://doi.org/10.1371/journal.pbio.1001293

Constantinidis, C., & Klingberg, T. (2016). The neuroscience of working memory capacity and training. *Nature Reviews Neuroscience*, *17*(7), 438-449. https://doi.org/10.1038/nrn.2016.43

Corbett, A., Owen, A., Hampshire, A., Grahn, J., Stenton, R., Dajani, S., Burns, A., Howard, R., Williams, N., Williams, G., & Ballard, C. (2015). The Effect of an Online Cognitive Training Package in Healthy Older Adults : An Online Randomized Controlled Trial. *Journal of the American Medical Directors Association*, *16*(11), 990-997. https://doi.org/10.1016/j.jamda.2015.06.014

Cornford, I. R. (2002). Learning-to-learn strategies as a basis for effective lifelong learning. *International Journal of Lifelong Education*, *21*(4), 357-368. https://doi.org/10.1080/02601370210141020

Cziksentmihalyi, M. (1990). Flow – The Psychology of optimal experience. *Harper*.

Danielmeier, C., & Ullsperger, M. (2011). Post-Error Adjustments. *Frontiers in Psychology*, *2*. https://doi.org/10.3389/fpsyg.2011.00233

Daw, N. D., Niv, Y., & Dayan, P. (2005). Uncertainty-based competition between prefrontal and dorsolateral striatal systems for behavioral control. *Nature Neuroscience*, *8*(12), 1704-1711. https://doi.org/10.1038/nn1560

Daw, N. D., & O'Doherty, J. P. (2014). Multiple Systems for Value Learning. In *Neuroeconomics* (p. 393-410). Elsevier. https://doi.org/10.1016/B978-0-12-416008-8.00021-8

Deci, E. L., & Ryan, R. M. (2000). The « What » and « Why » of Goal Pursuits : Human Needs and the Self-Determination of Behavior. *Psychological Inquiry*, *11*(4), 227-268. https://doi.org/10.1207/S15327965PLI1104_01

Di Chiara, G., & Bassareo, V. (2007). Reward system and addiction : What dopamine does and doesn't do. *Current Opinion in Pharmacology*, *7*(1), 69-76. https://doi.org/10.1016/j.coph.2006.11.003

Dignath, C., & Büttner, G. (2008). Components of fostering self-regulated learning among students. A meta-analysis on intervention studies at primary and secondary school level. *Metacognition and Learning*, *3*(3), 231-264. https://doi.org/10.1007/s11409-008-9029-x

Donoghue, T., Haller, M., Peterson, E. J., Varma, P., Sebastian, P., Gao, R., Noto, T., Lara, A. H., Wallis, J. D., Knight, R. T., Shestyuk, A., & Voytek, B. (2020). Parameterizing neural power spectra into periodic and aperiodic components. *Nature Neuroscience*, *23*(12), 1655-1665. https://doi.org/10.1038/s41593-020-00744-x

Doya, K. (2002). Metalearning and neuromodulation. *Neural Networks*, *15*(4-6), 495-506. https://doi.org/10.1016/S0893-6080(02)00044-8

Ducret, M., Giacometti, C., Dirheimer, M., Dureux, A., Autran-Clavagnier, D., Hadj-Bouziane, F., Verstraete, C., Lamberton, F., Wilson, C. R. E., Amiez, C., & Procyk, E. (2024). Medial to lateral frontal functional connectivity mapping reveals the organization of cingulate cortex. *Cerebral Cortex*, *34*(8), bhae322. https://doi.org/10.1093/cercor/bhae322

Dum, R., & Strick, P. (2002). Motor areas in the frontal lobe of the primate. *Physiology & Behavior*, *77*(4-5), 677-682. https://doi.org/10.1016/S0031-9384(02)00929-0

Duncan, J., Assem, M., & Shashidhara, S. (2020). Integrated Intelligence from Distributed Brain Activity. *Trends in Cognitive Sciences*, *24*(10), 838-852. https://doi.org/10.1016/j.tics.2020.06.012

Ericsson, K. A., Krampe, R. T., & Tesch-Romer, C. (1993). The Role of Deliberate Practice in the Acquisition of Expert Performance. *Psychological Review*, *100*(3), 363-406.

Faraut, M. C. M., Procyk, E., & Wilson, C. R. E. (2016). Learning to learn about uncertain feedback. *Learning & Memory*, *23*(2), 90-98. https://doi.org/10.1101/lm.039768.115

Federal Trade Commission. (2016). Lumosity to pay $2 million to settle FTC deceptive advertising charges for its « brain training » program. *FTC.gov*. https://www.ftc.gov/news-events/news/press-releases/2016/01/lumosity-pay-2-million-settle-ftc-deceptive-advertising-charges-its-brain-training-program

Ferrari, P. F., & Baldi, J. (2024). Social neuroscience : Primate research goes wireless. *Current Biology*, *34*(11).

Finn, C., Abbeel, P., & Levine, S. (2017). Model-Agnostic Meta-Learning for Fast Adaptation of Deep Networks. *Proceedings of the 34th International Conference on Machine Learning*, *70*, 1126-1135.

Fishbach, A., Zhang, Y., & Trope, Y. (2010). Counteractive evaluation : Asymmetric shifts in the implicit value of conflicting motivations. *Journal of Experimental Social Psychology*, *46*(1), 29-38. https://doi.org/10.1016/j.jesp.2009.09.008

Folstein, J. R., & Van Petten, C. (2008). Influence of cognitive control and mismatch on the N2 component of the ERP : A review. *Psychophysiology*, *45*(1), 152-170. https://doi.org/10.1111/j.1469-8986.2007.00602.x

Fu, Z., Beam, D., Chung, J. M., Reed, C. M., Mamelak, A. N., Adolphs, R., & Rutishauser, U. (2022). The geometry of domain-general performance monitoring in the human medial frontal cortex. *Science*, *376*(6593), eabm9922. https://doi.org/10.1126/science.abm9922

Fu, Z., Sajad, A., Errington, S. P., Schall, J. D., & Rutishauser, U. (2023). Neurophysiological mechanisms of error monitoring in human and non-human primates. *Nature Reviews Neuroscience*, *24*(3), 153-172. https://doi.org/10.1038/s41583-022-00670-w

Gabrieli, J. D. E. (2009). Dyslexia : A New Synergy Between Education and Cognitive Neuroscience. *Science*, *325*(5938), 280-283. https://doi.org/10.1126/science.1171999

Garey, L. J. (1999). *Brodmann's Localisation in the Cerebral Cortex : The Principles of Comparative Localisation in the Cerebral Cortex Based on Cytoarchitectonics*. Imperial College Press.

Gehring, W. J., Goss, B., Coles, M. G. H., Meyer, D. E., & Donchin, E. (1993). A neural system for error detection and compensation. *Psychological Science*, *4*(6), 385-390.

Godlove, D. C., Emeric, E. E., Segovis, C. M., Young, M. S., Schall, J. D., & Woodman, G. F. (2011). Event-Related Potentials Elicited by Errors during the Stop-Signal Task. I. Macaque Monkeys. *The Journal of Neuroscience*, *31*(44), 15640-15649. https://doi.org/10.1523/JNEUROSCI.3349-11.2011

Gosling, S. D. (2001). From mice to men : What can we learn about personality from animal research. *Psychological Bulletin*, *127*(1), 45-86.

Goussi-Denjean, C., Fontanier, V., Stoll, F. M., & Procyk, E. (2023). The Differential Weights of Motivational and Task Performance Measures on Medial and Lateral Frontal Neural Activity. *The Journal of Neuroscience*, *43*(23), 4329-4340. https://doi.org/10.1523/JNEUROSCI.0007-22.2023

Griffith, R. W., & Humphrey, D. R. (2006). Long-term gliosis around chronically implanted platinum electrodes in the Rhesus macaque motor cortex. *Neuroscience Letters*, *406*(1-2), 81-86. https://doi.org/10.1016/j.neulet.2006.07.018

Harlow, H. F. (1949). The formation of learning sets. *Psychological Review*, *56*(1), 51-65. https://doi.org/10.1037/h0062474

Harlow, H. F., & Warren, J. M. (1952). Formation and transfer of discrimination learning sets. *Journal of Comparative and Physiological Psychology*, *45*(5), 482-489. https://doi.org/10.1037/h0057267

Hattie, J., & Timperley, H. (2007). The Power of Feedback. *Review of Educational Research*, *77*(1), 81-112. https://doi.org/10.3102/003465430298487

Haufe, S., Nikulin, V. V., & Nolte, G. (2012). Alleviating the Influence of Weak Data Asymmetries on Granger-Causal Analyses. In F. Theis, A. Cichocki, A. Yeredor, & M. Zibulevsky (Éds.), *Latent Variable Analysis and Signal Separation* (Vol. 7191, p. 25-33). Springer Berlin Heidelberg. https://doi.org/10.1007/978-3-642-28551-6_4

Hayden, B. Y., & Platt, M. L. (2010). Neurons in Anterior Cingulate Cortex Multiplex Information about Reward and Action. *The Journal of Neuroscience*, *30*(9), 3339-3346. https://doi.org/10.1523/JNEUROSCI.4874-09.2010

Hermann, J. K., & Capadona, J. R. (2018). Understanding the Role of Innate Immunity in the Response to Intracortical Microelectrodes. *Critical Reviews in Biomedical Engineering*, *46*(4), 341-367. https://doi.org/10.1615/CritRevBiomedEng.2018027166

Hochman, E. Y., Vaidya, A. R., & Fellows, L. K. (2014). Evidence for a Role for the Dorsal Anterior Cingulate Cortex in Disengaging from an Incorrect Action. *PLoS ONE*, *9*(6), e101126. https://doi.org/10.1371/journal.pone.0101126

Holmes, J., Gathercole, S. E., Place, M., Dunning, D. L., Hilton, K. A., & Elliott, J. G. (2010). Working memory deficits can be overcome : Impacts of training and medication on working memory in children with ADHD. *Applied Cognitive Psychology*, *24*(6), 827-836. https://doi.org/10.1002/acp.1589

Holroyd, C. B., & Coles, M. G. H. (2002). The neural basis of human error processing : Reinforcement learning, dopamine, and the error-related negativity. *Psychological Review*, *109*(4), 679-709. https://doi.org/10.1037/0033-295X.109.4.679

Holroyd, C. B., Coles, M. G. H., Nieuwenhuis, S., Gehring, W. J., & Willoughby, A. R. (2002). Medial Prefrontal Cortex and Error Potentials. *Science, New Series*, *296*(5573), 1610-1611.

Izquierdo, A. (2017). Functional Heterogeneity within Rat Orbitofrontal Cortex in Reward Learning and Decision Making. *The Journal of Neuroscience*, *37*(44), 10529-10540. https://doi.org/10.1523/JNEUROSCI.1678-17.2017

Izquierdo, A., Suda, R. K., & Murray, E. A. (2004). Bilateral Orbital Prefrontal Cortex Lesions in Rhesus Monkeys Disrupt Choices Guided by Both Reward Value and Reward Contingency. *The Journal of Neuroscience*, *24*(34), 7540-7548. https://doi.org/10.1523/JNEUROSCI.1921-04.2004

Jaeggi, S. M., Buschkuehl, M., Jonides, J., & Perrig, W. J. (2008). Improving fluid intelligence with training on working memory. *Proceedings of the National Academy of Sciences*, *105*(19), 6829-6833. https://doi.org/10.1073/pnas.0801268105

Jocham, G., & Ullsperger, M. (2009). Neuropharmacology of performance monitoring. *Neurosci Biobehav Rev*, *33*(1), 48-60.

Kable, J. W., & Glimcher, P. W. (2009). The Neurobiology of Decision : Consensus and Controversy. *Neuron*, *63*(6), 733-745. https://doi.org/10.1016/j.neuron.2009.09.003

Kalcher-Sommersguter, E., Preuschoft, S., Franz-Schaider, C., Hemelrijk, C. K., Crailsheim, K., & Massen, J. J. M. (2015). Early maternal loss affects social integration of chimpanzees throughout their lifetime. *Scientific Reports*, *5*(1), 16439. https://doi.org/10.1038/srep16439

Karbach, J., & Verhaeghen, P. (2014). Making Working Memory Work : A Meta-Analysis of Executive-Control and Working Memory Training in Older Adults. *Psychological Science*, *25*(11), 2027-2037. https://doi.org/10.1177/0956797614548725

Kemp, C., Goodman, N. D., & Tenenbaum, J. B. (2010). Learning to Learn Causal Models. *Cognitive Science*, *34*(7), 1185-1243. https://doi.org/10.1111/j.1551-6709.2010.01128.x

Kennerley, S. W., Walton, M. E., Behrens, T. E. J., Buckley, M. J., & Rushworth, M. F. S. (2006). Optimal decision making and the anterior cingulate cortex. *Nature Neuroscience*, *9*(7), 940-947. https://doi.org/10.1038/nn1724

Khamassi, M., Enel, P., Dominey, P. F., & Procyk, E. (2013). Medial prefrontal cortex and the adaptive regulation of reinforcement learning parameters. In *Progress in Brain Research* (Vol. 202, p. 441-464). Elsevier. https://doi.org/10.1016/B978-0-444-62604-2.00022-8

Khamassi, M., & Humphries, M. D. (2012). Integrating cortico-limbic-basal ganglia architectures for learning model-based and model-free navigation strategies. *Frontiers in Behavioral Neuroscience*, *6*. https://doi.org/10.3389/fnbeh.2012.00079

Khamassi, M., Lallée, S., Enel, P., Procyk, E., & Dominey, P. F. (2011). Robot Cognitive Control with a Neurophysiologically Inspired Reinforcement Learning Model. *Frontiers in Neurorobotics*, *5*. https://doi.org/10.3389/fnbot.2011.00001

Khamassi, M., Quilodran, R., Enel, P., Dominey, P. F., & Procyk, E. (2015). Behavioral Regulation and the Modulation of Information Coding in the Lateral Prefrontal and Cingulate Cortex. *Cerebral Cortex*, *25*(9), 3197-3218. https://doi.org/10.1093/cercor/bhu114

Killcross, S., & Coutureau, E. (2003). Coordination of Actions and Habits in the Medial Prefrontal Cortex of Rats. *Cerebral Cortex*, *13*(4), 400-408. https://doi.org/10.1093/cercor/13.4.400

Kluger, A. N., & DeNisi, A. (1996). The effects of feedback interventions on performance : A historical review, a meta-analysis, and a preliminary feedback intervention theory. *Psychological Bulletin*, *119*(2), 254-284. https://doi.org/10.1037/0033-2909.119.2.254

Köhler, W. (1929). An old pseudoproblem. *Die Naturwissenschaften*, *17*(395-401).

Kolling, N., Wittmann, M. K., Behrens, T. E. J., Boorman, E. D., Mars, R. B., & Rushworth, M. F. S. (2016). Value, search, persistence and model updating in anterior cingulate cortex. *Nature Neuroscience*, *19*(10), 1280-1285. https://doi.org/10.1038/nn.4382

Kouneiher, F., Charron, S., & Koechlin, E. (2009). Motivation and cognitive control in the human prefrontal cortex. *Nature Neuroscience*, *12*(7), 939-945. https://doi.org/10.1038/nn.2321

Koziol, L. F., Budding, D., Andreasen, N., D'Arrigo, S., Bulgheroni, S., Imamizu, H., Ito, M., Manto, M., Marvel, C., Parker, K., Pezzulo, G., Ramnani, N., Riva, D., Schmahmann, J., Vandervert, L., & Yamazaki, T. (2014). Consensus Paper : The Cerebellum's Role in Movement and Cognition. *The Cerebellum*, *13*(1), 151-177. https://doi.org/10.1007/s12311-013-0511-x

Kyndt, E., & Baert, H. (2013). Antecedents of Employees' Involvement in Work-Related Learning : A Systematic Review. *Review of Educational Research*, *83*(2), 273-313. https://doi.org/10.3102/0034654313478021

Lansdell, B. J., & Kording, K. P. (2019). Towards learning-to-learn. *Current Opinion in Behavioral Sciences*, *29*, 45-50. https://doi.org/10.1016/j.cobeha.2019.04.005

Luman, M., Tripp, G., & Scheres, A. (2010). Identifying the neurobiology of altered reinforcement sensitivity in ADHD : A review and research agenda. *Neuroscience & Biobehavioral Reviews*, *34*(5), 744-754. https://doi.org/10.1016/j.neubiorev.2009.11.021

McGaugh, J. L. (2000). Memory—A Century of Consolidation. *Science*, *287*(5451), 248-251. https://doi.org/10.1126/science.287.5451.248

McGonigle, B., & Chalmers, M. (2006). Ordering and Executive Functioning as a Window on the Evolution and Development of Cognitive Systems. *International Journal of Comparative Psychology*, *19*(2). https://doi.org/10.46867/IJCP.2006.19.02.01

Melby-Lervåg, M., & Hulme, C. (2013a). Can Working Memory Training Ameliorate ADHD and Other Learning Disorders? A Systematic Meta-Analytic Review. *The ADHD Report*, *21*(2), 1-5. https://doi.org/10.1521/adhd.2013.21.2.1

Melby-Lervåg, M., & Hulme, C. (2013b). Is working memory training effective? A meta-analytic review. *Developmental Psychology*, *49*(2), 270-291. https://doi.org/10.1037/a0028228

Meyer, T., Qi, X.-L., Stanford, T. R., & Constantinidis, C. (2011). Stimulus Selectivity in Dorsal and Ventral Prefrontal Cortex after Training in Working Memory Tasks. *The Journal of Neuroscience*, *31*(17), 6266-6276. https://doi.org/10.1523/JNEUROSCI.6798-10.2011

Miller, E. K., & Cohen, J. D. (2001). An Integrative Theory of Prefrontal Cortex Function. *Annual Review of Neuroscience*, *24*(1), 167-202. https://doi.org/10.1146/annurev.neuro.24.1.167

Morecraft, R. J., Stilwell-Morecraft, K. S., Cipolloni, P. B., Ge, J., McNeal, D. W., & Pandya, D. N. (2012). Cytoarchitecture and cortical connections of the anterior cingulate and adjacent somatomotor fields in the rhesus monkey. *Brain Research Bulletin*, *87*(4-5), 457-497. https://doi.org/10.1016/j.brainresbull.2011.12.005

Nicol, D. J., & Macfarlane-Dick, D. (2006). Formative assessment and self-regulated learning : A model and seven principles of good feedback practice. *Studies in Higher Education*, *31*(2), 199-218. https://doi.org/10.1080/03075070600572090

Niv, Y., Daw, N. D., Joel, D., & Dayan, P. (2007). Tonic dopamine : Opportunity costs and the control of response vigor. *Psychopharmacology*, *191*(3), 507-520. https://doi.org/10.1007/s00213-006-0502-4

Norman, D. A., & Shallice, T. (1986). Attention to Action : Willed and Automatic Control of Behavior. In R. J. Davidson, G. E. Schwartz, & D. Shapiro (Éds.), *Consciousness and Self-Regulation* (p. 1-18). Springer US. https://doi.org/10.1007/978-1-4757-0629-1_1

O'Reilly, R. C., & Munakata, Y. (2003). Psychological Function in Computational Models of Neural Networks. In I. B. Weiner (Éd.), *Handbook of Psychology* (1re éd., p. 637-654). Wiley. https://doi.org/10.1002/0471264385.wei0322

Overbeek, T. J. M., Nieuwenhuis, S., & Ridderinkhof, K. R. (2005). Dissociable Components of Error Processing : On the Functional Significance of the Pe Vis-à-vis the ERN/Ne. *Journal of Psychophysiology*, *19*(4), 319-329. https://doi.org/10.1027/0269-8803.19.4.319

Owen, A. M., Hampshire, A., Grahn, J. A., Stenton, R., Dajani, S., Burns, A. S., Howard, R. J., & Ballard, C. G. (2010). Putting brain training to the test. *Nature*, *465*(7299), 775-778. https://doi.org/10.1038/nature09042

Pachitariu, M., Steinmetz, N., Kadir, S., Carandini, M., & Kenneth D., H. (2016). *Kilosort : Realtime spike-sorting for extracellular electrophysiology with hundreds of channels*. https://doi.org/10.1101/061481

Passingham, R. E. (2021). *Understanding the Prefrontal Cortex : Selective advantage, connectivity, and neural operations* (1re éd.). Oxford University Press. https://doi.org/10.1093/oso/9780198844570.001.0001

Pavlov, I. P. (1927). Conditioned reflexes : An investigation of the psychological activity of the cerebral cortex. *Oxford Univ. Press.*

Petrides, M. (2005). Lateral prefrontal cortex : Architectonic and functional organization. *Philosophical Transactions of the Royal Society B: Biological Sciences*, *360*(1456), 781-795. https://doi.org/10.1098/rstb.2005.1631

Petrides, M., & Pandya, D. N. (1994). Comparative architectonic analysis of the human and the macaque frontal cortex. *In Boller, F. & Grafman, J. (eds.), Handbook of Neuropsychology Elsevier, Amsterdam*, *9*, 17-58.

Petrides, M., & Pandya, D. N. (1999). Dorsolateral prefrontal cortex : Comparative cytoarchitectonic analysis in the human and the macaque brain and corticocortical connection patterns: Dorsolateral prefrontal cortex in human and monkey. *European Journal of Neuroscience*, *11*(3), 1011-1036. https://doi.org/10.1046/j.1460-9568.1999.00518.x

Petrides, M., & Pandya, D. N. (2002). Comparative cytoarchitectonic analysis of the human and the macaque ventrolateral prefrontal cortex and corticocortical connection patterns in the monkey : Ventrolateral prefrontal cortex in human and monkey. *European Journal of Neuroscience*, *16*(2), 291-310. https://doi.org/10.1046/j.1460-9568.2001.02090.x

Pintrich, P. R., & Groot, E. V. D. (1990). Motivational and Self-Regulated Learning Components of Classroom Academic Performance. *Journal of Educational Psychology*, *82*(1), 33-40.

Polich, J. (2007). Updating P300 : An integrative theory of P3a and P3b. *Clinical Neurophysiology*, *118*(10), 2128-2148. https://doi.org/10.1016/j.clinph.2007.04.019

Postman, L. (1947). The history and present status of the law of effect. *Psychological Bulletin*, *44*(6), 489-563. https://doi.org/10.1037/h0057716

Preuss, T. M., & Wise, S. P. (2022). Evolution of prefrontal cortex. *Neuropsychopharmacology*, *47*(1), 3-19. https://doi.org/10.1038/s41386-021-01076-5

Price, G. R., Holloway, I., Räsänen, P., Vesterinen, M., & Ansari, D. (2007). Impaired parietal magnitude processing in developmental dyscalculia. *Current Biology*, *17*(24), R1042-R1043. https://doi.org/10.1016/j.cub.2007.10.013

Procyk, E., Fontanier, V., Sarazin, M., Delord, B., Goussi, C., & Wilson, C. R. E. (2021). The midcingulate cortex and temporal integration. In *International Review of Neurobiology* (Vol. 158, p. 395-419). Elsevier. https://doi.org/10.1016/bs.irn.2020.12.004

Procyk, E., Wilson, C. R. E., Stoll, F. M., Faraut, M. C. M., Petrides, M., & Amiez, C. (2016). Midcingulate Motor Map and Feedback Detection : Converging Data from Humans and Monkeys. *Cerebral Cortex*, bhu213. https://doi.org/10.1093/cercor/bhu213

Qi, X.-L., & Constantinidis, C. (2013). Neural changes after training to perform cognitive tasks. *Behavioural Brain Research*, *241*, 235-243. https://doi.org/10.1016/j.bbr.2012.12.017

Qi, X.-L., Meyer, T., Stanford, T. R., & Constantinidis, C. (2011). Changes in Prefrontal Neuronal Activity after Learning to Perform a Spatial Working Memory Task. *Cerebral Cortex*, *21*(12), 2722-2732. https://doi.org/10.1093/cercor/bhr058

Qi, X.-L., Meyer, T., Stanford, T. R., & Constantinidis, C. (2012). Neural Correlates of a Decision Variable Before Learning to Perform a Match/Non-Match Task. *Journal of Neuroscience*, *32*(18), 6161-6169. https://doi.org/10.1523/JNEUROSCI.6365-11.2012

Quian Quiroga, R., & Panzeri, S. (2009). Extracting information from neuronal populations : Information theory and decoding approaches. *Nature Reviews Neuroscience*, *10*(3), 173-185. https://doi.org/10.1038/nrn2578

Quilodran, R., Rothé, M., & Procyk, E. (2008). Behavioral Shifts and Action Valuation in the Anterior Cingulate Cortex. *Neuron*, *57*(2), 314-325. https://doi.org/10.1016/j.neuron.2007.11.031

Ramaprasad, A. (1983). On the definition of feedback. *Behavioral Science*, *28*(1), 4-13. https://doi.org/10.1002/bs.3830280103

Redick, T. S., Shipstead, Z., Harrison, T. L., Hicks, K. L., Fried, D. E., Hambrick, D. Z., Kane, M. J., & Engle, R. W. (2013). No evidence of intelligence improvement after working memory training : A randomized, placebo-controlled study. *Journal of Experimental Psychology: General*, *142*(2), 359-379. https://doi.org/10.1037/a0029082

Reeve, J., & Lee, W. (2014). Students' classroom engagement produces longitudinal changes in classroom motivation. *Journal of Educational Psychology*, *106*(2), 527-540. https://doi.org/10.1037/a0034934

Ridderinkhof, K. R., Van Den Wildenberg, W. P. M., Segalowitz, S. J., & Carter, C. S. (2004). Neurocognitive mechanisms of cognitive control : The role of prefrontal cortex in action selection, response inhibition, performance monitoring, and reward-based learning. *Brain and Cognition*, *56*(2), 129-140. https://doi.org/10.1016/j.bandc.2004.09.016

Rothe, M., Quilodran, R., Sallet, J., & Procyk, E. (2011). Coordination of High Gamma Activity in Anterior Cingulate and Lateral Prefrontal Cortical Areas during Adaptation. *Journal of Neuroscience*, *31*(31), 11110-11117. https://doi.org/10.1523/JNEUROSCI.1016-11.2011

Sajad, A., Errington, S. P., & Schall, J. D. (2022). Functional architecture of executive control and associated event-related potentials in macaques. *Nature Communications*, *13*(1), 6270. https://doi.org/10.1038/s41467-022-33942-1

Santoro, A., Bartunov, S., Botvinick, M., Wierstra, D., & Lillicrap, T. (2016). *Meta-Learning with Memory-Augmented Neural Networks*. 9.

Schapiro, S. J., Bloomsmith, M. A., Suarez, S. A., & Porter, L. M. (1996). Effects of social and inanimate enrichment on the behavior of yearling rhesus monkeys. *American Journal of Primatology*, *40*(3), 247-260. https://doi.org/10.1002/(SICI)1098-2345(1996)40:3<247::AID-AJP3>3.0.CO;2-Y

Schraw, G. (1998). Promoting General Metacognitive Awareness. *Instructional Science*, *26*, 113-125. https://doi.org/10.1007/978-94-017-2243-8_1

Schrier, A. M. (1966). Learning-set formation by three species of macaque monkeys. *Journal of Comparative and Physiological Psychology*, *61*(3), 490-492. https://doi.org/10.1037/h0023268

Schultz, W. (1998). Predictive Reward Signal of Dopamine Neurons. *Journal of Neurophysiology*, *80*(1), 1-27. https://doi.org/10.1152/jn.1998.80.1.1

Schultz, W. (2007). Multiple Dopamine Functions at Different Time Courses. *Annual Review of Neuroscience*, *30*(1), 259-288. https://doi.org/10.1146/annurev.neuro.28.061604.135722

Schultz, W. (2015). Neuronal Reward and Decision Signals : From Theories to Data. *Physiological Reviews*, *95*(3), 853-951. https://doi.org/10.1152/physrev.00023.2014

Schultz, W. (2016). Dopamine reward prediction error coding. *Dialogues in Clinical Neuroscience*, *18*(1), 10.

Semendeferi, K., Armstrong, E., Schleicher, A., Zilles, K., & Hoesen, G. W. V. (2001). Prefrontal Cortex in Humans and Apes : A Comparative Study of Area 10. *American Journal of Physical Anthropology*, *114*, 224-241.

Semendeferi, K., Teffer, K., Buxhoeveden, D. P., Park, M. S., Bludau, S., Amunts, K., Travis, K., & Buckwalter, J. (2011). Spatial Organization of Neurons in the Frontal Pole Sets Humans Apart from Great Apes. *Cerebral Cortex*, *21*(7), 1485-1497. https://doi.org/10.1093/cercor/bhq191

Seo, H., & Lee, D. (2007). Temporal Filtering of Reward Signals in the Dorsal Anterior Cingulate Cortex during a Mixed-Strategy Game. *The Journal of Neuroscience*, *27*(31), 8366-8377. https://doi.org/10.1523/JNEUROSCI.2369-07.2007

Shaywitz, S. E., & Shaywitz, B. A. (2003). Dyslexia (Specific Reading Disability). *Pediatrics in Review*, *24*(5).

Shenhav, A., Botvinick, M. M., & Cohen, J. D. (2013). The Expected Value of Control : An Integrative Theory of Anterior Cingulate Cortex Function. *Neuron*, *79*(2), 217-240. https://doi.org/10.1016/j.neuron.2013.07.007

Simonyan, K., & Zisserman, A. (2015). *Very Deep Convolutional Networks for Large-Scale Image Recognition* (arXiv:1409.1556). arXiv. http://arxiv.org/abs/1409.1556

Skinner, B. F. (1953). Science and human behavior. *Macmillan*.

Smaers, J. B., Gómez-Robles, A., Parks, A. N., & Sherwood, C. C. (2017). Exceptional Evolutionary Expansion of Prefrontal Cortex in Great Apes and Humans. *Current Biology*, *27*(5), 714-720. https://doi.org/10.1016/j.cub.2017.01.020

Stoll, F. M., Fontanier, V., & Procyk, E. (2016). Specific frontal neural dynamics contribute to decisions to check. *Nature Communications*, *7*(1), 11990. https://doi.org/10.1038/ncomms11990

Suarez-Perez, A., Gabriel, G., Rebollo, B., Illa, X., Guimerà-Brunet, A., Hernández-Ferrer, J., Martínez, M. T., Villa, R., & Sanchez-Vives, M. V. (2018). Quantification of Signal-to-Noise Ratio in Cerebral Cortex Recordings Using Flexible MEAs With Co-localized Platinum Black, Carbon Nanotubes, and Gold Electrodes. *Frontiers in Neuroscience*, *12*, 862. https://doi.org/10.3389/fnins.2018.00862

Sutton, R. S., & Barto, A. (2014). *Reinforcement learning : An introduction* (Nachdruck). The MIT Press.

Sweller, J. (1988). Cognitive Load During Problem Solving : Effects on Learning. *Cognitive Science*, *12*(2), 257-285. https://doi.org/10.1207/s15516709cog1202_4

Tang, H., Riley, M. R., Singh, B., Qi, X.-L., Blake, D. T., & Constantinidis, C. (2022). Prefrontal cortical plasticity during learning of cognitive tasks. *Nature Communications*, *13*(1), 90. https://doi.org/10.1038/s41467-021-27695-6

Tanji, J., & Hoshi, E. (2008). Role of the Lateral Prefrontal Cortex in Executive Behavioral Control. *Physiological Reviews*, *88*(1), 37-57. https://doi.org/10.1152/physrev.00014.2007

Teffer, K., & Semendeferi, K. (2012). Human prefrontal cortex. In *Progress in Brain Research* (Vol. 195, p. 191-218). Elsevier. https://doi.org/10.1016/B978-0-444-53860-4.00009-X

Tenenbaum, J. B., Kemp, C., Griffiths, T. L., & Goodman, N. D. (2011). How to Grow a Mind : Statistics, Structure, and Abstraction. *Science*, *331*(6022), 1279-1285. https://doi.org/10.1126/science.1192788

Thrun, S. (1996). *Learning to learn : Introduction*.

Tolman, E. C. (1949). There is more than one kind of learning. *Psychological Review*, *56*(3), 144-155. https://doi.org/10.1037/h0055304

Tulving, E. (2002). Episodic Memory : From Mind to Brain. *Annual Review of Psychology*, *53*(1), 1-25. https://doi.org/10.1146/annurev.psych.53.100901.135114

Ullsperger, M., Harsay, H. A., Wessel, J. R., & Ridderinkhof, K. R. (2010). Conscious perception of errors and its relation to the anterior insula. *Brain Structure and Function*, *214*(5-6), 629-643. https://doi.org/10.1007/s00429-010-0261-1

Van Merriënboer, J. J. G., & Sweller, J. (2005). Cognitive Load Theory and Complex Learning : Recent Developments and Future Directions. *Educational Psychology Review*, *17*(2), 147-177. https://doi.org/10.1007/s10648-005-3951-0

Vezoli, J., & Procyk, E. (2009). Frontal Feedback-Related Potentials in Nonhuman Primates : Modulation during Learning and under Haloperidol. *The Journal of Neuroscience*, *29*(50), 15675-15683. https://doi.org/10.1523/JNEUROSCI.4943-09.2009

Vidal, F., Burle, B., Bonnet, M., Grapperon, J., & Hasbroucq, T. (2003). Error negativity on correct trials : A reexamination of available data. *Biological Psychology*, *64*(3), 265-282. https://doi.org/10.1016/S0301-0511(03)00097-8

Vidal, F., Hasbroucq, T., Grapperon, J., & Bonnet, M. (2000). Is the 'error negativity' specific to errors? *Biological Psychology*, *51*(2-3), 109-128. https://doi.org/10.1016/S0301-0511(99)00032-0

Vinck, M., Huurdeman, L., Bosman, C. A., Fries, P., Battaglia, F. P., Pennartz, C. M. A., & Tiesinga, P. H. (2015). How to detect the Granger-causal flow direction in the presence of additive noise? *NeuroImage*, *108*, 301-318. https://doi.org/10.1016/j.neuroimage.2014.12.017

Vogt, B. A. (2009). Regions and Subregions of the Cingulate Cortex. In B. A. Vogt (Éd.), *Cingulate Neurobiology and Disease* (p. 3-30). Oxford University PressOxford. https://doi.org/10.1093/oso/9780198566960.003.0001

Vogt, B. A. (2016). Midcingulate cortex : Structure, connections, homologies, functions and diseases. *Journal of Chemical Neuroanatomy*, *74*, 28-46. https://doi.org/10.1016/j.jchemneu.2016.01.010

Vogt, B. A., Berger, G. R., & Derbyshire, S. W. G. (2003). Structural and Functional Dichotomy of Human Midcingulate Cortex. *The European journal of neuroscience*, *18*(11), 3134-3144.

Vogt, B. A., Nimchinsky, E. A., Vogt, L. J., & Hof, P. R. (1995). Human cingulate cortex : Surface features, flat maps, and cytoarchitecture. *Journal of Comparative Neurology*, *359*(3), 490-506. https://doi.org/10.1002/cne.903590310

Volkow, N. D., Wang, G.-J., Fowler, J. S., Tomasi, D., & Telang, F. (2011). Addiction : Beyond dopamine reward circuitry. *Proceedings of the National Academy of Sciences*, *108*(37), 15037-15042. https://doi.org/10.1073/pnas.1010654108

Voloh, B., Maisson, D. J.-N., Cervera, R. L., Conover, I., Zambre, M., Hayden, B., & Zimmermann, J. (2023). Hierarchical action encoding in prefrontal cortex of freely moving macaques. *Cell Reports*, *42*(9), 113091. https://doi.org/10.1016/j.celrep.2023.113091

Vygotsky, L. S. (1978). *Mind in Society : Development of Higher Psychological Processes* (Harvard University Press).

Walton, M. E., Bannerman, D. M., Alterescu, K., & Rushworth, M. F. S. (2003). Functional Specialization within Medial Frontal Cortex of the Anterior Cingulate for Evaluating Effort-Related Decisions. *The Journal of Neuroscience*, *23*(16), 6475-6479. https://doi.org/10.1523/JNEUROSCI.23-16-06475.2003

Wang, J. X., Kurth-Nelson, Z., Kumaran, D., Tirumala, D., Soyer, H., Leibo, J. Z., Hassabis, D., & Botvinick, M. (2018). Prefrontal cortex as a meta-reinforcement learning system. *Nature Neuroscience*, *21*(6), 860-868. https://doi.org/10.1038/s41593-018-0147-8

Wang, Z., Bovik, A. C., Sheikh, H. R., & Simoncelli, E. P. (2004). Image Quality Assessment : From Error Visibility to Structural Similarity. *IEEE Transactions on Image Processing*, *13*(4), 600-612. https://doi.org/10.1109/TIP.2003.819861

Watson, J. B. (1913). *Psychology as the behaviorist views it*.

Wessel, J. R. (2018). An adaptive orienting theory of error processing. *Psychophysiology*, *55*(3), e13041. https://doi.org/10.1111/psyp.13041

Wiener, N. (1948). Cybernetics or Control and Communication in the Animal and the Machine. *John Wiley & Sons*.

Wilson, C. R. E., & Gaffan, D. (2008). Prefrontal-Inferotemporal Interaction Is Not Always Necessary for Reversal Learning. *Journal of Neuroscience*, *28*(21), 5529-5538. https://doi.org/10.1523/JNEUROSCI.0952-08.2008

Wilson, C. R. E., Vezoli, J., Stoll, F. M., Faraut, M. C. M., Leviel, V., Knoblauch, K., & Procyk, E. (2016). Prefrontal Markers and Cognitive Performance Are Dissociated during Progressive Dopamine Lesion. *PLOS Biology*, *14*(11), e1002576. https://doi.org/10.1371/journal.pbio.1002576

Wise, S. P. (2008). Forward frontal fields : Phylogeny and fundamental function. *Trends in Neurosciences*, *31*(12), 599-608. https://doi.org/10.1016/j.tins.2008.08.008

Yousuf, M., Heldmann, M., Münte, T. F., & Doñamayor, N. (2019). Electrophysiology of goal-directed versus habitual control during outcome devaluation. *Cortex*, *119*, 401-416. https://doi.org/10.1016/j.cortex.2019.08.002

Zhao, N., Zhong, C., Wang, Y., Zhao, Y., Gong, N., Zhou, G., Xu, T., & Hong, Z. (2008). Impaired hippocampal neurogenesis is involved in cognitive dysfunction induced by thiamine deficiency at early pre-pathological lesion stage. *Neurobiology of Disease*, *29*(2), 176-185. https://doi.org/10.1016/j.nbd.2007.08.014

Zimmerman, B. J. (2002). Becoming a Self-Regulated Learner : An Overview. *THEORY INTO PRACTICE*.